

NASA CR-175043
GARRETT 21-5705

DILUTION JET MIXING PROGRAM SUPPLEMENTARY REPORT

(NASA-CR-175043) DILUTION JET MIXING
PROGRAM, SUPPLEMENTARY REPORT (Garrett
Turbine Engine Co.) 397 p HC A17/MF A01
CSCL 20D

N86-23856

Unclas
G3/34 06020

by

R. SRINIVASAN
C. WHITE

Garrett Turbine Engine Company
A Division of The Garrett Corporation

March 1986

Prepared for

National Aeronautics and Space Administration
NASA-Lewis Research Center

Contract NAS3-22110



1 Report No NASA CR-175043		2 Government Accession No		3 Recipient's Catalog No	
4 Title and Subtitle Dilution Jet Mixing Program Supplementary Report				5 Report Date March 1986	
				6 Performing Organization Code 533-04-12	
7 Author(s) R. Srinivasan C. White				8 Performing Organization Report No Garrett 21-5705	
9 Performing Organization Name and Address Garrett Turbine Engine Company P.O. Box 5217 Phoenix, Arizona 85010				10 Work Unit No	
				11 Contract or Grant No NAS3-22110	
12 Sponsoring Agency Name and Address National Aeronautics and Space Administration Washington, D.C. 20546				13 Type of Report and Period Covered Supplementary Report	
				14 Sponsoring Agency Code	
15 Supplementary Notes Project Manager: Dr. J. D. Holdeman NASA-Lewis Research Center Cleveland, Ohio					
16 Abstract This report presents a comparison of the velocity and temperature distributions predicted by a 3-D numerical model and experimental measurements. In addition, empirical correlations for the jet velocity trajectory developed in this program are presented. The measured velocity distributions for all test cases of Phase I through Phase III in this program (Contract NAS3-22110) are presented in the form of contour and oblique plots.					
17 Key Words (Suggested by Author(s)) Dilution-Zone Jet-Mixing Combustion			18 Distribution Statement General Release		
19 Security Classif (of this report) Unclassified		20. Security Classif (of this page) Unclassified		21 No of Pages	
				22 Price*	

* For sale by the National Technical Information Service, Springfield, Virginia 22161

TABLE OF CONTENTS

	<u>Page</u>
1.0 SUMMARY	1
2.0 INTRODUCTION	3
3.0 DESCRIPTION OF TEST RIG, INSTRUMENTATION, AND DATA REDUCTION	5
4.0 RESULTS OF NUMERICAL CALCULATIONS	11
5.0 VELOCITY TRAJECTORY CORRELATIONS	15
6.0 RESULTS OF VELOCITY MEASUREMENTS	19
7.0 CONCLUSIONS	23
LIST OF SYMBOLS	25
REFERENCES	218

PRECEDING PAGE BLANK NOT FILMED

LIST OF ILLUSTRATIONS

<u>Figure</u>	<u>Title</u>	<u>Page</u>
1	Dilution Jet Mixing Rig Schematic	27
2	Schematics of Test Sections Used in the Program $H_0 = 10.16$ cm	28
3	Schematic of Orifice Plate Configurations	29
4	Total Pressure, Thermocouple, and Static Pressure Rake	30
5	Predicted Temperature Distributions for Test Case 1 - Table 1	31
6	Comparison Between Predicted and Measured Temperature Distributions for Test Case 1 - Table 1	32
7	Predicted Velocity Distributions for Test Case 1 - Table 1	33
8	Comparison Between Predicted and Measured Velocity Distributions for Test Case 1 - Table 1	34
9	Predicted Temperature Distributions for Test Case 2 - Table 1	35
10	Comparison Between Predicted and Measured Temperature Distributions for Test Case 2 - Table 1	36
11	Predicted Velocity Distributions for Test Case 2 - Table 1	37
12	Comparison Between Predicted and Measured Velocity Distributions for Test Case 2 - Table 1	38
13	Predicted Temperature Distributions for Test Case 3 - Table 1	39
14	Comparison Between Predicted and Measured Temperature Distributions for Test Case 3 - Table 1	40
15	Predicted Velocity Distributions for Test Case 3 - Table 1	41
16	Comparison Between Predicted and Measured Velocity Distributions for Test Case 3 - Table 1	42

LIST OF ILLUSTRATIONS (Contd)

<u>Figure</u>	<u>Title</u>	<u>Page</u>
17	Predicted Temperature Distributions for Test Case 4 - Table 1	43
18	Comparison Between Predicted and Measured Temperature Distributions for Test Case 4 - Table 1	44
19	Predicted Velocity Distributions for Test Case 4 - Table 1	45
20	Comparison Between Predicted and Measured Velocity Distributions for Test Case 4 - Table 1	46
21	Predicted Temperature Distributions for Test Case 5 - Table 1	47
22	Comparison Between Predicted and Measured Temperature Distributions for Test Case 5 - Table 1	48
23	Predicted Velocity Distributions for Test Case 5 - Table 1	49
24	Comparison Between Predicted and Measured Velocity Distributions for Test Case 5 - Table 1	50
25	Predicted Temperature Distributions for Test Case 6 - Table 1	51
26	Comparison Between Predicted and Measured Temperature Distributions for Test Case 6 - Table 1	52
27	Predicted Velocity Distributions for Test Case 6 - Table 1	53
28	Comparison Between Predicted and Measured Velocity Distributions for Test Case 6 - Table 1	54
29	Predicted Temperature Distributions for Test Case 7 - Table 1	55
30	Comparison Between Predicted and Measured Temperature Distributions for Test Case 7 - Table 1	56
31	Predicted Velocity Distributions for Test Case 7 - Table 1	57

LIST OF ILLUSTRATIONS (Contd)

<u>Figure</u>	<u>Title</u>	<u>Page</u>
32	Comparison Between Predicted and Measured Velocity Distributions for Test Case 7 - Table 1	58
33	Predicted Temperature Distributions for Test Case 8 - Table 1	59
34	Comparison Between Predicted and Measured Temperature Distributions for Test Case 8 - Table 1	60
35	Predicted Velocity Distributions for Test Case 8 - Table 1	61
36	Comparison Between Predicted and Measured Velocity Distributions for Test Case 8 - Table 1	62
37	Predicted Temperature Distributions for Test Case 9 - Table 1	63
38	Comparison Between Predicted and Measured Temperature Distributions for Test Case 9 - Table 1	64
39	Predicted Velocity Distributions for Test Case 9 - Table 1	65
40	Comparison Between Predicted and Measured Velocity Distributions for Test Case 9 - Table 1	66
41	Predicted Temperature Distributions for Test Case 10 - Table 1	67
42	Comparison Between Predicted and Measured Temperature Distributions for Test Case 10 - Table 1	68
43	Predicted Velocity Distributions for Test Case 10 - Table 1	69
44	Comparison Between Predicted and Measured Velocity Distributions for Test Case 10 - Table 1	70

LIST OF ILLUSTRATIONS (Contd)

<u>Figure</u>	<u>Title</u>	<u>Page</u>
45	Predicted Temperature Distributions for Test Case 11 - Table 1	71
46	Comparison Between Predicted and Measured Temperature Distributions for Test Case 11 - Table 1	72
47	Predicted Velocity Distributions for Test Case 11 - Table 1	73
48	Comparison Between Predicted and Measured Velocity Distributions for Test Case 11 - Table 1	74
49	Predicted Temperature Distributions for Test Case 12 - Table 1	75
50	Comparison Between Predicted and Measured Temperature Distributions for Test Case 12 - Table 1	76
51	Predicted Velocity Distributions for Test Case 12 - Table 1	77
52	Comparison Between Predicted and Measured Velocity Distributions for Test Case 12 - Table 1	78
53	Predicted Temperature Distributions for Test No. 13 - Table 2	79
54	Comparison Between Predicted and Measured Temperature Distributions for Test No. 13 - Table 2	80
55	Predicted Velocity Distributions for Test No. 13 - Table 2	81
56	Comparison Between Predicted and Measured Velocity Distributions for Test No. 13 - Table 2	82
57	Predicted Temperature Distributions for Test No. 14 - Table 2	83
58	Comparison Between Predicted and Measured Temperature Distributions for Test No. 14 - Table 2	84
59	Predicted Velocity Distributions for Test No. 14 - Table 2	85

LIST OF ILLUSTRATIONS (Contd)

<u>Figure</u>	<u>Title</u>	<u>Page</u>
60	Comparison Between Predicted and Measured Velocity Distributions for Test No. 14 - Table 2	86
61	Predicted Temperature Distributions for Test No. 15 - Table 2	87
62	Comparison Between Predicted and Measured Temperature Distributions for Test No. 15 - Table 2	88
63	Predicted Velocity Distributions for Test No. 15 - Table 2	89
64	Comparison Between Predicted and Measured Velocity Distributions for Test No. 15 - Table 2	90
65	Predicted Temperature Distributions for Test No. 16 - Table 2	91
66	Comparison Between Predicted and Measured Temperature Distributions for Test No. 16 - Table 2	92
67	Predicted Velocity Distributions for Test No. 16 - Table 2	93
68	Comparison Between Predicted and Measured Velocity Distributions for Test No. 16 - Table 2	94
69	Predicted Temperature Distributions for Test No. 17 - Table 2	95
70	Comparison Between Predicted and Measured Temperature Distributions for Test No. 17 - Table 2	96
71	Predicted Velocity Distributions for Test No. 17 - Table 2	97
72	Comparison Between Predicted and Measured Velocity Distributions for Test No. 17 - Table 2	98
73	Predicted Temperature Distributions for Test No. 18 - Table 2	99
74	Comparison Between Predicted and Measured Temperature Distributions for Test No. 18 - Table 2	100

LIST OF ILLUSTRATIONS (Contd)

<u>Figure</u>	<u>Title</u>	<u>Page</u>
75	Predicted Velocity Distributions for Test No. 18 - Table 2	101
76	Comparison Between Predicted and Measured Velocity Distributions for Test No. 18 - Table 2	102
77	Comparison Between Predicted and Measured Velocity Trajectories For $S/D = 2$ and $H_0/D = 4$	103
78	Comparison Between Predicted and Measured Velocity Trajectories Including Effects of Mainstream Profiles and Flow Area Convergence at Intermediate J for Orifice Plate 01/02/04	104
79	Comparison of Predicted and Measured Velocity Trajectories for Different Jet Diameters, $S/H = 0.5$	105
80	Predicted and Measured Velocity Trajectories for Non-Uniform Mainstream Profile and Flow Area Convergence, $S/D = 4$, $H_0/D = 8$	106
81	Predicted and Measured Velocity Trajectories for Different Convergence and Jet Injection Angles, $S/D = 4$, $H_0/D = 8$	107
82	Predicted and Measured Velocity Trajectories for $S/D = 4$, $H_0/D = 4$	108
83	Predicted and Measured Velocity Trajectories for a Straight Duct for $S/D = 2$, $H_0/D = 8$	109
84	Predicted and Measured Velocity Trajectories in Convergent Duct with Non-Uniform Mainstream Profile, $S/D = 4$, $H_0/D = 8$ (Test Section V)	110
85	Predicted and Measured Velocity Trajectories for Opposed Jets, $S/D = 2$, $H_0/D = 8$	111
86	Predicted and Measured Velocity Trajectories for Opposed Jets, $S/D = 4$, $H_0/D = 8$	112
87	Predicted and Measured Velocity Trajectories for Opposed Jets With Non-Uniform Mainstream Profile	113

LIST OF ILLUSTRATIONS (Contd)

<u>Figure</u>	<u>Title</u>	<u>Page</u>
88	Predicted and Measured Velocity Trajectories with Unequal Momentum Flux Ratios, Flow Area Convergence, for Opposed Jets; $S/D = 2$, $H_0/D = 8$	114
89	Predicted and Measured Velocity Trajectories for Opposed Jets in Convergent Ducts, $S/D = 4$, $H_0/D = 8$	115
90	Predicted and Measured Velocity Trajectories for Opposed Jets with $S/D = 4$, $H_0/D = 8$	116
91	Comparison Between Predicted and Measured Velocity Trajectories For Opposed In-line Jets with $H_0/D = 4$ in a Straight Duct	117
92	Predicted and Measured Velocity Trajectories with Opposed Jets in Convergent Ducts, $S/D = 2$, $H_0/D = 4$	118
93	Predicted and Measured Velocity Trajectories for 2-D Slots	119
94	Predicted and Measured Velocity Trajectories for the Remaining Test Cases in Phase II	120
95	Predicted and Measured Velocity Trajectories for Streamlined and Bluff Slots (Equivalent Size and Spacing to Orifice Plate 01/02/04)	121
96	Predicted and Measured Velocity Trajectories for Double Row of Jets (Plate M-3 and M-5)	122
97	Comparison of Predicted and Measured Velocity Trajectories for Plate 01/02/04, Plate M-4, and Equivalent Single Row of Jet Configurations	123
98	Predicted and Measured Velocity Trajectories for Double Row of Jets with Unequal Momentum Flux Ratios	124
99	Comparisons of Predicted and Measured Velocity Trajectories for 45-degree Slot and Equivalent Circular Holes	125
100	Measured Velocity Distributions for Test No. 1 of DJM Phase I Testing	127

LIST OF ILLUSTRATIONS (Contd)

<u>Figure</u>	<u>Title</u>	<u>Page</u>
101	Measured Velocity Distributions for Test No. 2 of DJM Phase I Testing	128
102	Measured Velocity Distributions for Test No. 3 of DJM Phase I Testing	129
103	Measured Velocity Distributions for Test No. 4 of DJM Phase I Testing	130
104	Measured Velocity Distributions for Test No. 5 of DJM Phase I Testing	131
105	Measured Velocity Distributions for Test No. 6 of DJM Phase I Testing	132
106	Measured Velocity Distributions for Test No. 7 of DJM Phase I Testing	133
107	Measured Velocity Distributions for Test No. 8 of DJM Phase I Testing	134
108	Measured Velocity Distributions for Test No. 9 of DJM Phase I Testing	135
109	Measured Velocity Distributions for Test No. 10 of DJM Phase I Testing	136
110	Measured Velocity Distributions for Test No. 11 of DJM Phase I Testing	137
111	Measured Velocity Distributions for Test No. 12 of DJM Phase I Testing	138
112	Measured Velocity Distributions for Test No. 13 of DJM Phase I Testing	139
113	Measured Velocity Distributions for Test No. 14 of DJM Phase I Testing	140
114	Measured Velocity Distributions for Test No. 15 of DJM Phase I Testing	141
115	Measured Velocity Distributions for Test No. 16 of DJM Phase I Testing	142

LIST OF ILLUSTRATIONS (Contd)

<u>Figure</u>	<u>Title</u>	<u>Page</u>
116	Measured Velocity Distributions for Test No. 17 of DJM Phase I Testing	143
117	Measured Velocity Distributions for Test No. 18 of DJM Phase I Testing	144
118	Measured Velocity Distributions for Test No. 23 of DJM Phase I Testing	145
119	Measured Velocity Distributions for Test No. 24 of DJM Phase I Testing	146
120	Measured Velocity Distributions for Test No. 25 of DJM Phase I Testing	147
121	Measured Velocity Distributions for Test No. 26 of DJM Phase I Testing	148
122	Measured Velocity Distributions for Test No. 27 of DJM Phase I Testing	149
123	Measured Velocity Distributions for Test No. 28 of DJM Phase I Testing	150
124	Measured Velocity Distributions for Test No. 29 of DJM Phase I Testing	151
125	Measured Velocity Distributions for Test No. 30 of DJM Phase I Testing	152
126	Measured Velocity Distributions for Test No. 31 of DJM Phase I Testing	153
127	Measured Velocity Distributions for Test No. 32 of DJM Phase I Testing	154
128	Measured Velocity Distributions for Test No. 33 of DJM Phase I Testing	155
129	Measured Velocity Distributions for Test No. 34 of DJM Phase I Testing	156
130	Measured Velocity Distributions for Test No. 3 of DJM Phase II Testing	157
131	Measured Velocity Distributions for Test No. 4 of DJM Phase II Testing	158

LIST OF ILLUSTRATIONS (Contd)

<u>Figure</u>	<u>Title</u>	<u>Page</u>
132	Measured Velocity Distributions for Test No. 5 of DJM Phase II Testing	159
133	Measured Velocity Distributions for Test No. 6 of DJM Phase II Testing	160
134	Measured Velocity Distributions for Test No. 12 of DJM Phase II Testing	161
135	Measured Velocity Distributions for Test No. 13 of DJM Phase II Testing	162
136	Measured Velocity Distributions for Test No. 14 of DJM Phase II Testing	163
137	Measured Velocity Distributions for Test No. 15 of DJM Phase II Testing	164
138	Measured Velocity Distributions for Test No. 16 of DJM Phase II Testing	165
139	Measured Velocity Distributions for Test No. 17 of DJM Phase II Testing	166
140	Measured Velocity Distributions for Test No. 18 of DJM Phase II Testing	167
141	Measured Velocity Distributions for Test No. 19 of DJM Phase II Testing	168
142	Measured Velocity Distributions for Test No. 20 of DJM Phase II Testing	169
143	Measured Velocity Distributions for Test No. 21 of DJM Phase II Testing	170
144	Measured Velocity Distributions for Test No. 22 of DJM Phase II Testing	171
145	Measured Velocity Distributions for Test No. 23 of DJM Phase II Testing	172
146	Measured Velocity Distributions for Test No. 24 of DJM Phase II Testing	173

LIST OF ILLUSTRATIONS (Contd)

<u>Figure</u>	<u>Title</u>	<u>Page</u>
147	Measured Velocity Distributions for Test No. 25 of DJM Phase II Testing	174
148	Measured Velocity Distributions for Test No. 26 of DJM Phase II Testing	175
149	Measured Velocity Distributions for Test No. 35 of DJM Phase II Testing	176
150	Measured Velocity Distributions for Test No. 36 of DJM Phase II Testing	177
151	Measured Velocity Distributions for Test No. 37 of DJM Phase II Testing	178
152	Measured Velocity Distributions for Test No. 38 of DJM Phase II Testing	179
153	Measured Velocity Distributions for Test No. 39 of DJM Phase II Testing	180
154	Measured Velocity Distributions for Test No. 40 of DJM Phase II Testing	181
155	Measured Velocity Distributions for Test No. 41 of DJM Phase II Testing	182
156	Measured Velocity Distributions for Test No. 42 of DJM Phase II Testing	183
157	Measured Velocity Distributions for Test No. 45A of DJM Phase II Testing	184
158	Measured Velocity Distributions for Test No. 45B of DJM Phase II Testing	185
159	Measured Velocity Distributions for Test No. 45C of DJM Phase II Testing	186
160	Measured Velocity Distributions for Test No. 49 of DJM Phase II Testing	187
161	Measured Velocity Distributions for Test No. 50 of DJM Phase II Testing	188

LIST OF ILLUSTRATIONS (Contd)

<u>Figure</u>	<u>Title</u>	<u>Page</u>
162	Measured Velocity Distributions for Test No. 1 of DJM Phase III Testing	189
163	Measured Velocity Distributions for Test No. 2 of DJM Phase III Testing	190
164	Measured Velocity Distributions for Test No. 3 of DJM Phase III Testing	191
165	Measured Velocity Distributions for Test No. 4 of DJM Phase III Testing	192
166	Measured Velocity Distributions for Test No. 5 of DJM Phase III Testing	193
167	Measured Velocity Distributions for Test No. 6 of DJM Phase III Testing	194
168	Measured Velocity Distributions for Test No. 7 of DJM Phase III Testing	195
169	Measured Velocity Distributions for Test No. 8 of DJM Phase III Testing	196
170	Measured Velocity Distributions for Test No. 9 of DJM Phase III Testing	197
171	Measured Velocity Distributions for Test No. 10 of DJM Phase III Testing	198
172	Measured Velocity Distributions for Test No. 11 of DJM Phase III Testing	199
173	Measured Velocity Distributions for Test No. 12 of DJM Phase III Testing	200
174	Measured Velocity Distributions for Test No. 13 of DJM Phase III Testing	201
175	Measured Velocity Distributions for Test No. 14 of DJM Phase III Testing	202
176	Measured Velocity Distributions for Test No. 15 of DJM Phase III Testing	203

LIST OF ILLUSTRATIONS (Contd)

<u>Figure</u>	<u>Title</u>	<u>Page</u>
177	Measured Velocity Distributions for Test No. 16 of DJM Phase III Testing	204
178	Measured Velocity Distributions for Test No. 17 of DJM Phase III Testing	205
179	Measured Velocity Distributions for Test No. 18 of DJM Phase III Testing	206
180	Measured Velocity Distributions for Test No. 19 of DJM Phase III Testing	207
181	Measured Velocity Distributions for Test No. 20 of DJM Phase III Testing	208
182	Measured Velocity Distributions for Test No. 21 of DJM Phase III Testing	209
183	Measured Velocity Distributions for Test No. 22 of DJM Phase III Testing	210

LIST OF TABLES

<u>Table</u>	<u>Title</u>	<u>Page</u>
1	Test Cases of 3-D Calculations Performed in Host Aerothermal Modeling Program	12
2	Test Cases of 3-D Calculations Performed in the NASA Dilution Jet Mixing Program	13
3	Configurations and Flow Conditions for Phase I, Series 1 Tests	211
4	Configurations and Flow Conditions for Phase I, Series 2 Tests	211
5	Configurations and Flow Conditions for Phase I, Series 3 Tests	212
6	Configurations and Flow Conditions for Phase I, Series 4 Tests	212
7	Configurations and Flow Conditions for Phase II, Series 5 Tests	213
8	Configurations and Flow Conditions for Phase II, Series 6 Tests	213
9	Configurations and Flow Conditions for Phase II, Series 7 Tests	214
10	Configurations and Flow Conditions for Phase II, Series 8 Tests	215
11	Configurations and Flow Conditions for Phase III, Series 9 Tests	217
12	Configurations and Flow Conditions for Phase III, Series 10 Tests	217

1.0 SUMMARY

In this report, velocity and temperature distributions predicted by a 3-D numerical model are presented and compared with measurements taken during the Dilution Jet Mixing program (Contract NAS3-22110). In addition, empirical correlations for the jet velocity trajectory developed in this program are presented. For all of the configurations tested in the Dilution Jet Mixing program (Phases I through III), measurements of both temperature and velocity distributions were made at several axial stations. The measured temperature distributions were reported in the three previous reports. The measured velocity distributions for all test cases performed in this program are presented in this report in the form of contour and oblique plots. The velocity distributions show characteristics similar to those observed in temperature distributions.

2.0 INTRODUCTION

Advanced aircraft propulsion gas turbine engines for civil and military applications require increased thrust or horsepower per unit airflow. The increased power density often results in higher average combustor discharge temperature with attendant reduction of the available dilution air. Effective use must be made of the available dilution air to tailor the combustor discharge temperature distribution.

The combustor discharge temperature quality is influenced by nearly all aspects of the combustor design and in particular by the dilution zone. To tailor the combustor discharge temperature pattern, the discharge temperature distribution must be characterized in terms of the dilution zone geometric and flow parameters. Such characterization requires an improved understanding of the dilution jet mixing processes.

The present program has been undertaken to acquire a data base of dilution jet mixing characteristics, to develop empirical jet mixing correlations and to validate combustor analytical design models.

The main objectives of the NASA Dilution Jet Mixing Program are to quantify the effects of the following on the jet mixing characteristics with a confined cross-flow:

- o Orifice geometry, momentum flux ratio, and density ratio
- o Nonuniform mainstream temperature and velocity profiles upstream of dilution orifices
- o Cold versus hot jet injection

- o Cross-stream flow area convergence (accelerating cross-stream) as encountered in practical dilution-zone geometries.
- o 2-D slots versus circular orifices
- o Discrete noncircular orifices
- o Single-sided versus opposed (in-line and staggered) jets
- o Single row versus double row of jets

Besides generating a data base, a limited number of 3-D numerical computations were made for several dilution jet configurations. The comparison between the numerical predictions and the test data are presented in Section 4.

As a part of the program, an empirical model describing the jet mixing characteristics was developed. The model results for temperature field are reported in References 1 through 3. The empirical model also predicts the jet velocity trajectory for all the configurations tested in the program. A description of the empirical model for velocity trajectory and the comparison between data and model results are provided in Section 5.

The temperature measurements obtained in this program are reported in References 1 through 3. This report contains all the velocity data obtained in the NASA Dilution Jet Mixing Program under Contract NAS3-22110.

3.0 DESCRIPTION OF TEST RIG, INSTRUMENTATION, AND DATA REDUCTION

3.1 Test Rig

A schematic layout of the jet mixing test rig is presented in Figure 1. The mainstream airflow is ducted from the test cell main air supply through a 15.24-cm internal diameter pipe. A transition section connects the inlet pipe to a rectangular cross section of constant width (30.48 cm) and adjustable height.

A perforated plate with 25 holes of 1.43-cm diameter provides a relatively uniform airstream at the profile generator plenum. The profile generator duct incorporates an adjustable bottom wall to match the test section inlet height, which can vary from 10.16 cm to 15.24 cm.

A separate air supply enables the profile generator to provide the desired radial profile of temperature and velocity upstream of the jet-injection plane.

A third air supply allows the dilution injection orifices to vary jet velocity and density. A number of interchangeable dilution orifice plates and test section geometries are used to study confined jet mixing with the mainstream. To minimize the rig thermal losses, the rig walls are insulated with a 2.54-cm thick layer of Kaolite insulation.

Detailed descriptions of the profile generator, test sections, and dilution orifice plates are provided in References 1 through 3. The test sections used in this program are shown in Figure 2, and the orifice plate configurations employed are illustrated in Figure 3.

The rig instrumentation includes a number of wall static pressure taps and flow thermocouples, in addition to a traversing $P_t/P_s/T$ rake.

3.2 Instrumentation

The dilution jet mixing characteristics were determined by measuring temperature and pressure distributions within the test section at different axial stations. A traversing probe (Figure 4) is used for this purpose.

The probe consists of a 20-element thermocouple rake with 20 total-pressure sensors on one side and 20 static-pressure rakes on the other side. The nominal transverse spacing between the thermocouple rake and the total pressure rake is 0.508 cm. The spacing between the thermocouple and the static pressure elements is 0.508 cm.

The height of the probe between the top and the bottom elements is 9.35 cm. The first element is located 0.405 cm from the top wall of the constant-height test section (Test Section I). All the elements are equally spaced in the vertical direction, providing a nominal spacing of 0.492 cm.

The total-pressure sensor elements are made of Inconel tubes with an outside diameter of 0.16 cm and a wall thickness of 0.023 cm. The internal conical design of the tube at the inlet provides a ± 15 degree flow insensitivity angle. The static pressure tubes, similar to the total pressure sensors, are dead-ended with four bleeding holes of 0.03-cm diameter 90 degrees apart and 0.7 cm from the tip. The total temperature sensors are type K thermocouple wires with insulated junctions encased in 0.10-cm inside diameter tubes, supported by 0.21-cm inside diameter enveloping tubes. The insulated junction tubes exposed to the air stream are 0.76-cm long. The sensing elements have a straight length of 1.52 cm or more

before the first bend to the probe core, where all tubes are inserted in a rectangular probe shield, 4.32 x 0.67 cm.

The probe is mounted on a traversing system that allows travel in three directions. This system allows for a 30.48-cm traverse in the X-direction (mainstream flow direction) and 22.86 cm in the radial (Y) and transverse (Z) directions with an accuracy of ± 0.015 percent. The flow field mapping in the Z direction is made at several planes starting at $Z/S = -0.5$ at intervals of 0.1. The measurements in the X-direction were made at axial planes between $X/H_0 = 0.25$ and $X/H_0 = 2.0$.

The temperature and pressure values from the test rig instrumentation are recorded on magnetic tape through a central computerized data acquisition system. An on-line data display system provides real-time information on selected raw data for monitoring the flow conditions. The raw data from the magnetic tape is used for detail data reduction, analysis, and correlation.

3.3 Data Reduction

The pressure recordings from the probe rake were used to compute the velocity $V(X,Y,Z)$ at the point (X,Y,Z) . An interpolation scheme was used to compute pressure (P_s) values at the point where probe thermocouples are located. From these total and static pressures, a nondimensionalized velocity, $V(X,Y,Z)/V_j$, was computed. $V(X,Y,Z)$ is obtained from

$$V(X,Y,Z) = \left\{ 2 [P_t (X,Y,Z) - P_s (X,Y,Z)] / \rho(X,Y,Z) \right\}^{1/2}$$

The jet velocity, V_j , is calculated from

$$V_j = 4 \dot{m}_j / (\rho_j N \pi D^2 C_D)$$

where D is the orifice diameter, N is the number of orifices, ρ_j is the jet density (P_j/RT_j), and C_D is the orifice discharge coefficient.

The orifice discharge coefficients were determined by measuring the pressure drop across the orifice plate (without cross flow) for a range of mass flow rates. The discharge coefficient, C_D , was obtained from the relation

$$\frac{\Delta P}{P} = 1.99 \left[\frac{\dot{w}_c}{AC_D} \right]^2$$

where, \dot{w}_c is the corrected flow rate in lbm/sec and A is the geometric area of the orifices in square inches.

$$\text{Note: } \dot{w}_c = \dot{w}_a \frac{\sqrt{\beta}}{\delta}, \text{ where } \beta = \frac{T(OR)}{518.67}, \text{ and } \delta = \frac{P(\text{psi})}{14.696}$$

The velocity vector in the vicinity of the jet injection plane is predominantly in the radial direction. In such regions, the velocity values obtained from the rake probe are not expected to be accurate.

An important parameter relevant to the jet description is the jet momentum flux ratio, J , defined as

$$J = \rho_j V_j^2 / (\rho_m V_m^2)$$

where

ρ_j = Jet density

ρ_m = Mainstream density = $P_m/(RT_m)$

V_j or V_{JET} = Jet velocity at the orifice Vena Contracta

V_m or V_{MAIN} = Mainstream Velocity = $\dot{m}_m/(\rho_m A_m)$

A_m = Effective mainstream flow area.

\dot{m}_m = Mainstream flow rate

Other flow parameters of interest are:

Mass flux ratio (blowing rate), M or BLORAT = $\rho_j V_j / \rho_m V_m$

Temperature ratio, TRATIO = T_j / T_m

Density ratio, DENRATIO = ρ_j / ρ_m

Velocity ratio = V_j / V_m .

The geometric parameters of importance associated with the orifice configuration are: S/D_j and H_0/D_j , where D_j is the effective jet diameter defined by

$$D_j = D \left(C_D \right)^{0.5}$$

The quantities described in this section define the geometric and flow conditions of each test and are reported along with the reduced data.

The average mainstream velocity, V_m and the average jet velocity, V_j , are mass weighted average values for the test. They represent the correct momentum flux for the mainstream and the jet, respectively.

4.0 RESULTS OF NUMERICAL CALCULATIONS

The empirical correlations developed in this program and other existing empirical models describing the jet mixing characteristics are applicable only within the scope of the experiments from which these models are generated. Many practical combustion systems have geometries that are not investigated in these experiments. The jet mixing behavior in such systems can be predicted by 3-D numerical calculations. In the Host Aerothermal Modeling Program Phase I (Contract NAS3-23523), 3-D numerical calculations were performed for 10 dilution jet mixing test cases. The predicted temperature distributions are reported in Reference 4.

The 3-D calculations performed in that program include the test configurations shown in Table 1. The predicted temperature and velocity distributions by the 3-D model for these cases are presented in Figures 5 through 52 in the form of oblique and contour plots. The velocity distributions show the same characteristics as the predicted temperature distributions.

The 3-D model underestimates the mixing of the velocity field. Decreasing the number of finite-difference grids tends to increase the mixing, which demonstrates that the solution is grid dependent and that the numerical diffusion effects are significant. The jet velocity penetration (corresponding to maximum velocity point) and the acceleration of the cross flow around the jet are correctly predicted by the model; but the magnitudes of the predicted velocity are only within 20 percent of the measured values.

As a part of the Phase III Dilution Jet Mixing Program, similar 3-D numerical calculations were made for six dilution jet configurations shown in Table 2.

The predicted temperature and velocity distributions for these six cases are presented in Figures 53 through 76. These figures

}

TABLE 1. SAMPLE CASES OF 3-D CALCULATIONS PERFORMED IN
HOST AEROTHERMAL MODELING PROGRAM

Case No.	Orifice Configuration	Number of Nodes	Orifice Dia (cm)	S/D	H ₀ /D	J	DJM Test Case No.	
							Phase	Test No.
1	Single-Sided	35x33x17	1.27	2.0	8.0	22.32	I	5
2	Single-Sided	27x26x8	1.27	2.0	8.0	22.32	I	5
3	Single-Sided	35x33x17	1.27	2.0	8.0	92.63	I	6
4	Single-Sided	27x26x8	1.27	2.0	8.0	92.63	I	6
5	Single-Sided	35x33x17	1.80	2.83	5.66	25.48	II	50
6	Single-Sided	32x29x21	1.80	2.83	5.66	25.48	II	50
7	Single-Sided	45x23x19	2.54	2.0	4.0	18.59	I	2
8	Single-Sided	40x23x21	2.54	4.0	4.0	23.51	I	4
9	Single-Sided	40x23x21	2.54	4.0	4.0	5.31	I	3
10	Top Cold Profile	45x23x19	2.54	2.0	4.0	31.79	I	13
11	Opposed In-Line	35x33x17	1.27	2.0	8.0	24.94	II	2
12	Opposed Staggered	22x27x33	2.54	4.0	4.0	26.41	II	28

TABLE 2. SAMPLE CASES OF 3-D CALCULATIONS PERFORMED IN
THE NASA DILUTION JET MIXING PROGRAM

Case No.	Orifice Configuration	Number of Nodes	Orifice Dia (cm)	S/D	H ₀ /D	J	DJM Test Case No.	
							Phase	Test No.
13	Single-Sided	36x29x19	1.27	4.0	8.0	28.37	I	7
14	In-Line, 2 Rows	41x23x21	1.80	2.83	5.66	26.27	III	6
			1.80	2.83	5.66	26.85		
15	Single-Sided Conv. Duct	42x28x17	2.54	2.0	4.0	26.36	I	26
16	45-Deg. Slot	45x23x19	2.54	2.0	4.0	27.13	III	19
17	Offset, 2 Rows	41x23x21	1.80	2.83	5.66	26.79	III	11
			1.27	2.00	8.00	26.63		
18	Single-Sided	45x23x19	2.54	2.00	4.00	26.24	III	22

show the contour and oblique plots of nondimensionalized temperature and velocity distributions, along with their vertical profiles along the jet centerplane. The following general conclusions are made from these figures:

- o The jet velocity penetration is farther than the temperature penetration.
- o The 3-D model underestimates the mixing of velocity and temperature fields, especially in the transverse direction.
- o The predicted centerplane velocity profiles are in good agreement with the data. The centerplane velocity profiles are more accurately predicted by the 3-D model than the temperature profiles.
- o For 45-degree slots, the 3-D numerical model correctly predicts the transverse shift of the centerplane profiles, as well as the rotation of the theta contours. The rotation of theta contours is not predicted by the Garrett empirical model for angled slots.
- o The 3-D model predictions are in qualitative agreement with the data. Improvements in the numerics and turbulence models are needed to accurately correlate with the measurements.

5.0 VELOCITY TRAJECTORY CORRELATIONS

The interaction of dilution jets injected normally into a confined cross flow is highly complex and three-dimensional in nature. Accurate characterization of this interaction requires multidimensional models. Such models are currently in development and are not yet validated. Furthermore, the multidimensional models are not currently cost effective for making hardware changes in the combustor to meet the combustor exit profile requirements. In order to aid the combustor design efforts, GTEC developed empirical models for characterizing the dilution jet mixing in confined cross flows, by using the data obtained in this program. The empirical model is based upon the correlations reported in Reference 5. The GTEC correlations are applicable to the following configurations:

- o Single sided and opposed jets
- o Single row as well as multiple rows of jets
- o Circular and noncircular jets
- o 2-D slots and discrete angled slots.
- o Nonuniform cross flow temperature and velocity profiles
- o Flow area convergence.

Descriptions of the empirical model and its results were reported in References 1 through 3. In these references, only the temperature field was presented. In addition to correlating the temperature field, the empirical model also estimates velocity trajectory.

The expression for jet velocity trajectory developed in the GTEC empirical model is based upon the following form proposed by Walker and Eberhardt (Reference 6):

$$Y_v/D_j = 0.549 J^{0.12} (S/D_j)^{0.23} (H_0/D_j)^{0.57} (X/D_j)^{0.18} \quad (1)$$

where,

Y_v is the jet velocity penetration

D_j is the effective jet diameter

S is the orifice spacing

H_0 is the channel height at jet injection plane

J is the momentum flux ratio.

Preliminary comparison between data and this expression indicated poor agreement between the two. Based upon the data obtained in this Dilution Jet Mixing Program, the following expression was developed at GTEC for correlating the jet velocity trajectory:

$$\left(\frac{Y_v}{D_j}\right) = a_0 J^{0.12} \left(\frac{S}{D_j}\right)^{0.23} \left(\frac{H_0}{D_j}\right)^{0.57} \left(\frac{X}{D_j}\right)^{\alpha} \quad (2)$$

where,

$$a_0 = 0.765 \left[1 + \frac{dH}{dx}\right]^{0.35} \quad (3)$$

$$\alpha = 0.12 \left[1 + \frac{dH}{dx}\right]^{1.25} \quad (4)$$

and $\frac{dH}{dx}$ is a measure of the rate of area change.

For a straight duct

$$(dH/dx = 0) \quad a_0 = 0.765 \text{ and } \alpha = 0.12.$$

Note the difference between equations (1) and (2), namely, larger value of empirical constant a_0 and slower decay in the stream-wise direction. Both these equations give the same jet trajectory for $X/D_j = 250$.

The results obtained from equation (2) and their comparison with test data are presented in Figures 77 through 99. In these figures, the locations of measured jet trajectories are shown by symbols, and predictions are shown by solid lines. For opposed and double rows of holes, the trajectories corresponding to the bottom injections or aft row of jets, whichever is applicable, are shown by the broken lines. In these figures, the data points were obtained by interpolating between the measured values. It is important to note that the velocity measurements were made using a probe rake. Such measurements are not expected to be accurate close to the jet injection plane. Consequently, the velocity trajectory data in those regions are not accurate. The following general conclusions are made by comparing the trajectories obtained from the empirical model with the test data:

- o The empirical model correctly predicts, within measurement accuracy, the trajectories for $S/D = 2$ and underestimates it for $S/D = 4$.
- o The model underestimates jet velocity trajectories for tests using convergent ducts.
- o For opposed jets, the empirical model accurately predicts the jet penetrations for in-line arrangements; the agreement between data and model results are poor for staggered configurations.
- o The empirical model underestimates the jet penetrations for 2-D slots when equation (2) is used with $S/D_j=1$ and H_0/D_j is replaced by H_0/w , where w is the slot width.
- o Jet velocity trajectories for bluff slots and 45-degree slots are accurately predicted by the model, while those

for streamlined slots are underestimated. For these discrete slots, the D_j values employed in equation (2) correspond to those of equivalent area circular holes.

- o For double rows of jets, the model accurately estimates jet penetrations for in-line arrangement and underestimates them for staggered and offset configurations. For multiple rows of jets, the lead row jet penetrations correlate well with the measurements.
- o The empirical model for velocity trajectory must be evaluated against more accurate data on trajectory.

6.0 RESULTS OF VELOCITY MEASUREMENTS

In References 1 through 3, the measured temperature distributions were presented for all test cases performed in Phases I through III. The test configurations and flow conditions for these tests are presented in Tables 3 through 12. In all these test cases, total and static pressure measurements were made in addition to obtaining thermocouple data, as described in paragraph 4.1. From the total and static pressure data, the axial velocity component is computed in the form described in paragraph 4.2. The measurements obtained from the rake probe are not reliable in some regions, especially in regions close to the injection plane where the velocity vectors are not aligned with the total pressure elements. In these regions, the measured rake probe static pressures show higher values than the corresponding total pressure data. The velocity values in such situations are set equal to zero. The measured velocity distributions are presented in nondimensional form as $(U-V_{\text{main}})/V_{\text{jet}}$.

Evaluation of the test data showed that for some of the test cases, the accuracy of velocity data was very poor. For these test cases, the velocity data will not be presented:

- o Phase I - Tests 19 through 22 and 35 through 38.
- o Phase II - Tests 1, 2, 7, 8, 9, 10, 11, 27 through 34, 43, and 44, 46, 47, 48 and 51.

For the remaining test cases performed in Phases I through III, the nondimensionalized velocity distributions are presented in the form of contour plots and oblique plots. These results are shown in Figures 100 through 183. The following conclusions are drawn from the velocity data:

- o The jet velocity penetration (location of maximum velocity) is farther than the jet temperature penetration. However, when the jet penetration is close to the opposite wall, the jet velocity and temperature centerlines are close to each other.
- o The rate at which laterally two-dimensional profiles are obtained for velocity is faster than the rate for temperature distributions.
- o The jet-to-mainstream density ratio, ρ_j/ρ_m , has at best a second order influence on the velocity distributions for a given momentum flux ratio.
- o The influence of nonuniform mainstream velocity profile on the velocity distribution is significant; but the superposition scheme applicable to temperature distributions may not be applicable to velocity distributions (Figures 112-117 and 135-140).
- o Flow area convergence enhances jet mixing. Velocity distributions in an asymmetrically convergent duct with jet injection from the flat wall (Figures 122-125) are very similar to those in an equivalent symmetrically convergent duct (Figures 118-121) at the same momentum flux ratio. For an asymmetrically convergent duct with jet injection from the slant wall, the velocity gradients in the vertical direction (Figures 126-129) are steeper than those with flat wall injection or symmetrical convergence. The jet spreading rates in the transverse direction are faster for slant wall jets than the other two configurations.
- o Opposed jets injected into an asymmetrically convergent duct produce velocity distributions (Figures 149-156) similar to those in a symmetrically convergent duct

(Figures 141-148) beyond $X/H_0 = 0.5$. In the regions closer to the injection plane, the jets from the slant wall show deeper penetration than those from the flat wall.

- o Orifice plates having the same S/H_0 ratio produce similar velocity distributions at the same momentum flux ratios.
- o The velocity distributions produced by streamlined slots are similar to those of equivalent area circular holes with the same S/H_0 and momentum flux ratio in regions beyond $X/H_0 = 1$. In the regions closer to the jet injection plane, the velocity profiles for streamlined slots show smaller vertical gradients compared to equivalent area circular holes.
- o The bluff slots have smaller jet velocity penetration compared to streamlined slots or equivalent area circular holes, but the velocity distributions are more two-dimensional in nature. The bluff slots produce larger vertical velocity gradients compared to equivalent area circular holes.
- o Double rows of in-line jets with $S/D = 2.83$, $H_0/D = 5.66$ (Plate M-3, Figure 3) produce velocity distributions very similar to those of single row of jets with the same spacing and diameter at the same momentum flux ratio. The velocity profiles for these two orifices are similar, while the magnitudes are different. Plate M-3 produces smaller velocity gradients in the vertical direction than the equivalent area circular holes (Plate 01/02/04) at the same momentum flux ratio.
- o The configuration with a double row of dissimilar holes (Plate M-5, Figure 3) produces steeper velocity gradients

in the vertical direction compared to Plate M-3. These gradients are still smaller compared to those produced by a single row of jet of equivalent area.

- o In orifice Plate M-5, increasing the flows in the downstream row of jets increases the velocity gradients in the vertical direction.
- o Plate M-6 (with leading row of holes having $S/D = 2$ and $H_0/D = 8$) produces velocity profiles very similar to those of orifice plate 01/02/08 (single row with $S/D = 2$ and $H_0/D = 8$) (See Figure 3 for orifice configurations.).
- o The 45-degree slot generates a skewed vortex field, which shifts the velocity centerplanes in the direction of slot. In addition, the vortex field rotates the velocity contours about the axis of the slot.

7.0 CONCLUSIONS

The NASA Dilution Jet Mixing program under Contract NAS3-2210, was directed toward characterizing mixing processes of jets injected into a confined cross flow. Measurements of temperature and velocity were made for several orifice shapes and configurations. The velocity distributions for these test cases are presented in this report. In addition, empirical correlations were developed to quantify the jet velocity trajectory. Comparison between the data and the empirical model shows agreement within the accuracy of measurements for most of the jet configurations studied.

As a part of the program, 3-D numerical calculations were performed for several different orifice configurations. The 3-D model underestimates the mixing of velocity and temperature fields. Advanced numerics and turbulence models are needed to improve the accuracy of 3-D model predictions.

LIST OF SYMBOLS

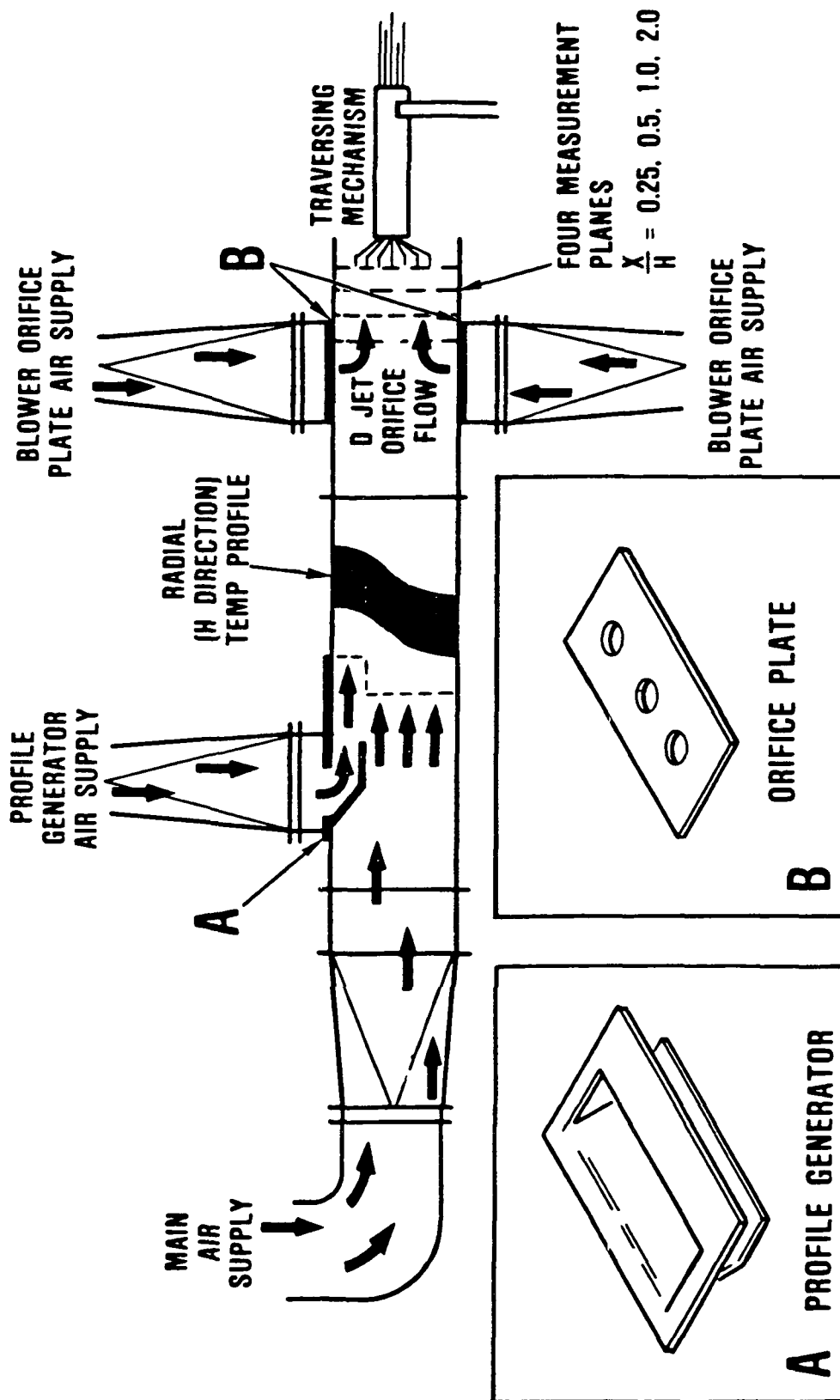
A	Test section cross-sectional area at survey plane
AR	Aspect Ratio (frontal width/streamwise length)
C_D	Orifice discharge coefficient
D	Geometric orifice diameter
D_j	Effective orifice diameter
H_0	Duct height at the jet injection plane
J	Momentum flux ratio $\rho_j V_j^2 / \rho_m V_m^2$
P_t	Stagnation pressure
P_s	Static pressure
S	Orifice spacing
T	Temperature
V	Velocity
X	x direction, parallel to duct axis
Y	y direction, parallel to orifice centerline (radial direction)
Y_v	Centerplane velocity trajectory
Z	z direction, normal to duct axis (transverse direction)

Greek

θ	Temperature difference ratio
ρ	Density

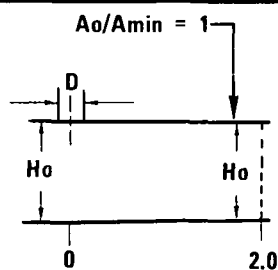
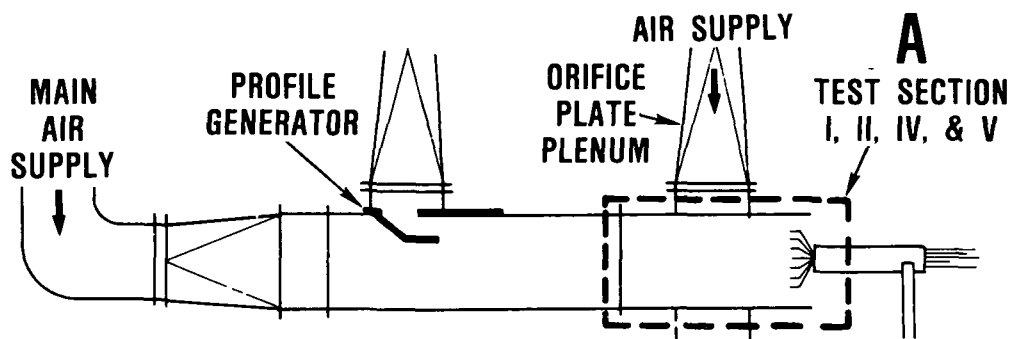
Subscripts

av	Average
EB	Equilibrium value
j	Jet property
max	Maximum
m	Cross-flow property, average value
F	First or lead row jet conditions
B	Back or aft row jet conditions

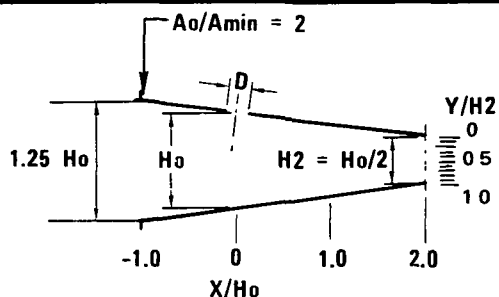


23-SVG1657-2

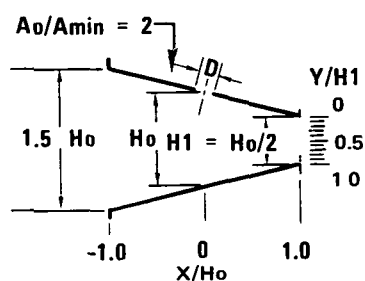
Figure 1. Dilution Jet Mixing Rig Schematic.



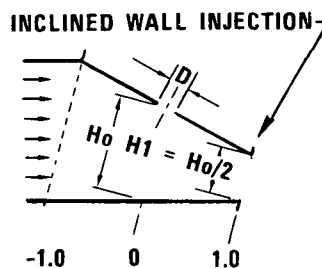
TEST SECTION I



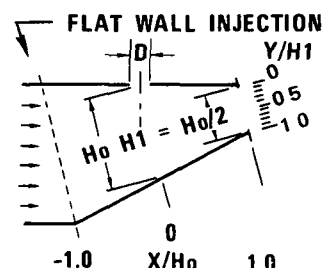
TEST SECTION II



TEST SECTION IV



TEST SECTION V



TEST SECTION VI

Figure 2. Schematics of Test Sections Used in the Program $H_0=10.16$ cm.

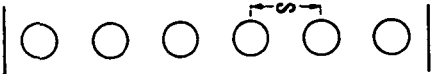
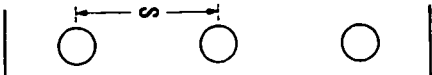
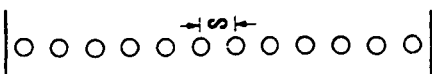
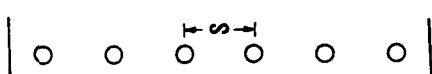
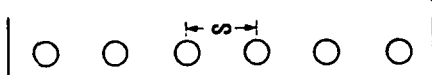



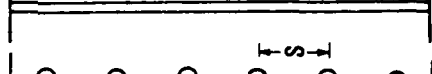



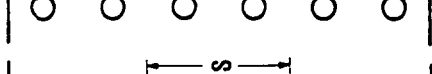
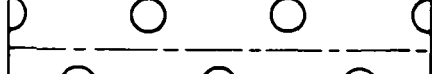
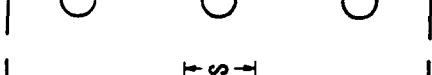
CONFIGURATION	SYMBOL	ORIFICE DIAMETER (CM)	S/D	H ₀ /D
	01/02/04	2.54	2	4
	01/04/04	2.54	4	4
	01/02/08	1.27	2	8
	01/04/08	1.27	4	8
	01/03/06	1.80	2.83	5.66
	SQUARE	2.25	4	4
	WIDE SLOT	1.024	1	9.92
	NARROW SLOT	0.5144	1	19.75
	STREAMLINED SLOT	2.54	2	4
	BLUFF SLOT	2.54	2	4
	PLATE M-3	1.80 1.80	2.83 2.83	5.66 5.66
	PLATE M-4	2.54 2.54	4 4	4 4
	PLATE M-5	1.80 1.27	2.83 2.0	5.66 8.0
	PLATE M-6	1.27 1.83	2.0 2.83	8.0 5.66
	PLATE M-7	2.54	2	4

Figure 3. Orifice Plate Configurations.

ORIGINAL PAGE IS
OF POOR QUALITY

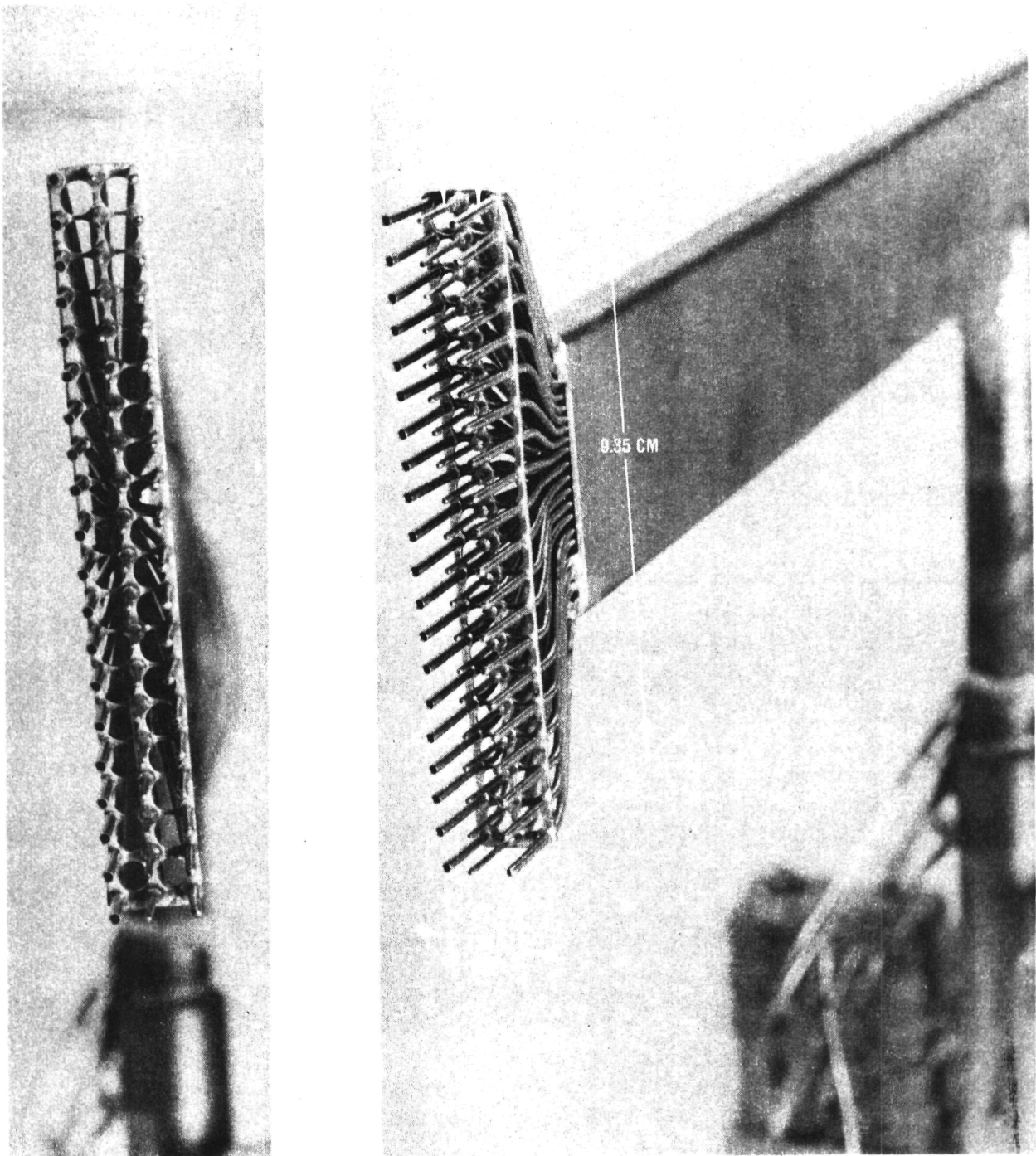
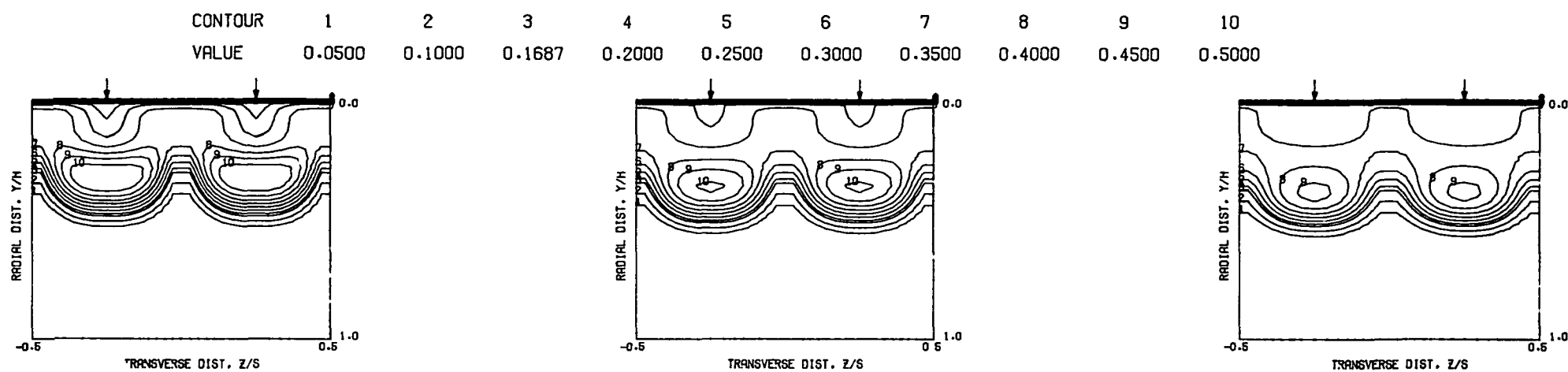


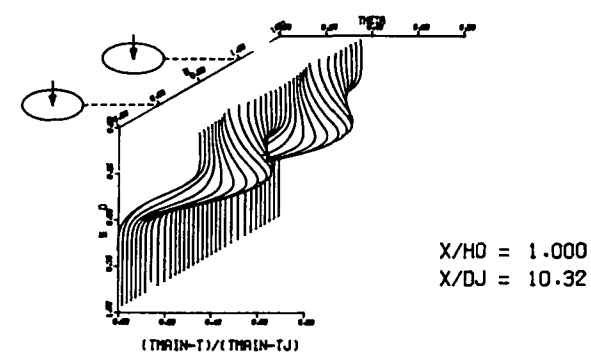
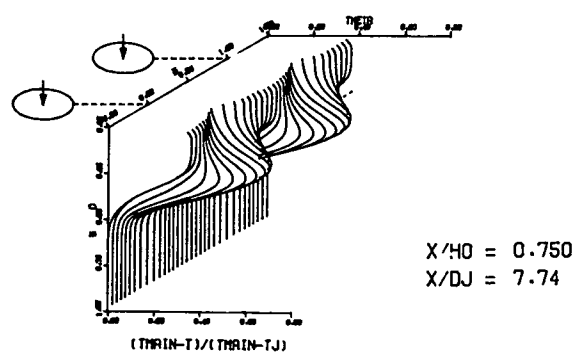
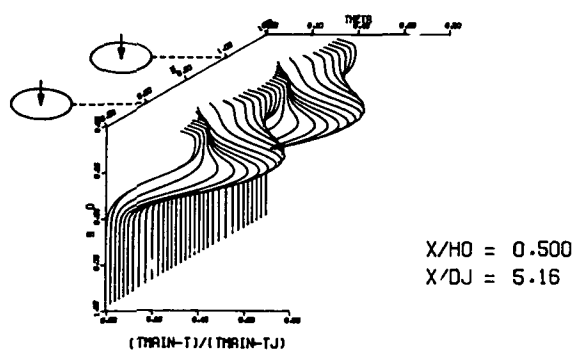
Figure 4. Total Pressure, Thermocouple, and Static Pressure Rake.

FOLDOUT FRAME

FOLDOUT FRAME



PREDICTED THETA CONTOURS FOR TEST NO.1, FINE GRID, $J=25.32$, $S/D=2.0$, $H/D=8.0$

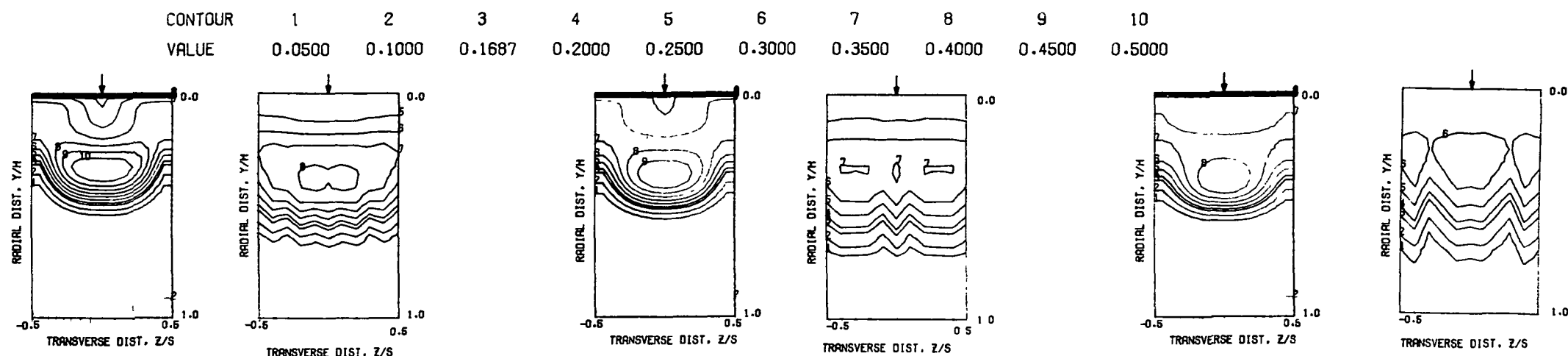


PREDICTED THETA DISTRIBUTIONS FOR TEST NO. 1, FINE GRID, $J=25.32$, $S/D=2.0$, $H/D=8.0$

Figure 5. Predicted Temperature Distributions for Test Case 1 - Table 1.

FOLDOUT FRAME

FOLDOUT FRAME



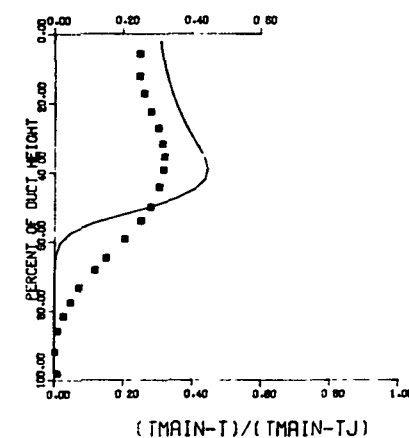
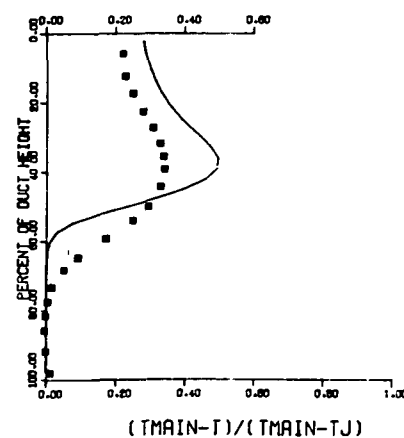
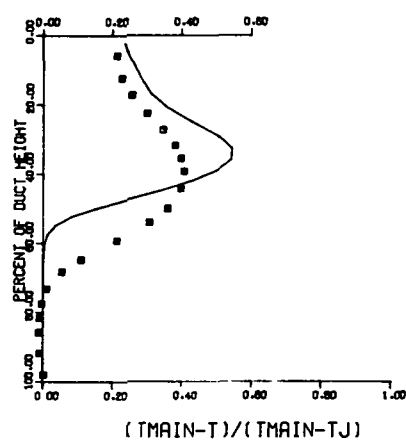
THETA CONTOURS FOR TEST NO. 1, $H=CONST$, $J=25.32$, $S/D=2.0$, $H/D=8.0$

$S/DJ = 2.58$ $HO/DJ = 10.33$ $VRATIO = 3.45$ $TRATIO = 0.475$ $DENRATIO=2.128$ $TMAIN = 648.7 \text{ K}$ $TJET = 308.3 \text{ K}$ $THEB = 0.169$

$X/H = 0.50$ $X/DJ = 5.16$

$X/H = 0.75$ $X/DJ = 7.75$

$X/H = 1.00$ $X/DJ = 10.33$



COMPARISON BETWEEN DATA AND PREDICTIONS FOR TEST NO. 1, STRAIGHT DUCT, $T_M = CONST$,

$J = 25.32$, $S/D = 2.00$, $H/D = 8.00$

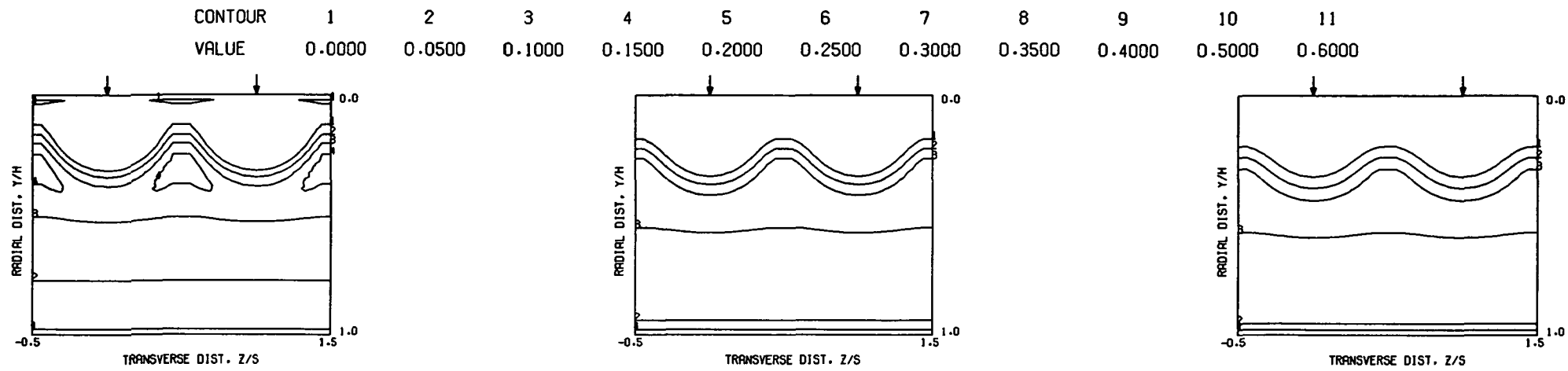
Figure 6. Comparison Between
Predicted and Measured
Temperature Distributions
for Test Case 1 - Table 1.

ORIGINAL PAGE IS
OF POOR QUALITY

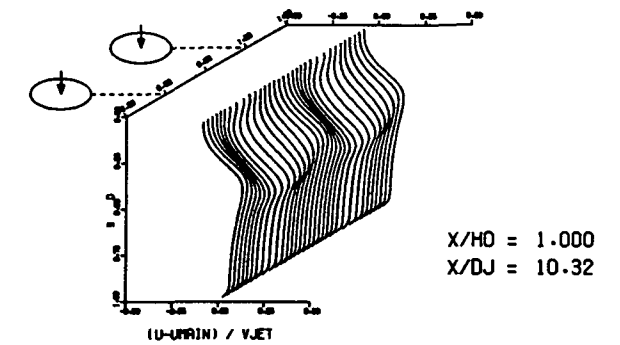
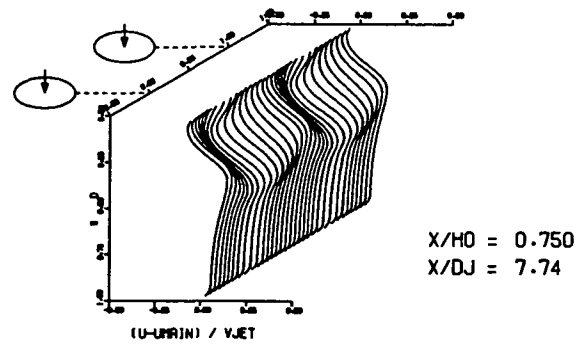
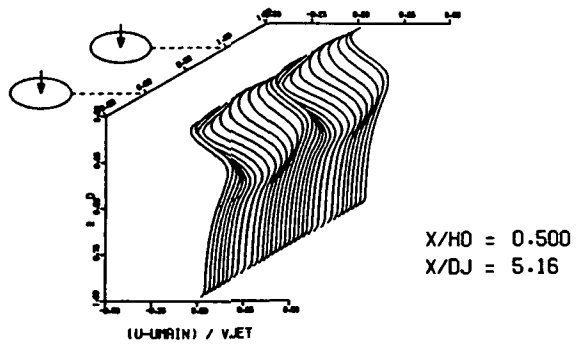
ORIGINAL PAGE IS
OF POOR QUALITY

FOLDOUT FRAME

FOLDOUT FRAME



PREDICTED VELOCITY CONTOURS FOR TEST NO. 1.35X33X17, J=22.32, S/D=2.00, H/D=8.00



PREDICTED VELOCITY DISTRIBUTIONS FOR TEST NO. 1.35X33X17, J=22.32, S/D=2.00, H/D=8.00

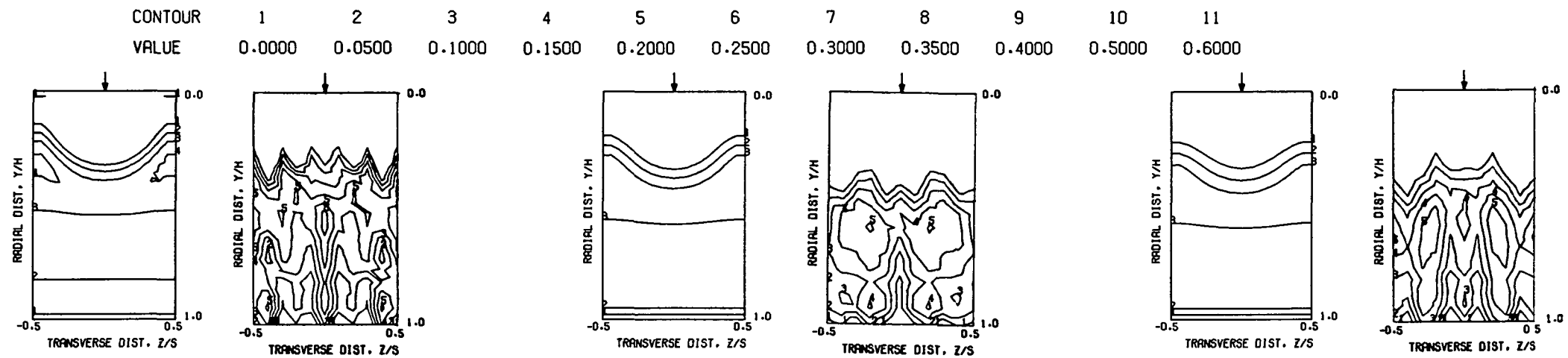
Figure 7. Predicted Velocity Distributions for Test Case 1 - Table 1.

ORIGINAL PAGE IS
OF POOR QUALITY

ORIGINAL PAGE IS
OF POOR QUALITY

FOLDOUT FRAME

FOLDOUT FRAME

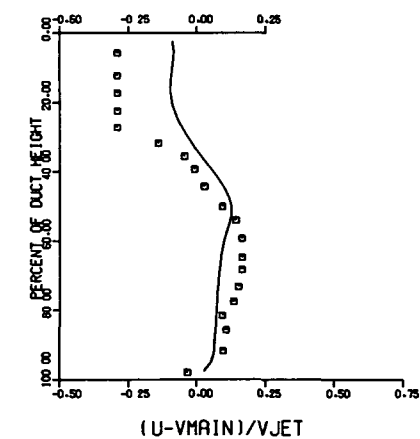
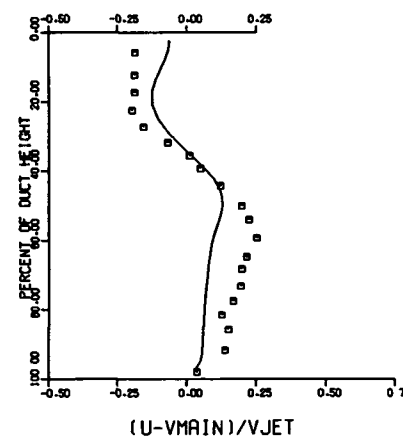
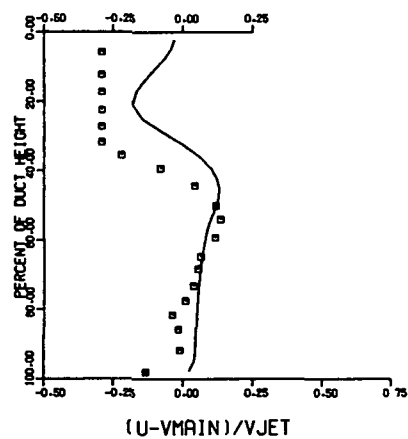


S/DJ = 2.58 HO/DJ = 10.33 VRATIO = 3.45 TRATIO = 0.475 DENRATIO=2.128 TMAIN = 360.4 K TJET = 171.3 K THEB = 0.169

X/H = 0.50 X/DJ = 5.16

X/H = 0.75 X/DJ = 7.75

X/H = 1.00 X/DJ = 10.33

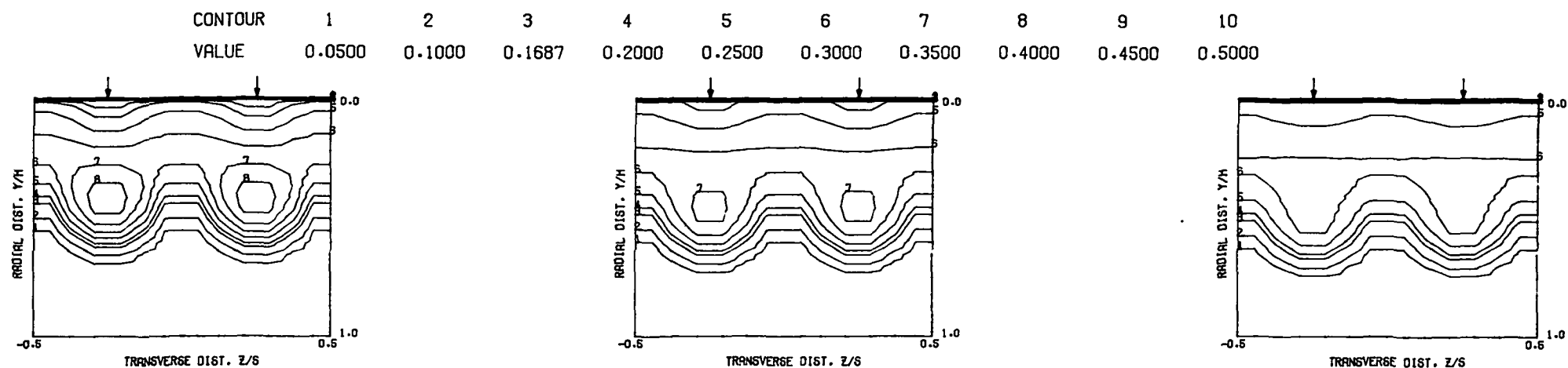


COMPARISON BETWEEN DATA AND PREDICTIONS FOR TEST 1.35X33X17, SINGLE SIDED ROW OF JETS, J = 22.32, S/D = 2.00, H/D = 8.00

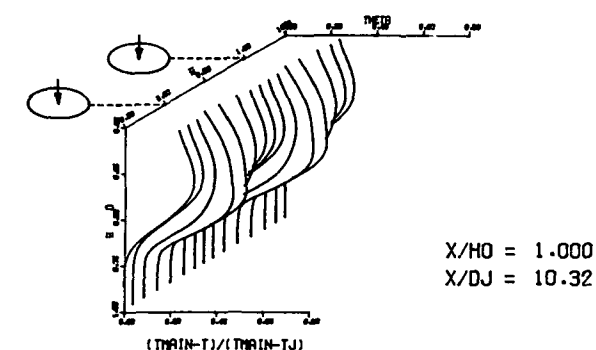
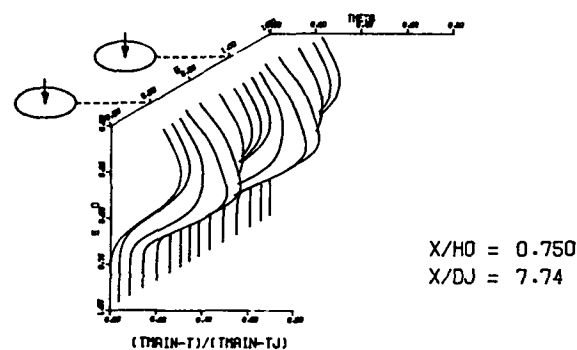
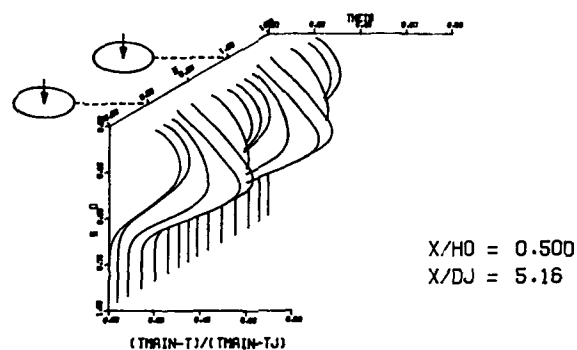
Figure 8. Comparison Between Predicted and Measured Velocity Distributions for Test Case 1 - Table 1.

FOLDOUT FRAME

2 FOLDOUT FRAME



PREDICTED THETA CONTOURS FOR TEST NO.1,4-NODE JET, $J=25.32$, $S/D=2.0$, $H/D=8.0$



PREDICTED THETA DISTRIBUTIONS FOR TEST NO. 1,4-NODE JET, $J=25.32$, $S/D=2.0$, $H/D=8.0$

Figure 9. Predicted Temperature Distributions for Test Case 2 - Table 1.

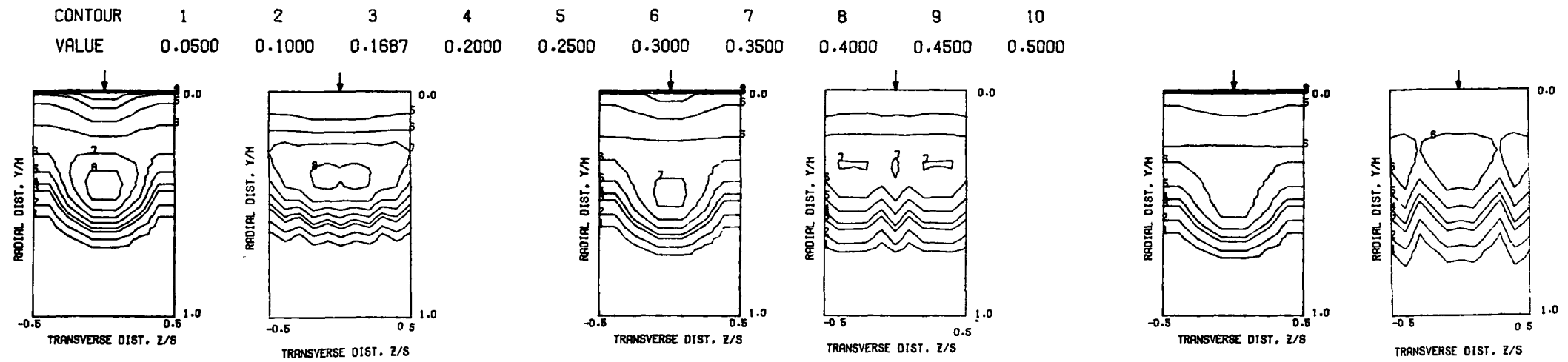
ORIGINAL PAGE IS
OF POOR QUALITY

ORIGINAL PAGE IS
OF POOR QUALITY

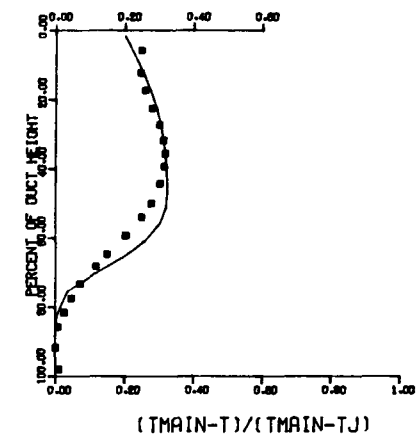
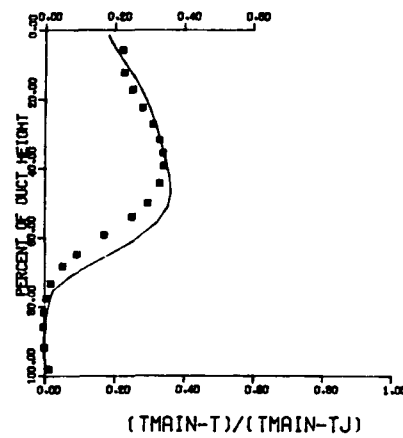
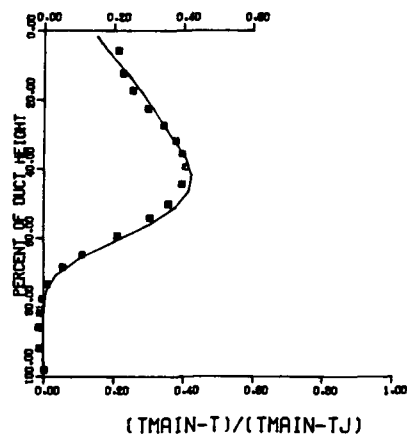
FOLDOUT FRAME

2 FOLDOUT FRAME

FOLDOUT FRAME



S/DJ = 2.58 HO/DJ = 10.33 VRATIO = 3.45 TRATIO = 0.475 DENRATIO=2.128 TMAIN = 648.7 K TJET = 308.3 K THEB = 0.169
X/H = 0.50 X/DJ = 5.16 X/H = 0.75 X/DJ = 7.75 X/H = 1.00 X/DJ = 10.33



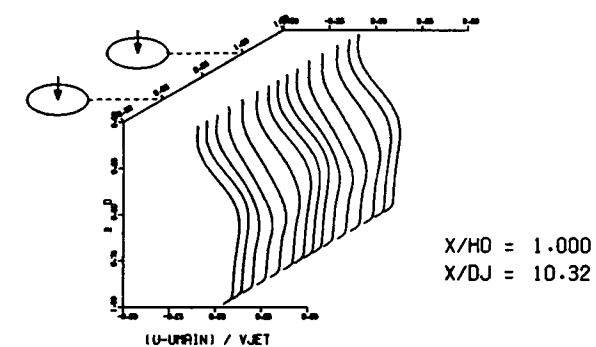
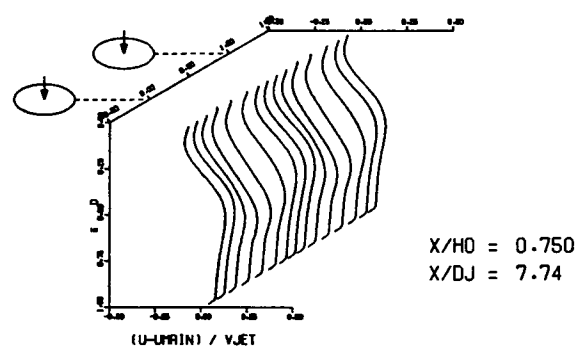
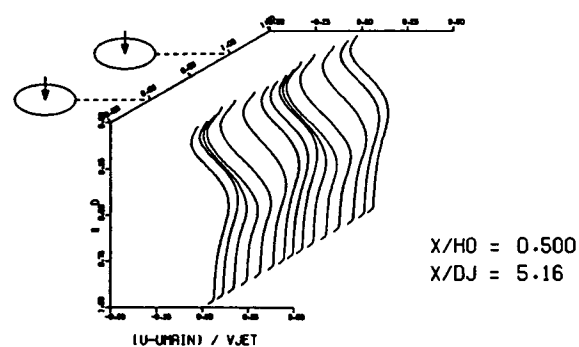
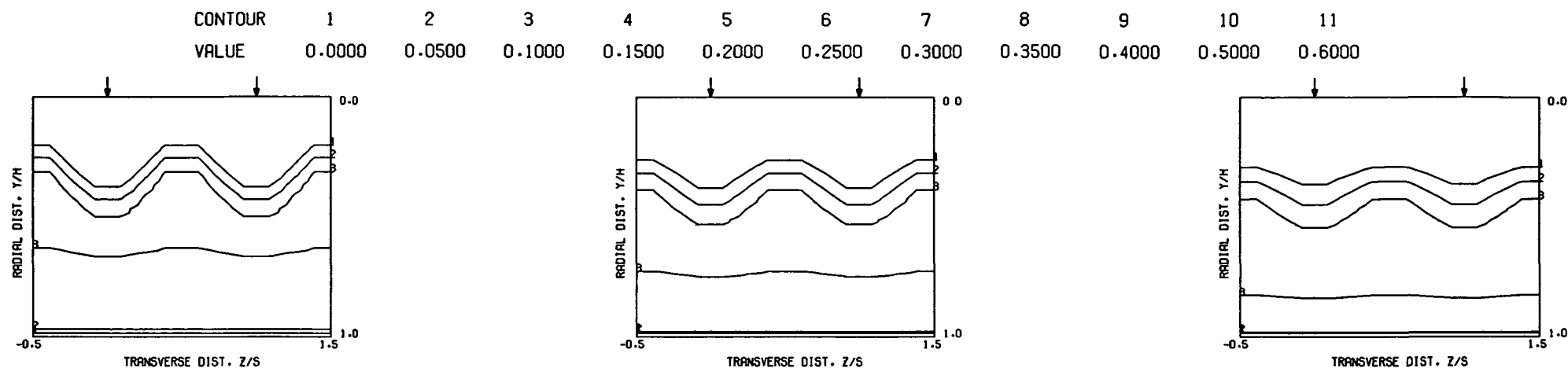
COMPARISON BETWEEN DATA AND PREDICTIONS FOR TEST NO. 1, STRAIGHT DUCT, 4-NODE JET,

J = 25.32 , S/D = 2.00 , H/D = 8.00

Figure 10. Comparison Between Predicted and Measured Temperature Distributions for Test Case 2 - Table 1.

ORIGINAL PAGE IS
OF POOR QUALITY

2 FOLDOUT FRAME



PREDICTED VELOCITY DISTRIBUTIONS FOR TEST NO. 2, 27X26X8, J=22.32, S/D=2.00, H/D=8.00

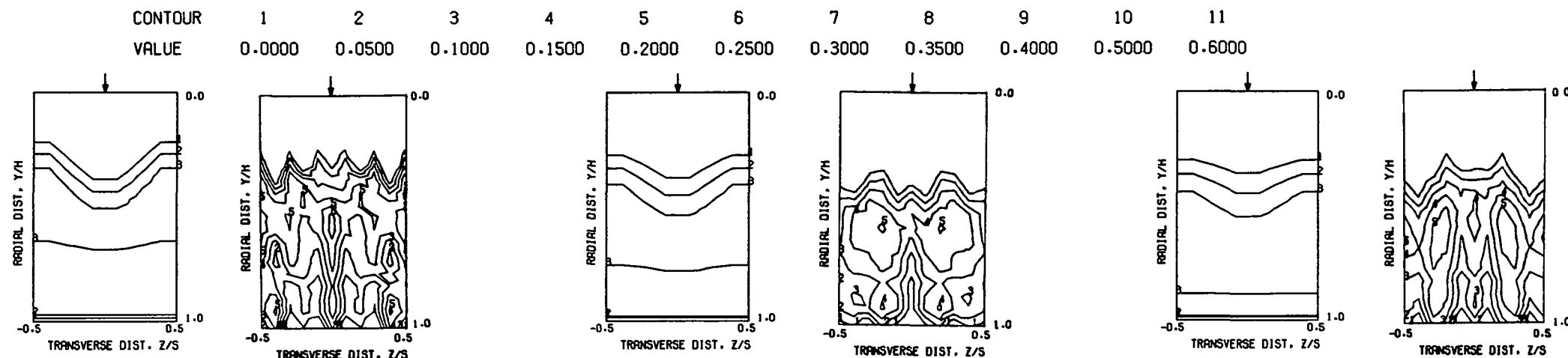
Figure 11. Predicted Velocity
Distributions for Test Case 2 -
Table 1.

FOLDOUT FRAME

ORIGINAL PAGE IS
OF POOR QUALITY

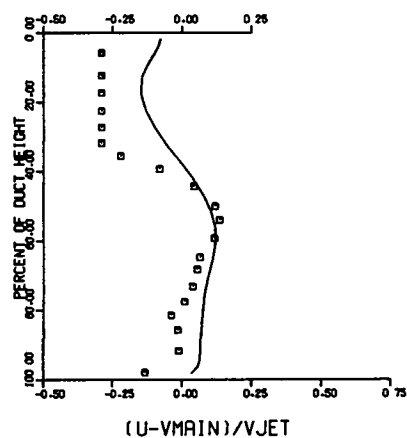
FOLDOUT FRAME

ORIGINAL PAGE IS
OF POOR QUALITY

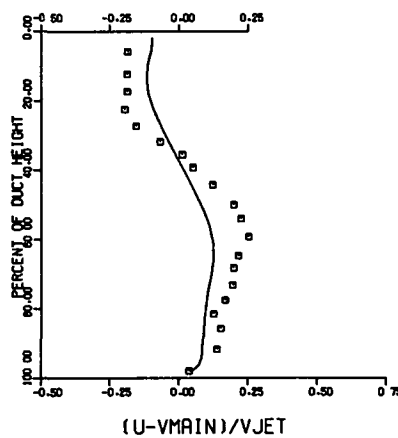


S/DJ = 2.58 H/DJ = 10.33 VRATIO = 3.45 TRATIO = 0.475 DENRATIO=2.128 TMAIN = 360.4 K TJET = 171.3 K THEB = 0.169

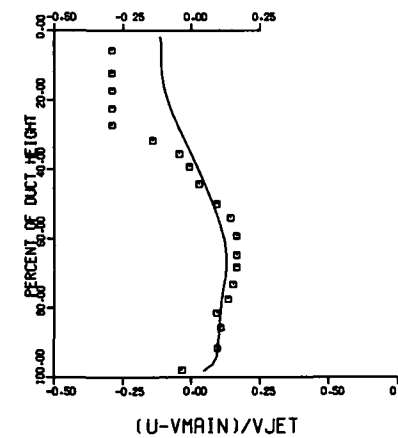
X/H = 0.50 X/DJ = 5.16



X/H = 0.75 X/DJ = 7.75



X/H = 1.00 X/DJ = 10.33



COMPARISON BETWEEN DATA AND PREDICTIONS FOR TEST 2, 27X26X8, SINGLE SIDED ROW OF JETS, J = 22.32, S/D = 2.00, H/D = 8.00

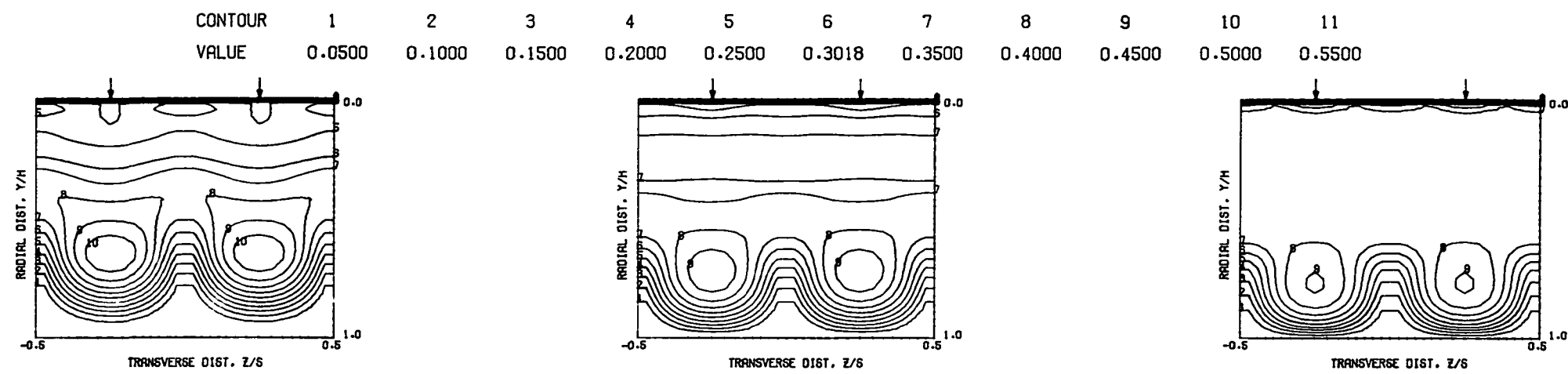
Figure 12. Comparison Between Predicted and Measured Velocity Distributions for Test Case 2 - Table 1.

ORIGINAL PAGE IS
OF POOR QUALITY

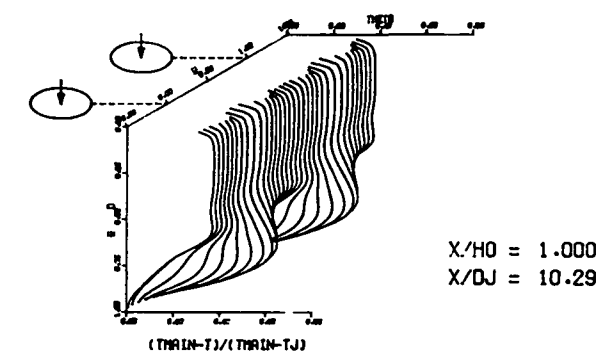
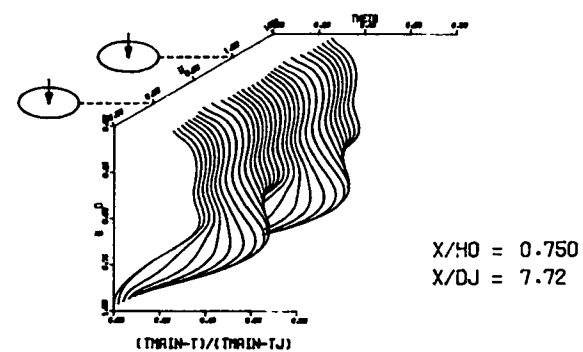
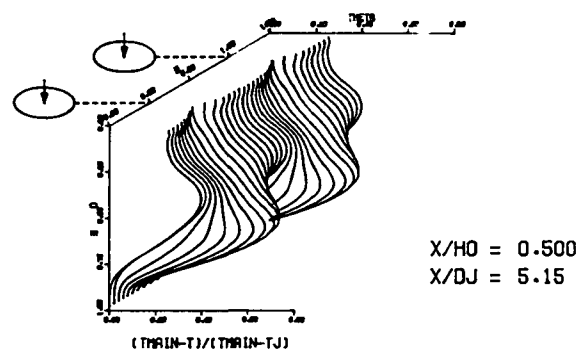
FOLDOUT FRAME

1 FOLDOUT FRAME

2 FOLDOUT FRAME

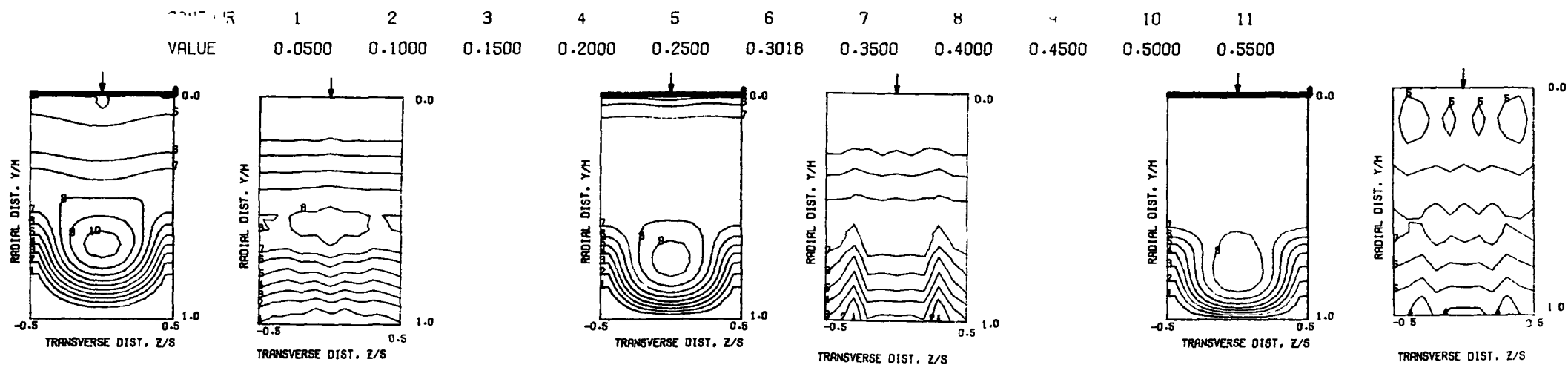


PREDICTED THETA CONTOURS FOR TEST NO.6, FINE GRID, $J=107.8$, $S/D=2.0$, $H/D=8.0$



PREDICTED THETA DISTRIBUTIONS FOR TEST NO. 6, FINE GRID, $J=107.8$, $S/D=2.0$, $H/D=8.0$

Figure 13. Predicted Temperature Distributions for Test Case 3 - Table 1.

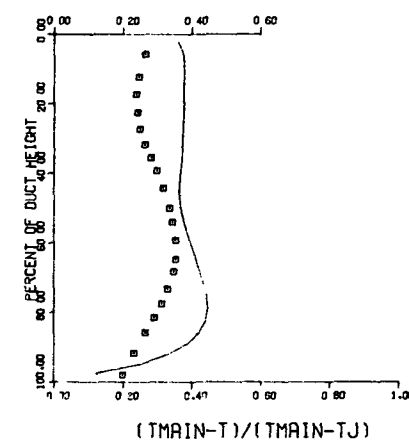
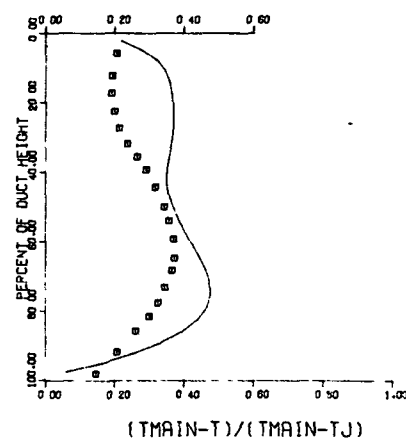
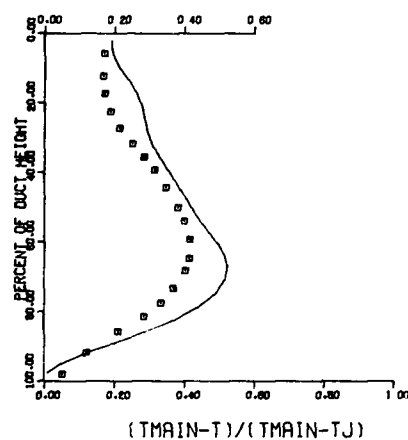


$S/DJ = 2.57$ $HO/DJ = 10.29$ $VRATIO = 6.86$ $TRATIO = 0.460$ $DENRATIO = 2.287$ $T_{MAIN} = 649.7 \text{ K}$ $T_{JET} = 299.2 \text{ K}$ $T_{HEB} = 0.302$

$X/H = 0.50$ $X/DJ = 5.14$

$X/H = 0.75$ $X/DJ = 7.71$

$X/H = 1.00$ $X/DJ = 10.29$



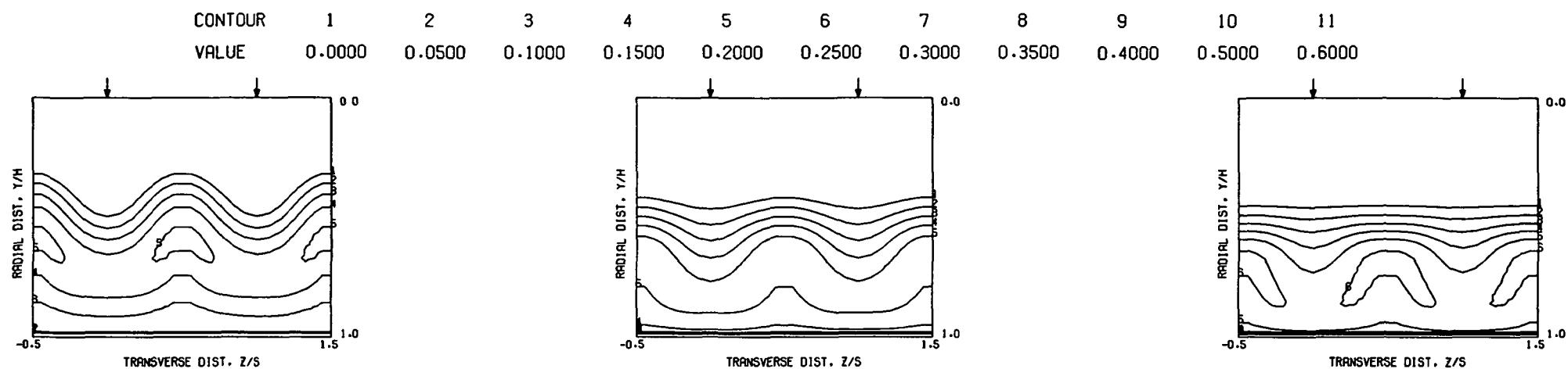
COMPARISON BETWEEN DATA AND PREDICTIONS FOR TEST NO. 6, TEST SECTION I, $T_{MAIN} = \text{CONST}$.

$J = 107.78$, $S/D = 2.00$, $H/D = 8.00$

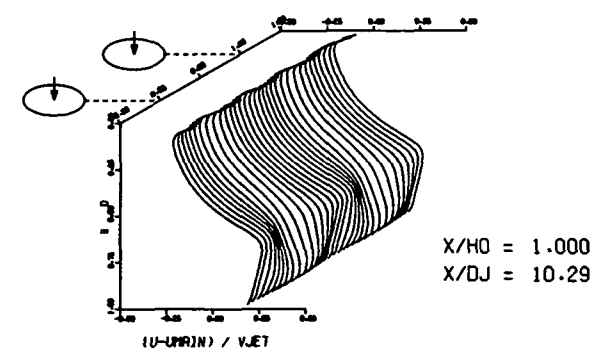
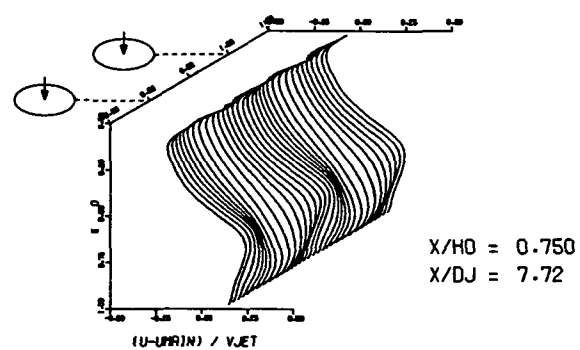
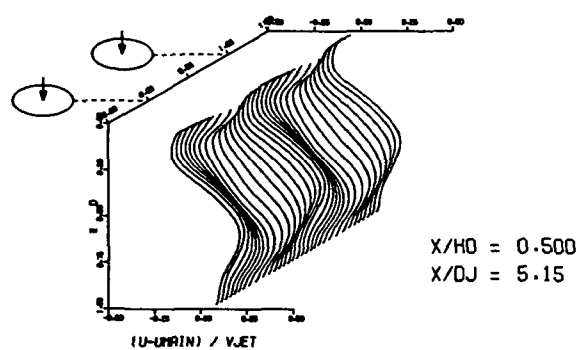
Figure 14. Comparison Between Predicted and Measured Temperature Distributions for Test Case 3 - Table 1.

FOLDOUT FRAME

FOLDOUT FRAME



PREDICTED VELOCITY CONTOURS FOR TEST NO. 3.35X33X17, $J=92.63$, $S/D=2.00$, $H/D=8.00$



PREDICTED VELOCITY DISTRIBUTIONS FOR TEST NO. 3.35X33X17, $J=92.63$, $S/D=2.00$, $H/D=8.00$

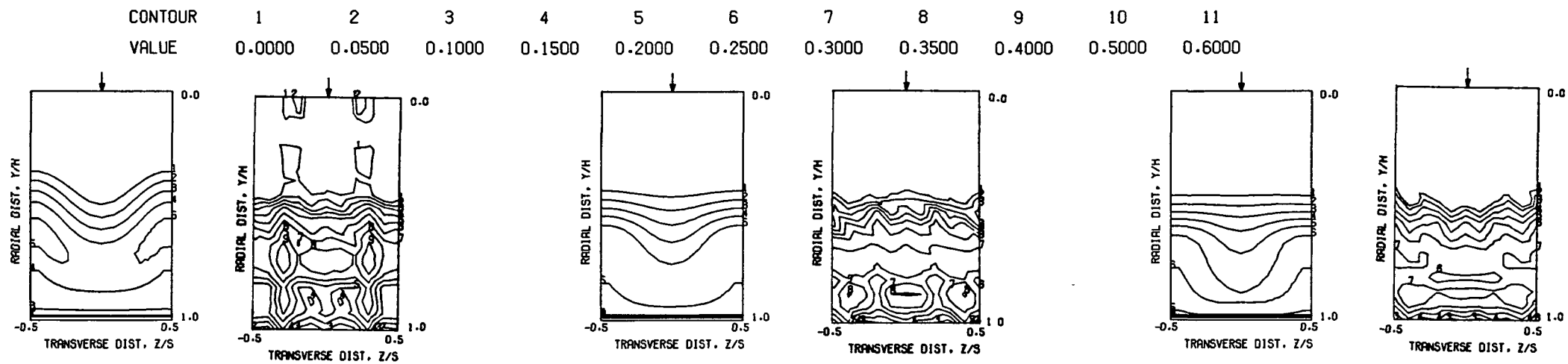
Figure 15. Predicted Velocity Distributions for Test Case 3 - Table 1.

FOLDOUT FRAME

2 FOLDOUT FRAME

ORIGINAL PAGE IS
OF POOR QUALITY

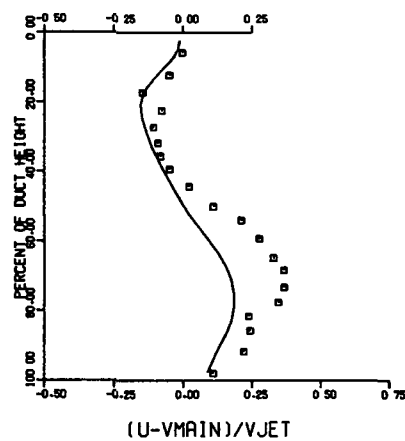
ORIGINAL PAGE IS
OF POOR QUALITY



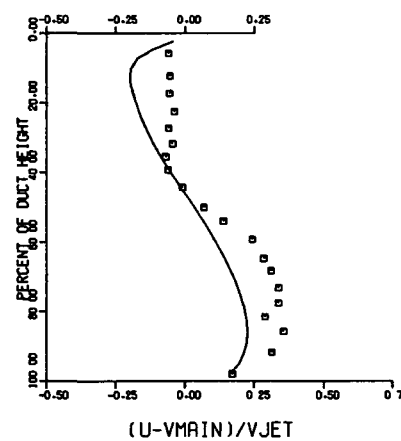
PREDICTED VELOCITY CONTOURS FOR TEST NO. 3.35X33X17, $J=92.63$, $S/D=2.00$, $H/D=8.00$

$S/DJ = 2.57$ $H/DJ = 10.29$ $VRATIO = 6.86$ $TRATIO = 0.460$ $DENRATIO=2.287$ $TMAIN = 360.9$ K $TJET = 166.2$ K $THEB = 0.302$

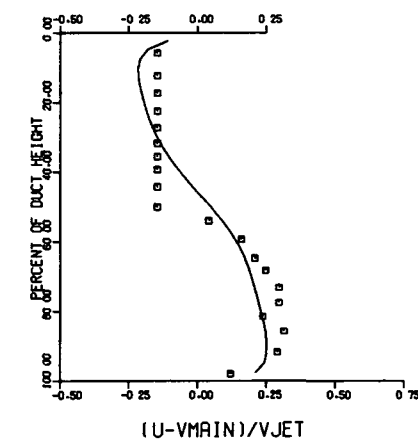
$X/H = 0.50$ $X/DJ = 5.14$



$X/H = 0.75$ $X/DJ = 7.71$



$X/H = 1.00$ $X/DJ = 10.29$



COMPARISON BETWEEN DATA AND PREDICTIONS FOR TEST 3.35X33X17, SINGLE SIDED ROW OF JETS, $J = 92.63$, $S/D = 2.00$, $H/D = 8.00$

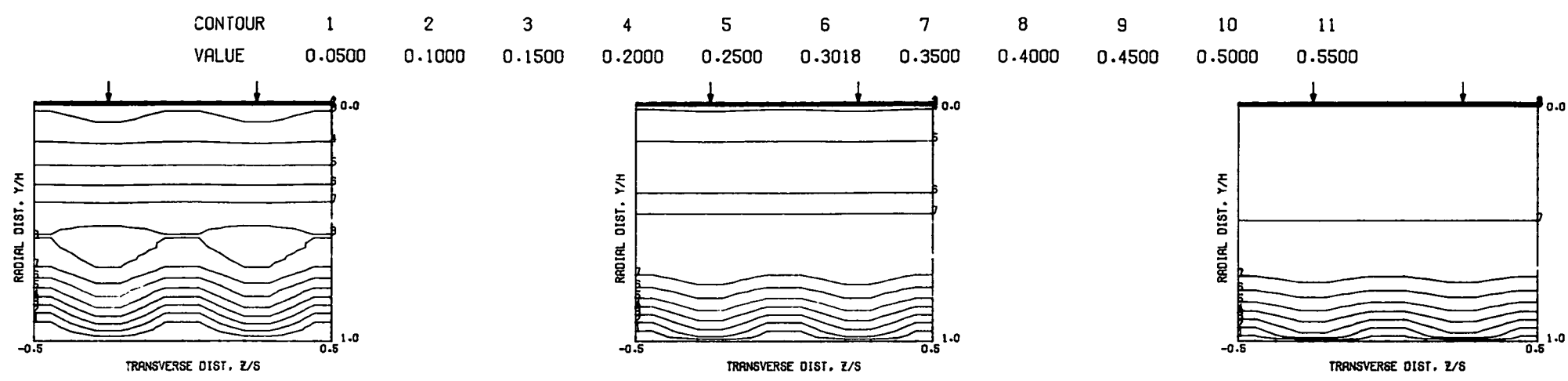
Figure 16. Comparison Between Predicted and Measured Velocity Distributions for Test Case 3 - Table 1.

FOLDOUT FRAME

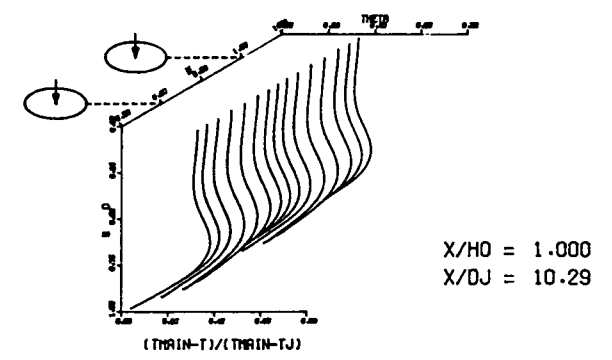
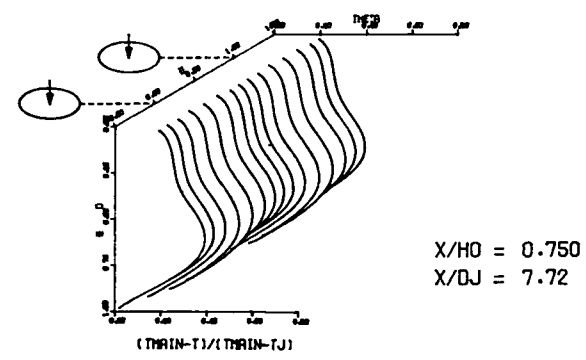
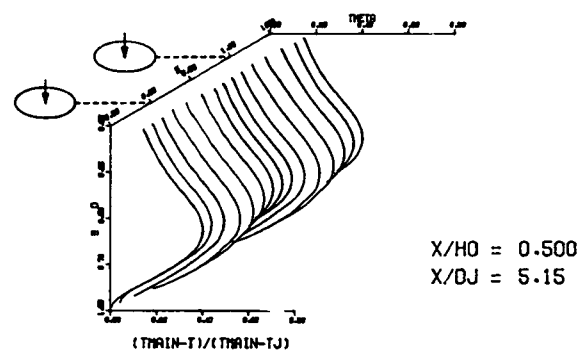
2 FOLDOUT FRAME

ORIGINAL PAGE IS
OF POOR QUALITY

ORIGINAL PAGE IS
OF POOR QUALITY



PREDICTED THETA CONTOURS FOR TEST NO. 6, 4-NODE JET, $J=107.8$, $S/D=2.0$, $H/D=8.0$

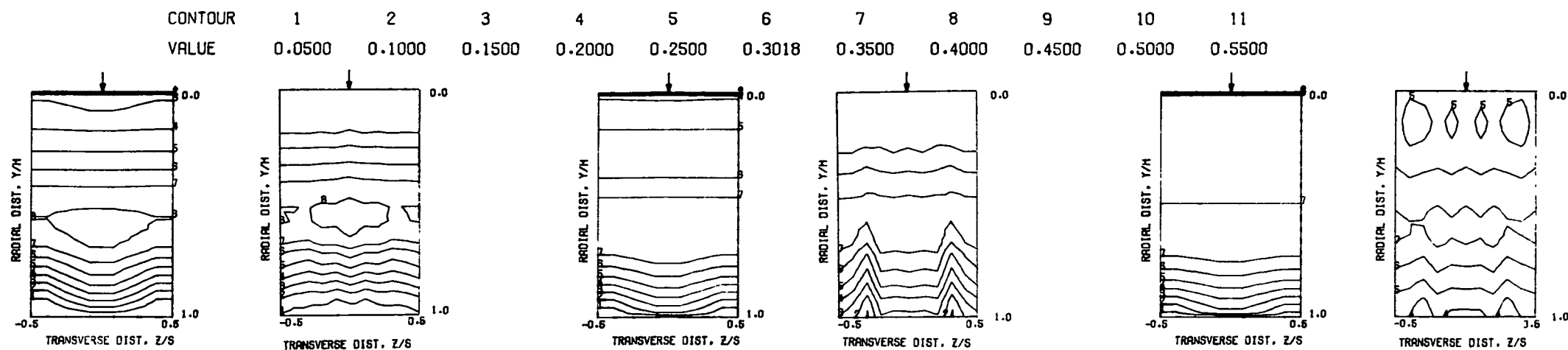


PREDICTED THETA DISTRIBUTIONS FOR TEST NO. 6, 4-NODE JET, $J=107.8$, $S/D=2.0$, $H/D=8.0$

Figure 17. Predicted Temperature
Distributions for Test Case 4 -
Table 1.

2 FOLDOUT FRAME

FOLDOUT FRAME

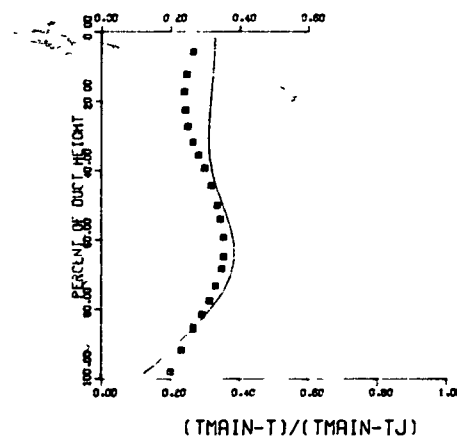
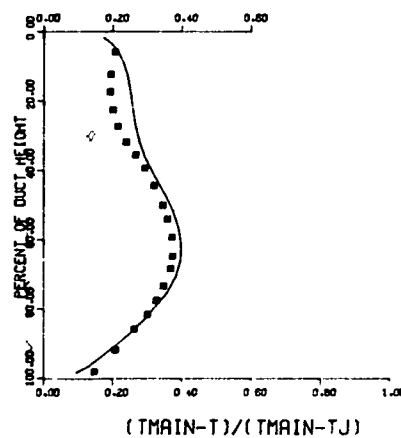
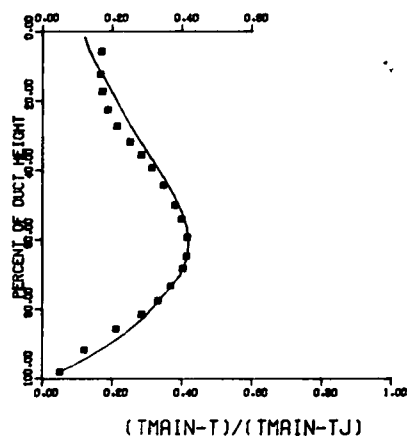


$S/DJ = 2.57$ $H/DJ = 10.29$ $VRATIO = 6.86$ $TRATIO = 0.460$ $DENRATIO = 2.287$ $TMAIN = 649.7$ K $TJET = 299.2$ K $THEB = 0.302$

$X/H = 0.50$ $X/DJ = 5.14$

$X/H = 0.75$ $X/DJ = 7.71$

$X/H = 1.00$ $X/DJ = 10.29$



COMPARISON BETWEEN DATA AND PREDICTIONS FOR TEST NO. 6, STRAIGHT DUCT, 4-NODE JET, $J = 107.78$, $S/D = 2.00$, $H/D = 8.00$

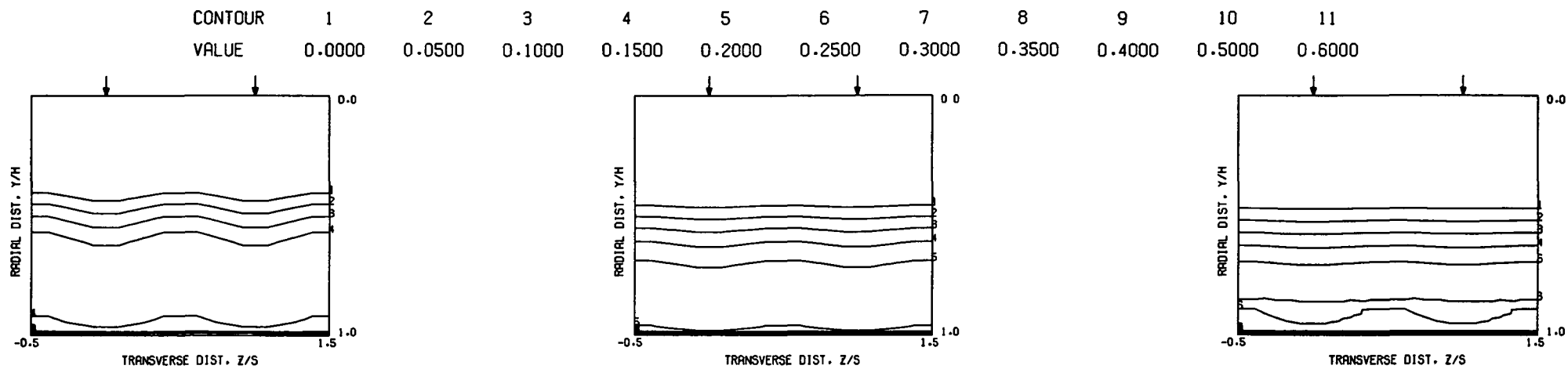
Figure 18. Comparison Between Predicted and Measured Temperature Distributions for Test Case 4 - Table 1.

FOLDOUT FRAME

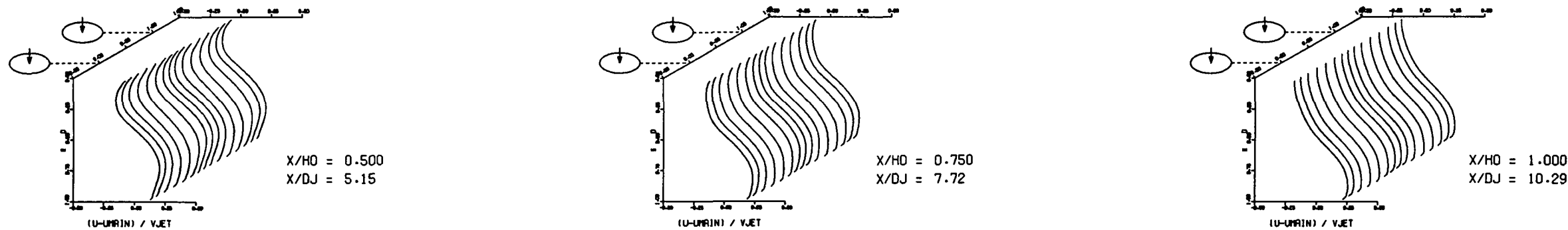
FOLDOUT FRAME

ORIGINAL PAGE IS
OF POOR QUALITY

ORIGINAL PAGE IS
OF POOR QUALITY



PREDICTED VELOCITY CONTOURS FOR TEST NO. 4, 27X26X8, J=92.63, S/D=2.00, H/D=8.00



PREDICTED VELOCITY DISTRIBUTIONS FOR TEST NO. 4, 27X26X8, J=92.63, S/D=2.00, H/D=8.00

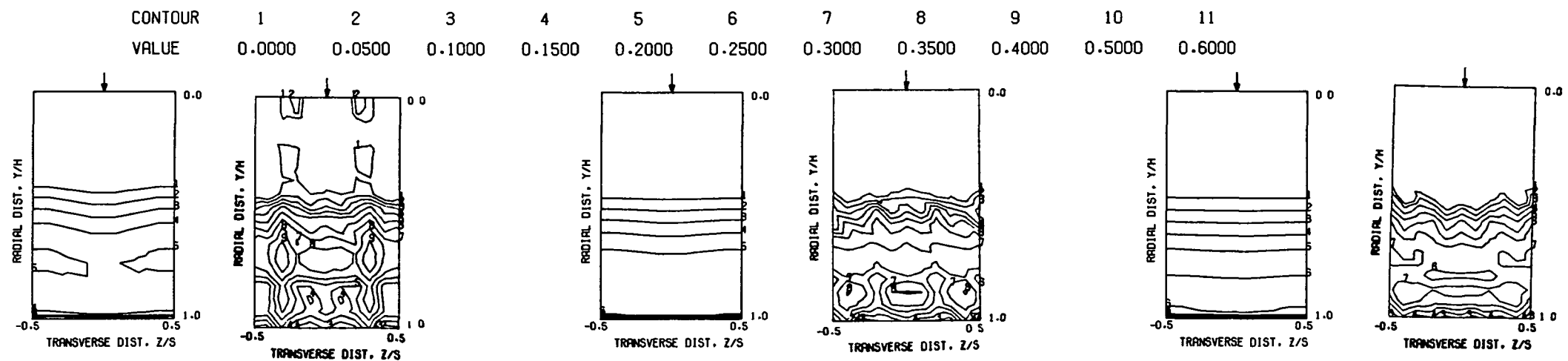
Figure 19. Predicted Velocity
Distributions for Test Case 4 -
Table 1.

FOLDOUT FRAME

2 FOLDOUT FRAME

ORIGINAL PAGE IS
OF POOR QUALITY

ORIGINAL PAGE IS
OF POOR QUALITY

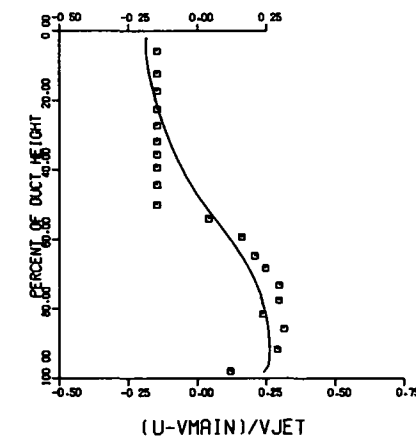
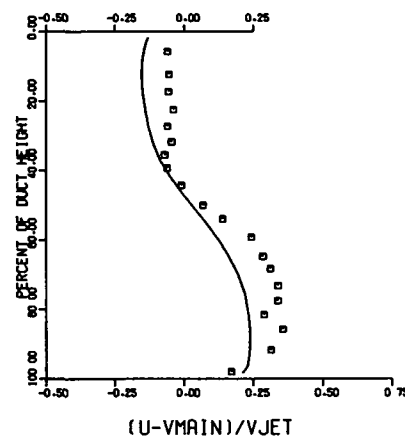
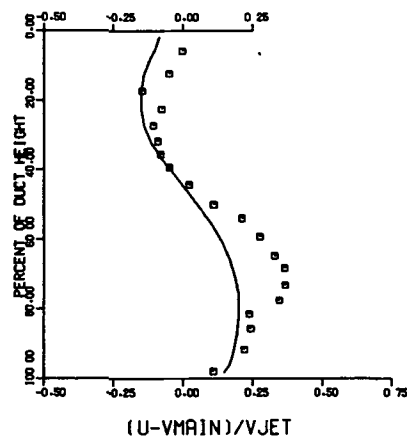


S/DJ = 2.57 HO/DJ = 10.29 VRATIO = 6.86 TRATIO = 0.460 DENRATIO=2.287 TMAIN = 360.9 K TJET = 166.2 K THEB = 0.302

X/H = 0.50 X/DJ = 5.14

X/H = 0.75 X/DJ = 7.71

X/H = 1.00 X/DJ = 10.29

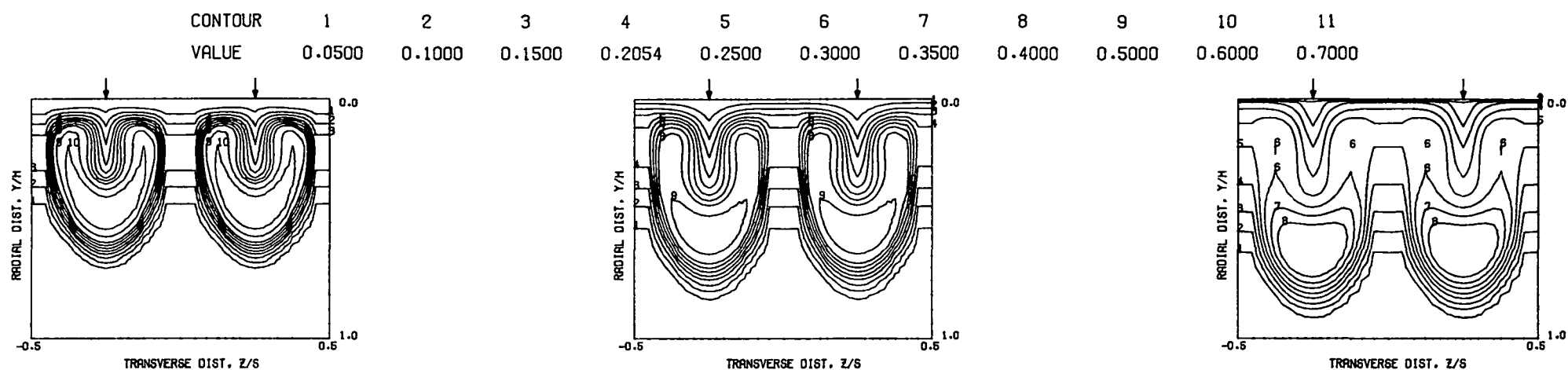


COMPARISON BETWEEN DATA AND PREDICTIONS FOR TEST 4, 27X26X8, SINGLE SIDED ROW OF JETS, J = 92.63, S/D = 2.00, H/D = 8.00

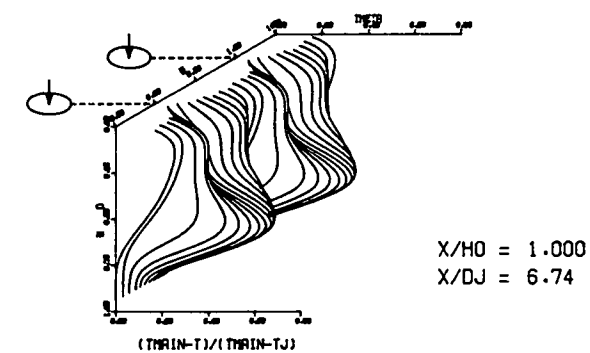
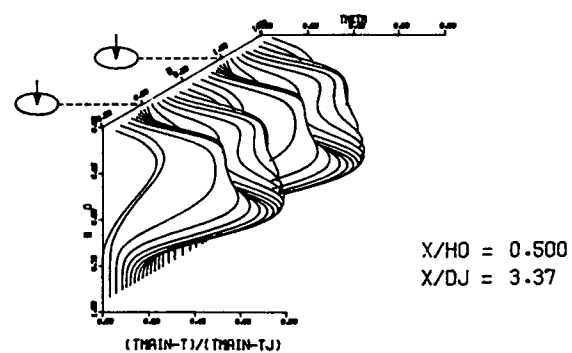
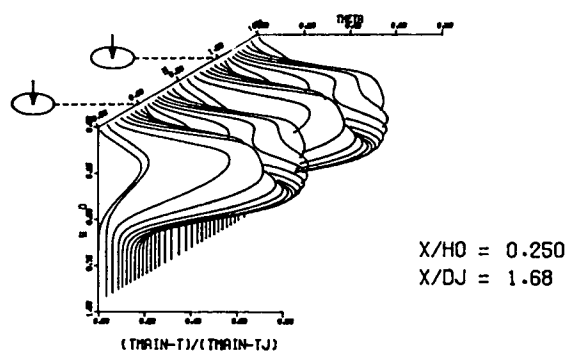
Figure 20. Comparison Between Predicted and Measured Velocity Distributions for Test Case 4 - Table 1.

FOLDOUT FRAME

FOLDOUT FRAME



PREDICTED THETA CONTOURS FOR TEST NO.50, $T_M=CONST$, $J=25.48$, $S/D=2.83$, $H/D=5.66$

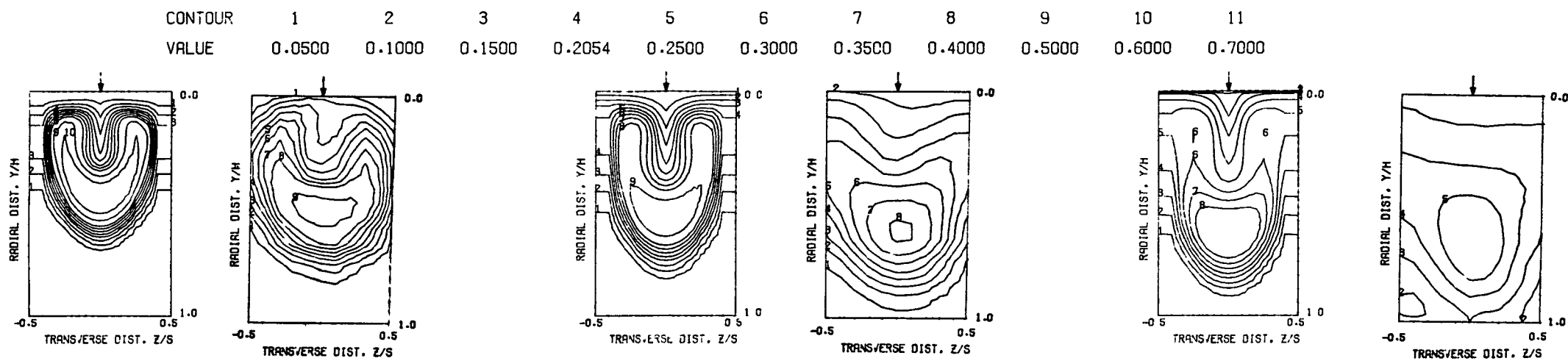


PREDICTED THETA DISTRIBUTIONS FOR TEST NO. 50, $T_M=CONST$, $J=25.48$, $S/D=2.83$, $H/D=5.66$

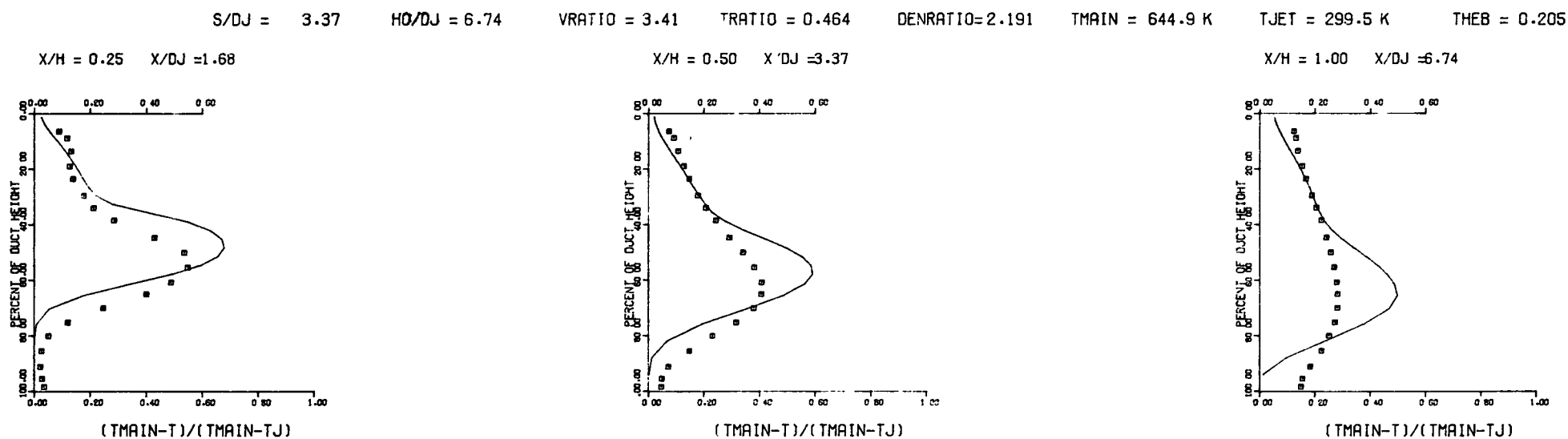
Figure 21. Predicted Temperature Distributions for Test Case 5 - Table 1.

FOLDOUT FRAME

2 FOLDOUT FRAME



THETA CONTOURS FOR TEST NO.50, $T_M = \text{CONST}$, $J = 25.48$, $S/D = 2.8$, $H/D = 5.7$



COMPARISON BETWEEN DATA AND PREDICTIONS FOR TEST NO. 50, TEST SECTION I, $T_M = \text{CONST}$

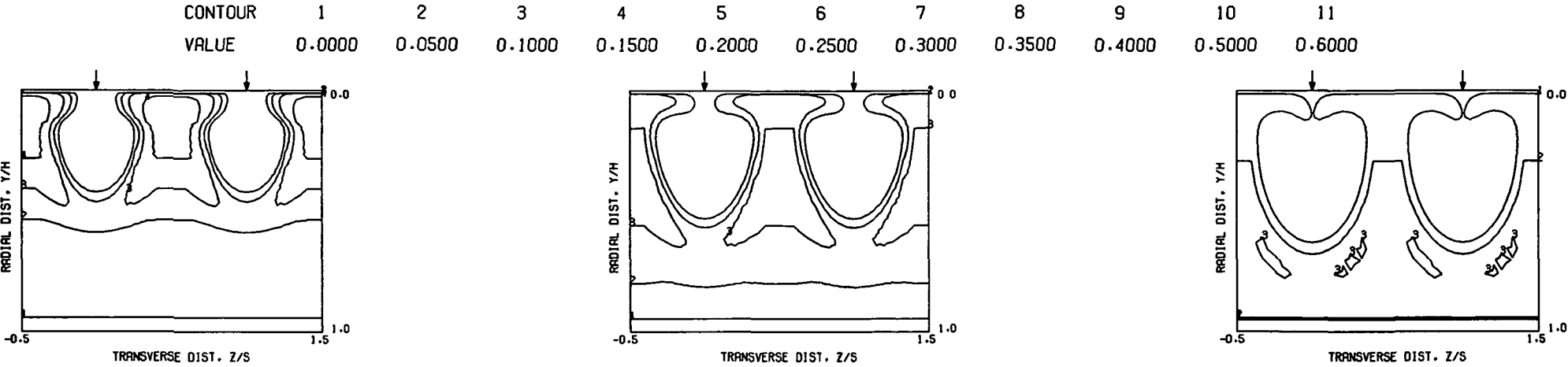
$J = 25.48$, $S/D = 2.83$, $H/D = 5.66$

Figure 22. Comparison Between Predicted and Measured Temperature Distributions for Test Case 5 - Table 1.

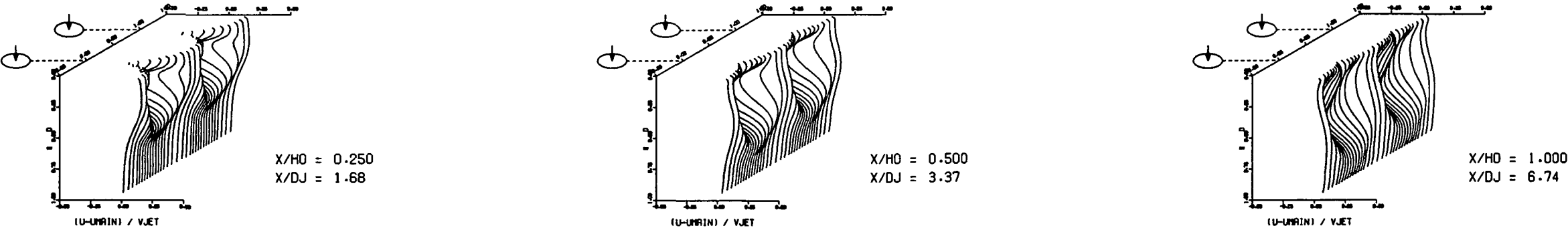
FOLDOUT FRAME

FOLDOUT FRAME

ORIGINAL PAGE IS
OF POOR QUALITY



PREDICTED VELOCITY CONTOURS FOR TEST NO. 5.35X33X17, J=25.48, S/D=2.83, H/D=5.66

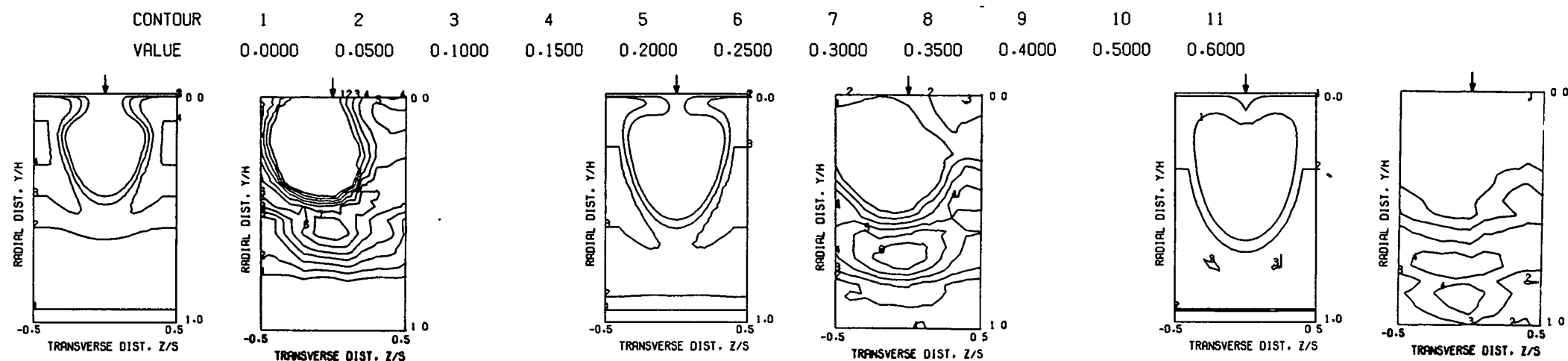


PREDICTED VELOCITY DISTRIBUTIONS FOR TEST NO. 5.35X33X17, J=25.48, S/D=2.83, H/D=5.66

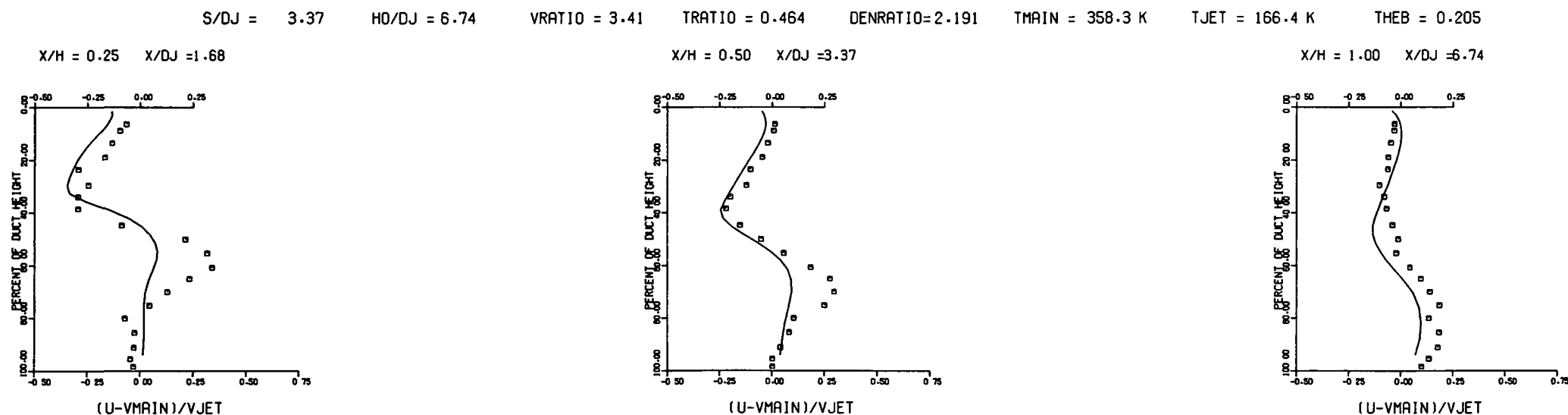
Figure 23. Predicted Velocity
Distributions for Test Case 5 -
Table 1.

FOLDOUT FRAMES

FOLDOUT FRAME



PREDICTED VELOCITY CONTOURS FOR TEST NO. 5.35X33X17, $J=25.48$, $S/D=2.83$, $H/D=5.66$

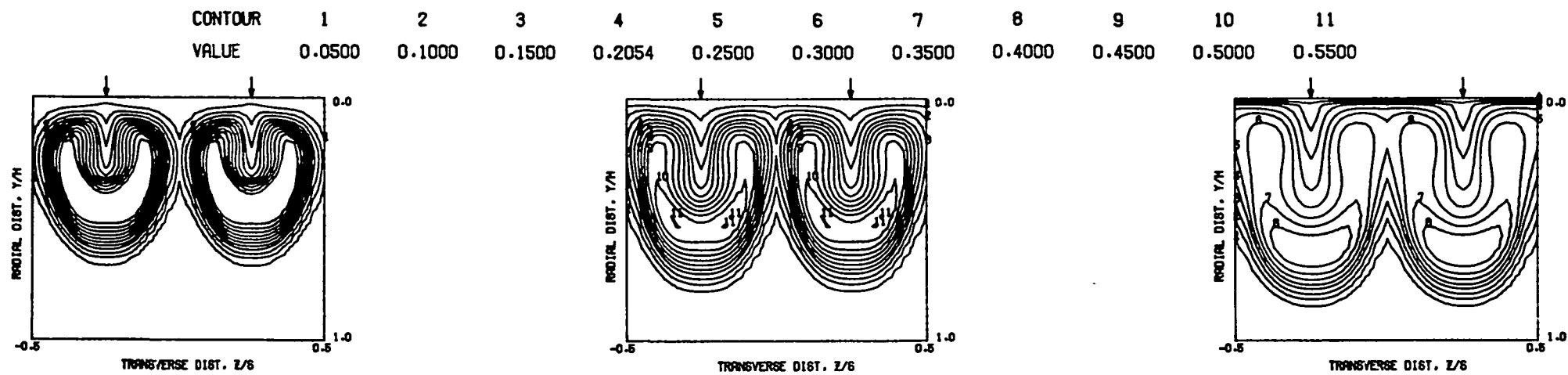


COMPARISON BETWEEN DATA AND PREDICTIONS FOR TEST 5. 35X33X17, SINGLE SIDED ROW OF JETS, $J = 25.48$, $S/D = 2.83$, $H/D = 5.66$

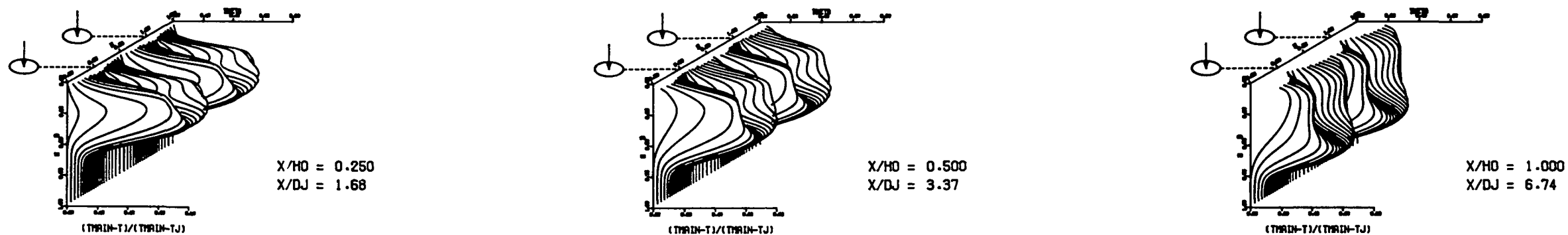
Figure 24. Comparison Between Predicted and Measured Velocity Distributions for Test Case 5 - Table 1.

FOLDOUT FRAME

FOLDOUT FRAME



PREDICTED THETA CONTOURS FOR TEST NO.50, $T_M=CONST$, $J=25.48$, $S/D=2.83$, $H/D=5.66$

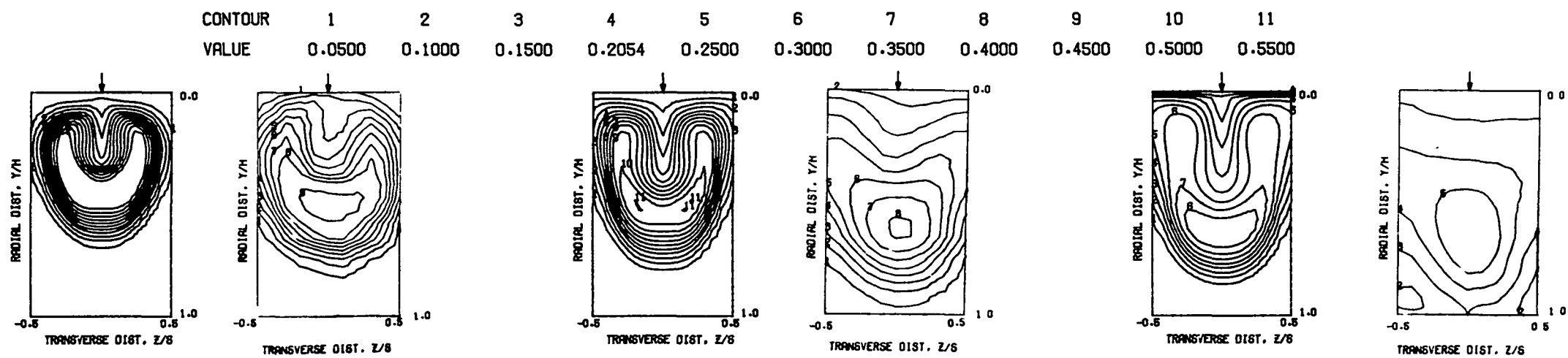


PREDICTED THETA DISTRIBUTIONS FOR TEST NO. 50, $T_M=CONST$, $J=25.48$, $S/D=2.83$, $H/D=5.66$

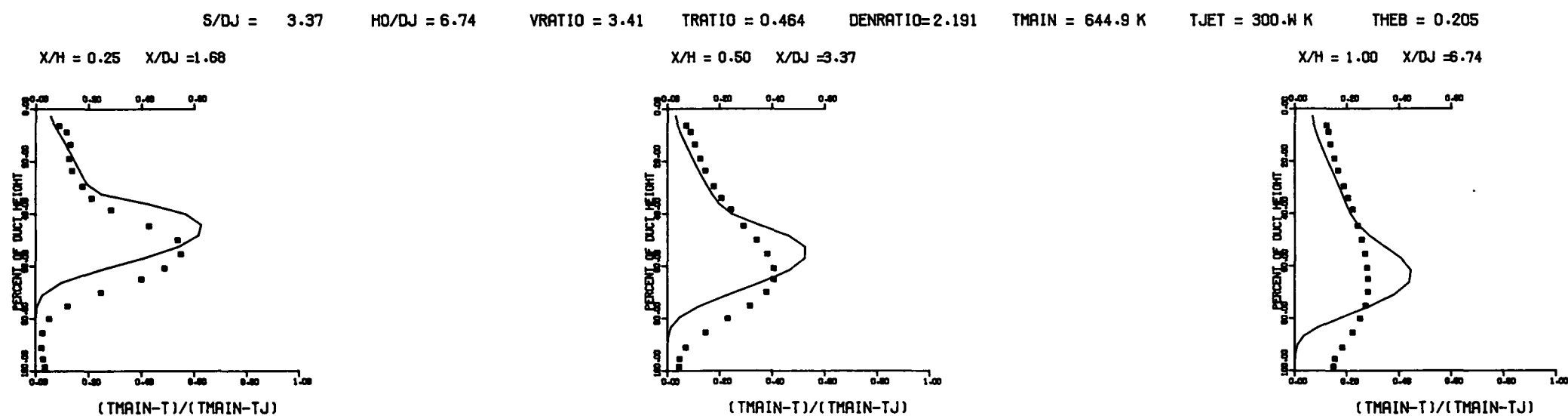
Figure 25. Predicted Temperature Distributions for Test Case 6 - Table 1.

FOLDOUT FRAME

2 FOLDOUT FRAME



THETA CONTOURS FOR TEST NO.50, $T_M = \text{CONST}$, $J = 25.48$, $S/D = 2.83$, $H/D = 5.66$



COMPARISON BETWEEN DATA AND PREDICTIONS FOR TEST 50, $T_M = \text{CONST}$, TEST SECTION I, $J = 25.48$, $S/D = 2.83$, $H/D = 5.66$

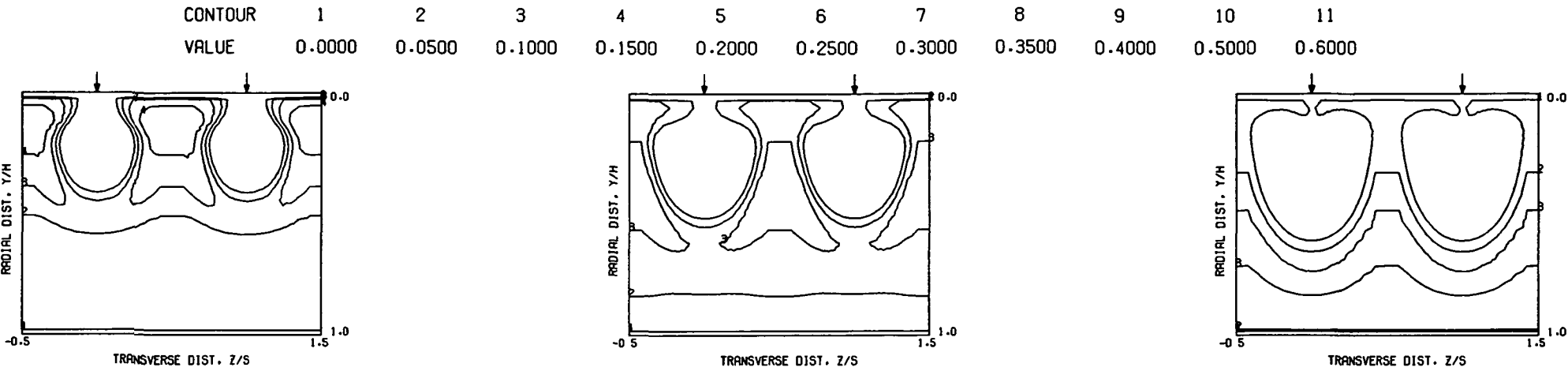
Figure 26. Comparison Between Predicted and Measured Temperature Distributions for Test Case 6 - Table 1.

FOLDOUT FRAME

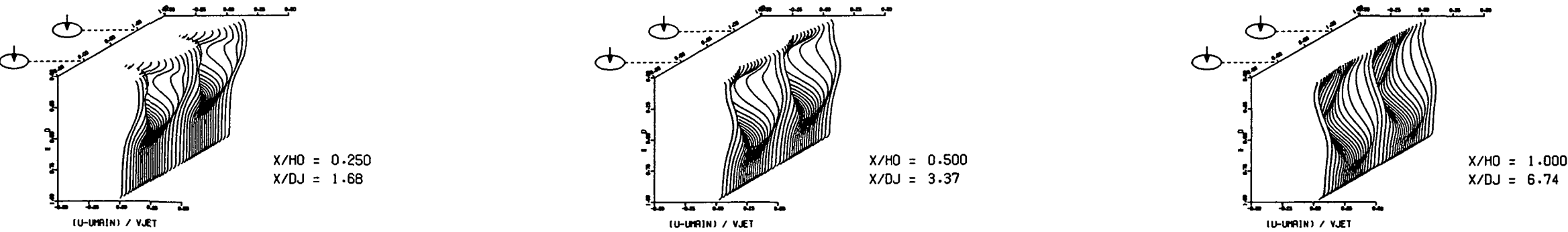
FOLDOUT FRAME

ORIGINAL PAGE IS
OF POOR QUALITY

ORIGINAL PAGE IS
OF POOR QUALITY



PREDICTED VELOCITY CONTOURS FOR TEST NO. 6.32X29X21, J=25.48, S/D=2.83, H/D=5.66

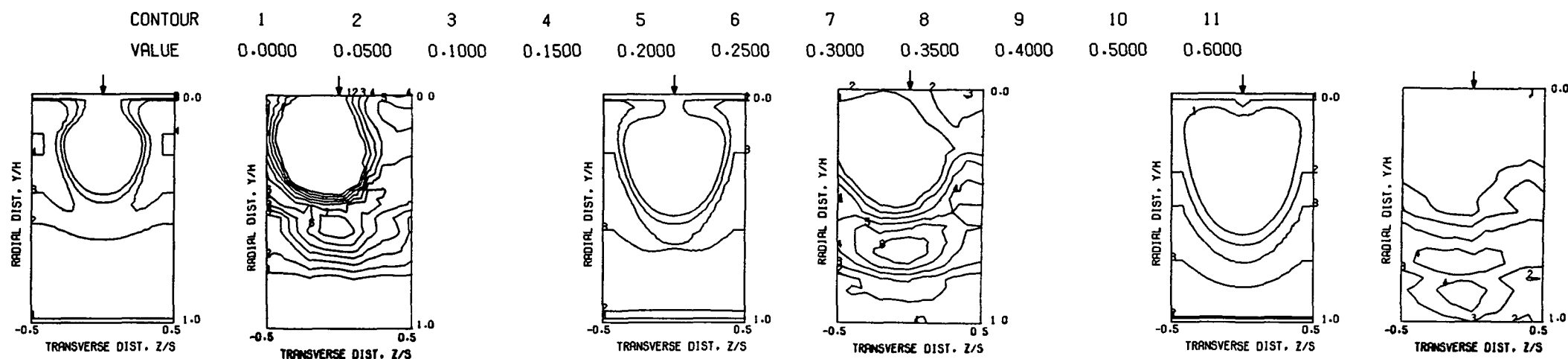


PREDICTED VELOCITY DISTRIBUTIONS FOR TEST NO. 6.32X29X21, J=25.48, S/D=2.83, H/D=5.66

Figure 27. Predicted Velocity
Distributions for Test Case 6 - Table 1.

FOLDOUT FRAME

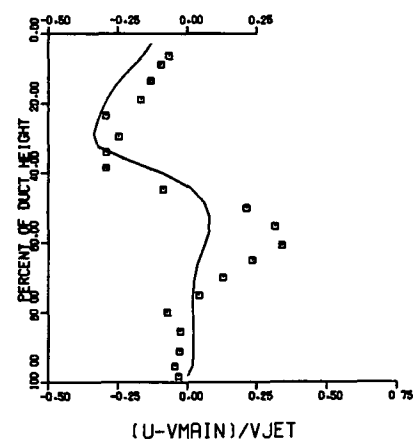
FOLDOUT FRAME



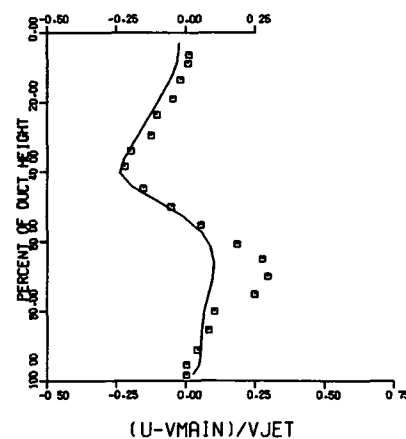
PREDICTED VELOCITY CONTOURS FOR TEST NO. 6, 32X29X21, J=25.48, S/D=2.83, H/D=5.66

S/DJ = 3.37 HO/DJ = 6.74 VRATIO = 3.41 TRATIO = 0.464 DENRATIO=2.191 TMAIN = 358.3 K TJET = 166.4 K THEB = 0.205

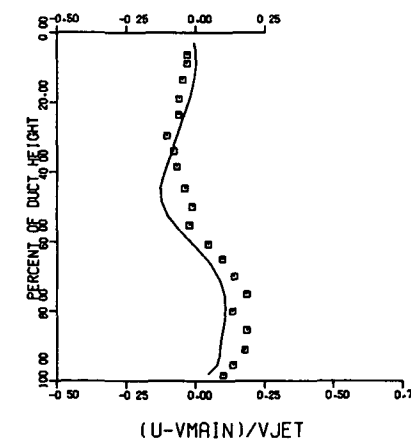
X/H = 0.25 X/DJ = 1.68



X/H = 0.50 X/DJ = 3.37



X/H = 1.00 X/DJ = 6.74

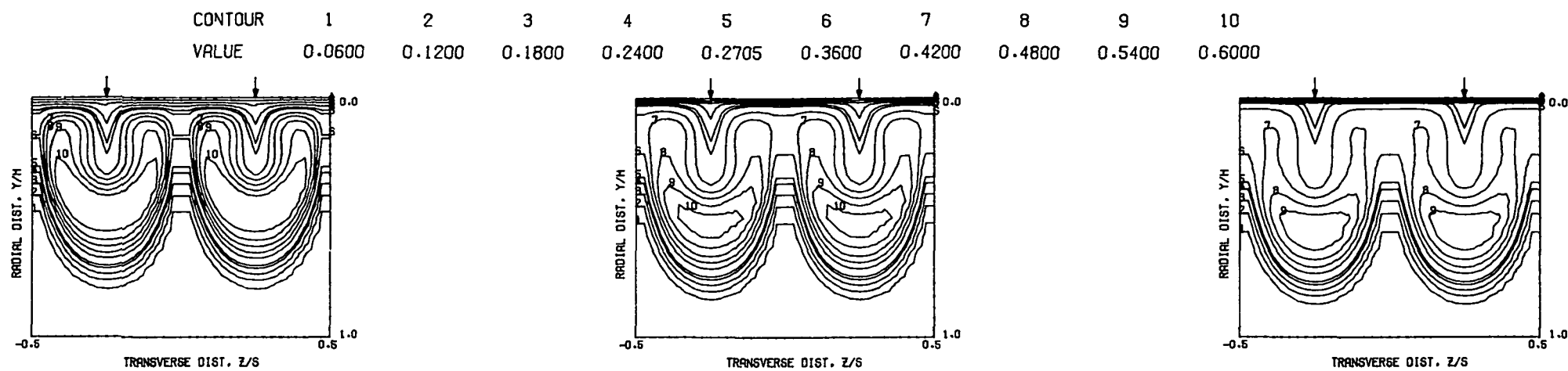


COMPARISON BETWEEN DATA AND PREDICTIONS FOR TEST 6, 32X29X21, SINGLE SIDED ROW OF JETS, J = 25.48 , S/D =2.83 , H/D =5.66

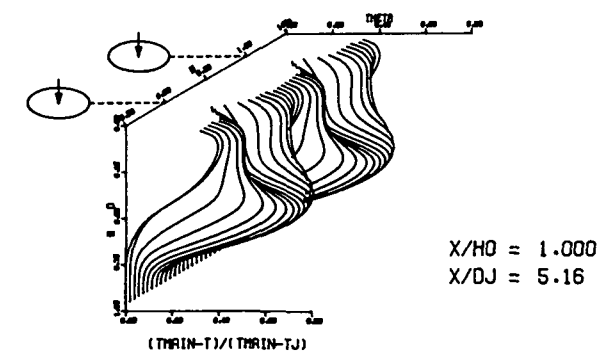
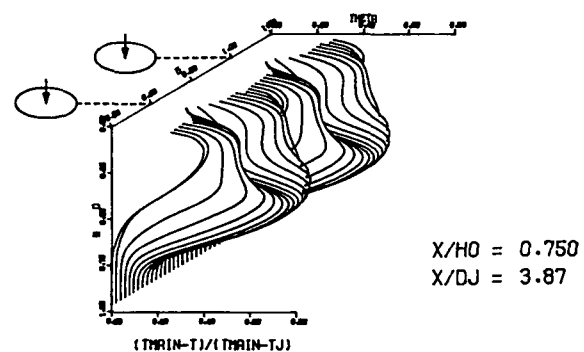
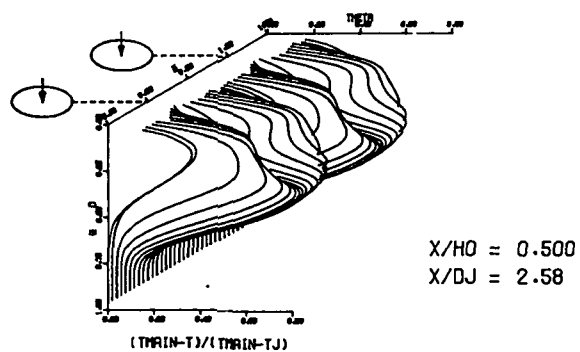
Figure 28. Comparison Between Predicted and Measured Velocity Distributions for Test Case 6 - Table 1.

FOLDOUT FRAME

FOLDOUT FRAME



PREDICTED THETA CONTOURS FOR TEST NO.2, FINE GRID, $J=21.59$, $S/D=2.0$, $H/D=4.0$

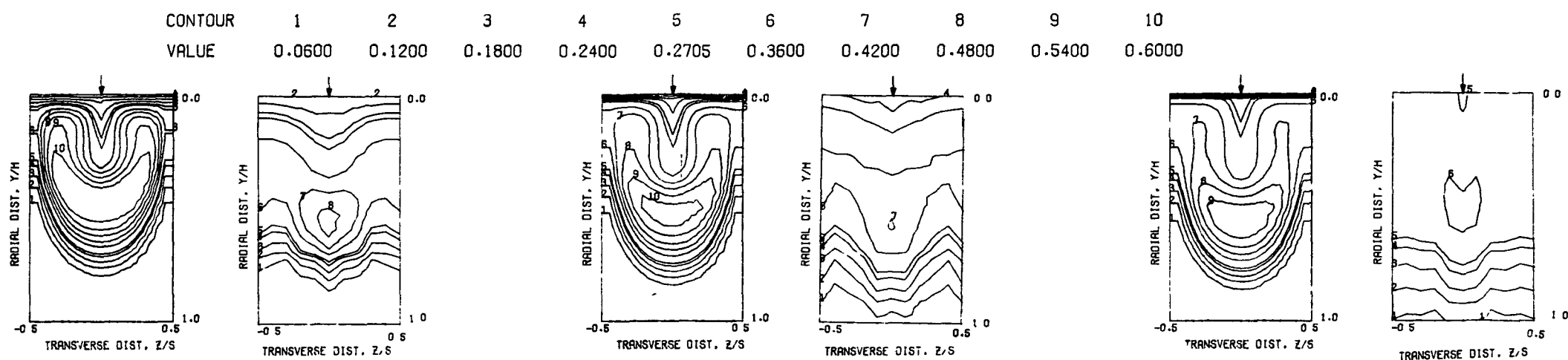


PREDICTED THETA DISTRIBUTIONS FOR TEST NO. 2, FINE GRID, $J=21.59$, $S/D=2.0$, $H/D=4.0$

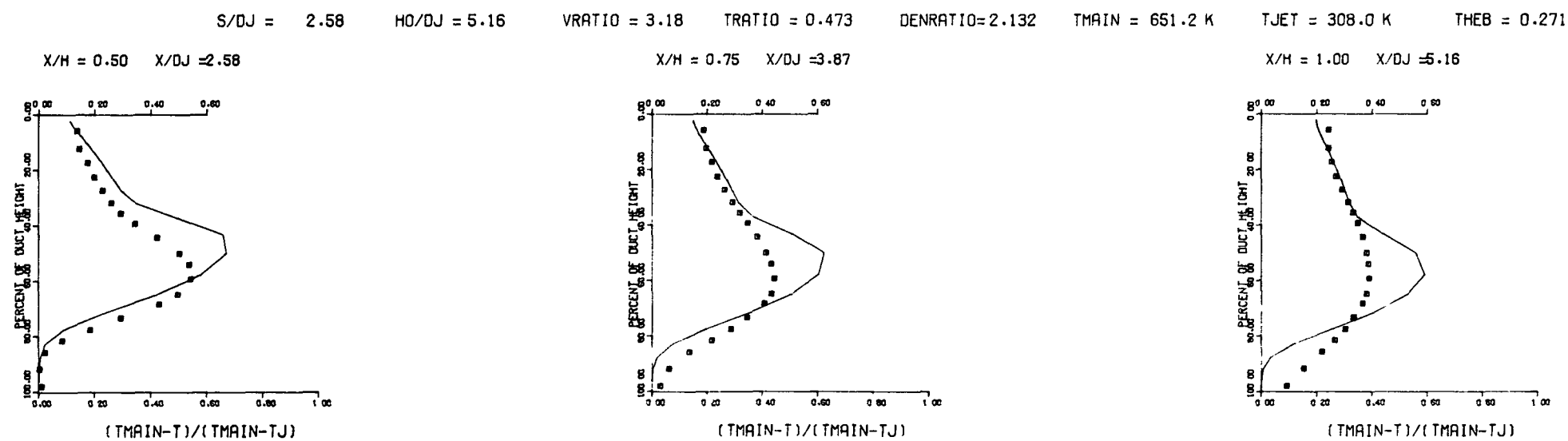
Figure 29. Predicted Temperature Distributions for Test Case 7 - Table 1.

FOLDOUT FRAME

2 FOLDOUT FRAME



THETA CONTOURS FOR TEST NO. 2, $T_M = \text{CONST}$, $J = 21.59$, $S/D = 2.0$, $H/D = 4.0$

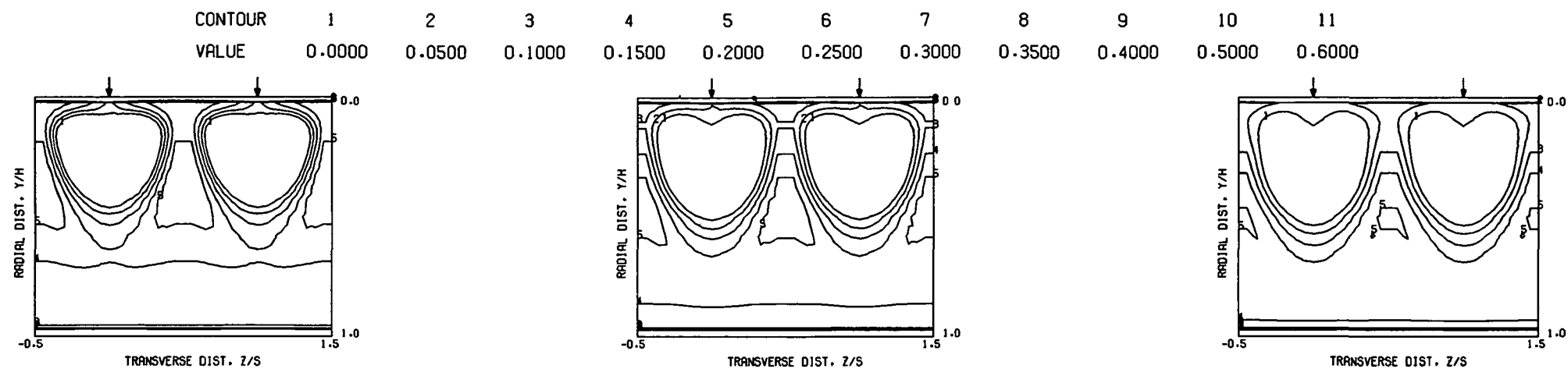


COMPARISON BETWEEN DATA AND PREDICTIONS FOR TEST NO. 02, TEST SECTION I, $T_M = \text{CONST}$, $J = 21.59$, $S/D = 2.00$, $H/D = 4.00$

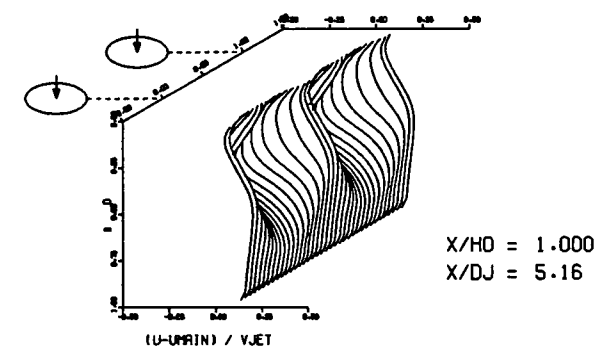
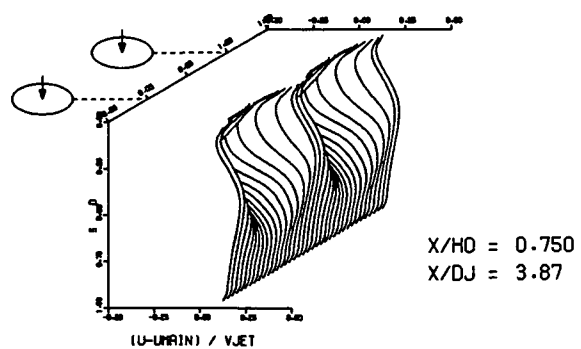
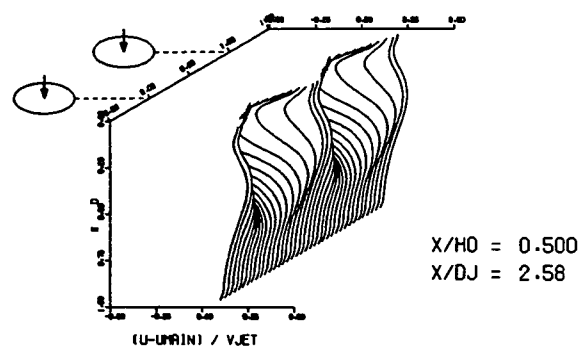
Figure 30. Comparison Between Predicted and Measured Temperature Distributions for Test Case 7 - Table 1.

FOLDOUT FRAME

FOLDOUT FRAME



PREDICTED VELOCITY CONTOURS FOR TEST NO. 7, 45X23X19, J=18.59, S/D=2.00, H/D=4.00



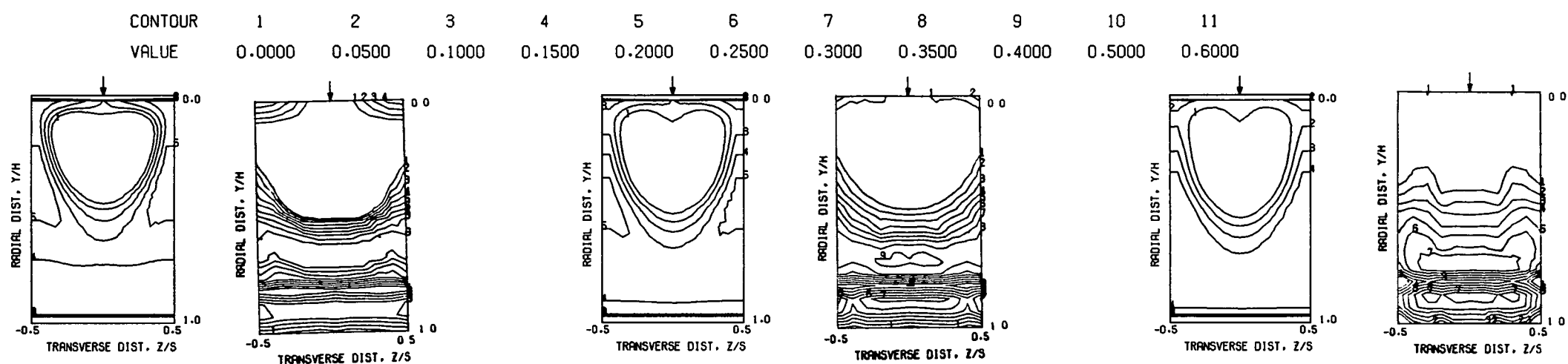
PREDICTED VELOCITY DISTRIBUTIONS FOR TEST NO. 7, 45X23X19, J=18.59, S/D=2.00, H/D=4.00

Figure 31. Predicted Velocity Distributions for Test Case 7 - Table 1.

FOLDOUT FRAME

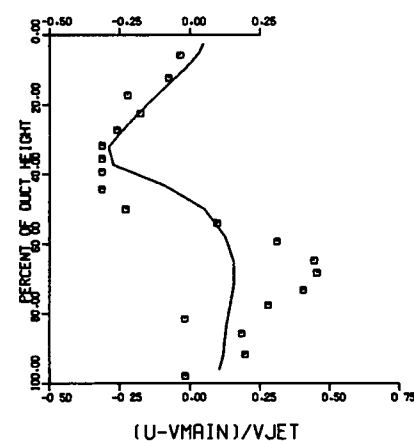
2 FOLDOUT FRAME

ORIGINAL PAGE IS
OF POOR QUALITY

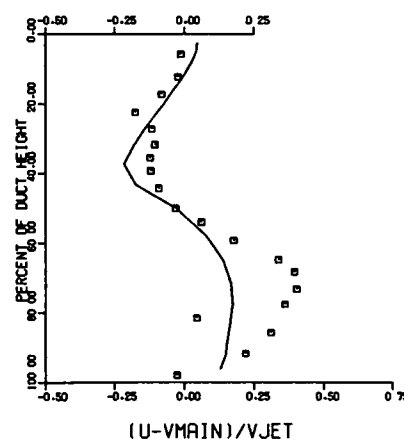


S/DJ = 2.58 HO/DJ = 5.16 VRATIO = 3.18 TRATIO = 0.473 DENRATIO=2.132 TMAIN = 361.8 K TJET = 171.1 K THEB = 0.271

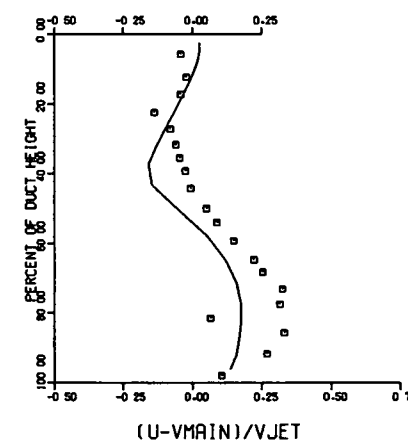
X/H = 0.50 X/DJ = 2.58



X/H = 0.75 X/DJ = 3.87



X/H = 1.00 X/DJ = 5.16

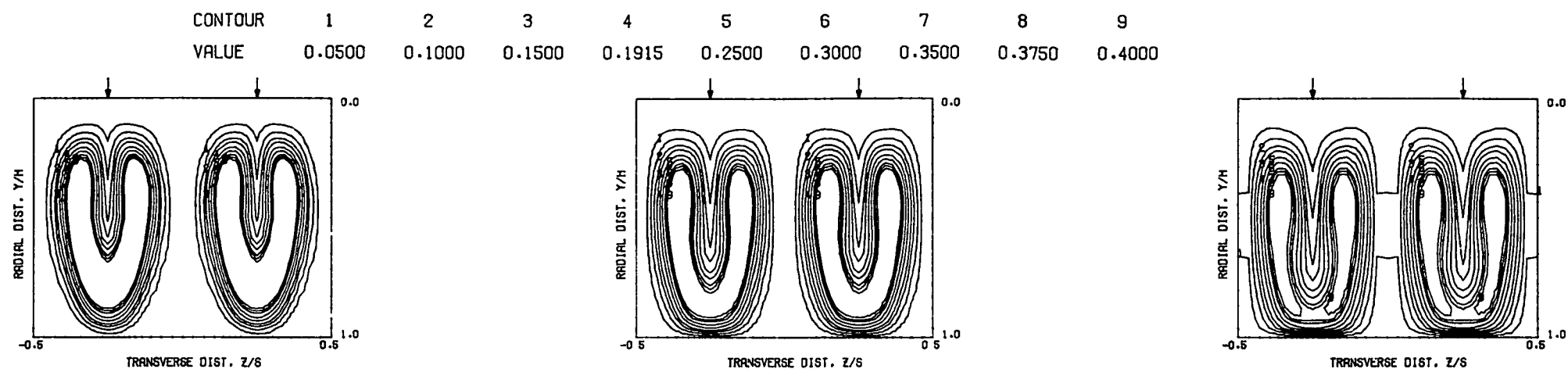


COMPARISON BETWEEN DATA AND PREDICTIONS FOR TEST 7. 45X23X19. SINGLE SIDED ROW OF JETS. J = 18.59 , S/D =2.00 , H/D =4.00

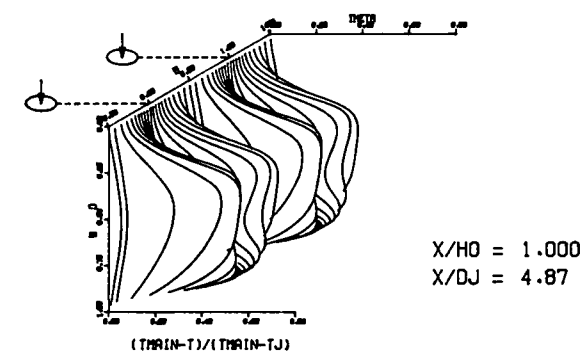
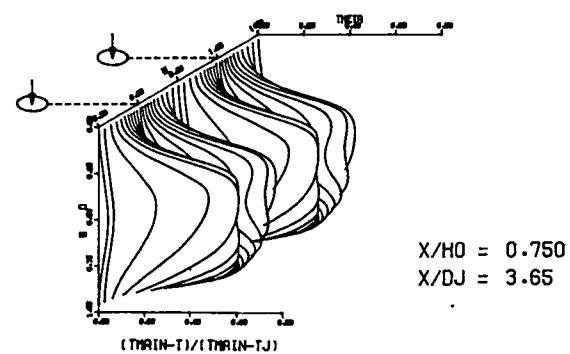
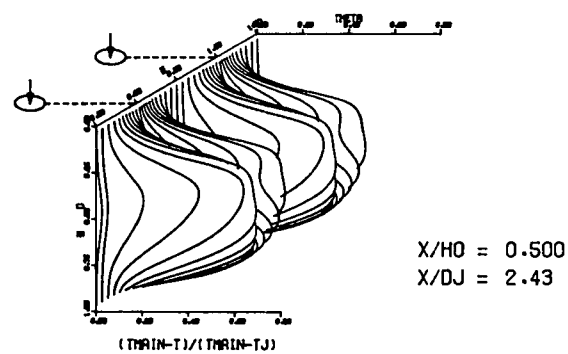
Figure 32. Comparison Between Predicted and Measured Velocity Distributions for Test Case 7 - Table 1.

FOLDOUT FRAME

FOLDOUT FRAME



PREDICTED THETA CONTOURS FOR TEST NO.4, FINE GRID, $J=26.68$, $S/D=4.0$, $H/D=4.0$

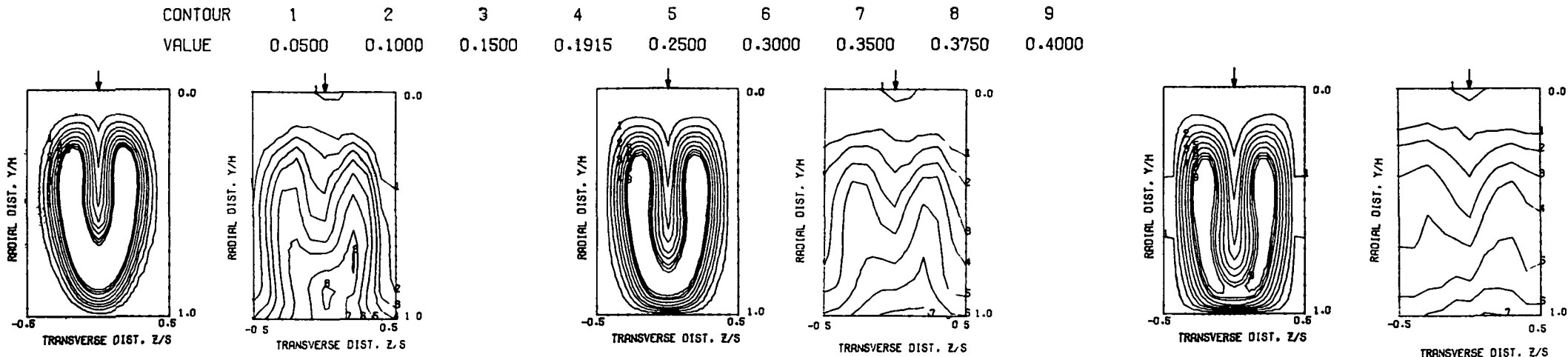


PREDICTED THETA DISTRIBUTIONS FOR TEST NO. 4, FINE GRID, $J=26.68$, $S/D=4.0$, $H/D=4.0$

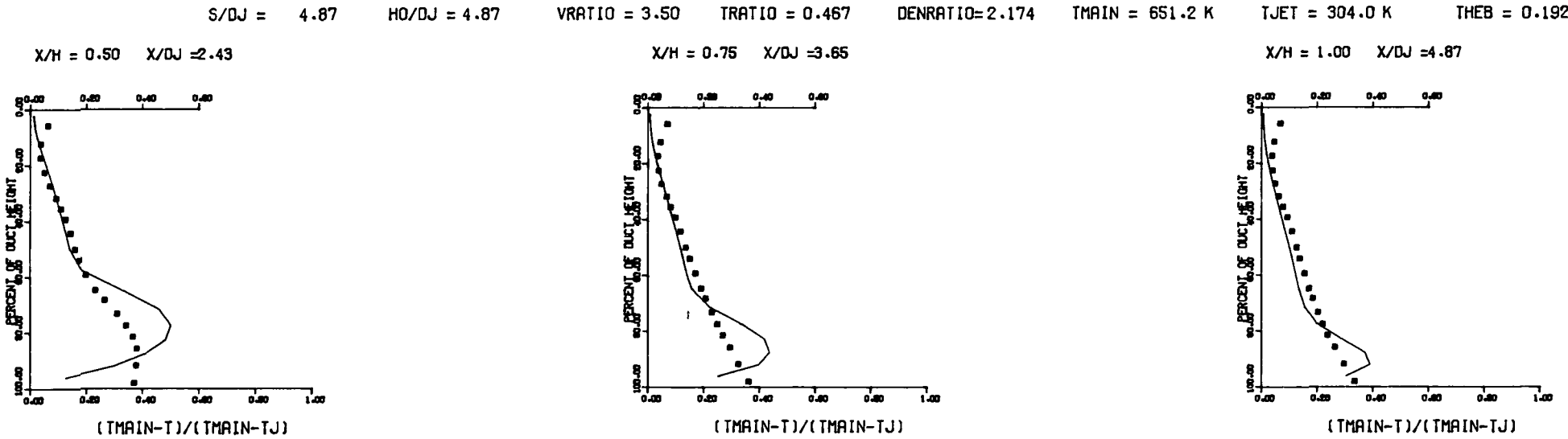
Figure 33. Predicted Temperature Distributions for Test Case 8 - Table 1.

FOLDOUT FRAME

FOLDOUT FRAME



THETA CONTOURS FOR TEST NO 4, $T_M=CONST$, $J=26.7$, $S/D=4.0$, $H/D=4.0$

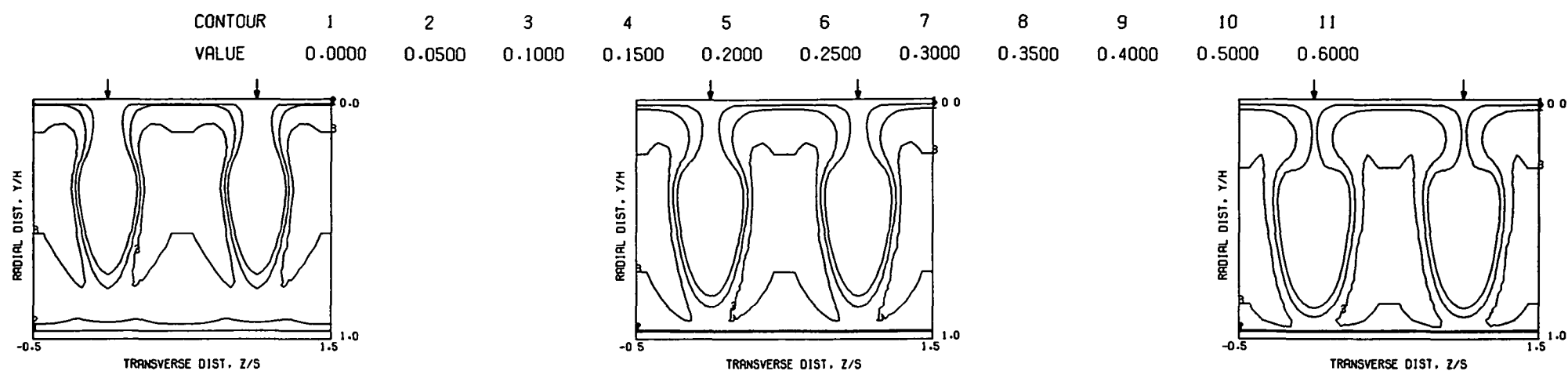


COMPARISON BETWEEN DATA AND PREDICTIONS FOR TEST NO. 4, TEST SECTION I, ONE SIDED , $J = 26.68$, $S/D = 4.00$, $H/D = 4.00$

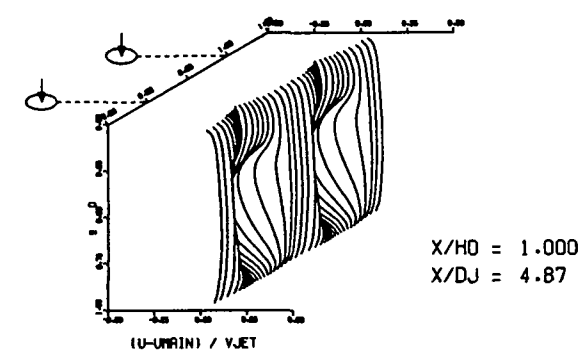
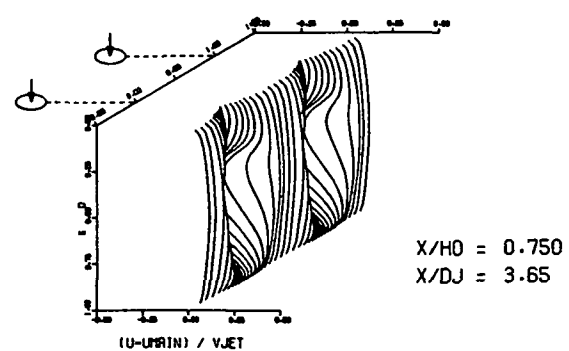
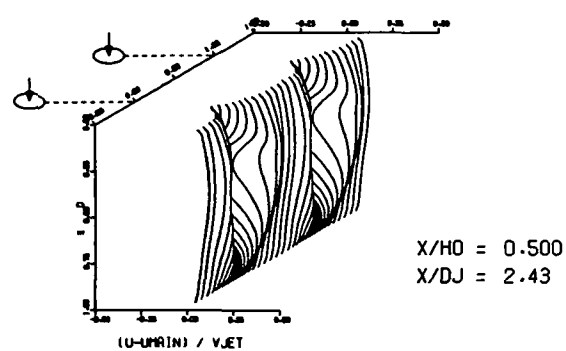
Figure 34. Comparison Between Predicted and Measured Temperature Distributions for Test Case 8 - Table 1.

FOLDOUT FRAME

2 FOLDOUT FRAME



PREDICTED VELOCITY CONTOURS FOR TEST NO. 8, 40X23X21, $J=23.51$, $S/D=4.00$, $H/D=4.00$

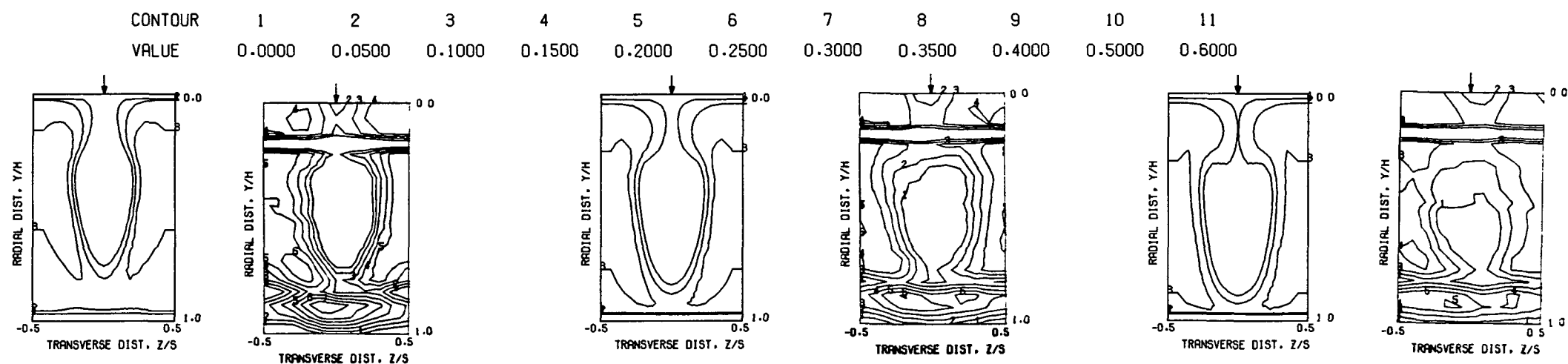


PREDICTED VELOCITY DISTRIBUTIONS FOR TEST NO. 8, 40X23X21, $J=23.51$, $S/D=4.00$, $H/D=4.00$

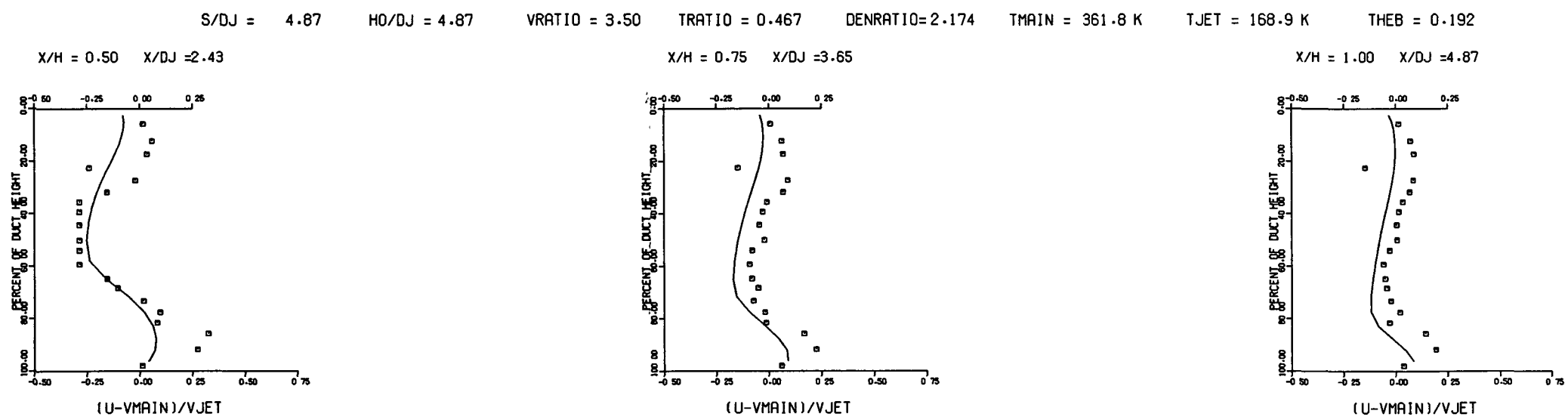
Figure 35. Predicted Velocity Distributions for Test Case 8 - Table 1.

FOLDOUT FRAME

FOLDOUT FRAME



PREDICTED VELOCITY CONTOURS FOR TEST NO. 8, 40X23X21, J=23.51, S/D=4.00, H/D=4.00

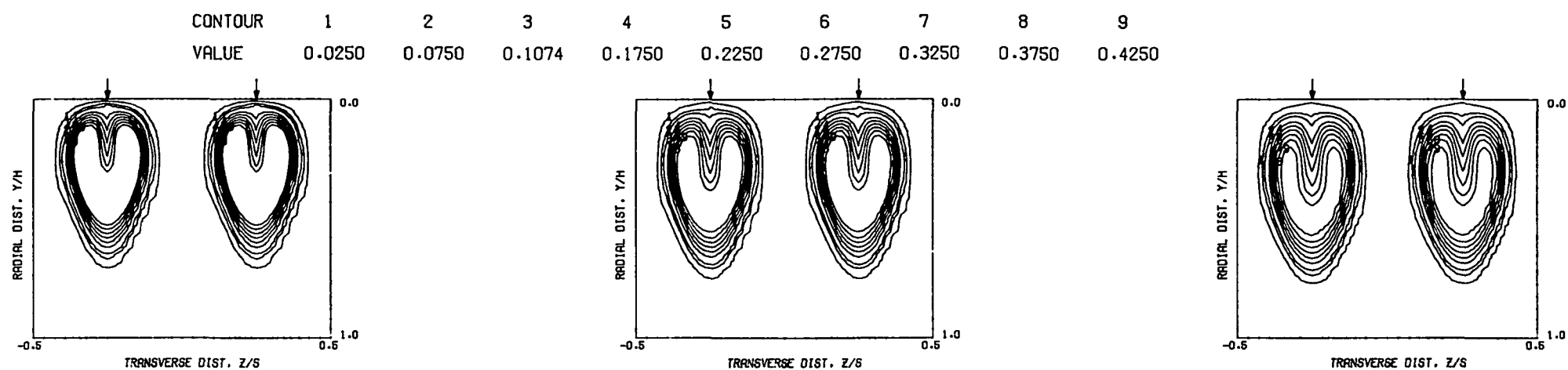


COMPARISON BETWEEN DATA AND PREDICTIONS FOR TEST 8, 40X23X21, SINGLE SIDED ROW OF JETS, J = 23.51, S/D = 4.00, H/D = 4.00

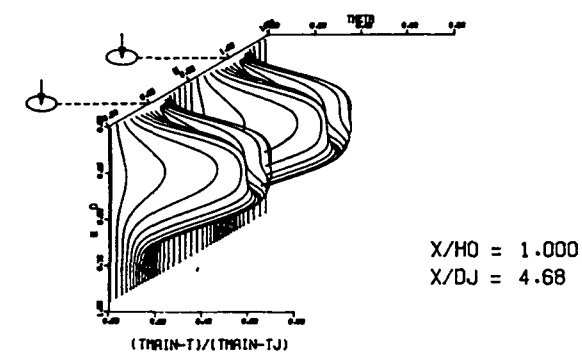
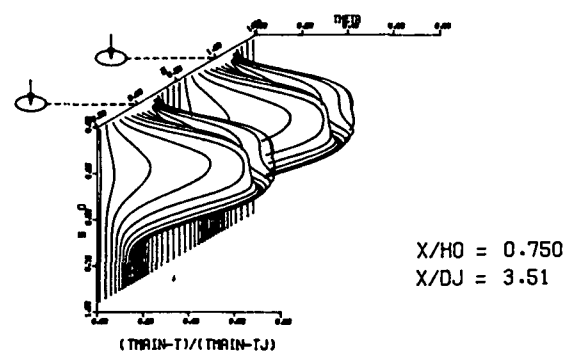
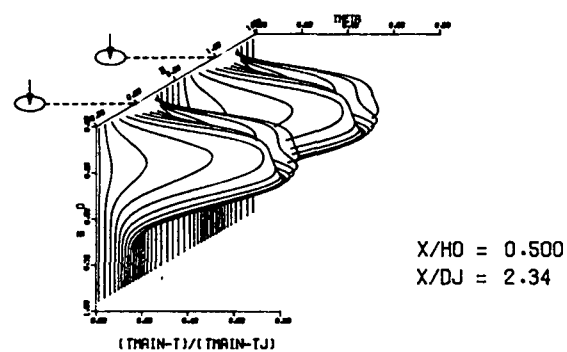
Figure 36. Comparison Between Predicted and Measured Velocity Distributions for Test Case 8 - Table 1.

FOLDOUT FRAME

2 FOLDOUT FRAME



PREDICTED THETA CONTOURS FOR TEST NO.2, FINE GRID, $J=6.14$, $S/D=4.0$, $H/D=4.0$

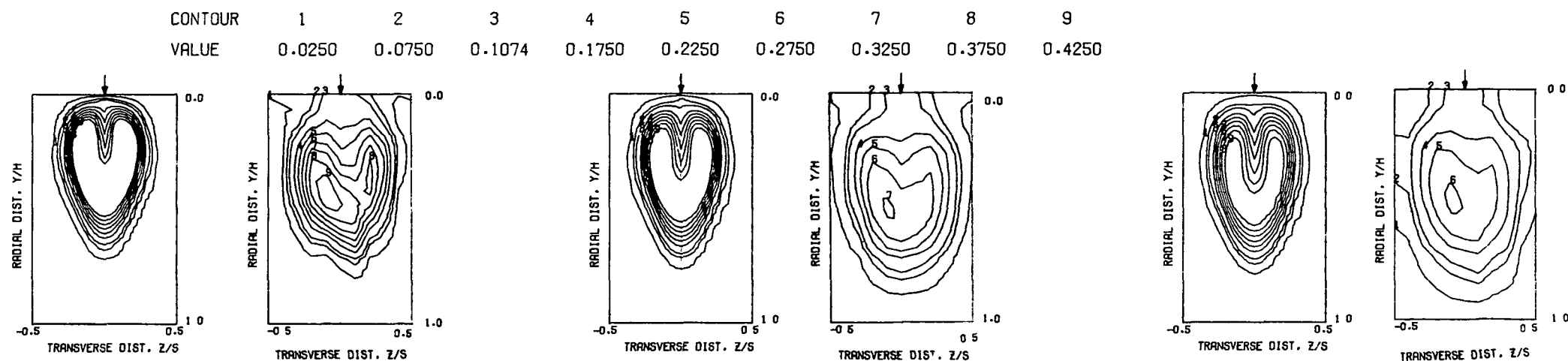


PREDICTED THETA DISTRIBUTIONS FOR TEST NO. 2, FINE GRID, $J=6.14$, $S/D=4.0$, $H/D=4.0$

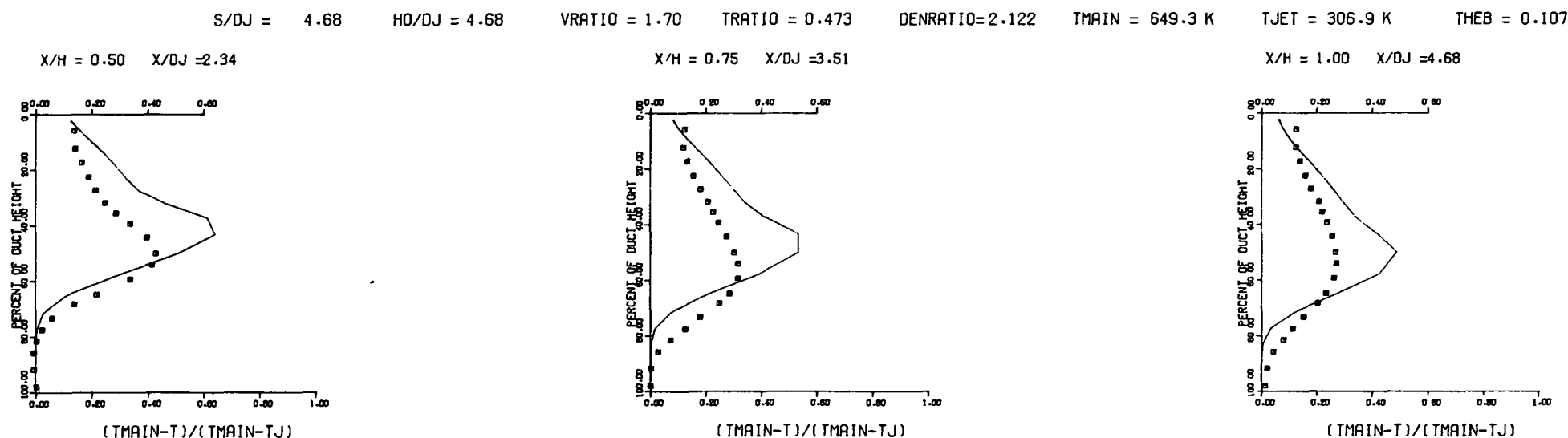
Figure 37. Predicted Temperature Distributions for Test Case 9 - Table 1.

FOLDOUT FRAME

2 FOLDOUT FRAME



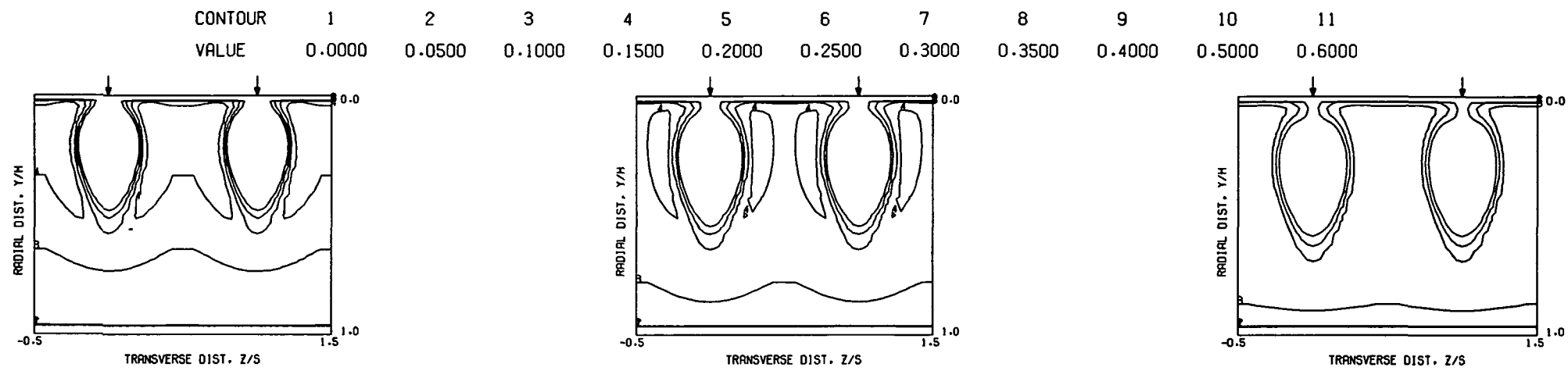
THETA CONTOURS FOR TEST NO.2, $T_M = \text{CONST}$, $J = 6.14$, $S/D = 4.0$, $H/D = 4.0$



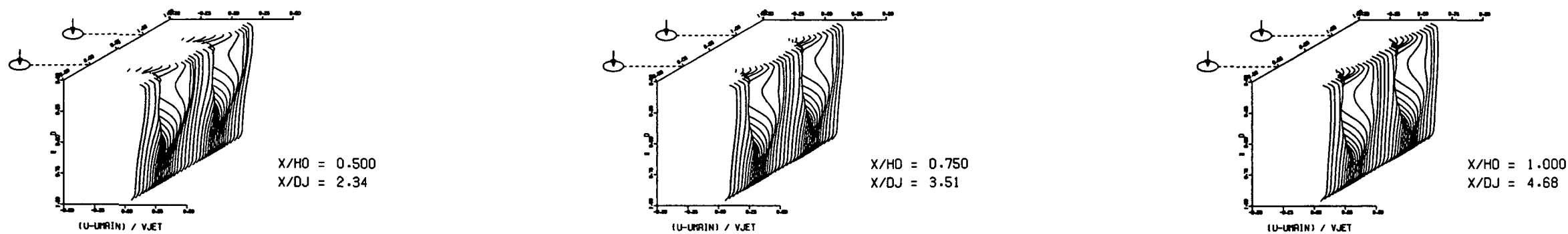
COMPARISON BETWEEN DATA AND PREDICTIONS FOR TEST NO. 2, TEST SECTION I, $T_M = \text{CONST}$, $J = 6.14$, $S/D = 4.00$, $H/D = 4.00$

Figure 38. Comparison Between Predicted and Measured Temperature Distributions for Test Case 9 - Table 1.

ORIGINAL PAGE IS
OF POOR QUALITY



PREDICTED VELOCITY CONTOURS FOR TEST NO. 9, 40X23X21, J=5.31, S/D=4.00, H/D=4.00

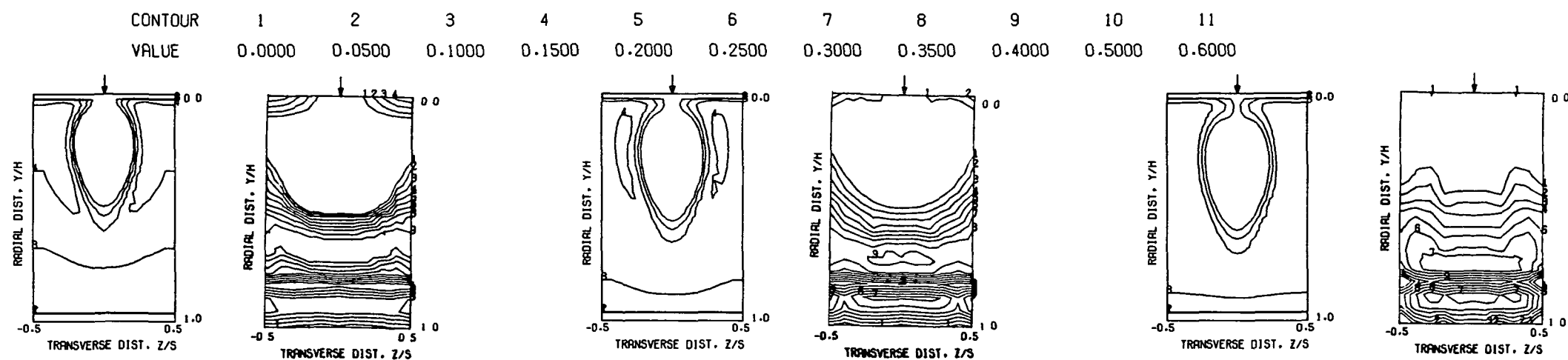


PREDICTED VELOCITY DISTRIBUTIONS FOR TEST NO. 9, 40X23X21, J=5.31, S/D=4.00, H/D=4.00

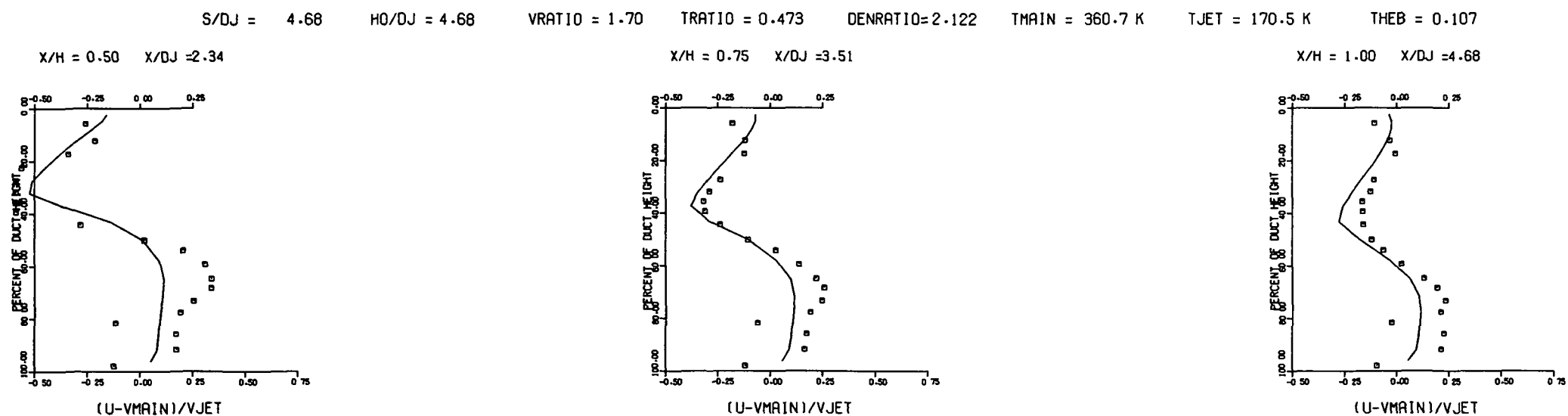
Figure 39. Predicted Velocity
Distributions for Test Case 9 - Table 1.

FOLDOUT FRAME

FOLDOUT FRAME



PREDICTED VELOCITY CONTOURS FOR TEST NO. 9, 40X23X21, J=5.31, S/D=4.00, H/D=4.00

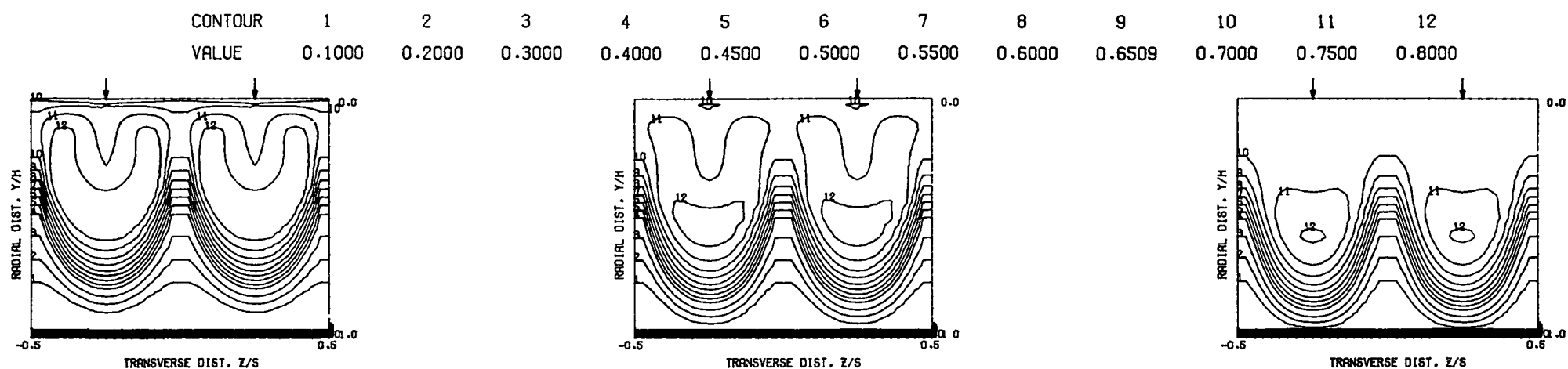


COMPARISON BETWEEN DATA AND PREDICTIONS FOR TEST 9, 40X23X21, SINGLE SIDED ROW OF JETS, J = 5.31 , S/D =4.00 , H/D =4.00

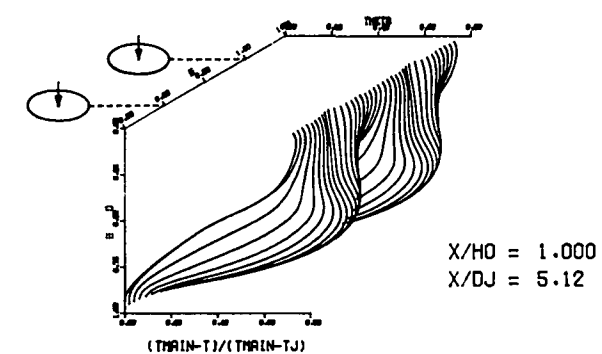
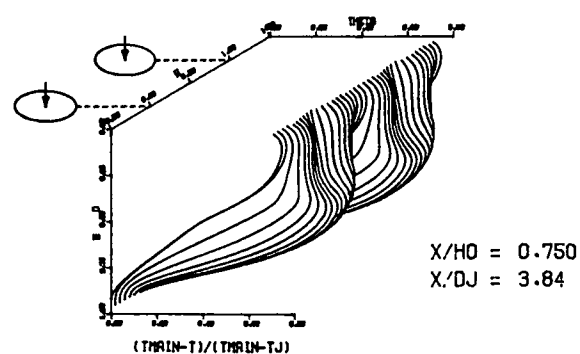
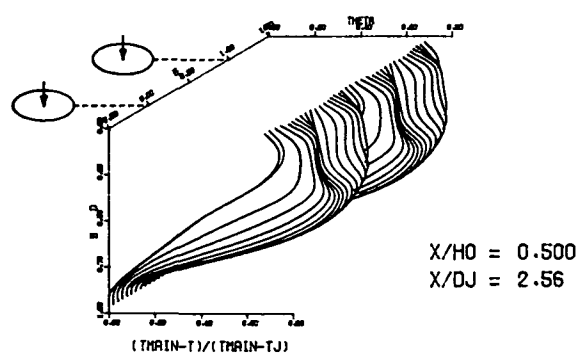
Figure 40. Comparison Between Predicted and Measured Velocity Distributions for Test Case 9 - Table 1.

FOLDOUT FRAME

2 FOLDOUT FRAME



PREDICTED THETA CONTOURS FOR TEST NO.13, TOP COLD, $J=22.63$, $S/D=2.0$, $H/D=4.0$

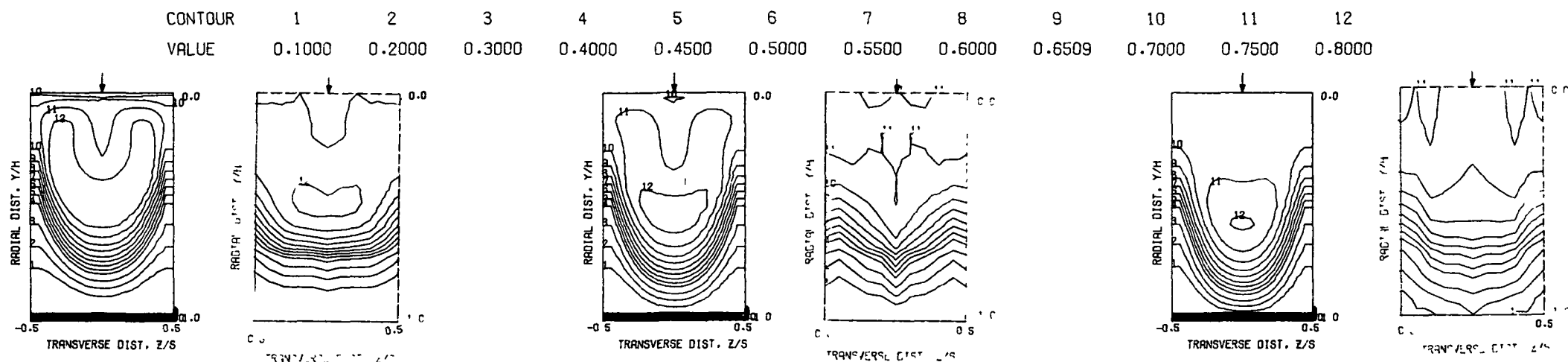


PREDICTED THETA DISTRIBUTIONS FOR TEST NO. 13, TOP COLD, $J=22.63$, $S/D=2.0$, $H/D=4.0$

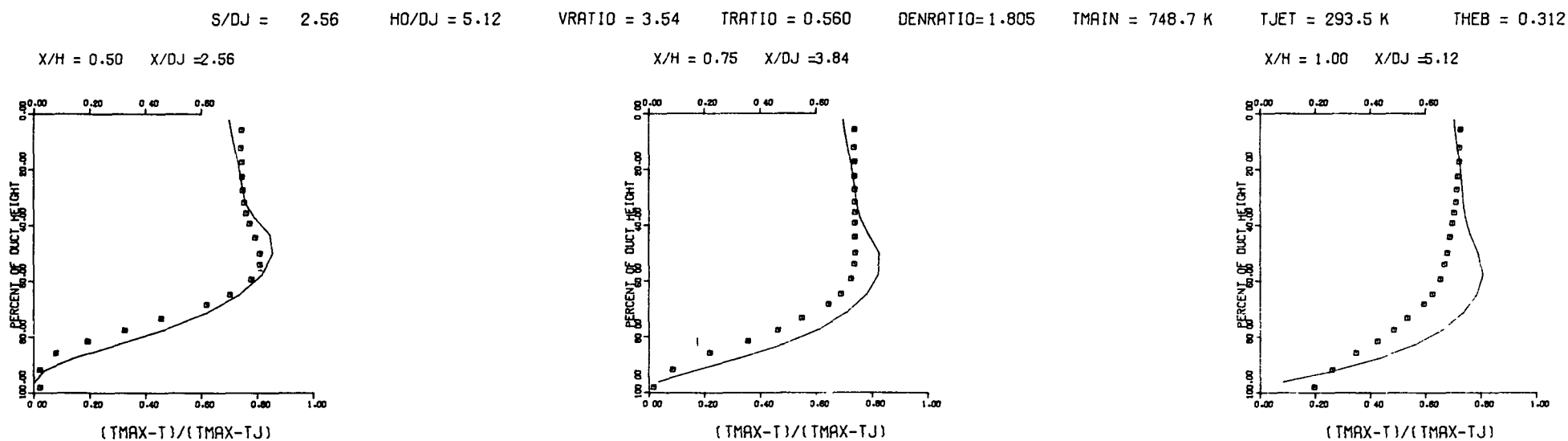
Figure 41. Predicted Temperature Distributions for Test Case 10 - Table 1.

FOLDOUT FRAME

2 FOLDOUT FRAME



THETA CONTOURS FOR TEST NO. 13, TOP COLD, $J=22.63$, $S/D=2.0$, $H/D=4.0$

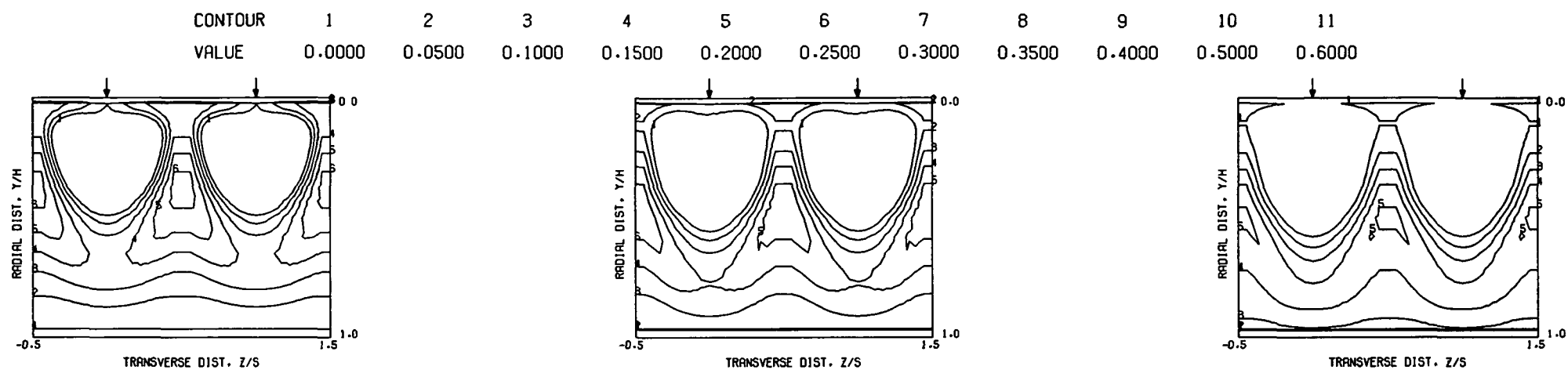


COMPARISON BETWEEN DATA AND PREDICTIONS FOR TEST NO. 13, TEST SECTION I, TOP COLD TM, $J = 22.63$, $S/D = 2.00$, $H/D = 4.00$

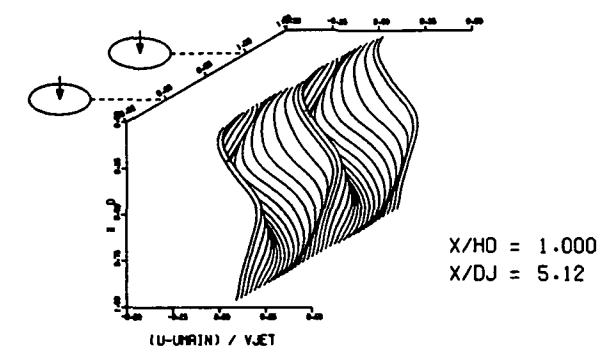
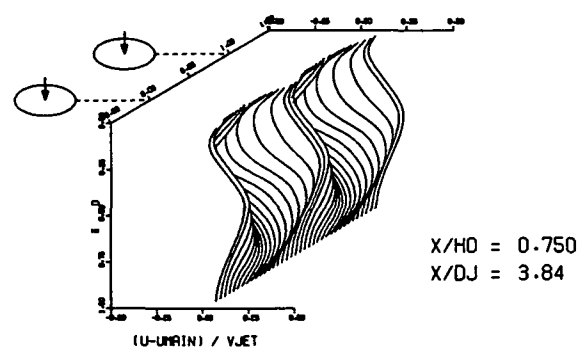
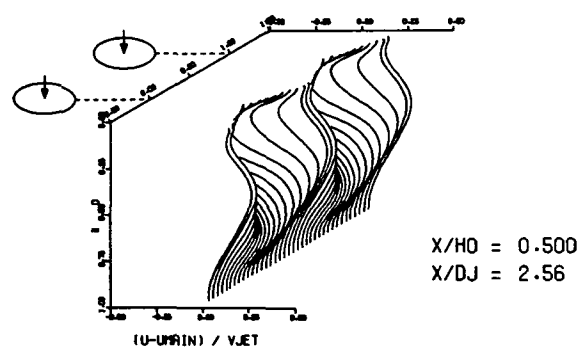
Figure 42. Comparison Between Predicted and Measured Temperature Distributions for Test Case 10 - Table 1.

FOLDOUT FRAME

FOLDOUT FRAME



PREDICTED VELOCITY CONTOURS FOR TEST NO.10, TOP COLD, $J=31.79$, $S/D=2.00$, $H/D=4.00$



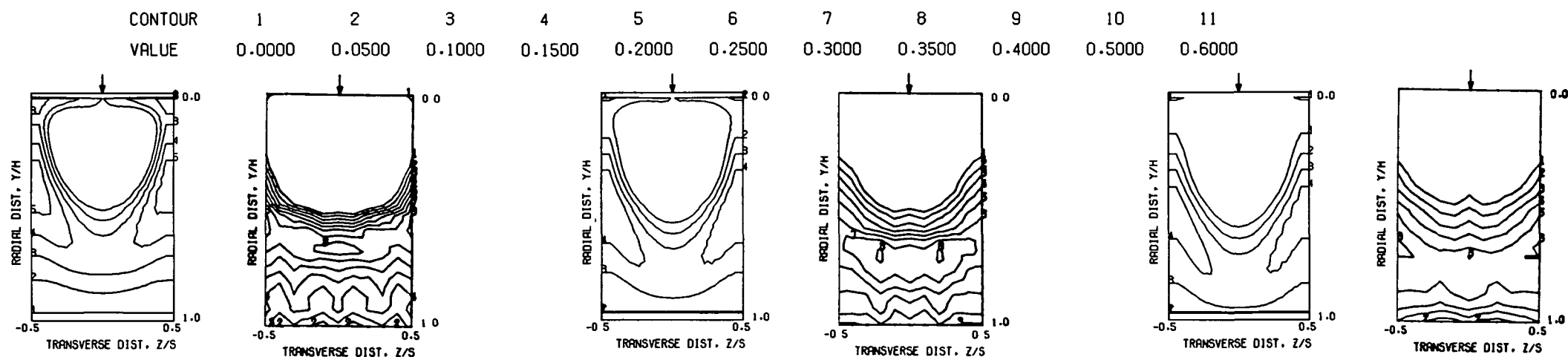
PREDICTED VELOCITY DISTRIBUTIONS FOR TEST NO. 10, 45X23X19, $J=31.79$, $S/D=2.00$, $H/D=4.00$

Figure 43. Predicted Velocity Distributions for Test Case 10 - Table 1.

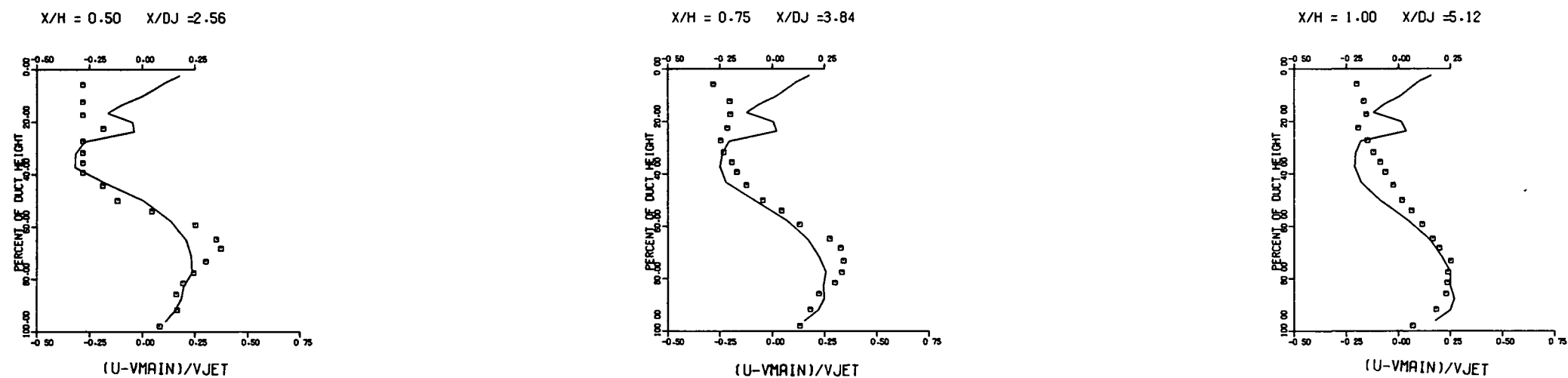
FOLDOUT FRAME

FOLDOUT FRAME

ORIGINAL PAGE IS
OF POOR QUALITY



$S/DJ = 2.56$ $H/DJ = 5.12$ $VRATIO = 3.54$ $TRATIO = 0.560$ $DENRATIO=1.805$ $TMAIN = 415.0 K$ $TJET = 163.1 K$ $THEB = 0.651$

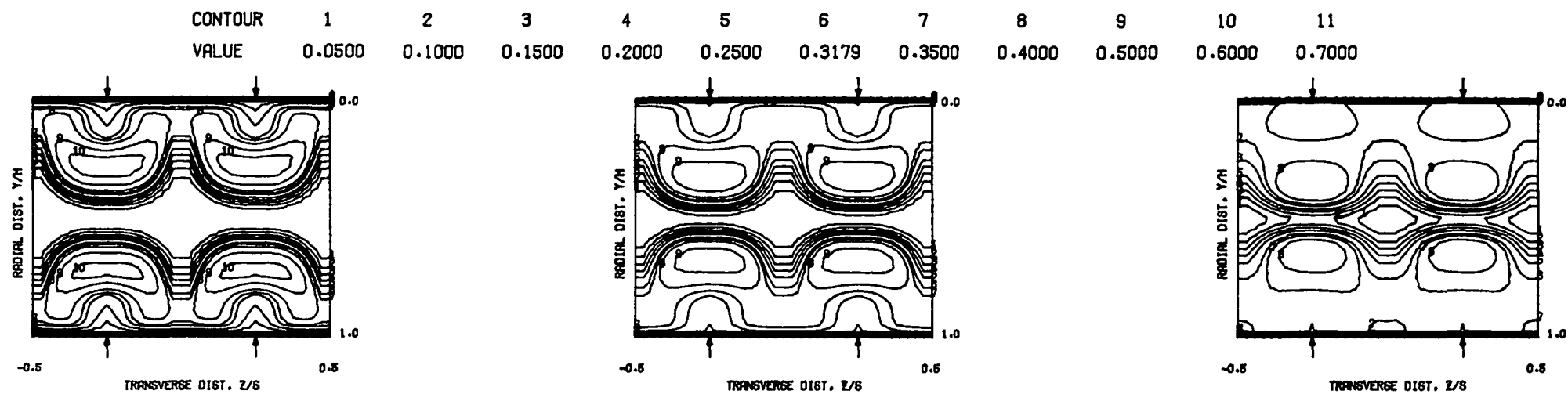


COMPARISON BETWEEN DATA AND PREDICTIONS FOR TEST 10, 45X23X19, TOP COLD MAINSTREAM PROFILE, $J = 31.79$, $S/D = 2.00$, $H/D = 4.00$

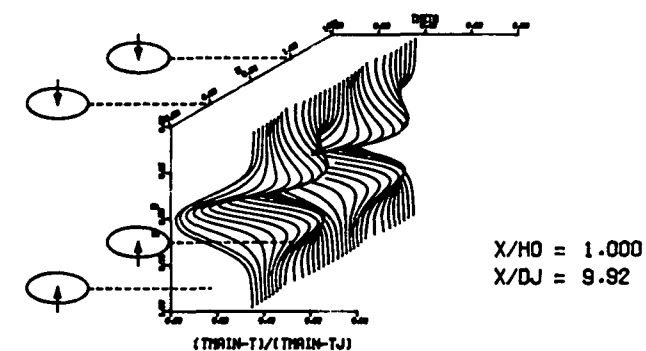
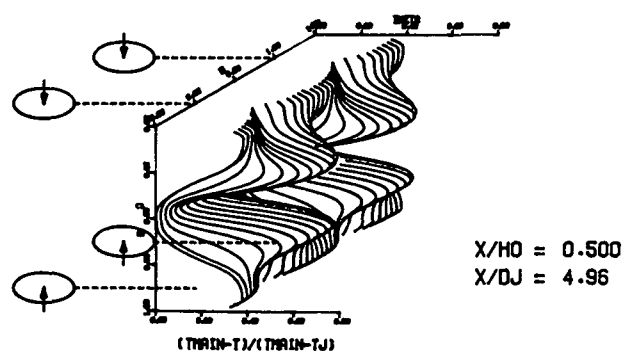
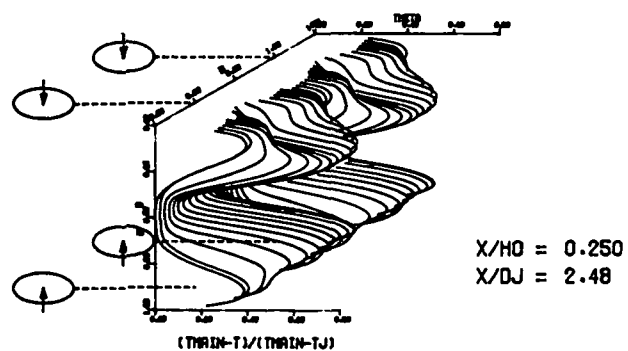
Figure 44. Comparison Between Predicted and Measured Velocity Distributions for Test Case 10 - Table 1.

FOLDOUT FRAME

FOLDOUT FRAME



PREDICTED THETA CONTOURS FOR TEST NO.2,OPPOSED(INL), J=24.95, S/D=2.0, H/D=8.0



PREDICTED THETA DISTRIBUTIONS FOR TEST NO. 02, IN-LINE, J=24.95, S/D=2.0, H/D=8.0

Figure 45. Predicted Temperature Distributions for Test Case 11 - Table 1.

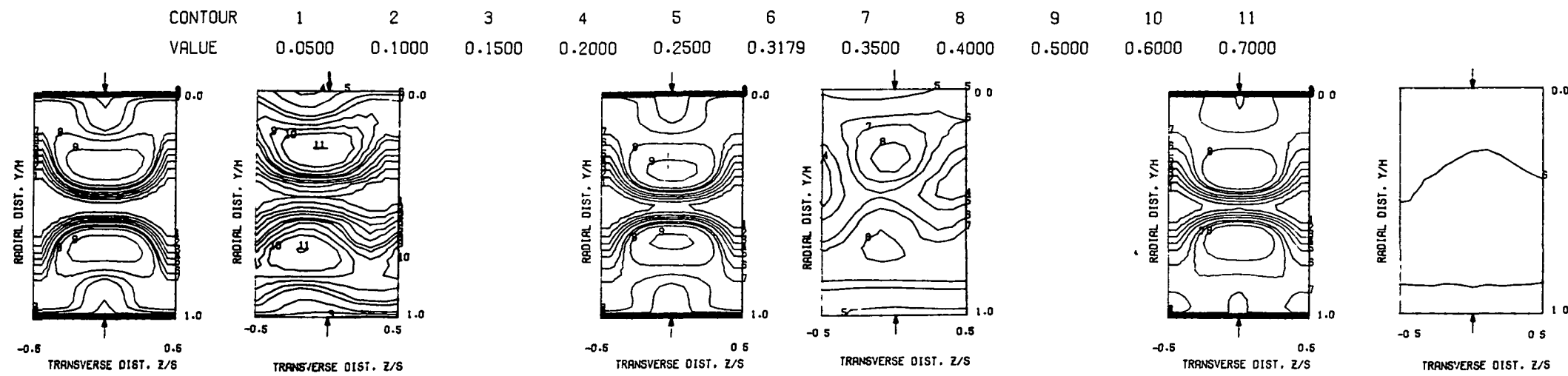
FOLDOUT FRAME

FOLDOUT FRAME

2 FOLDOUT FRAME

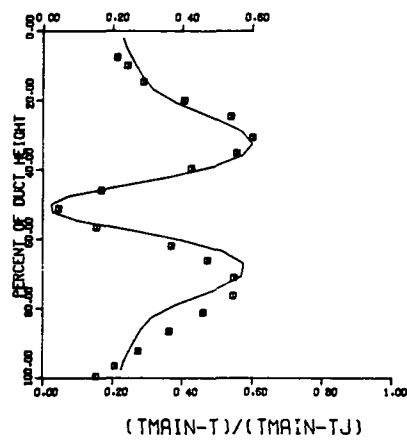
ORIGINAL PAGE IS
OF POOR QUALITY

ORIGINAL PAGE IS
OF POOR QUALITY

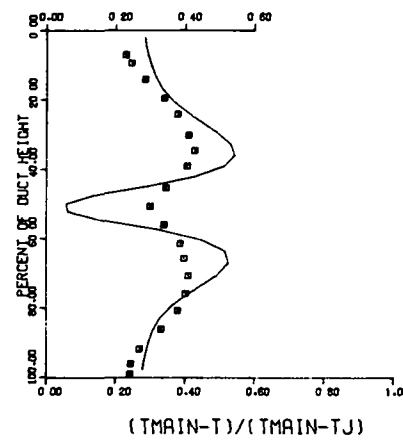


S/DJ = 2.48 HO/DJ = 9.92 VRATIO = 3.42 TRATIO = 0.474 DENRATIO = 2.135 TMAIN = 646.6 K TJET = 306.8 K THEB = 0.318

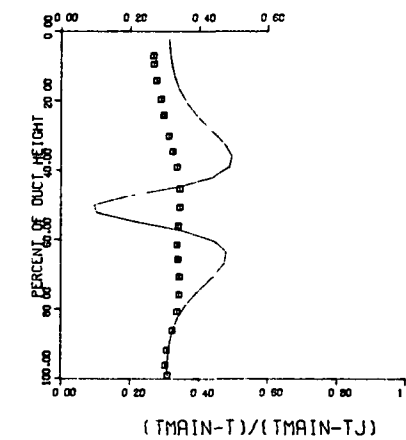
X/H = 0.25 X/DJ = 2.48



X/H = 0.50 X/DJ = 4.96



X/H = 1.00 X/DJ = 9.92

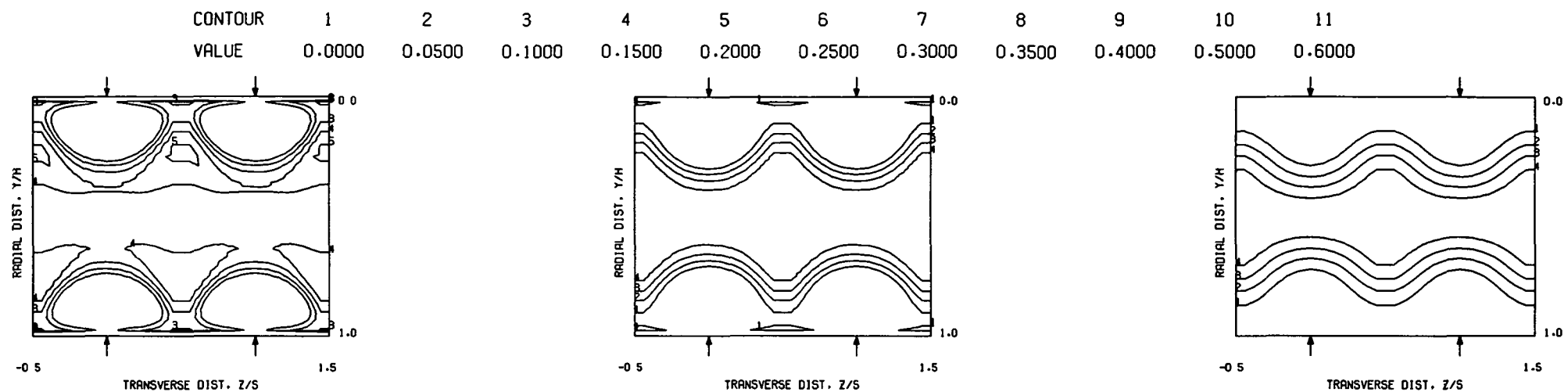


COMPARISON BETWEEN DATA AND PREDICTIONS FOR TEST NO. 2, TEST SECTION 1, OPPOSED (INL), J = 24.95, S/D = 2.00, H/D = 8.00

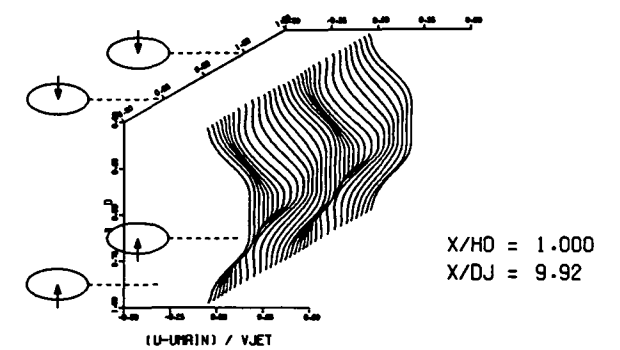
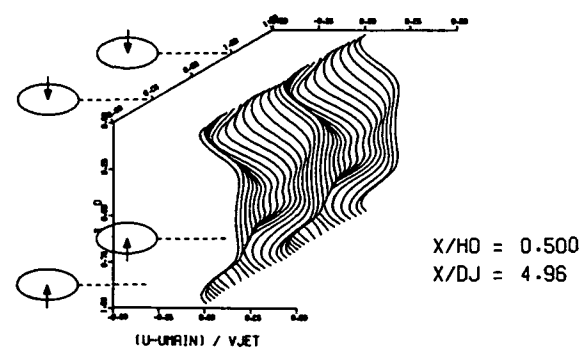
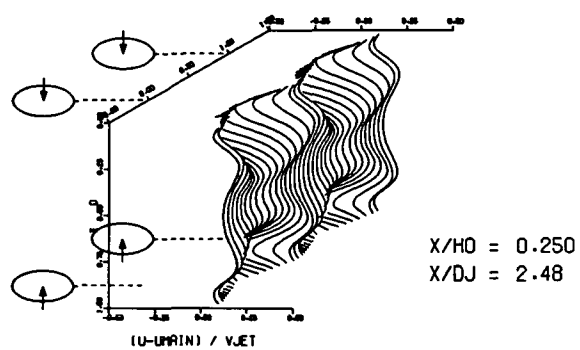
Figure 46. Comparison Between Predicted and Measured Temperature Distributions for Test Case 11 - Table 1.

FOLDOUT FRAME

FOLDOUT FRAME



PREDICTED VELOCITY CONTOURS FOR TEST NO. 11, IN-LINE, $J=24.94$, $S/D=2.00$, $H/D=8.00$

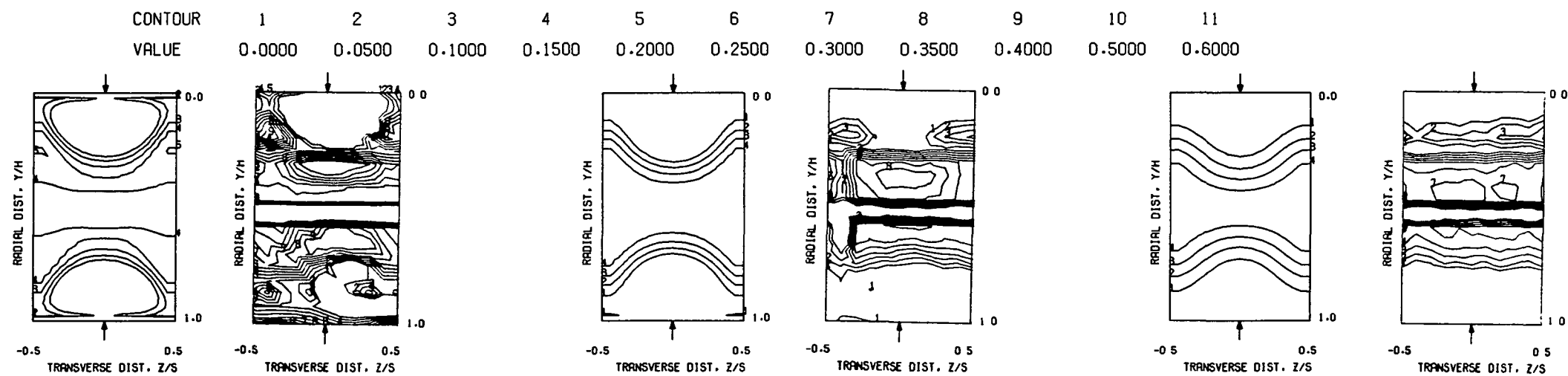


PREDICTED VELOCITY DISTRIBUTIONS FOR TEST NO. 11, 35X33X17, $J=24.94$, $S/D=2.00$, $H/D=8.00$

Figure 47. Predicted Velocity Distribution for Test Case 11 - Table 1.

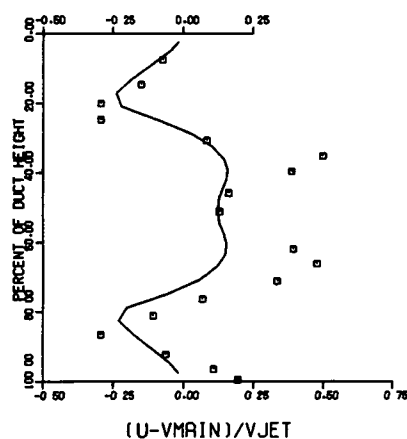
FOLDOUT FRAME

2 FOLDOUT FRAME

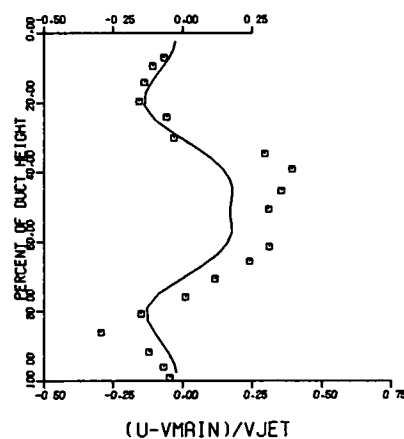


S/DJ = 2.48 HO/DJ = 9.92 VRATIO = 3.42 TRATIO = 0.474 DENRATIO=2.135 TMAIN = 359.2 K TJET = 170.4 K THEB = 0.318

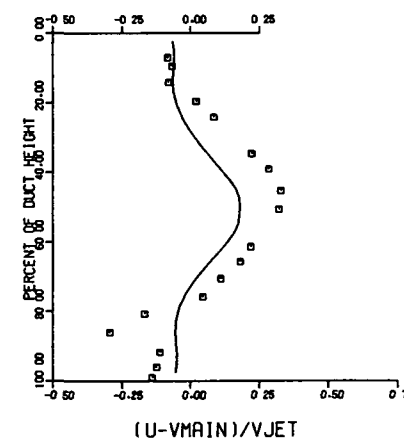
X/H = 0.25 X/DJ = 2.48



X/H = 0.50 X/DJ = 4.96



X/H = 1.00 X/DJ = 9.92

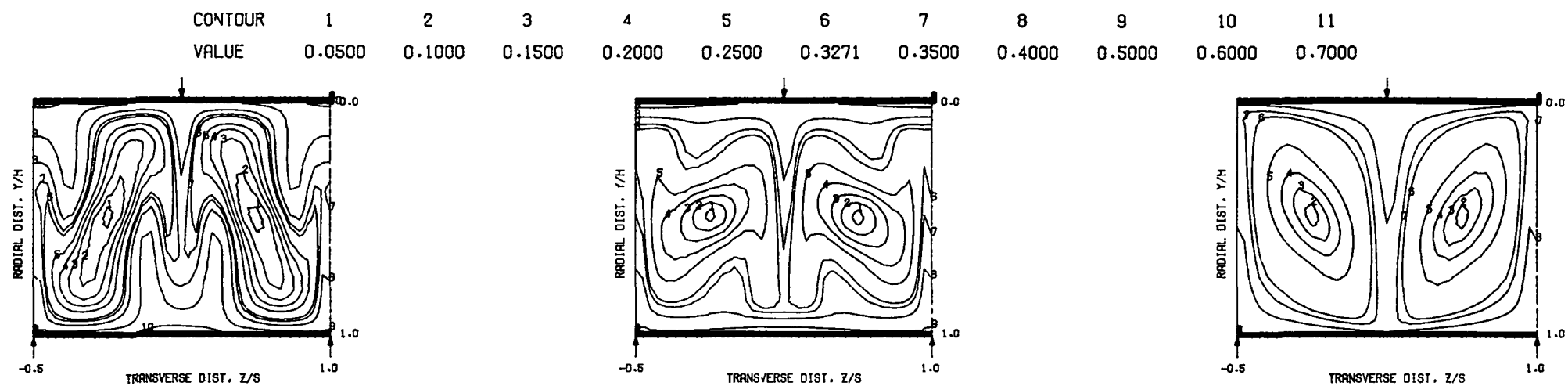


COMPARISON BETWEEN DATA AND PREDICTIONS FOR TEST 11, 35X33X17, OPPOSED IN-LINE ROW OF JETS, J = 24.94, S/D = 2.00, H/D = 8.00

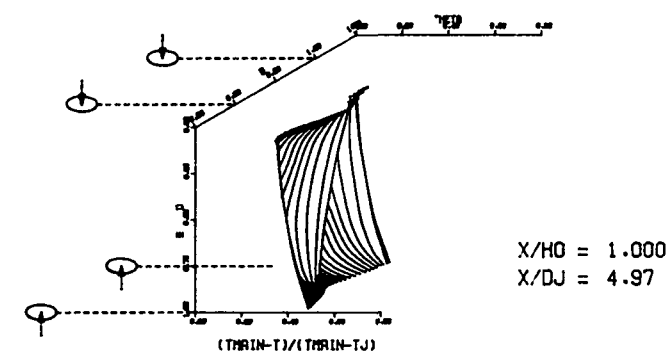
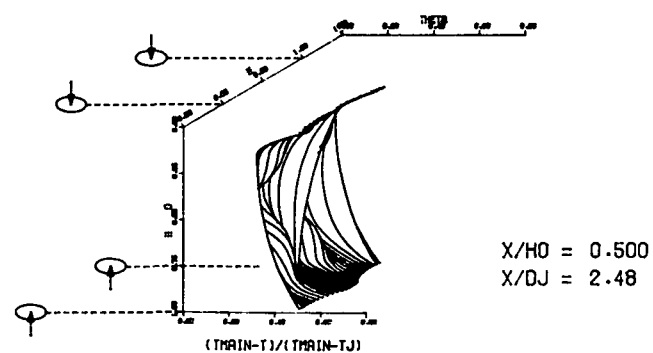
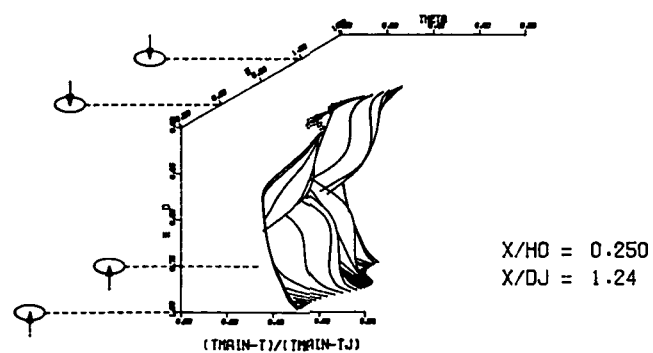
Figure 48. Comparison Between Predicted and Measured Velocity Distributions for Test Case 11 - Table 1.

FOLDOUT FRAME

2 FOLDOUT FRAME



PREDICTED THETA CONTOURS FOR TEST NO.28,OPPOSED(STG), J=26.42, S/D=4.0, H/D=4.0

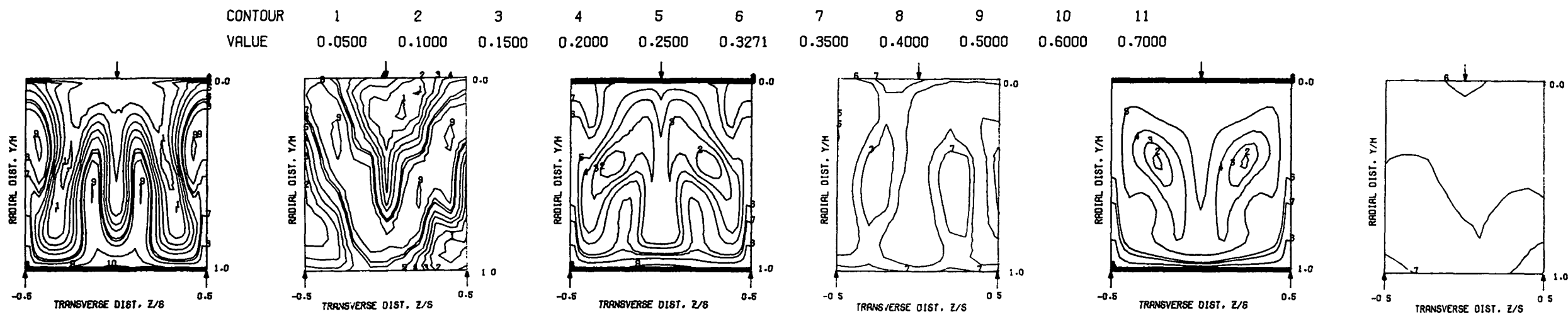


PREDICTED THETA DISTRIBUTIONS FOR TEST NO. 28, STAGGERED, J=26.42, S/D=4.0, H/D=4.

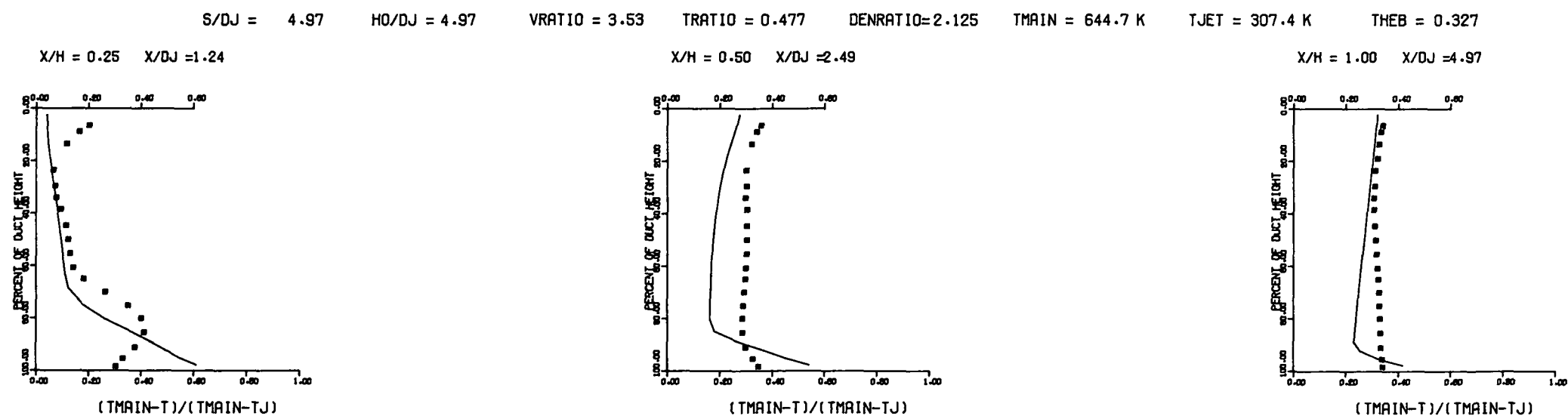
Figure 49. Predicted Temperature Distributions for Test Case 12 - Table 1.

FOLDOUT FRAME

2 FOLDOUT FRAME



THETA CONTOURS FOR TEST NO. 28, STAGGERED, J=26.4, S/D=4.0, H/D=4.0



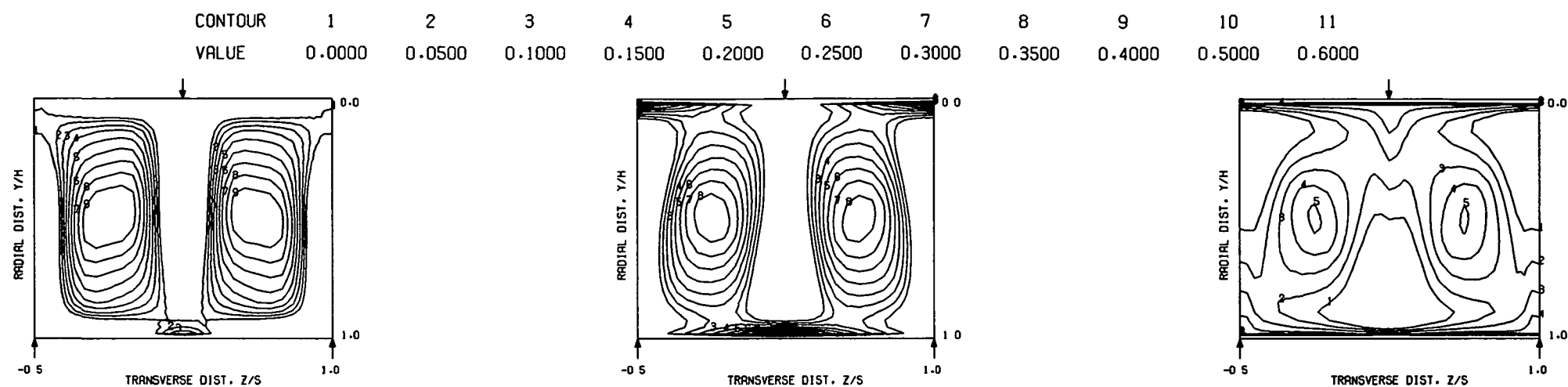
COMPARISON BETWEEN DATA AND PREDICTIONS FOR TEST NO. 28, TEST SECTION I, OPPOSED (STG), J = 26.42, S/D = 4.00, H/D = 4.00

Figure 50. Comparison Between Predicted and Measured Temperature Distributions for Test Case 12 - Table 1.

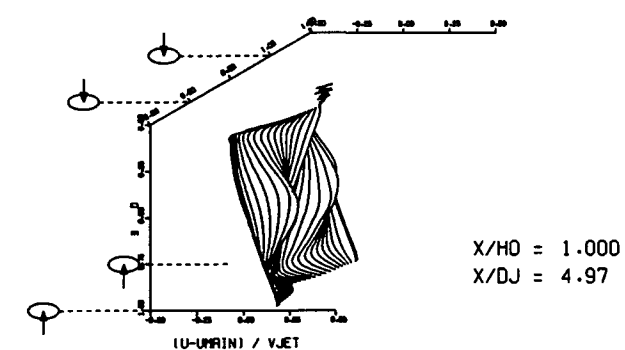
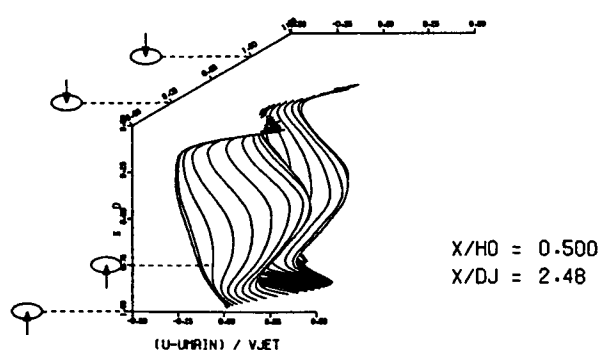
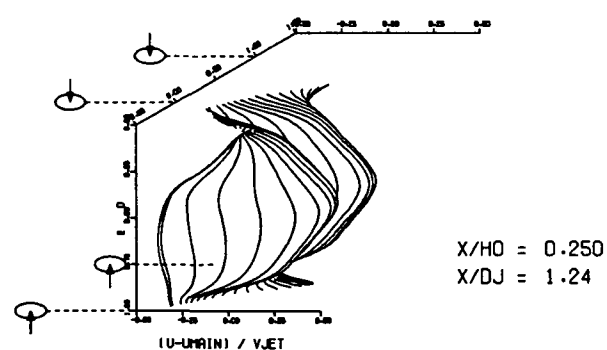
FOLDOUT FRAME

2 FOLDOUT FRAME

ORIGINAL PAGE IS
OF POOR QUALITY



PREDICTED VELOCITY CONTOURS FOR TEST NO.12, STAGGERED, $J=26.41$, $S/D=4.00$, $H/D=4.00$

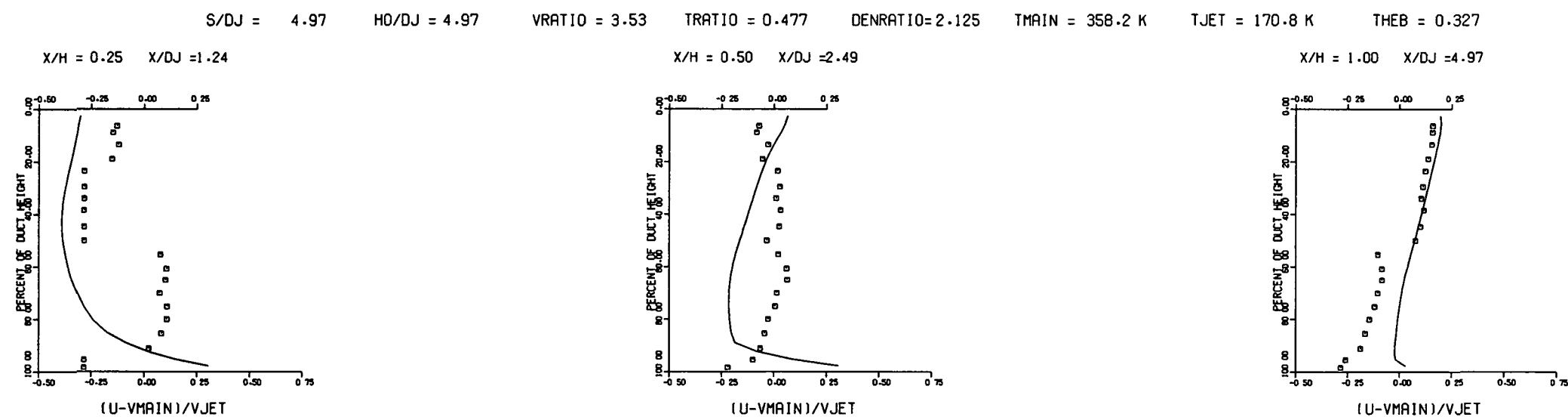
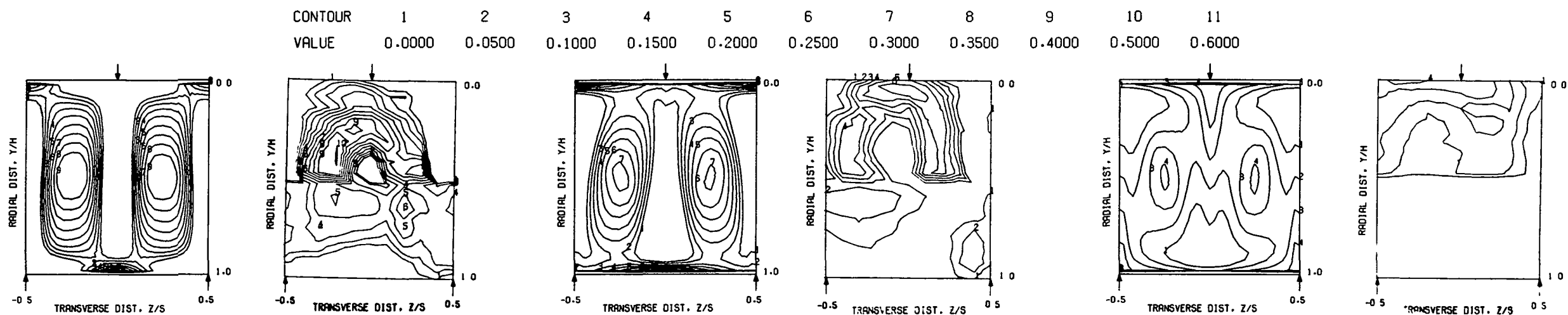


PREDICTED VELOCITY DISTRIBUTIONS FOR TEST NO. 12, 22X27X33, $J=26.41$, $S/D=4.00$, $H/D=4.00$

Figure 51. Predicted Velocity
Distributions for Test Case 12 - Table 1.

FOLDOUT FRAME

2 FOLDOUT FRAME

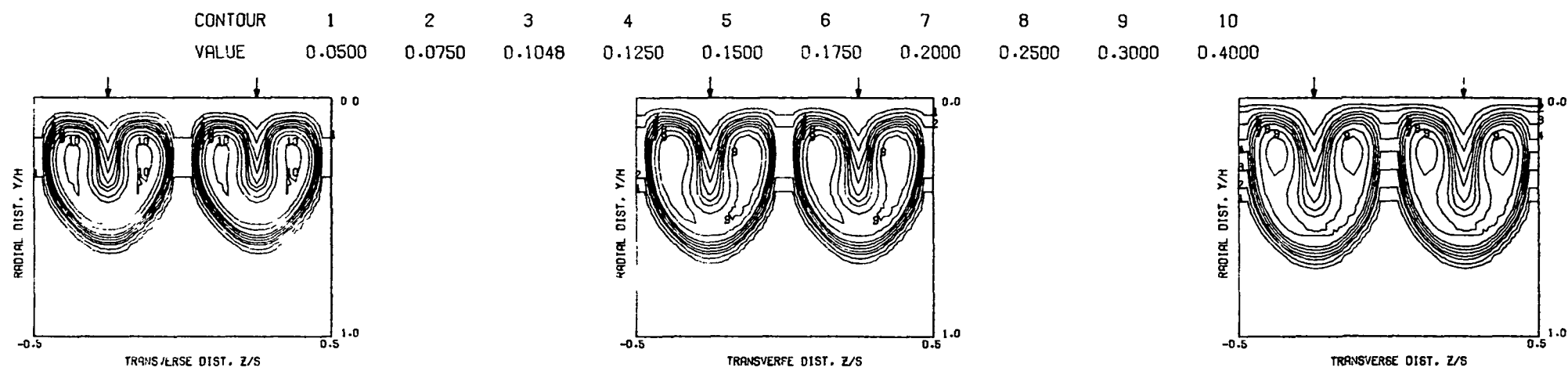


COMPARISON BETWEEN DATA AND PREDICTIONS FOR TEST 12, 22X27X33, OPPOSED STAGGERED JETS, J = 26.41, S/D = 4.00, H/D = 4.00

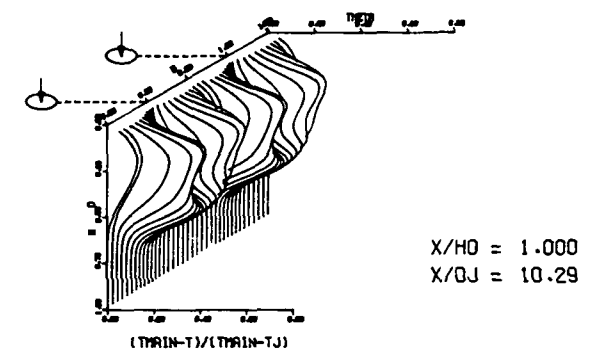
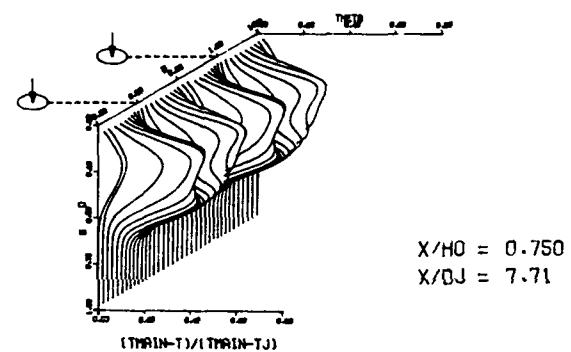
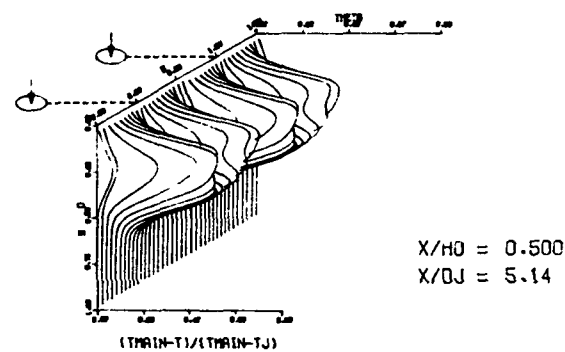
Figure 52. Comparison Between Predicted and Measured Velocity Distributions for Test Case 12 - Table 1.

FOLDOUT FRAME

2 FOLDOUT FRAME

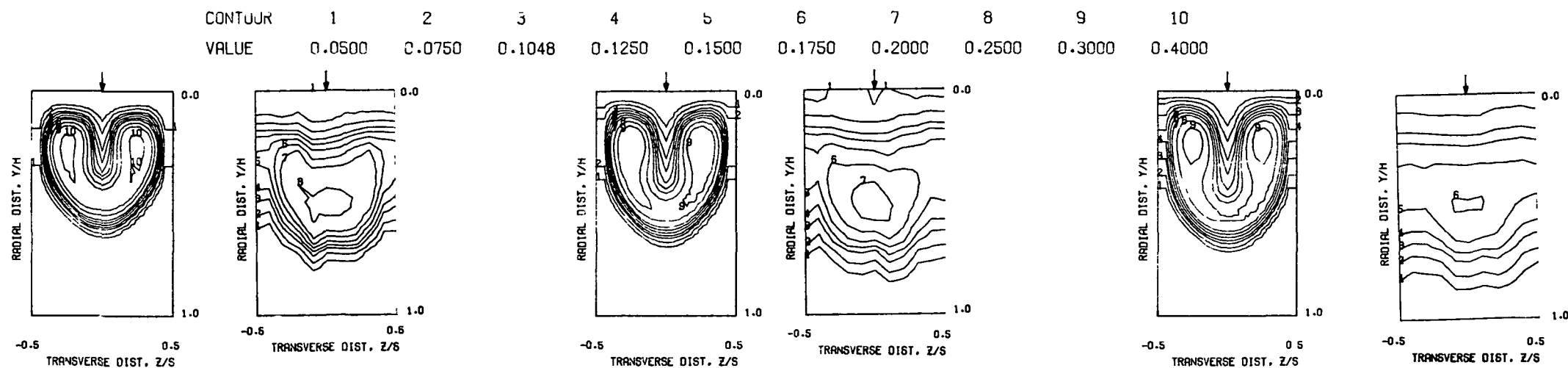


PREDICTED THETA CONTOURS FOR TEST NO. 1, $T_M=CONST$, $J=28.37$, $S/D=4.0$, $H/D=8.0$



PREDICTED THETA DISTRIBUTIONS FOR TEST NO. 13, $T_M=CONST$, $J=28.37$, $S/D=4.0$, $H/D=8.0$

Figure 53. Predicted Temperature Distributions for Test No. 13 - Table 2.



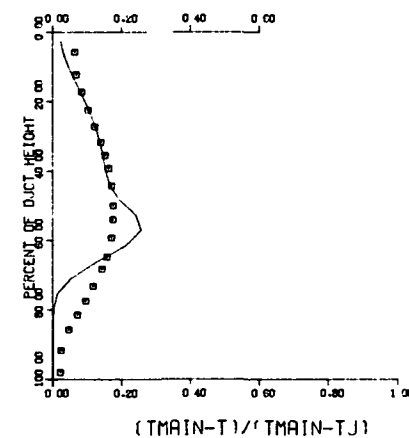
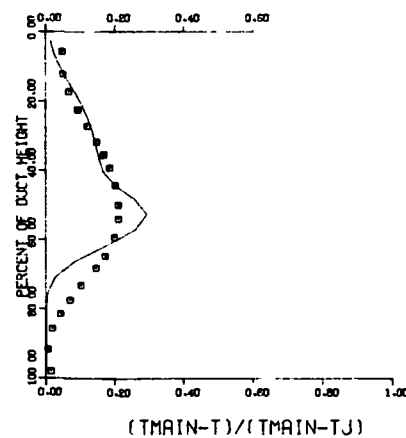
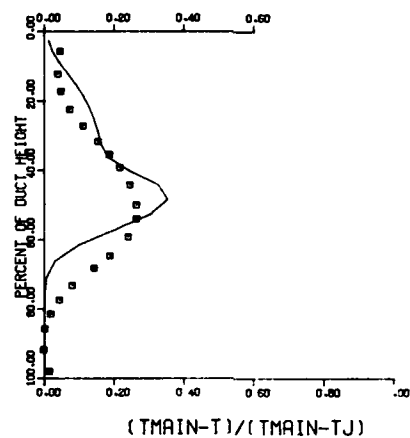
PREDICTED THETA CONTOURS FOR TEST NO. 1, $T_M = \text{CONST}$, $J = 28.37$, $S/D = 4.0$, $H/D = 8.0$

$S/DJ = 5.14$ $H/DJ = 10.29$ $VRATIO = 3.47$ $TRATIO = 0.464$ $DENRATIO = 2.192$ $T_{MAIN} = 651.4 \text{ K}$ $T_{JET} = 302.1 \text{ K}$ $THEB = 0.105$

$X/H = 0.50$ $X/DJ = 5.14$

$X/H = 0.75$ $X/DJ = 7.71$

$X/H = 1.00$ $X/DJ = 10.29$

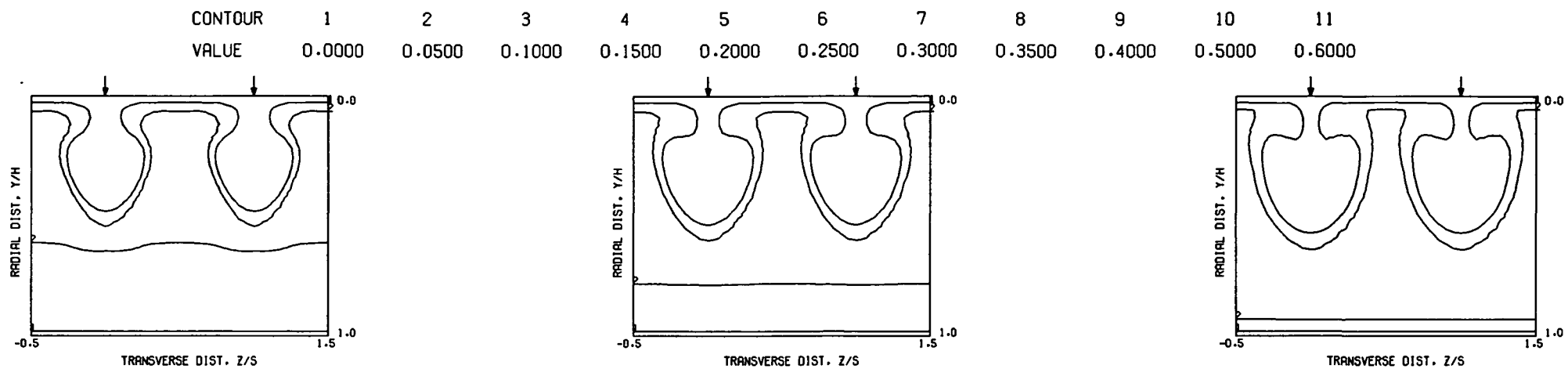


COMPARISON BETWEEN DATA AND PREDICTIONS FOR TEST 13, $T_M = \text{CONST}$, SINGLE SIDED INJECTION, $J = 28.37$, $S/D = 4.00$, $H/D = 8.00$

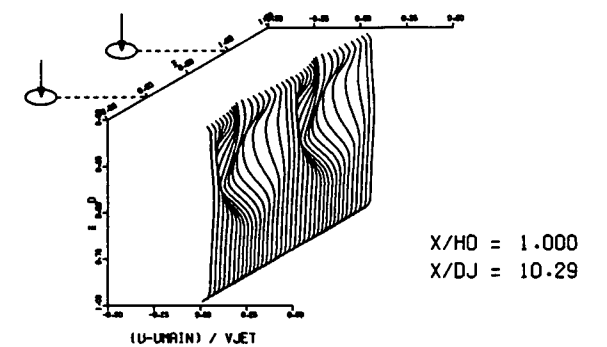
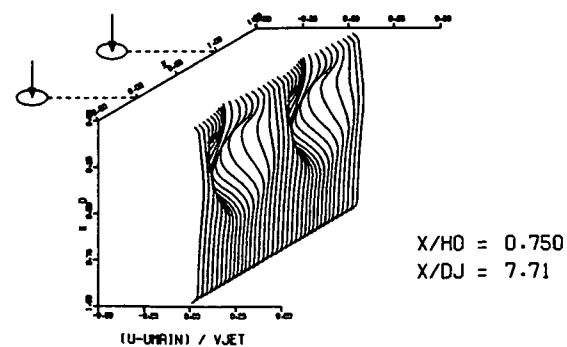
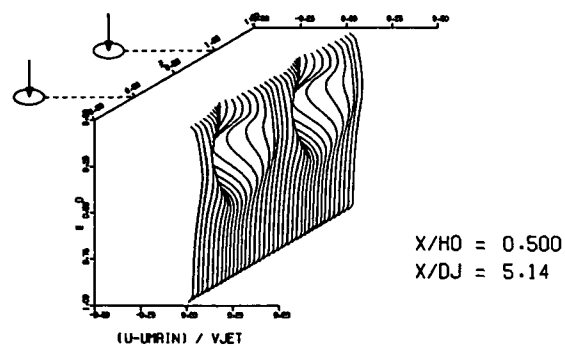
Figure 54. Comparison Between Predicted and Measured Temperature Distributions for Test No. 13 - Table 2.

FOLDOUT FRAME

FOLDOUT FRAME

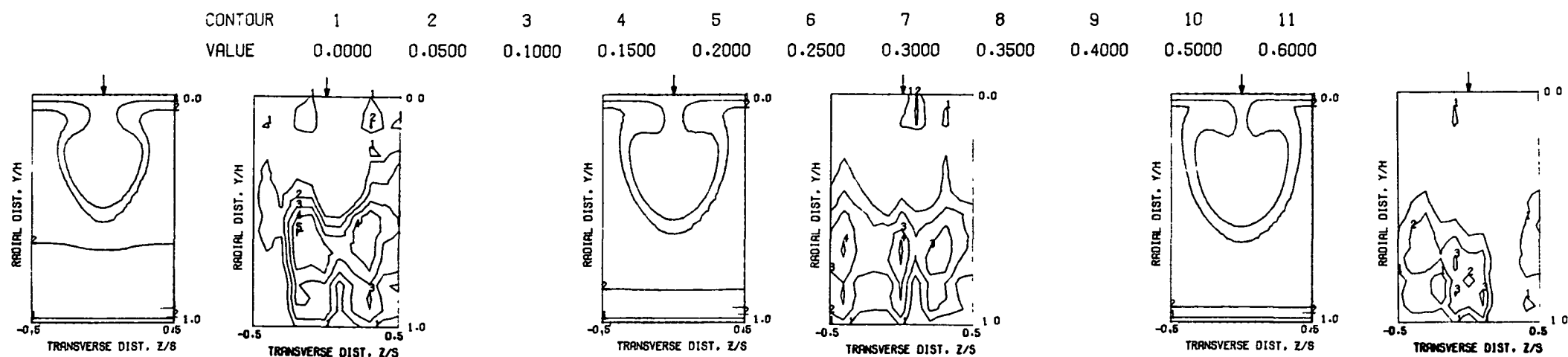


PREDICTED VELOCITY CONTOURS FOR TEST NO. 136X29X19, $J=28.37$, $S/D=4.00$, $H/D=8.00$



PREDICTED VELOCITY DISTRIBUTIONS FOR TEST 136X29X19, $J=28.37$, $S/D=4.00$, $H/D=8.00$

Figure 55. Predicted Velocity Distributions for Test No. 13 - Table 2.



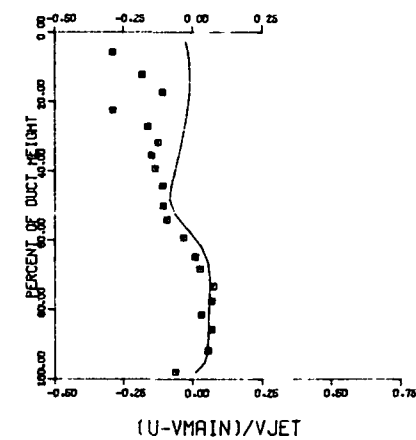
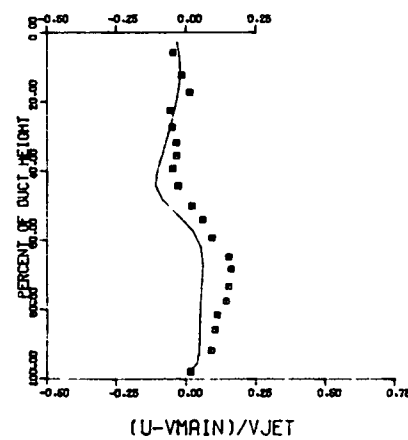
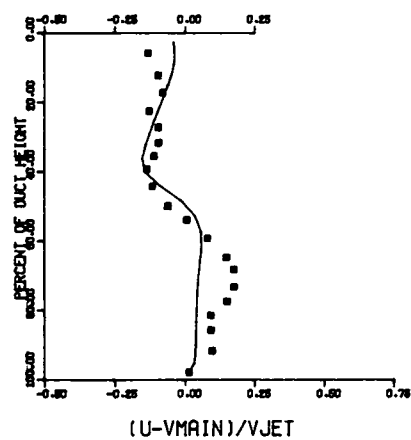
PREDICTED VELOCITY CONTOURS FOR TEST NO. 1, $T_M = \text{CONST}$, $J = 28.37$, $S/D = 4.00$, $H/D = 8.00$

$S/DJ = 5.14$ $H/DJ = 10.29$ $VRATIO = 3.47$ $TRATIO = 0.464$ $DENRATIO = 2.192$ $T_{MAIN} = 651.4 \text{ K}$ $T_{JET} = 302.1 \text{ K}$ $T_{HEB} = 0.105$

$X/H = 0.50$ $X/DJ = 5.14$

$X/H = 0.75$ $X/DJ = 7.71$

$X/H = 1.00$ $X/DJ = 10.29$

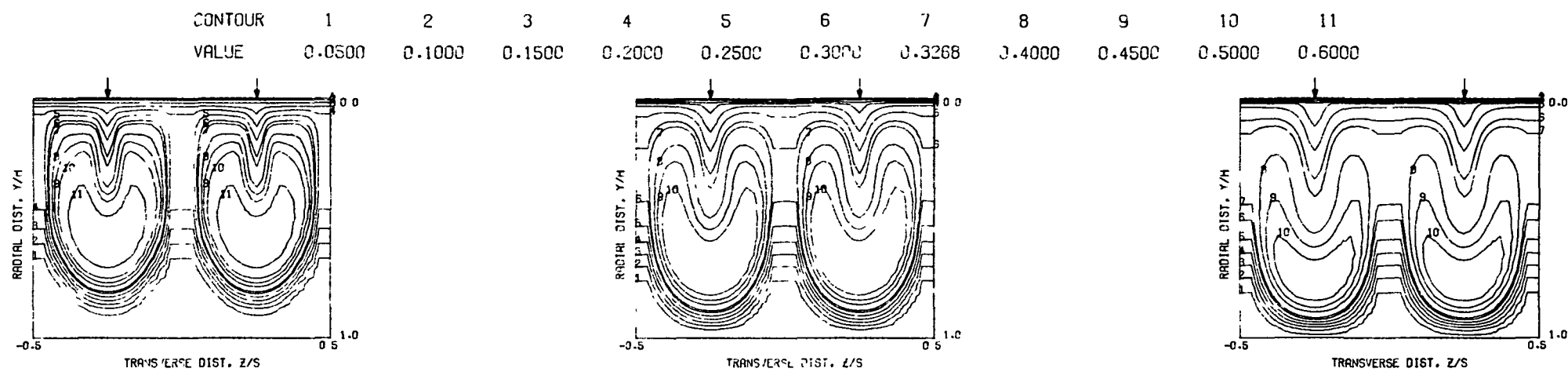


COMPARISON BETWEEN DATA AND PREDICTIONS FOR TEST 13, $T_M = \text{CONST}$, SINGLE SIDED INJECTION $J = 28.37$, $S/D = 4.00$, $H/D = 8.00$

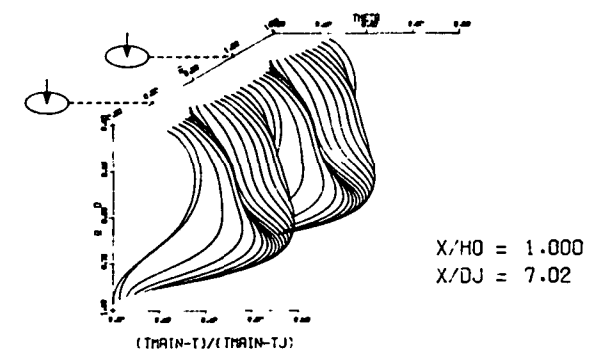
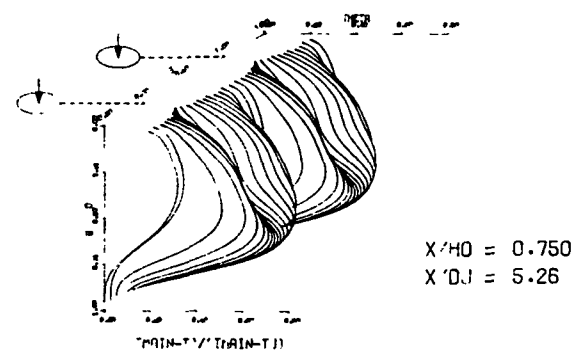
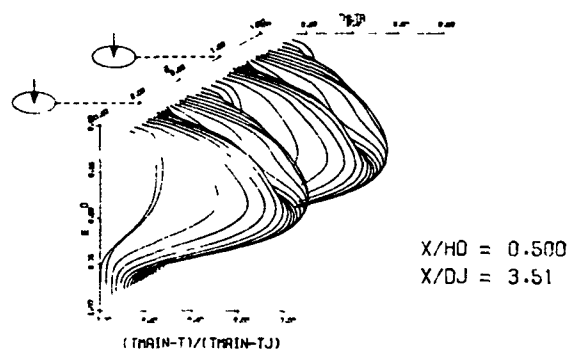
Figure 56. Comparison Between Predicted and Measured Velocity Distributions for Test No. 13 - Table 2.

FOLDOUT FRAME

FOLDOUT FRAME



PREDICTED THETA CONTOURS FOR TEST NO. 2, PLATE M3, $J=26.27$, $S/D=2.83$, $H/D=5.66$

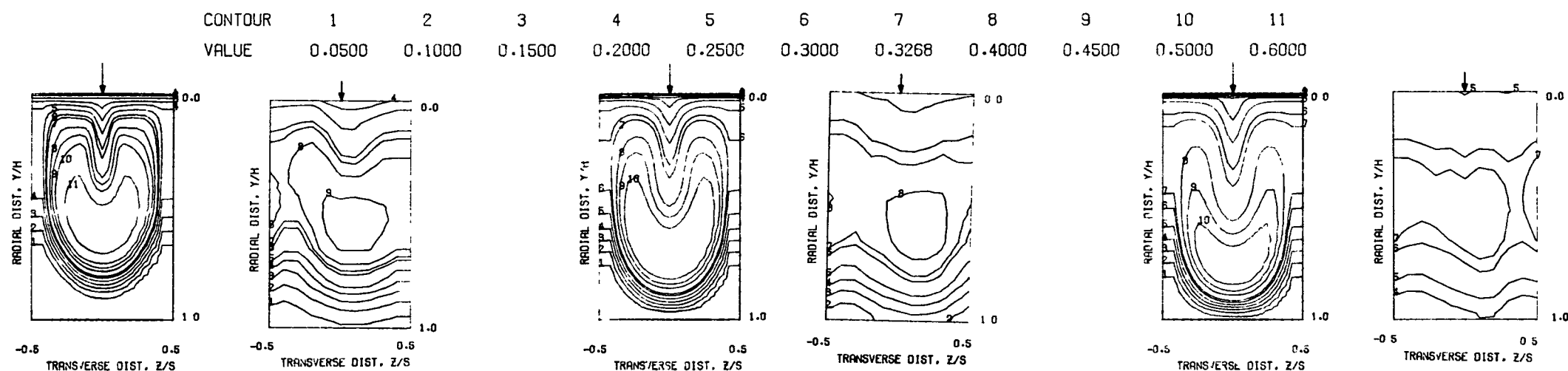


PREDICTED THETA DISTRIBUTIONS FOR TEST NO. 14, $TM=CONST$, $J=26.27$, $S/D=2.83$, $H/D=5.66$

Figure 57. Predicted Temperature Distributions for Test No. 14 - Table 2.

ORIGINAL PAGE IS
OF POOR QUALITY

ORIGINAL PAGE IS
OF POOR QUALITY

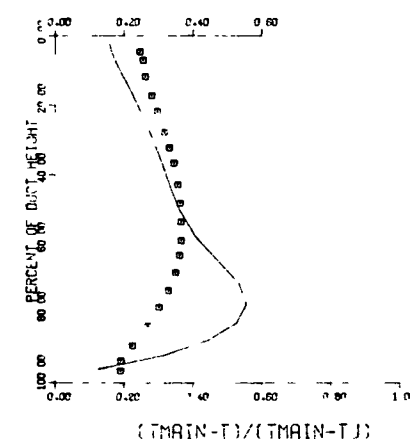
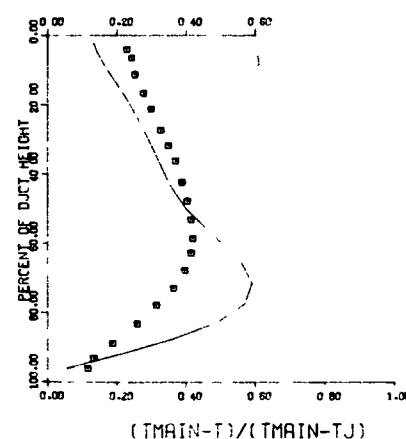
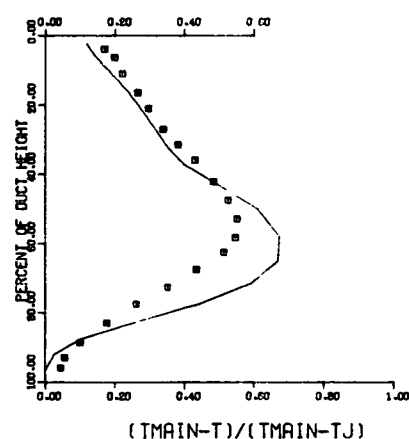


S/DJ = 3.51 H/DJ = 7.02 VRATIO = 3.47 TRATIO = 0.466 DENRATIO = 2.184 TMAIN = 665.9 K TJET = 310.4 K THEB = 0.327

X/H = 0.50 X/DJ = 3.51

X/H = 0.75 X/DJ = 5.26

X/H = 1.00 X/DJ = 7.02

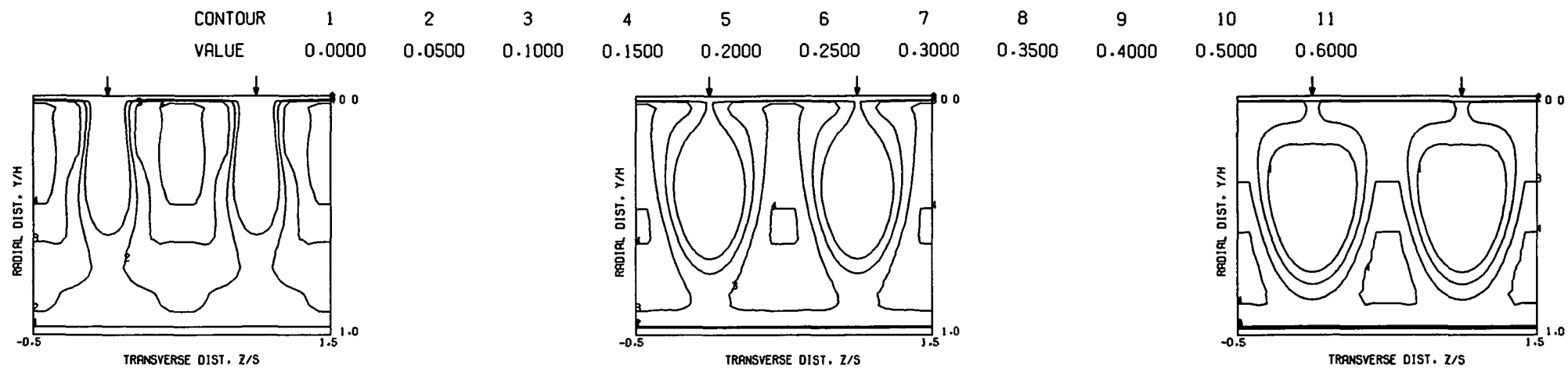


COMPARISON BETWEEN DATA AND PREDICTIONS FOR TEST 14, PLATE M3, AXIAL STAGED INJECTION, J = 26.27, S/D = 2.83, H/D = 5.66

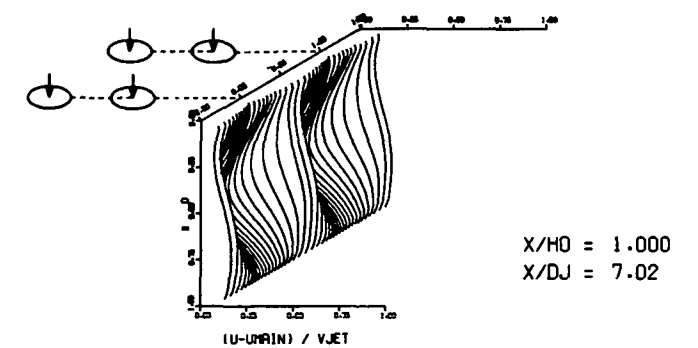
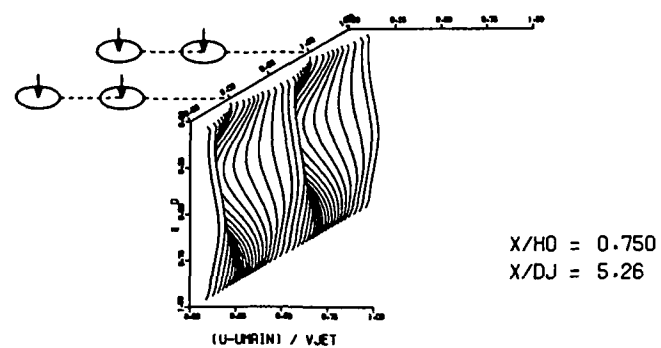
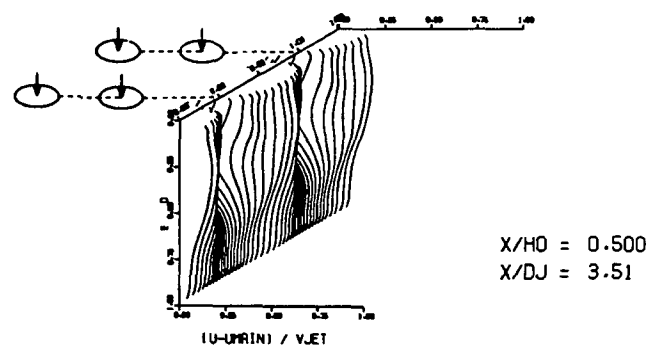
Figure 58. Comparison Between Predicted and Measured Temperature Distributions for Test No. 14 - Table 2.

FOLDOUT FRAME

FOLDOUT FRAME



PREDICTED VELOCITY CONTOURS FOR TEST NO. 2.41X23X21, J=26.27, S/D=2.83, H/D=5.66



PREDICTED VELOCITY DISTRIBUTIONS FOR TEST 14, PLATE M3, J=26.27, S/D=2.83, H/D=5.66

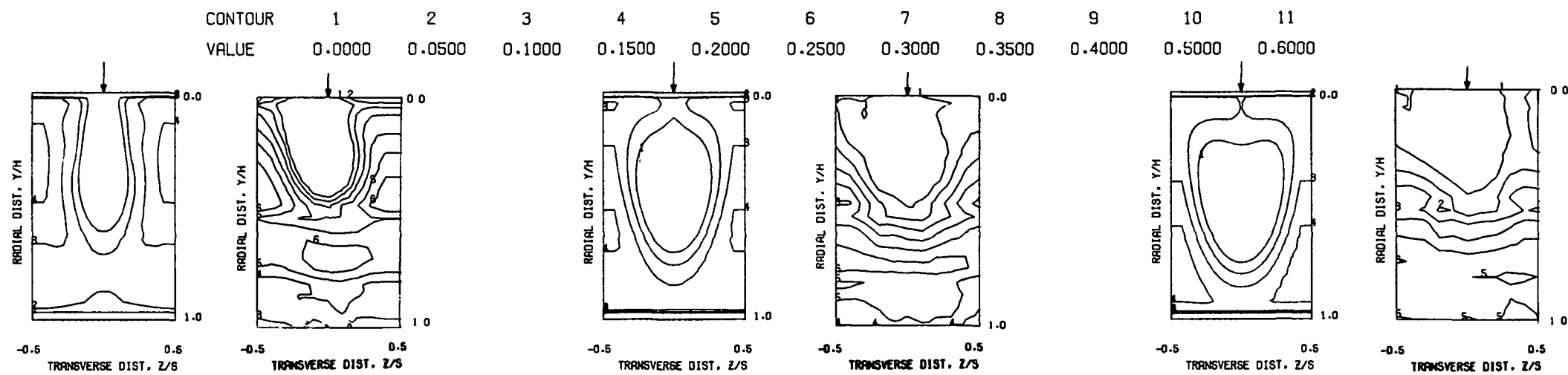
Figure 59. Predicted Velocity Distributions for Test No. 14 - Table 2.

FOLDOUT FRAME

2 FOLDOUT FRAME

ORIGINAL PAGE IS
OF POOR QUALITY

ORIGINAL PAGE IS
OF POOR QUALITY

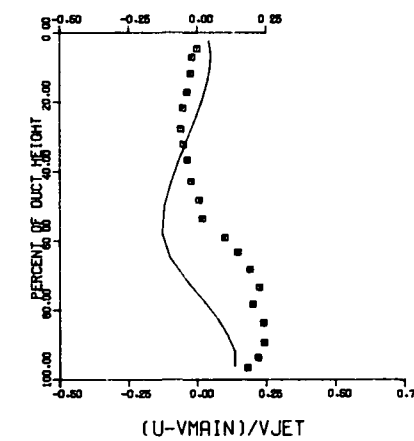
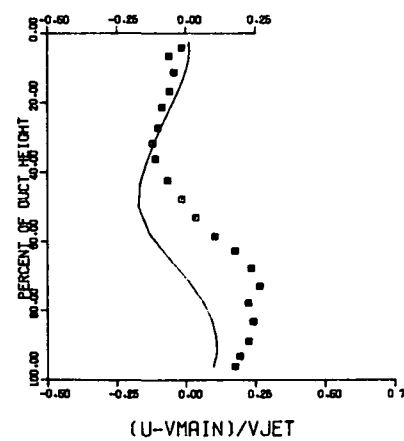
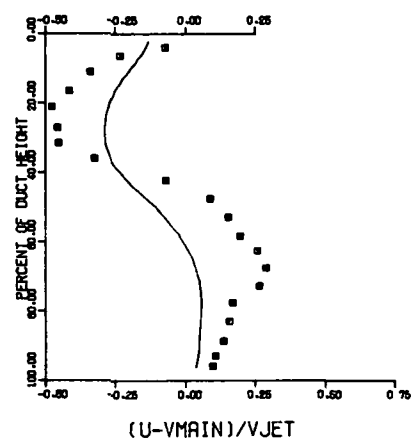


$S/DJ = 3.51$ $H/DJ = 7.02$ $VRATIO = 3.47$ $TRATIO = 0.466$ $DENRATIO = 2.184$ $TMAIN = 665.9$ $TJET = 310.4$ $THEB = 0.327$

$X/H = 0.50$ $X/DJ = 3.51$

$X/H = 0.75$ $X/DJ = 5.26$

$X/H = 1.00$ $X/DJ = 7.02$

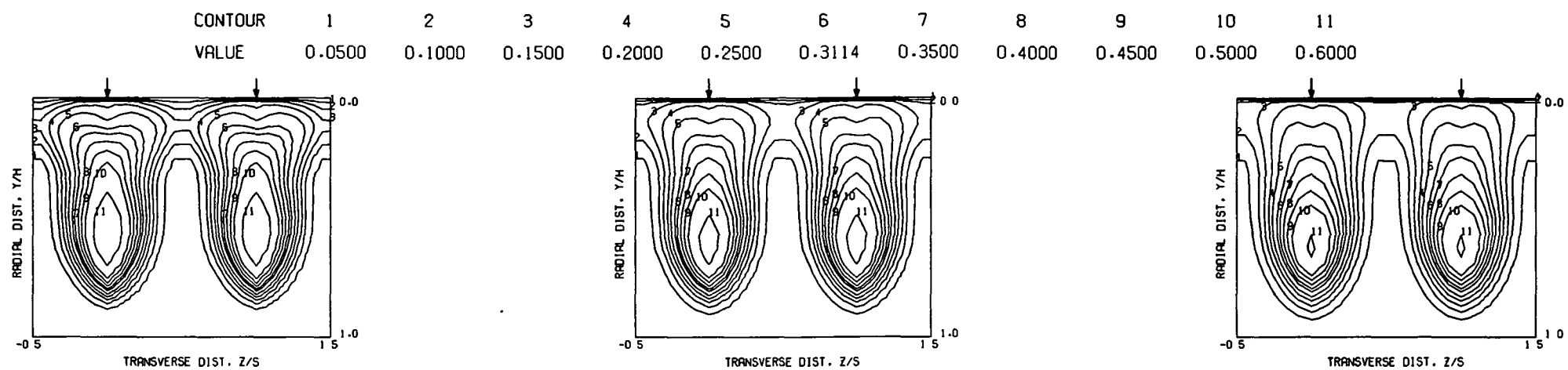


COMPARISON BETWEEN DATA AND PREDICTIONS FOR TEST 14, PLATE M3, AXIALLY STAGED INJECTION $J = 26.27$, $S/D = 2.83$, $H/D = 5.66$

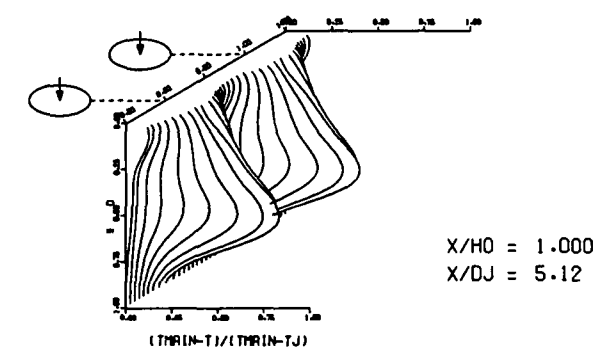
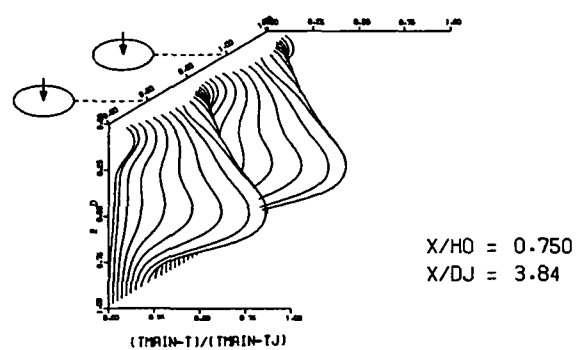
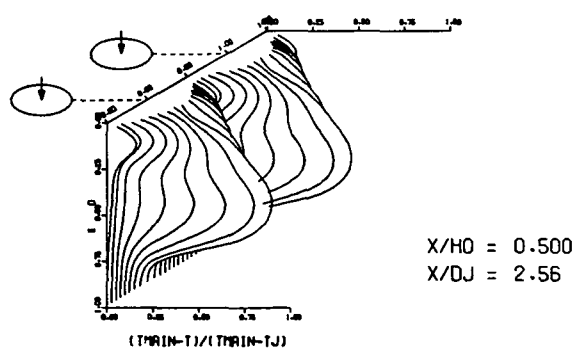
Figure 60. Comparison Between Predicted and Measured Velocity Distributions for Test No. 14 - Table 2.

FOLDOUT FRAME

FOLDOUT FRAME



PREDICTED THETA CONTOURS FOR TEST NO. 3, CONV DUCT, $J=26.36$, $S/D=2.00$, $H/D=4.00$

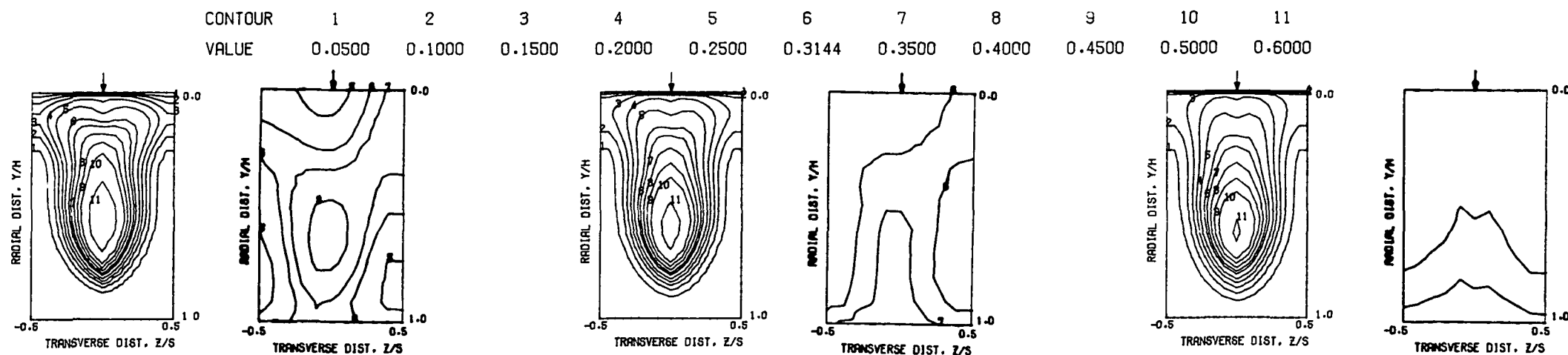


PREDICTED THETA DISTRIBUTIONS FOR TEST NO. 15, 42X28X17, $J=26.36$, $S/D=2.00$, $H/D=4.00$

Figure 61. Predicted Temperature Distributions for Test No. 15 - Table 2.

ORIGINAL PAGE IS
OF POOR QUALITY

ORIGINAL PAGE IS
OF POOR QUALITY



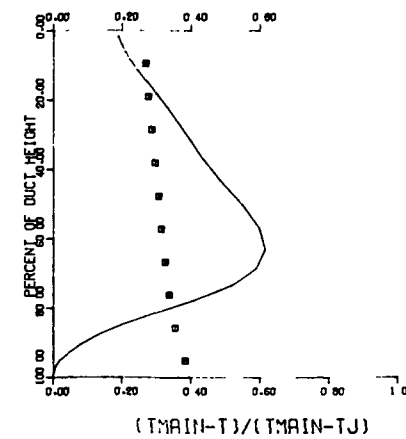
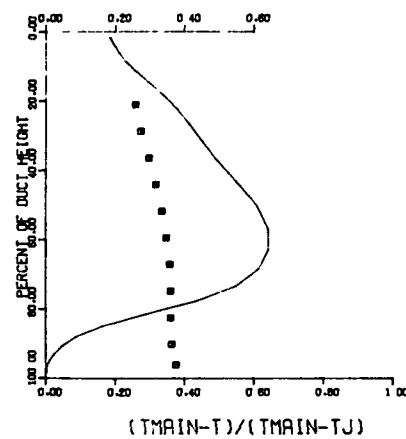
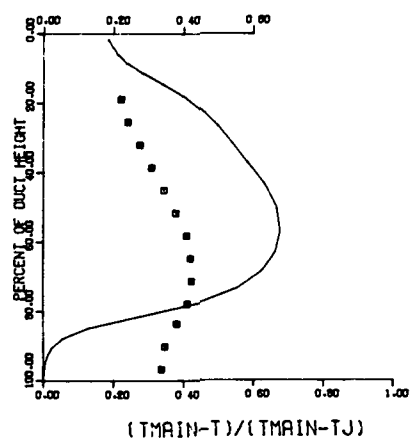
PREDICTED THETA CONTOURS FOR TEST NO. 3, CONV DUCT, $J=26.36$, $S/D=2.00$, $H/D=4.00$

$S/DJ = 2.56$ $H/DJ = 5.12$ $VRATIO = 3.44$ $TRATIO = 0.456$ $DENRATIO = 2.225$ $TMAIN = 650.8 \text{ K}$ $TJET = 296.9 \text{ K}$ $THEB = 0.314$

$X/H = 0.50$ $X/DJ = 2.56$

$X/H = 0.75$ $X/DJ = 3.84$

$X/H = 1.00$ $X/DJ = 5.12$

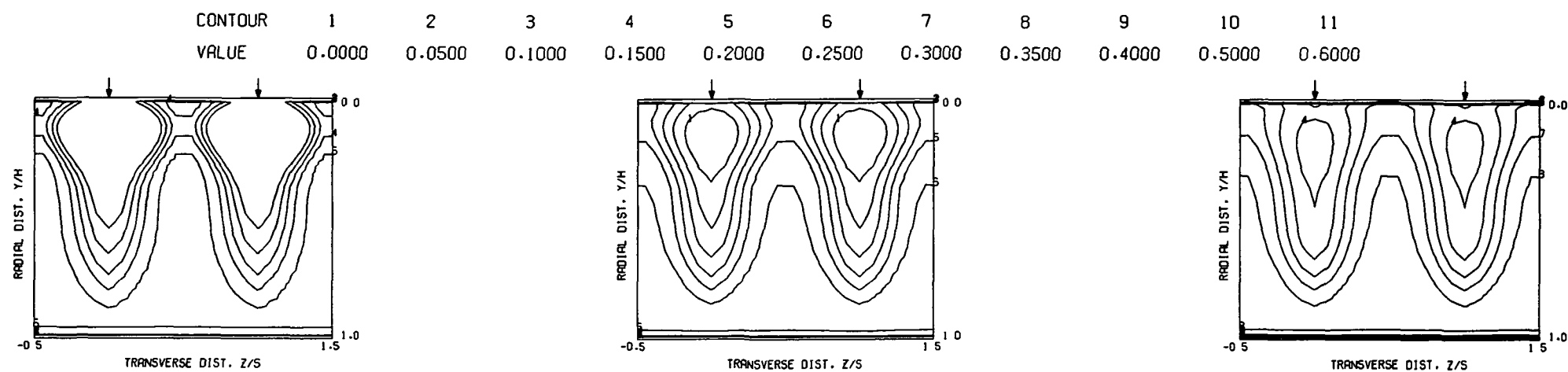


COMPARISON BETWEEN DATA AND PREDICTIONS FOR TEST 15, CONV DUCT, INCLINED WALL INJECTION, $J = 26.36$, $S/D = 2.00$, $H/D = 4.00$

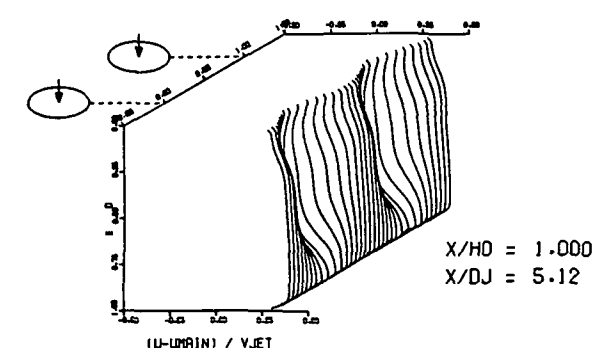
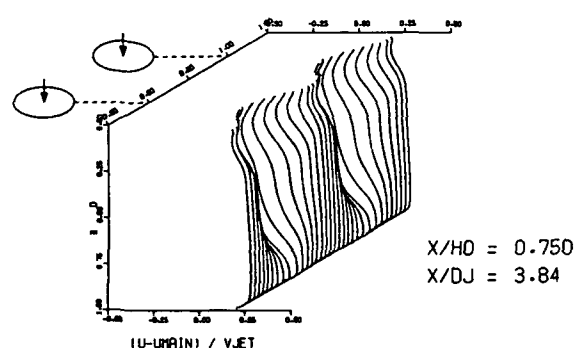
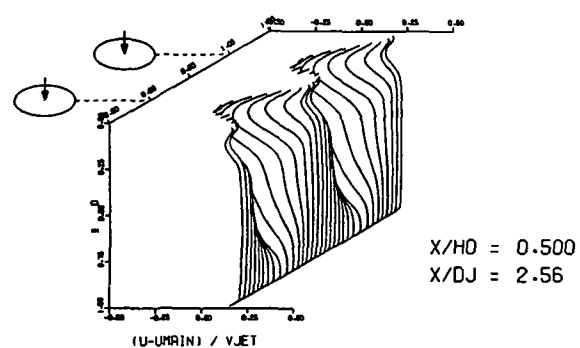
Figure 62. Comparison Between Predicted and Measured Temperature Distributions for Test No. 15 - Table 2.

FOLDOUT FRAME

2 FOLDOUT FRAME



PREDICTED VELOCITY CONTOURS FOR TEST NO. 3, CONV DUCT, $J=26.36$, $S/D=2.00$, $H/D=4.00$

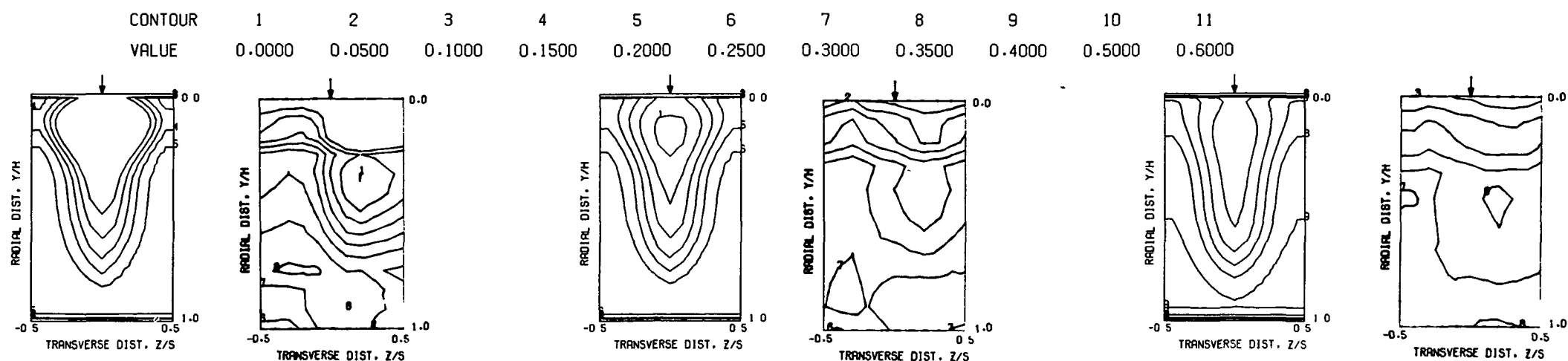


PREDICTED VELOCITY DISTRIBUTIONS FOR TEST NO. 15, 42X28X17, $J=26.36$, $S/D=2.00$, $H/D=4.00$

Figure 63. Predicted Velocity Distributions for Test No. 15 - Table 2.

FOLDOUT FRAME

2 FOLDOUT FRAME

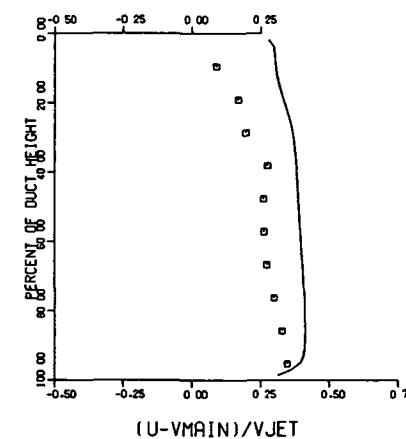
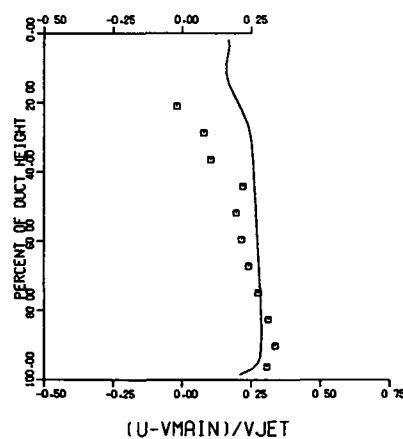
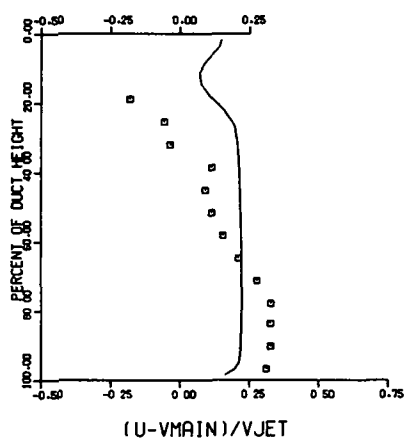


S/DJ = 2.56 HO/DJ = 5.12 VRATIO = 3.44 TRATIO = 0.456 DENRATIO = 2.225 TMAIN = 361.6 K TJET = 164.9 K THEB = 0.314

X/H = 0.50 X/DJ = 2.56

X/H = 0.75 X/DJ = 3.84

X/H = 1.00 X/DJ = 5.12

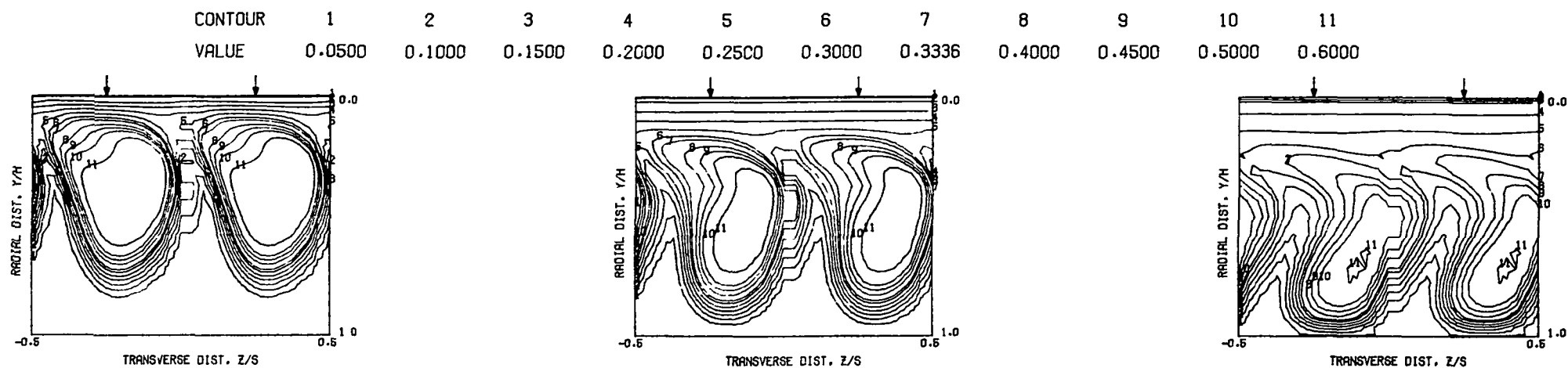


COMPARISON BETWEEN DATA AND PREDICTIONS FOR TEST 15, 42X28X17, CONV DUCT, SLANT WALL JETS, J = 26.36, S/D = 2.00, H/D = 4.00

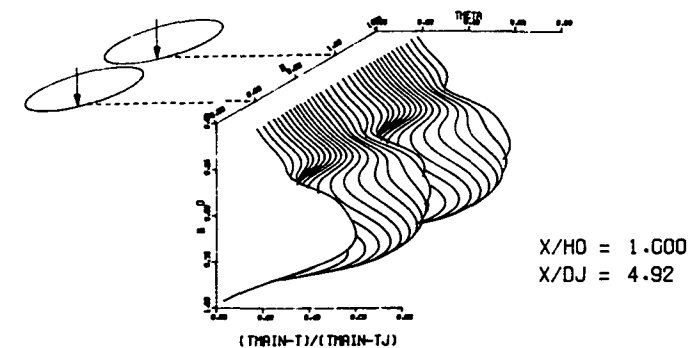
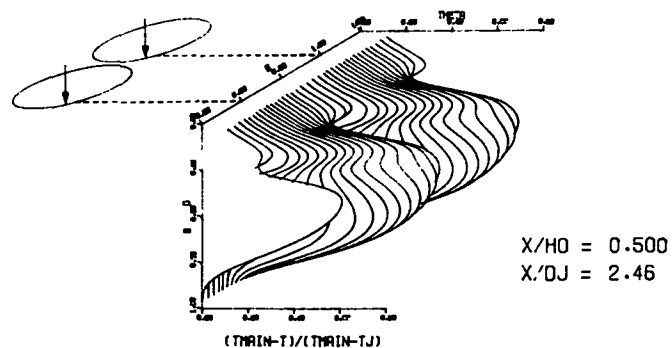
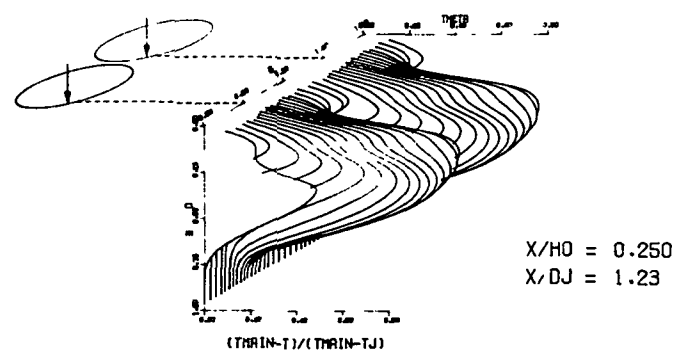
Figure 64. Comparison Between Predicted and Measured Velocity Distributions for Test No. 15 - Table 2.

FOLDOUT FRAME

FOLDOUT FRAME



PREDICTED THETA CONTOURS FOR TEST NO. 4, 45 DEG SLOT, $J=27.13$, $S/D=2.00$, $H/D=4.00$



PREDICTED THETA DISTRIBUTIONS FOR TEST NO. 16, 45 DEG SLOT, $J=27.13$, $S/D=2.00$, $H/D=4.00$

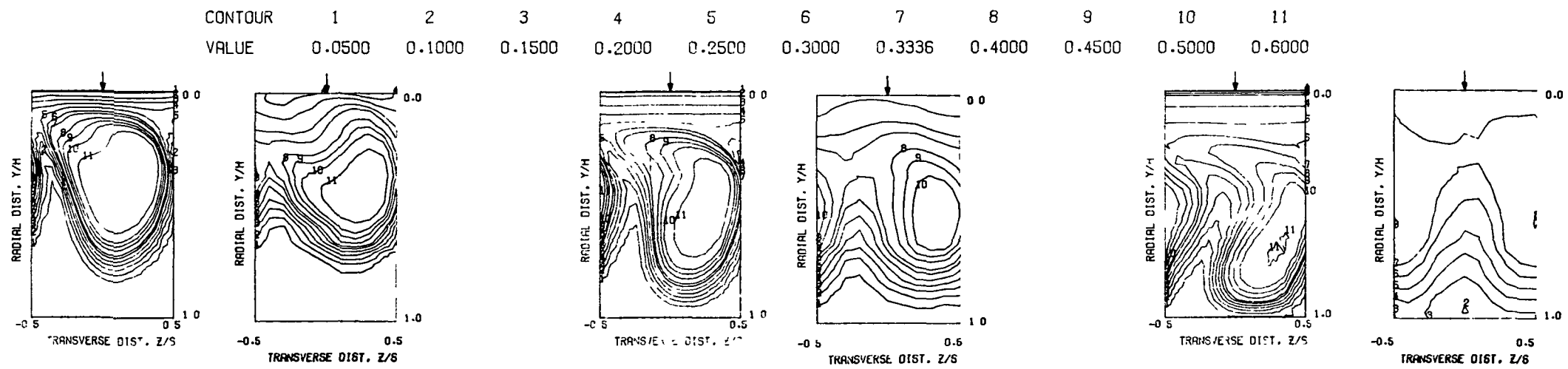
Figure 65. Predicted Temperature Distributions for Test No. 16 - Table 2.

FOLDOUT FRAME

2 FOLDOUT FRAME

ORIGINAL PAGE IS
OF POOR QUALITY

ORIGINAL PAGE IS
OF POOR QUALITY

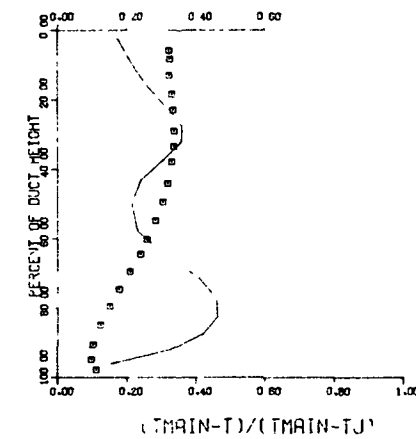
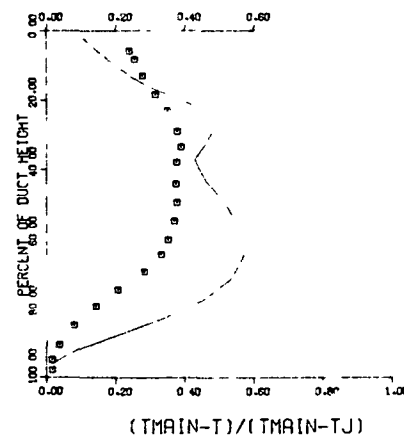
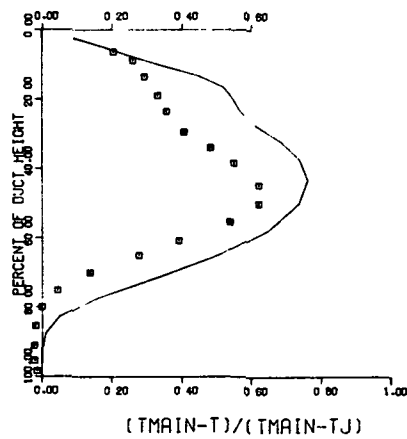


$S/DJ = 2.46$ $H/DJ = 4.92$ $VRATIO = 3.52$ $TRATIO = 0.466$ $DENRATIO = 2.186$ $TMAIN = 615.5 \text{ K}$ $TJET = 314.5 \text{ K}$ $THEB = 0.334$

$X/H = 0.25$ $X/DJ = 1.23$

$X/H = 0.50$ $X/DJ = 2.46$

$X/H = 1.00$ $X/DJ = 4.92$



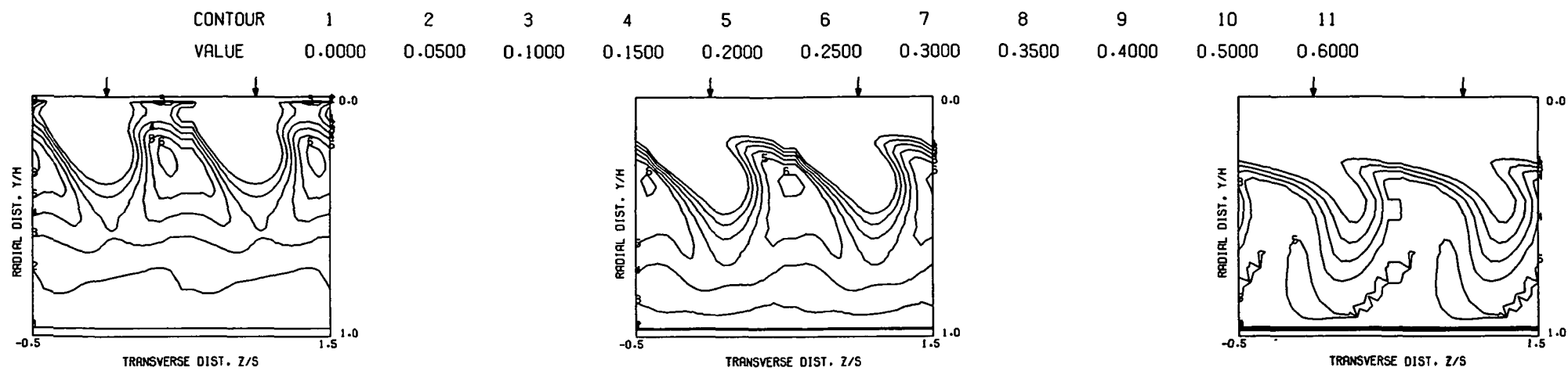
COMPARISON BETWEEN DATA AND PREDICTIONS FOR TEST 16.45 DEG SLOT, SINGLE SIDED INJECTION $J = 27.13$, $S/D = 2.00$, $H/D = 4.00$

Figure 66. Comparison Between Predicted and Measured Temperature Distributions for Test No. 16 - Table 2.

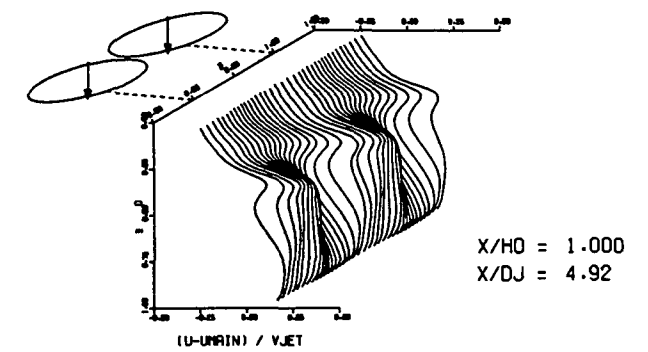
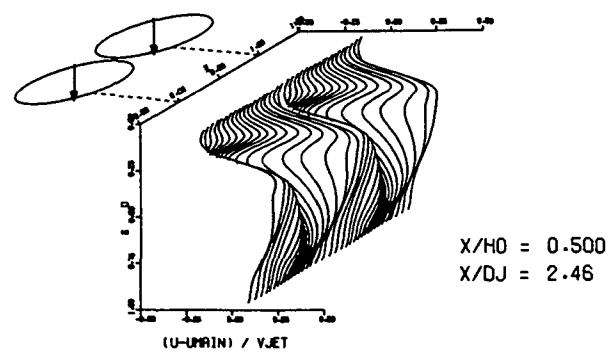
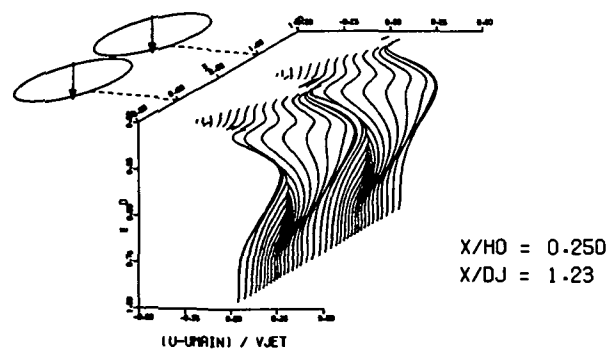
FOLDOUT FRAME

2 FOLDOUT FRAME

ORIGINAL PAGE IS
OF POOR QUALITY



PREDICTED VELOCITY CONTOURS FOR TEST NO. 4.45X23X19, $J=27.13$, $S/D=2.00$, $H/D=4.00$

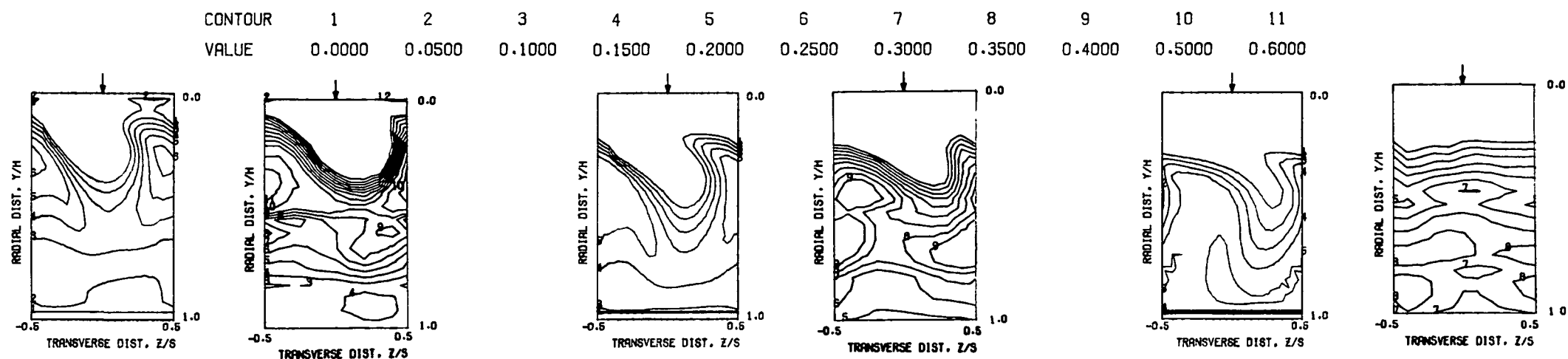


PREDICTED VELOCITY DISTRIBUTIONS FOR TEST 16, 45 DEGREE SLOT, $J=27.13$, $S/D=2.00$

Figure 67. Predicted Velocity
Distributions for Test No. 16 - Table 2.

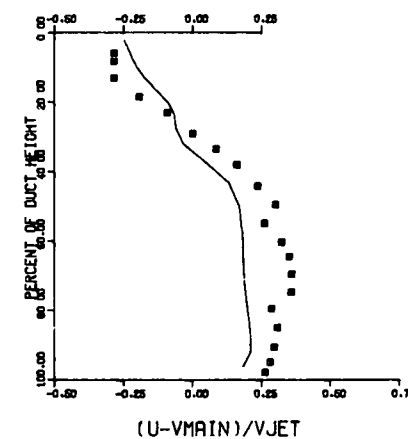
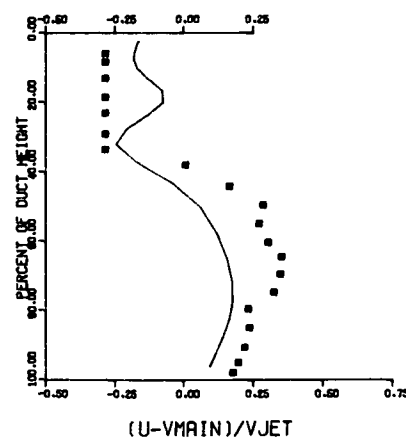
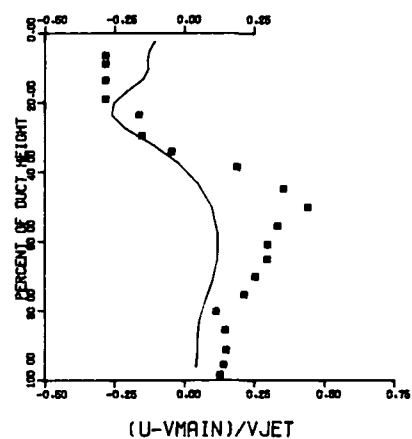
FOLDOUT FRAME

2 FOLDOUT FRAME



PREDICTED VELOCITY CONTOURS FOR TEST NO. 4.45 DEG SLOT, J=27.13, S/D=2.00, H/D=4.00

S/DJ = 2.46 H/DJ = 4.92 VRATIO = 3.52 TRATIO = 0.466 DENRATIO = 2.186 TMAIN = 675.5 K TJET = 314.5 K THEB = 0.334
X/H = 0.25 X/DJ = 1.23 X/H = 0.50 X/DJ = 2.46 X/H = 1.00 X/DJ = 4.92

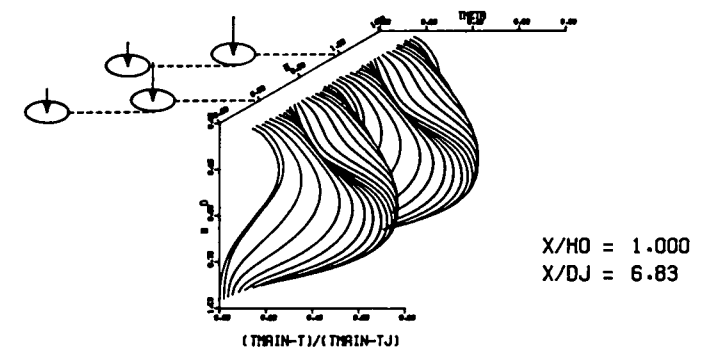
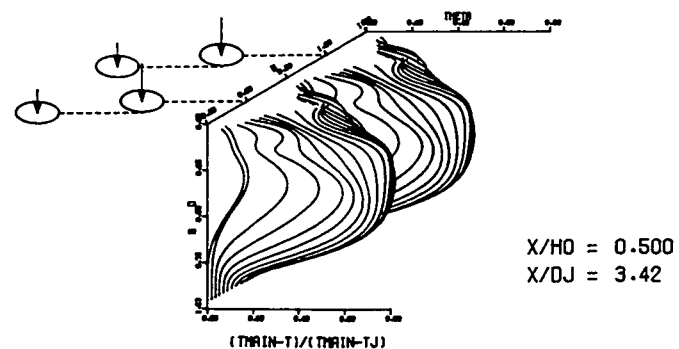
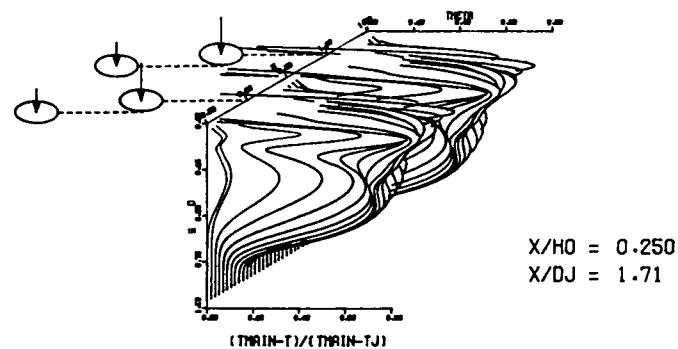
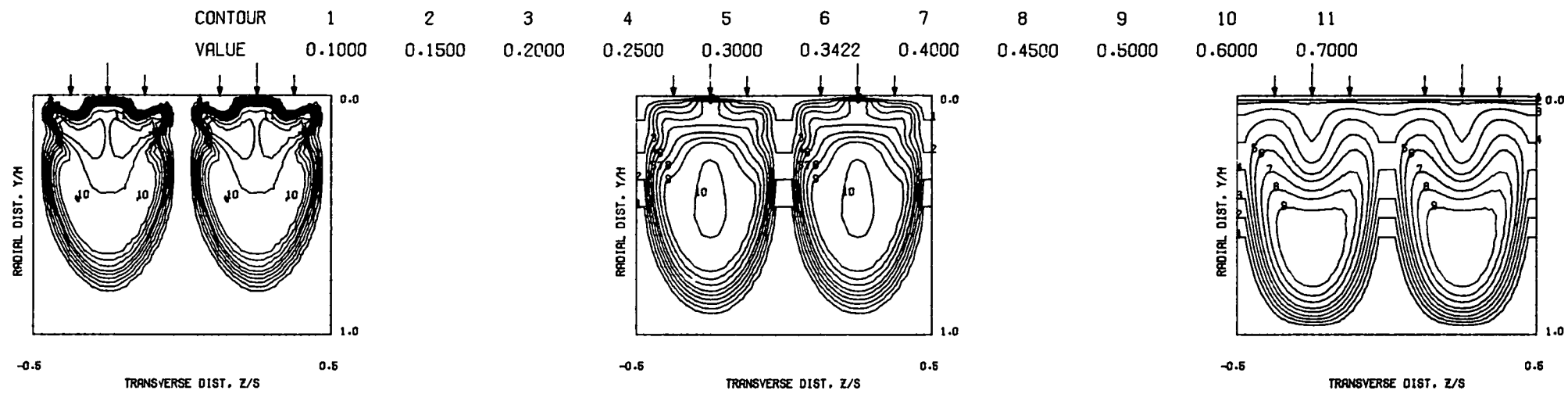


COMPARISON BETWEEN DATA AND PREDICTIONS FOR TEST 16, TM=CONST, 45 DEG SLOT (ONE-SIDED) J = 27.13 , S/D = 2.00 , H/D = 4.00

Figure 68. Comparison Between Predicted and Measured Velocity Distributions for Test No. 16 - Table 2.

FOLDOUT FRAME

2 FOLDOUT FRAME

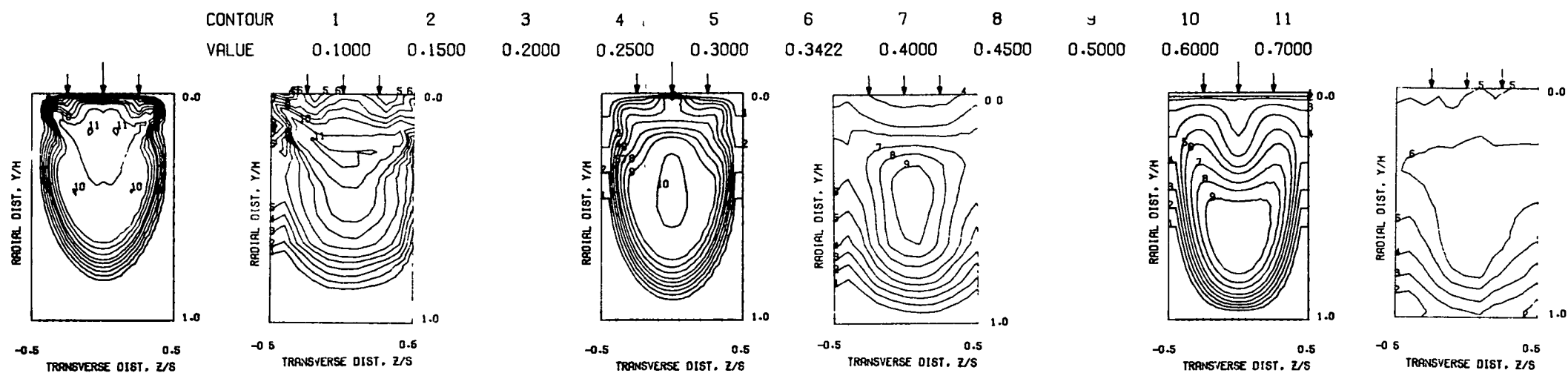


PREDICTED THETA DISTRIBUTIONS FOR TEST NO. 17, PLATE M5, $J=26.79$, $S/D=2.83$, $H/D=5.66$

Figure 69. Predicted Temperature Distributions for Test No. 17 - Table 2.

FOLDOUT FRAME

2 FOLDOUT FRAME



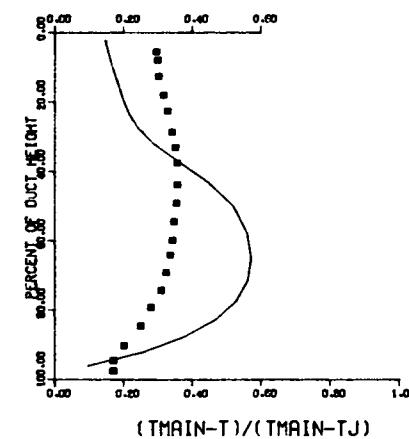
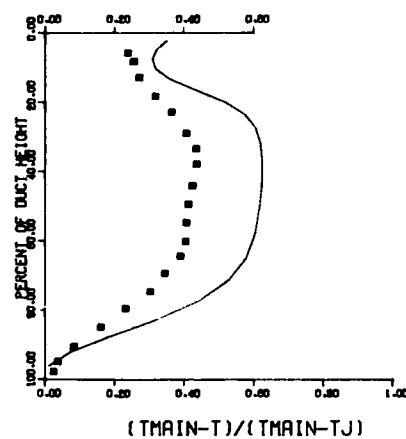
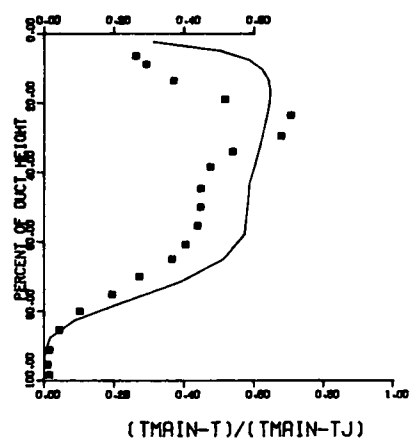
PREDICTED THETA CONTOURS FOR TEST NO. 5, PLATE M5, $J=26.79$, $S/D=2.83$, $H/D=5.66$

$S/DJ = 3.42$ $HO/DJ = 6.83$ $VRATIO = 3.49$ $TRATIO = 0.463$ $DENRATIO = 2.203$ $TMAIN = 677.2 \text{ K}$ $TJET = 313.5 \text{ K}$ $THEB = 0.342$

$X/H = 0.25$ $X/DJ = 1.71$

$X/H = 0.50$ $X/DJ = 3.42$

$X/H = 1.00$ $X/DJ = 6.83$



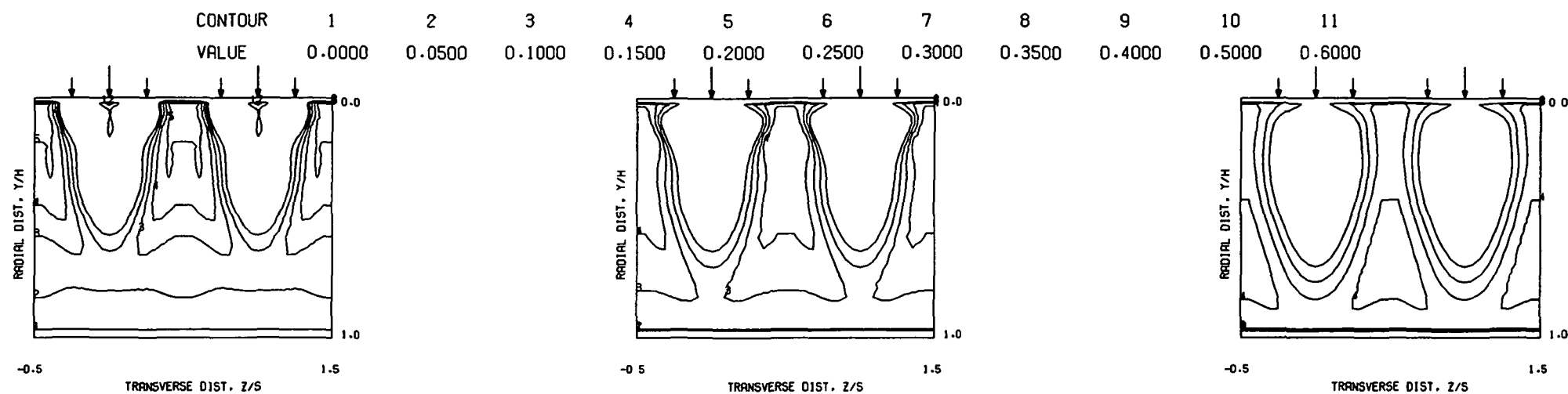
COMPARISON BETWEEN DATA AND PREDICTIONS FOR TEST 17, PLATE M5, AXIAL STAGED INJECTION

$J = 26.79$, $S/D = 2.83$, $H/D = 5.66$

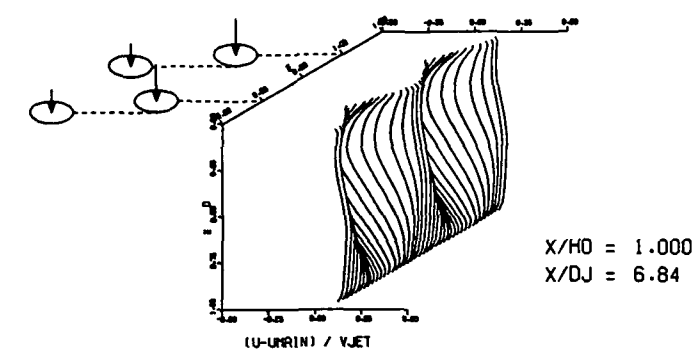
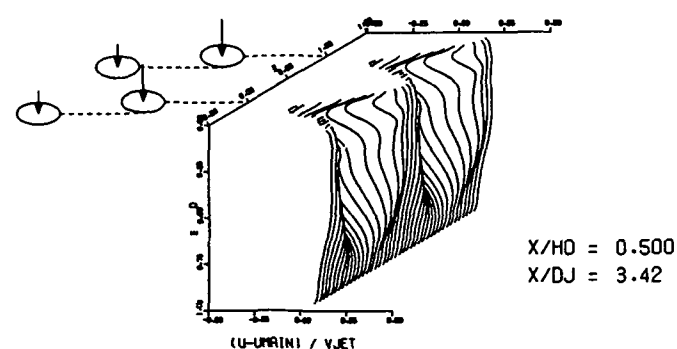
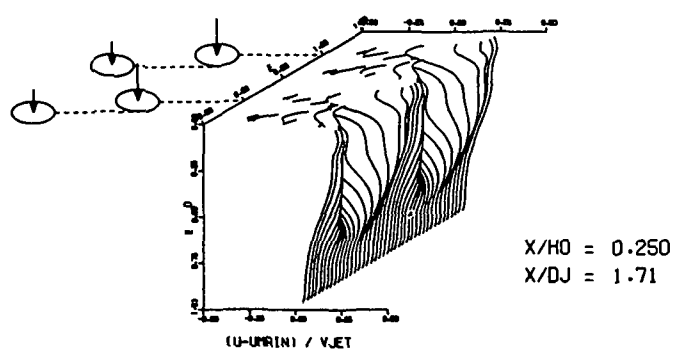
Figure 70. Comparison Between Predicted and Measured Temperature Distributions for Test No. 17 - Table 2.

FOLDOUT FRAME

FOLDOUT FRAME



PREDICTED VELOCITY CONTOURS FOR TEST NO. 5, 41X23X21, $J=26.79$, $S/D=2.83$, $H/D=5.66$



PREDICTED VELOCITY DISTRIBUTIONS FOR TEST NO. 17, 41X23X21, $J=26.79$, $S/D=2.83$, $H/D=5.66$

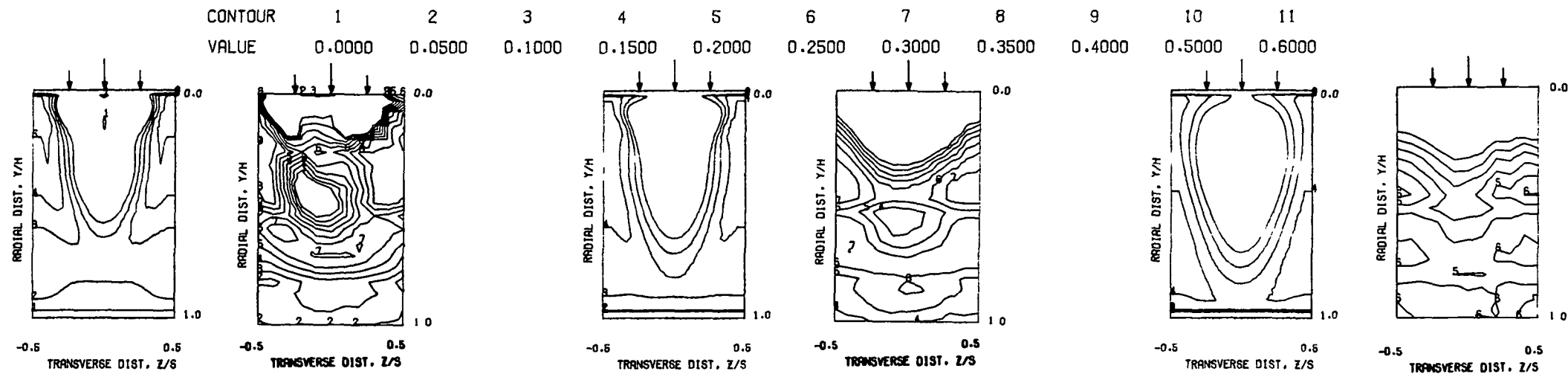
Figure 71. Predicted Velocity Distributions for Test No. 17 - Table 2.

FOLDOUT FRAME

FOLDOUT FRAME

ORIGINAL PAGE IS
OF POOR QUALITY

ORIGINAL PAGE IS
OF POOR QUALITY

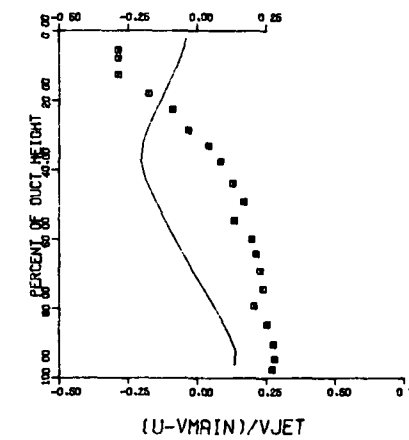
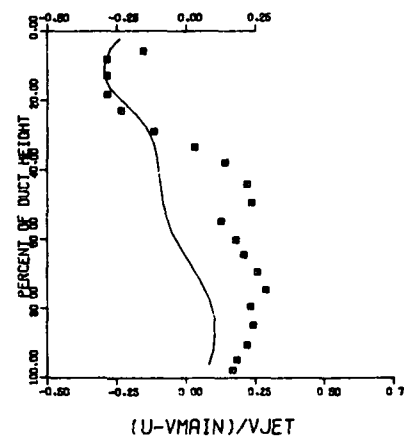
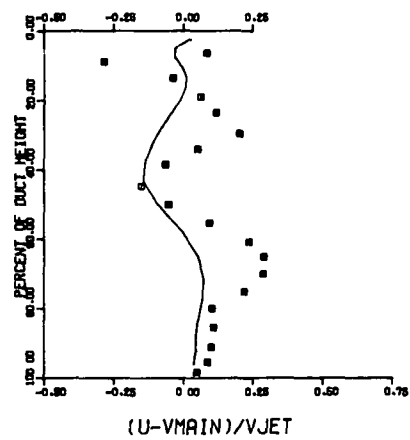


$S/DJ = 3.42$ $HO/DJ = 6.83$ $VRATIO = 3.49$ $TRATIO = 0.463$ $DENRATIO = 2.203$ $TMAIN = 677.2 \text{ K}$ $TJET = 313.5 \text{ K}$ $THEB = 0.342$

$X/H = 0.25$ $X/DJ = 1.71$

$X/H = 0.50$ $X/DJ = 3.42$

$X/H = 1.00$ $X/DJ = 6.83$



COMPARISON BETWEEN DATA AND PREDICTIONS FOR TEST 17, $TM=CONST$, AXIALLY STAGED INJECTION $J = 26.79$, $S/D = 2.83$, $H/D = 5.66$

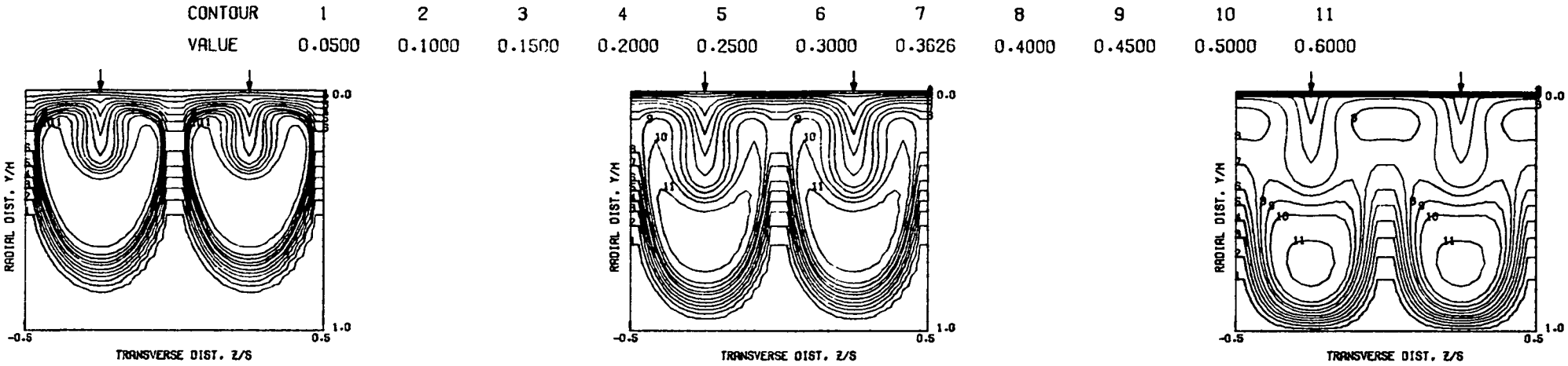
Figure 72. Comparison Between Predicted and Measured Velocity Distributions for Test No. 17 - Table 2.

FOLDOUT FRAME

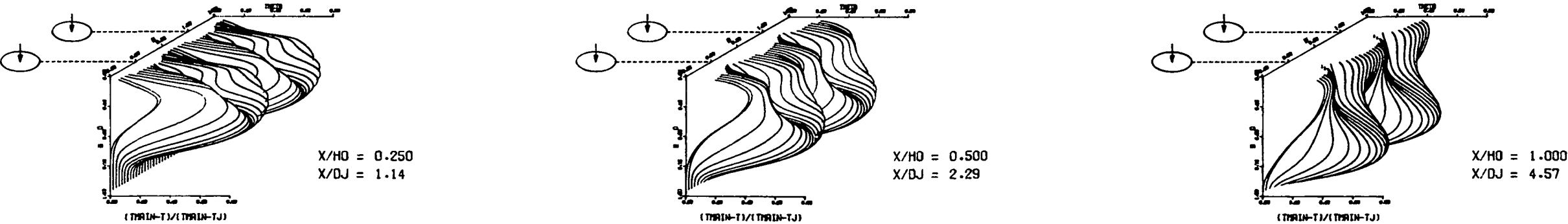
FOLDOUT FRAME

ORIGINAL PAGE IS
OF POOR QUALITY

ORIGINAL PAGE IS
OF POOR QUALITY



PREDICTED THETA CONTOURS FOR TEST NO. 6, $T_M=CONST$, $J=26.24$, $S/D=2.00$, $H/D=4.00$



PREDICTED THETA DISTRIBUTIONS FOR TEST NO. 18, $T_M=CONST$, $J=26.24$, $S/D=2.00$, $H/D=4.00$

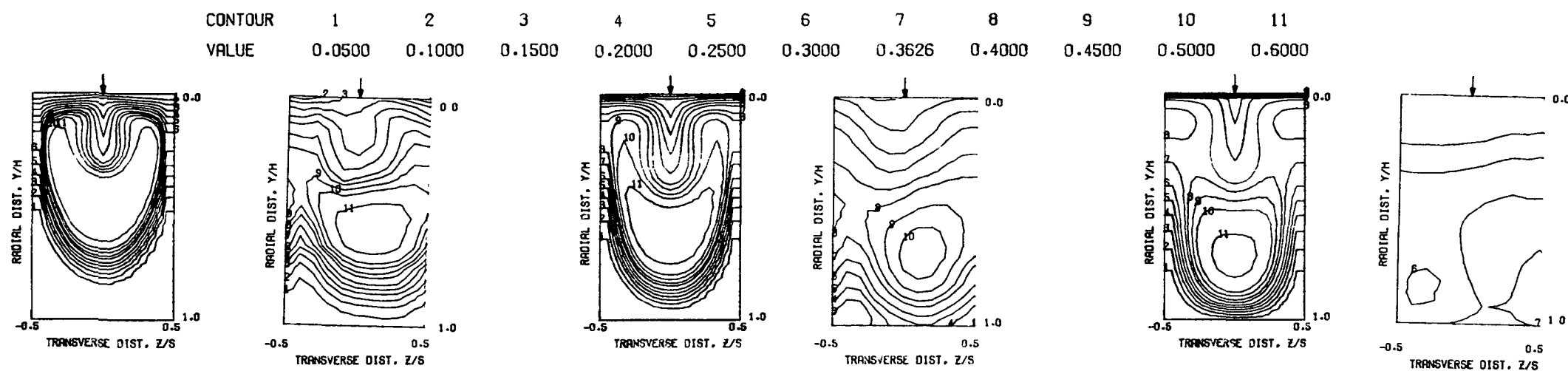
Figure 73. Predicted Temperature
Distributions for Test No. 18 - Table 2.

FOLDOUT FRAME

2 FOLDOUT FRAME

ORIGINAL PAGE IS
OF POOR QUALITY

ORIGINAL PAGE IS
OF POOR QUALITY



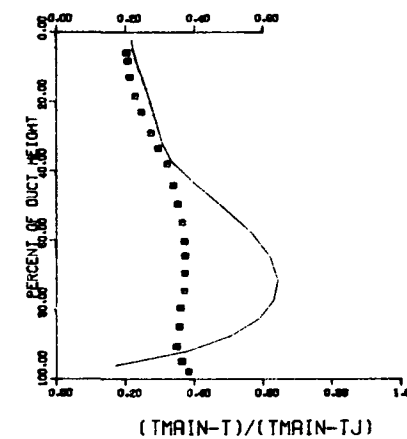
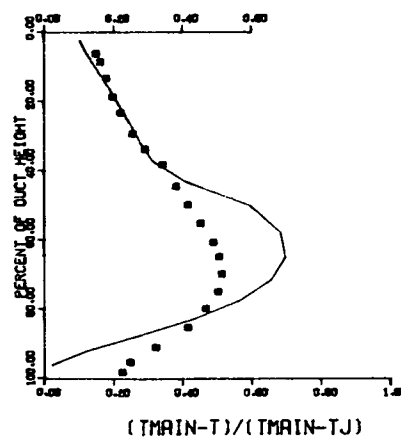
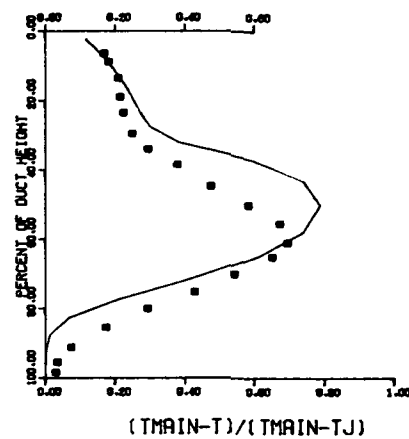
PREDICTED THETA CONTOURS FOR TEST NO. 6, $T_M=CONST$, $J=26.24$, $S/D=2.00$, $H/D=4.00$

$S/DJ = 2.29$ $H/DJ = 4.57$ $VRATIO = 3.47$ $TRATIO = 0.468$ $DENRATIO=2.185$ $T_{MAIN} = 668.5 \text{ K}$ $T_{JET} = 312.7 \text{ K}$ $T_{HEB} = 0.363$

$X/H = 0.25$ $X/DJ = 1.14$

$X/H = 0.50$ $X/DJ = 2.29$

$X/H = 1.00$ $X/DJ = 4.57$

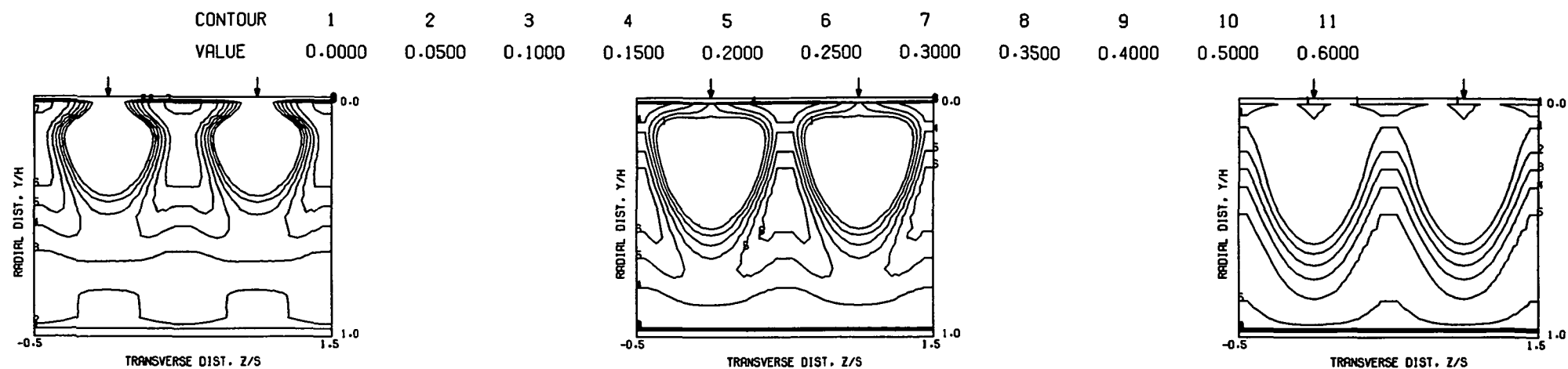


COMPARISON BETWEEN DATA AND PREDICTIONS FOR TEST 18, $T_M=CONST$, SINGLE SIDED INJECTION $J = 26.24$, $S/D = 2.00$, $H/D = 4.00$

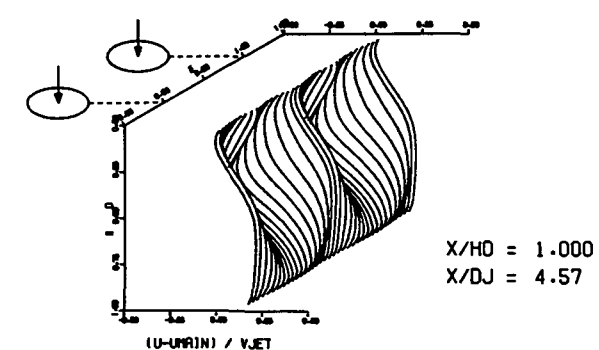
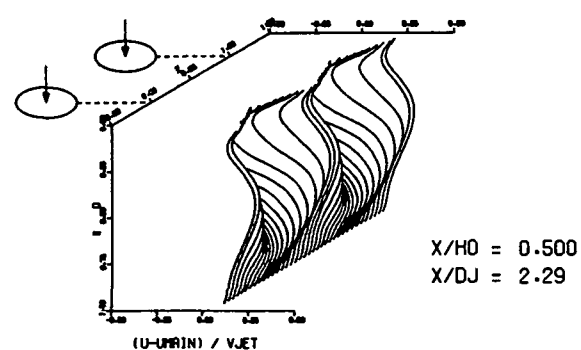
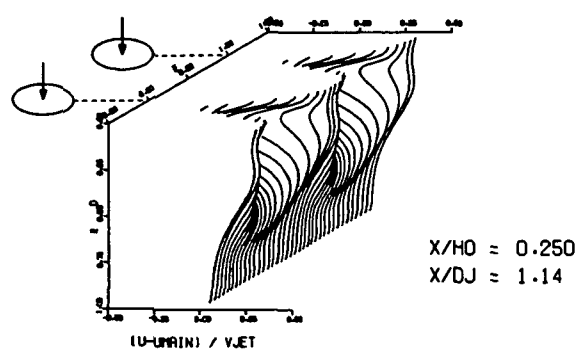
Figure 74. Comparison Between Predicted and Measured Temperature Distributions for Test No. 18 - Table 2.

FOLDOUT FRAME

FOLDOUT FRAME



PREDICTED VELOCITY CONTOURS FOR TEST NO. 6.45X23X19, J=26.24, S/D=2.00, H/D=4.00

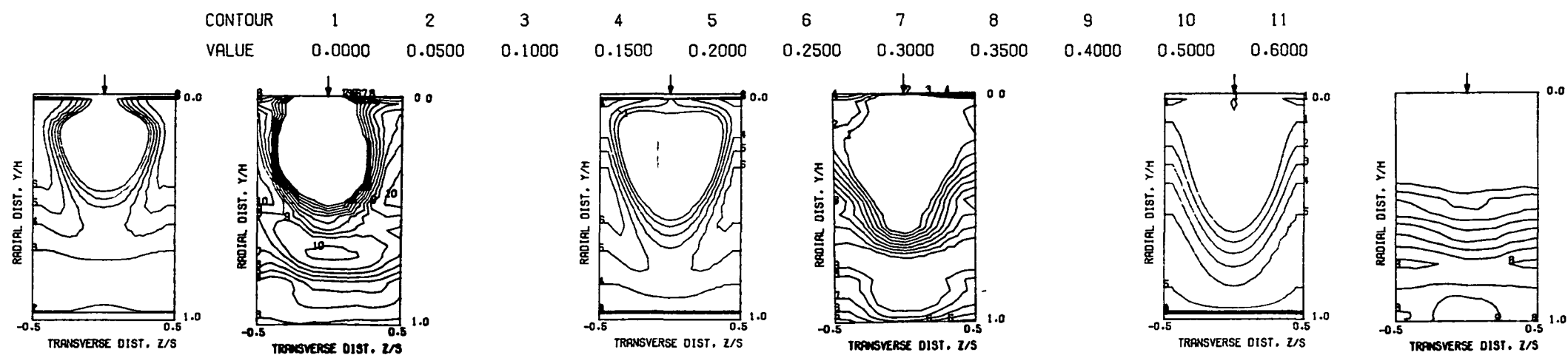


PREDICTED VELOCITY DISTRIBUTIONS FOR TEST 18.45X23X19, J=26.24, S/D=2.00, H/D=4.00

Figure 75. Predicted Velocity Distributions for Test No. 18 - Table 2.

FOLDOUT FRAME

FOLDOUT FRAME



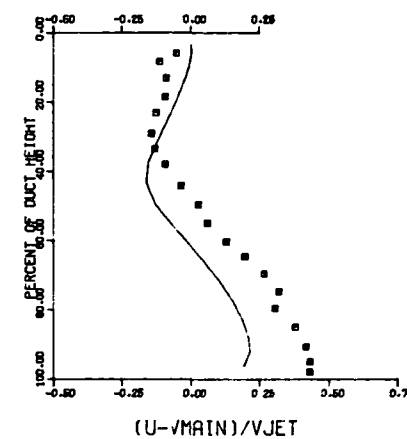
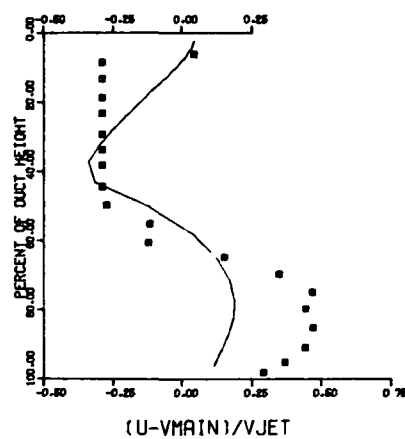
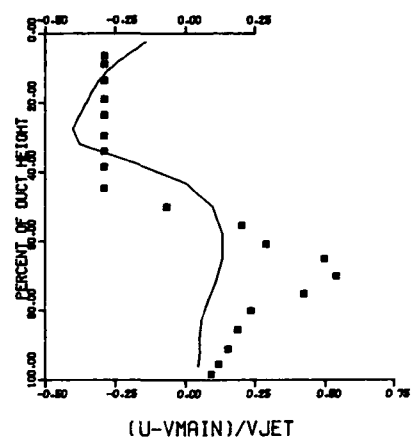
PREDICTED VELOCITY CONTOURS FOR TEST NO. 6, $T_M=CONST$, $J=26.24$, $S/D=2.0$, $H/D=4.0$

$S/DJ = 2.29$ $H/DJ = 4.57$ $VRATIO = 3.47$ $TRATIO = 0.468$ $DENRATIO=2.185$ $TMAIN = 668.5 \text{ K}$ $TJET = 312.7 \text{ K}$ $THEB = 0.363$

$X/H = 0.25$ $X/DJ = 1.14$

$X/H = 0.50$ $X/DJ = 2.29$

$X/H = 1.00$ $X/DJ = 4.57$



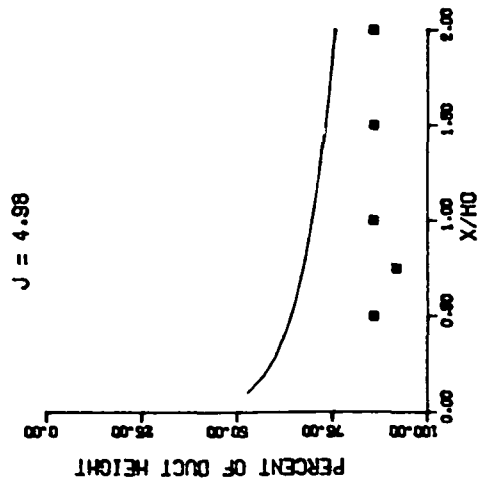
COMPARISON BETWEEN DATA AND PREDICTIONS FOR TEST 18, $T_M=CONST$, SINGLE SIDED INJECTION $J = 26.24$ $S/D = 2.00$ $H/D = 4.00$

Figure 76. Comparison Between Predicted and Measured Velocity Distributions for Test No. 18 - Table 2.

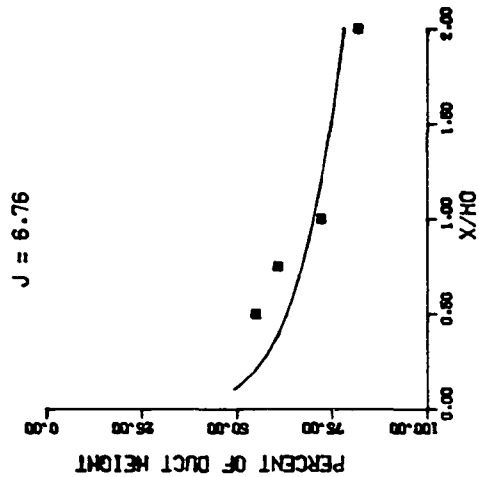
FOLDOUT FRAME

FOLDOUT FRAME

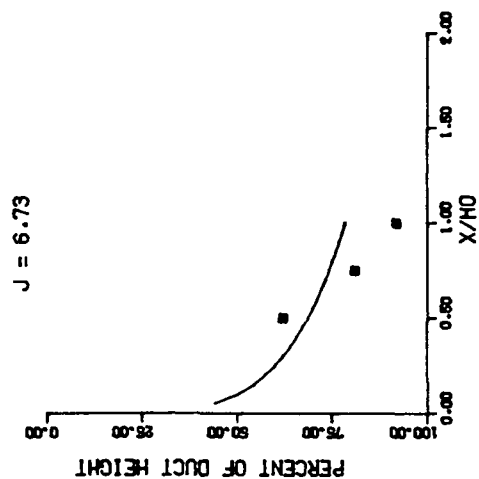
TEST NO 1. ISOTHERMAL THIN, PHASE I
ORIFICE PLATE 01/02/04



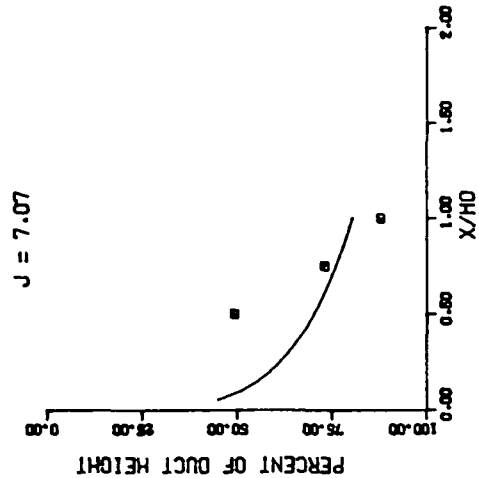
TEST NO 21. CONV DUCT II, PHASE I
ORIFICE PLATE 01/02/04



TEST NO 25. CONV DUCT IV, PHASE I
ORIFICE PLATE 01/02/04



TEST NO 29. FLAT WALL JET, PHASE I
ORIFICE PLATE 01/02/04



TEST NO 33. SLANT WALL JET, PHASE I
ORIFICE PLATE 01/02/04

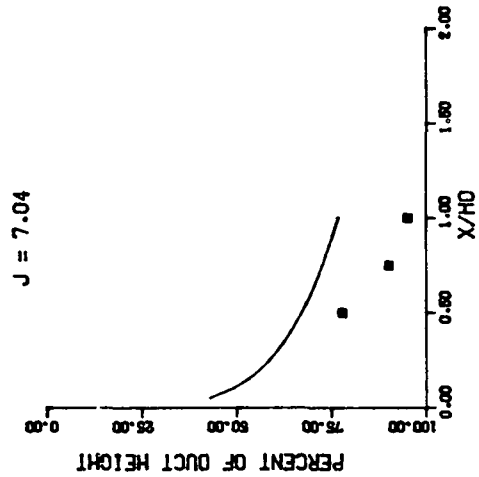
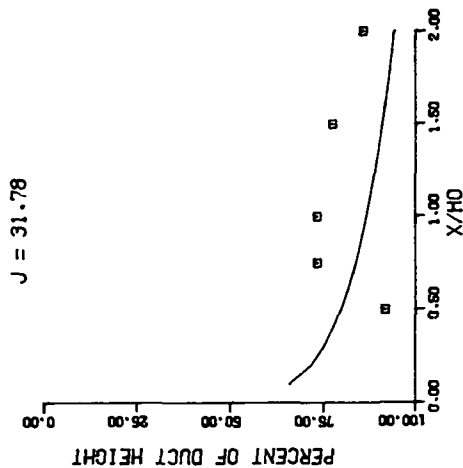
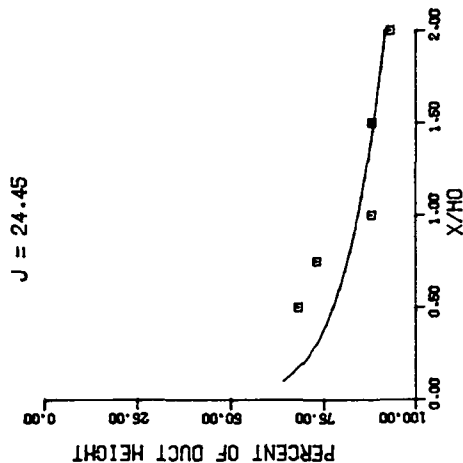


Figure 77. Comparison Between Predicted and Measured Velocity Trajectories
For $S/D = 2$ and $H_0/D = 4$.

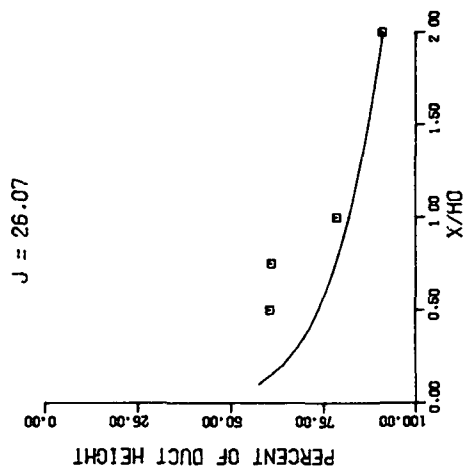
TEST NO 13. TOP COLD PROFILE, PHASE I
ORIFICE PLATE 01/02/04



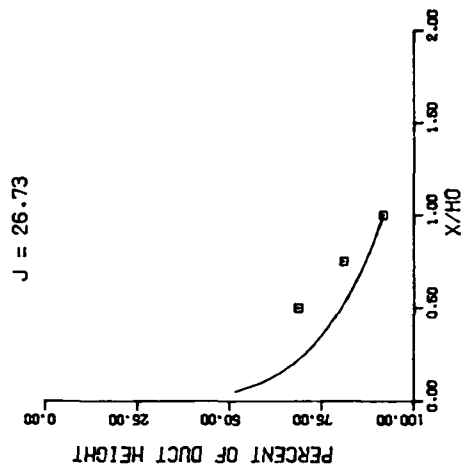
TEST NO 17. TOP HOT PROFILE, PHASE I
ORIFICE PLATE 01/02/04



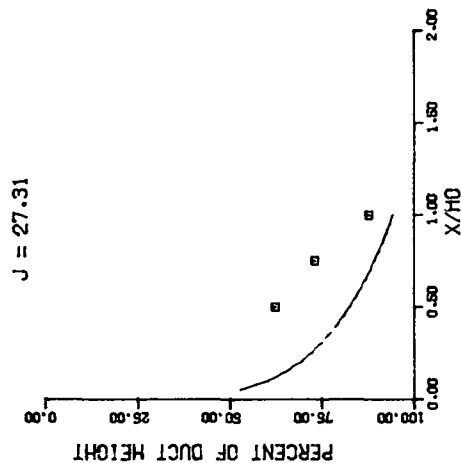
TEST NO 22. CONV DUCT II, PHASE I
ORIFICE PLATE 01/02/04



TEST NO 26. CONV DUCT IV, PHASE I
ORIFICE PLATE 01/02/04



TEST NO 30. FLAT WALL JET, PHASE I
ORIFICE PLATE 01/02/04



TEST NO 34. SLANT WALL JET, PHASE I
ORIFICE PLATE 01/02/04

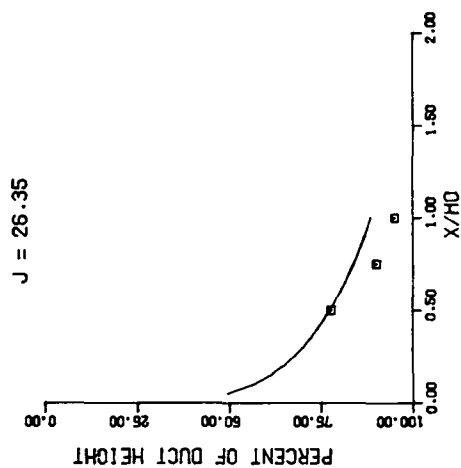
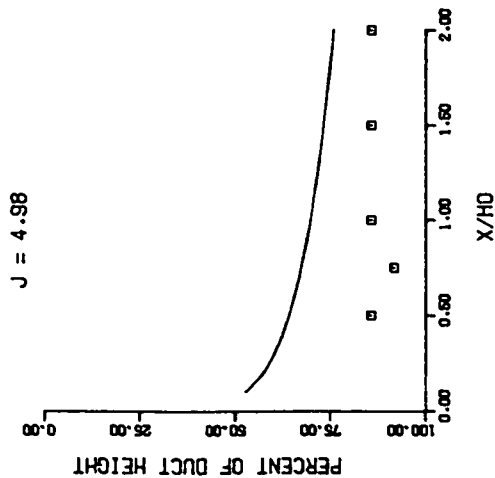
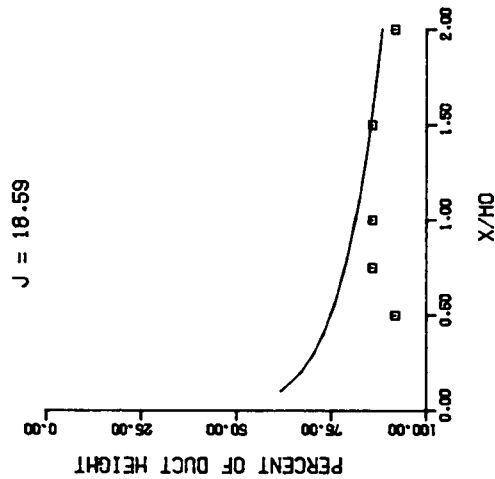


Figure 78. Comparison Between Predicted and Measured Velocity Trajectories Including Effects of Mainstream Profiles and Flow Area Convergence at Intermediate J for Orifice Plate 01/02/04.

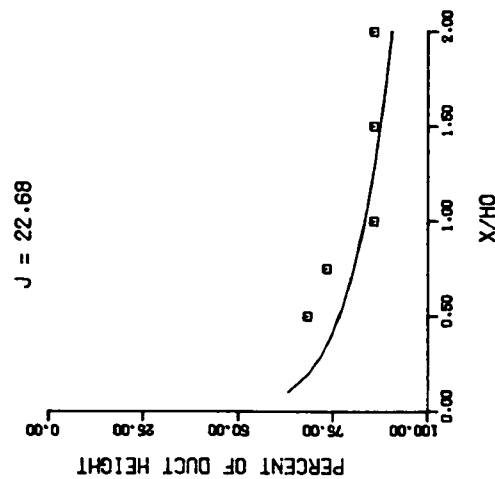
TEST NO 1. HOT MAINSTREAM, PHASE I
ORIFICE PLATE 01/02/04



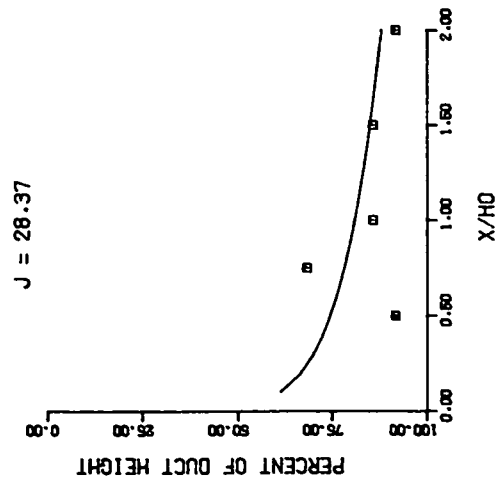
TEST NO 2. HOT MAINSTREAM, PHASE I
ORIFICE PLATE 01/02/04



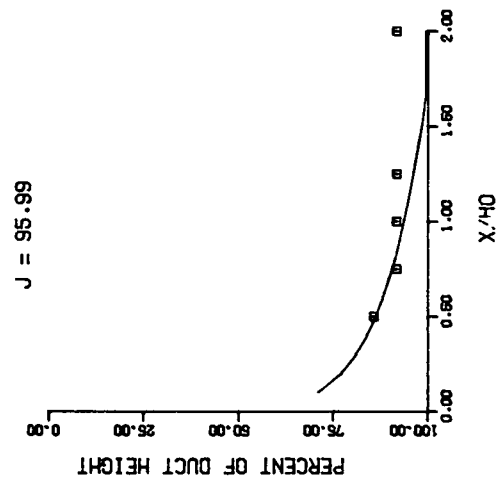
TEST NO 9. COLD MAINSTREAM, PHASE I
ORIFICE PLATE 01/02/04



TEST NO 7. HOT MAINSTREAM, PHASE I
ORIFICE PLATE 01/04/08



TEST NO 8. HOT MAINSTREAM, PHASE I
ORIFICE PLATE 01/04/08



TEST NO 12. COLD MAINSTREAM, PHASE I
ORIFICE PLATE 01/04/08

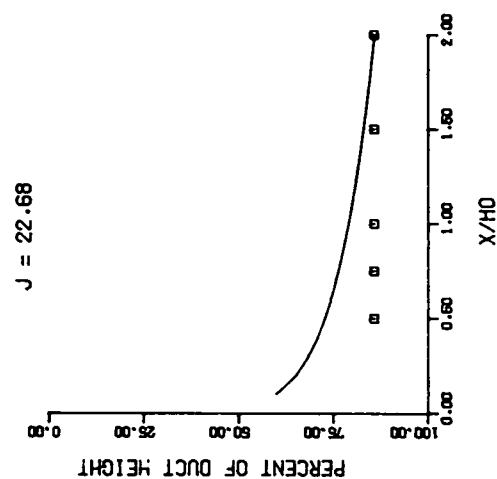


Figure 79. Comparison of Predicted and Measured Velocity Trajectories for Different Jet Diameters, $S/H = 0.5$.

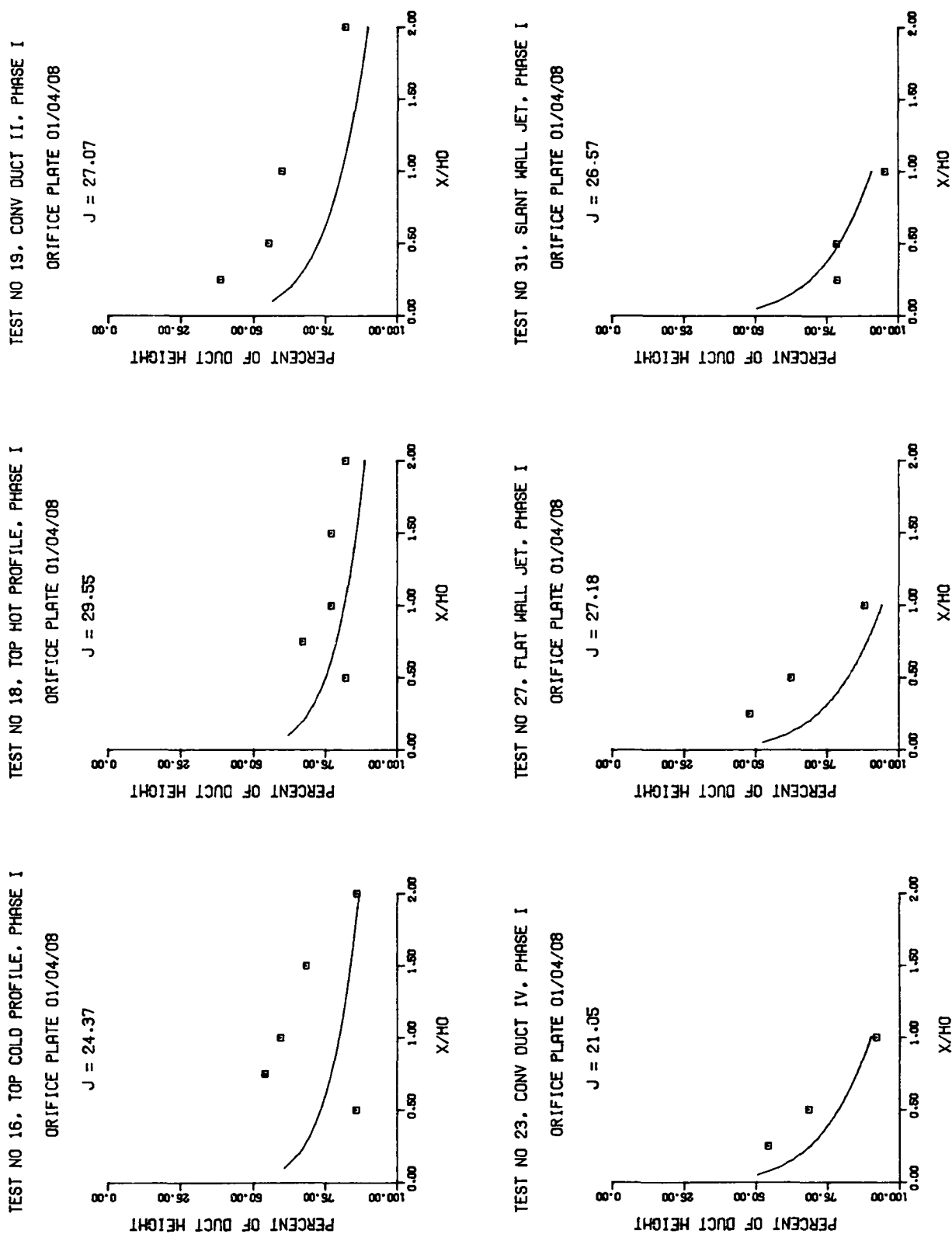


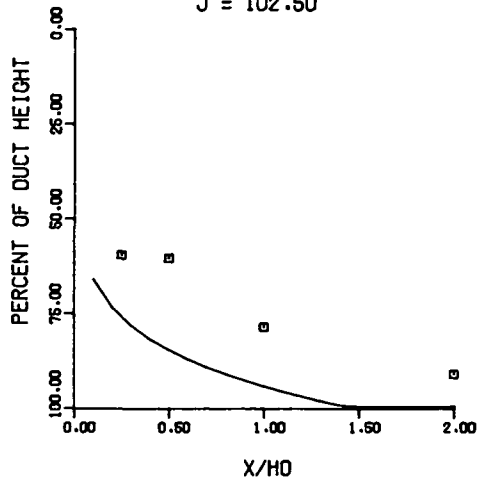
Figure 80. Predicted and Measured Velocity Trajectories for Non-Uniform Mainstream Profile and Flow Area Convergence, $S/D = 4$, $H_0/D = 8$.

ORIGINAL PAGE IS
OF POOR QUALITY

TEST NO 20, CONV DUCT II, PHASE I

ORIFICE PLATE 01/04/08

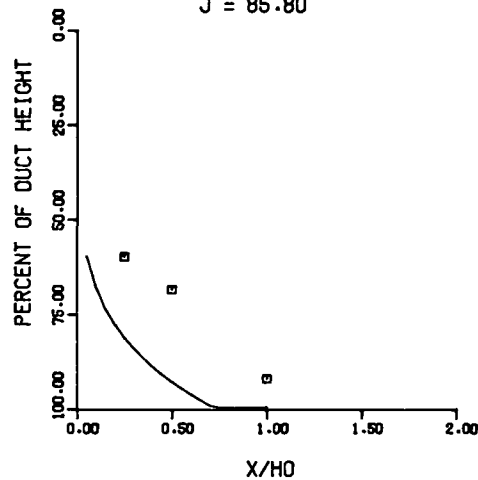
$J = 102.50$



TEST NO 24, CONV DUCT IV, PHASE I

ORIFICE PLATE 01/04/08

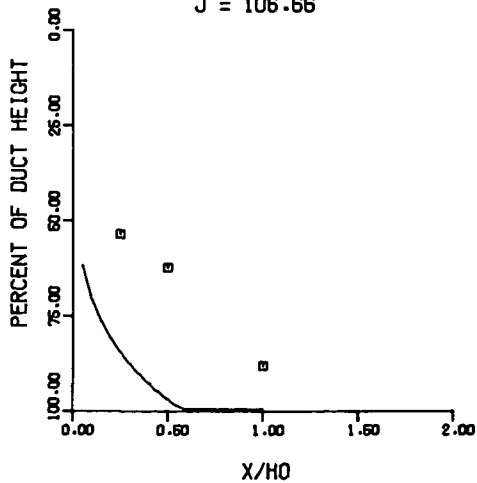
$J = 85.80$



TEST NO 28, FLAT WALL JET, PHASE I

ORIFICE PLATE 01/04/08

$J = 106.66$



TEST NO 32, SLANT WALL JET, PHASE I

ORIFICE PLATE 01/04/08

$J = 107.56$

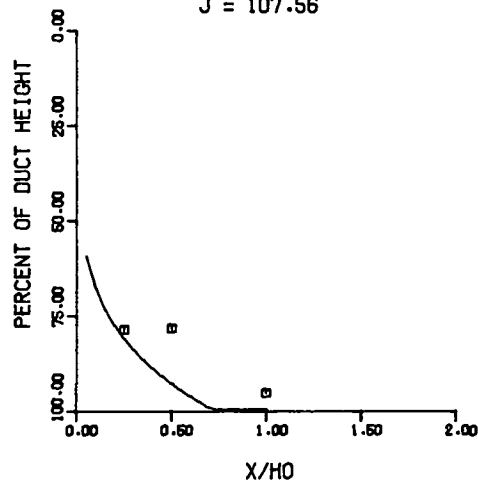
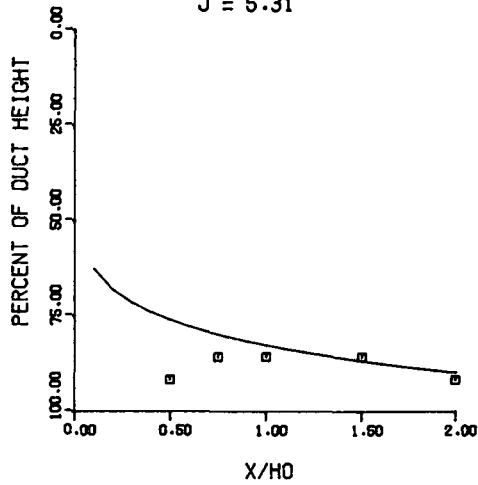


Figure 81. Predicted and Measured Velocity Trajectories for Different Convergence and Jet Injection Angles, $S/D = 4$, $H_0/D = 8$.

TEST NO 3, HOT MAINSTREAM, PHASE I

ORIFICE PLATE 01/04/04

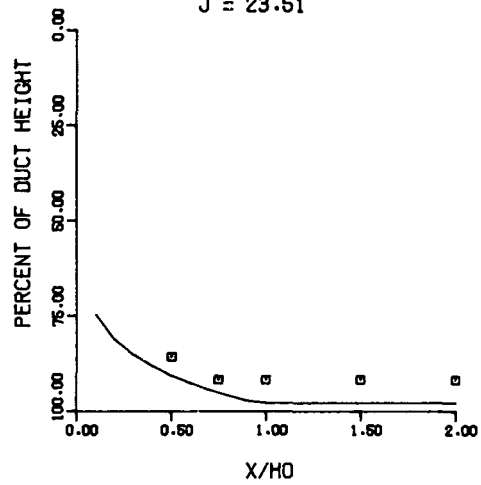
$J = 5.31$



TEST NO 4, HOT MAINSTREAM, PHASE I

ORIFICE PLATE 01/04/04

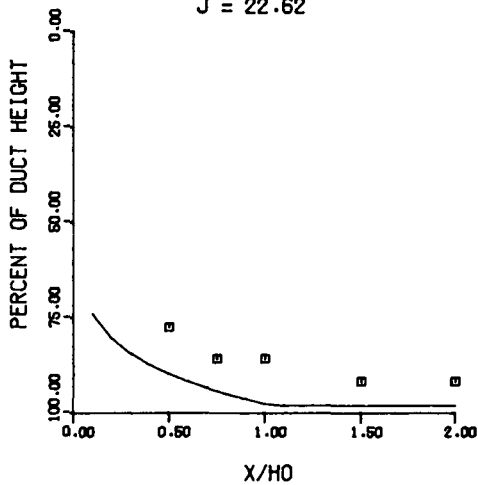
$J = 23.51$



TEST NO 10, COLD MAINSTREAM, PHASE I

ORIFICE PLATE 01/04/04

$J = 22.62$



TEST NO 18, TOP COLD PROFILE, PHASE I

ORIFICE PLATE 01/04/04

$J = 6.70$

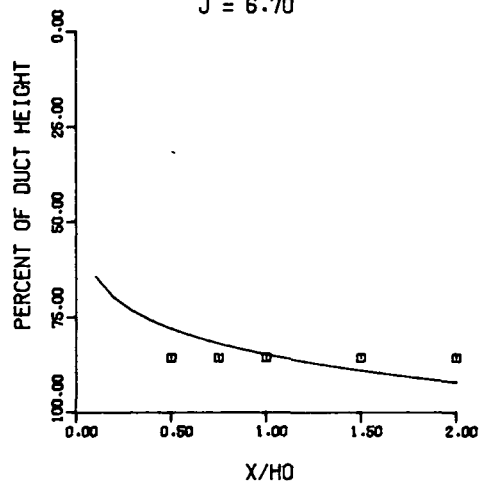
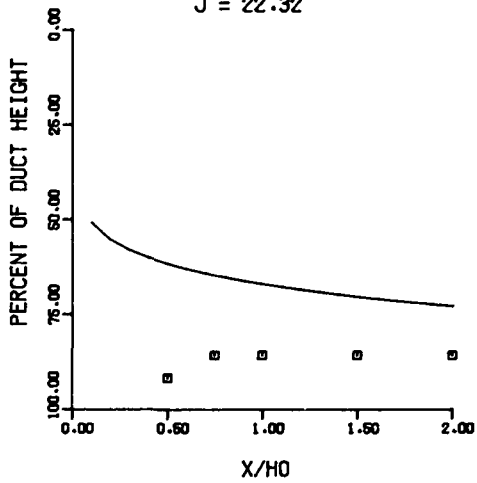


Figure 82. Predicted and Measured Velocity Trajectories in a Straight Duct for $S/D = 4$, $H_0/D = 4$.

TEST NO 5, HOT MAINSTREAM, PHASE I

ORIFICE PLATE 01/02/08

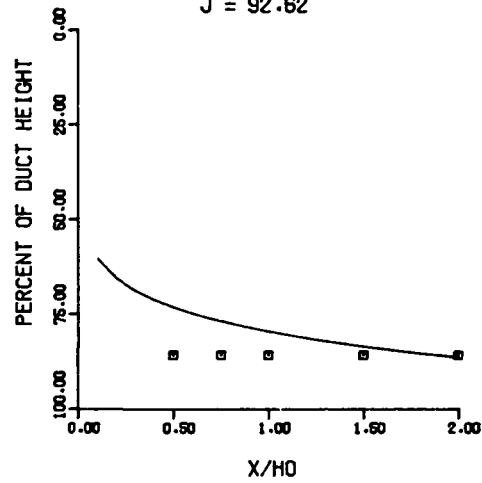
$J = 22.32$



TEST NO 6, HOT MAINSTREAM, PHASE I

ORIFICE PLATE 01/02/08

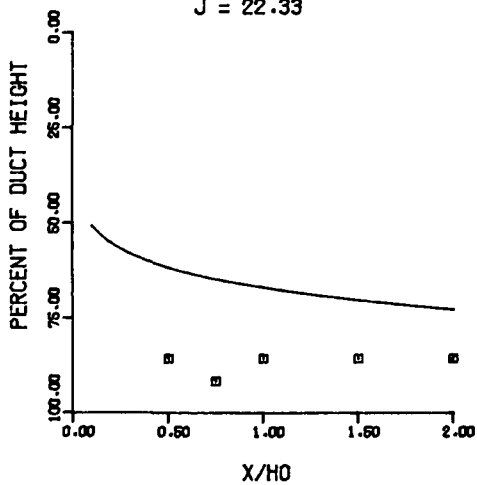
$J = 92.62$



TEST NO 11, COLD MAINSTREAM, PHASE I

ORIFICE PLATE 01/02/08

$J = 22.33$



TEST NO 15, TOP COLD PROFILE, PHASE I

ORIFICE PLATE 01/02/08

$J = 99.20$

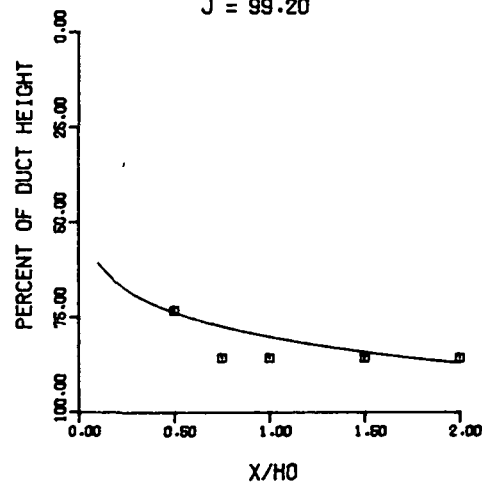
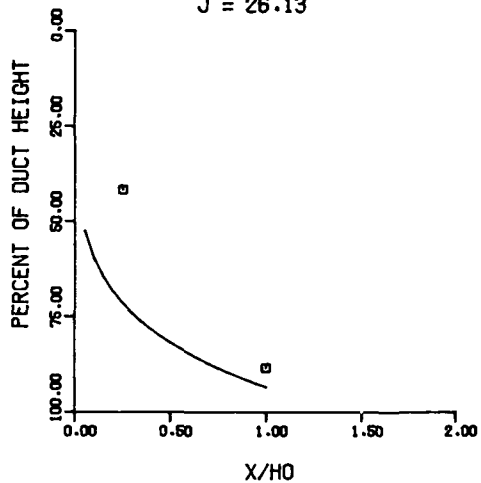


Figure 83. Predicted and Measured Velocity Trajectories in a Straight Duct for $S/D = 2$, $H_0/D = 8$.

TEST NO 35, TOP COLD PROFILE, T.S. V

ORIFICE PLATE 01/04/08

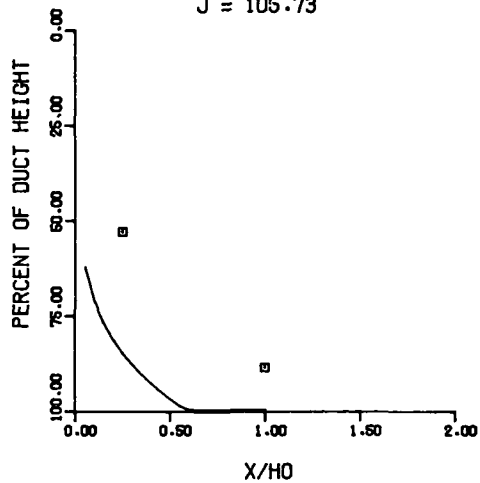
$J = 26.13$



TEST NO 36, TOP COLD PROFILE, T.S. V

ORIFICE PLATE 01/04/08

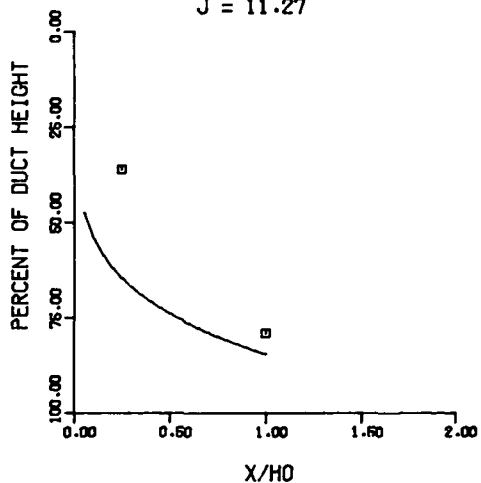
$J = 105.73$



TEST NO 37, TOP HOT PROFILE, T.S. V

ORIFICE PLATE 01/04/08

$J = 11.27$



TEST NO 38, TOP HOT PROFILE, T.S. V

ORIFICE PLATE 01/04/08

$J = 40.18$

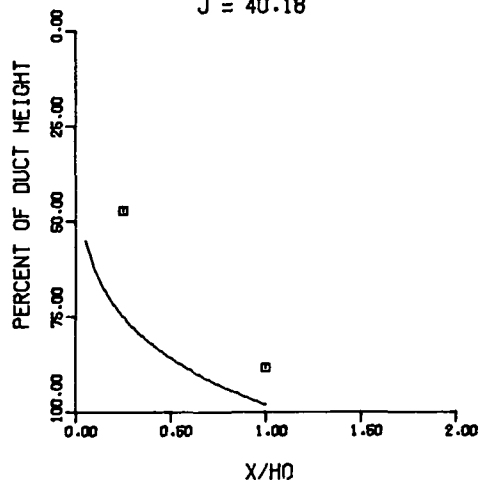
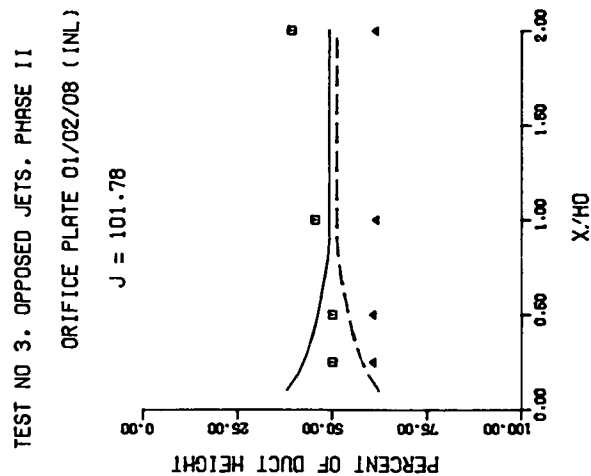
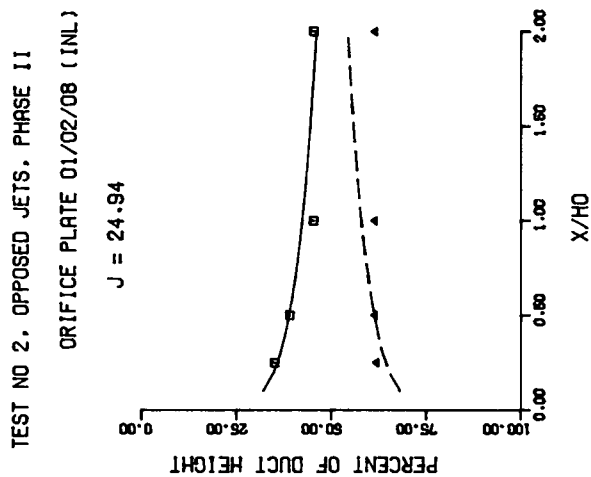
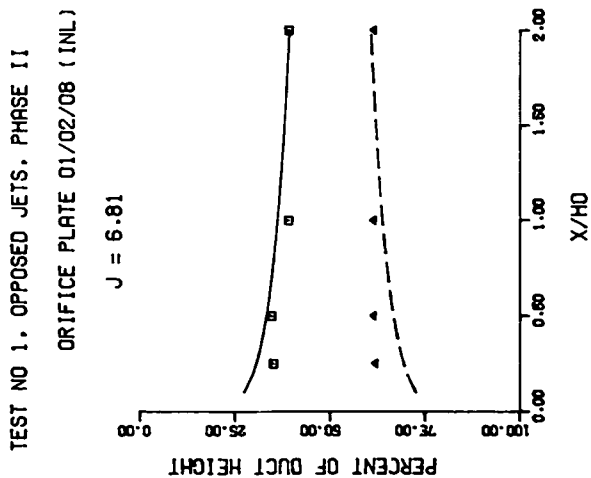


Figure 84. Predicted and Measured Velocity Trajectories in a Symmetrically Convergent Duct with Non-Uniform Mainstream Profile, $S/N = 4$, $H_0/D = 8$ (Test Section V).



—— TOP ROW JET TRAJECTORY - - - - BOTTOM ROW JET TRAJECTORY

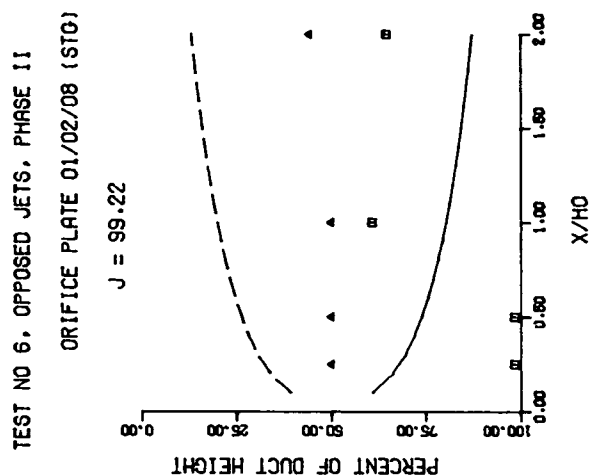
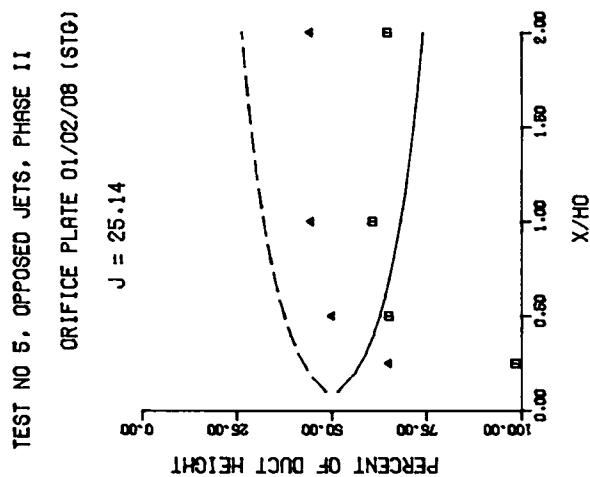
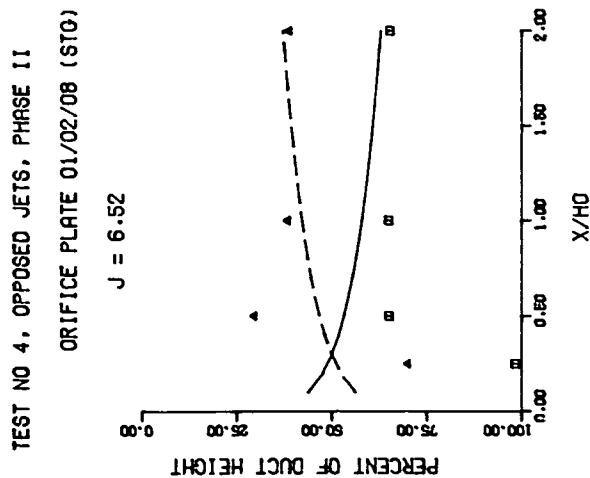


Figure 85. Predicted and Measured Velocity Trajectories for Opposed Jets, $S/D = 2$, $H_0/D = 8$.

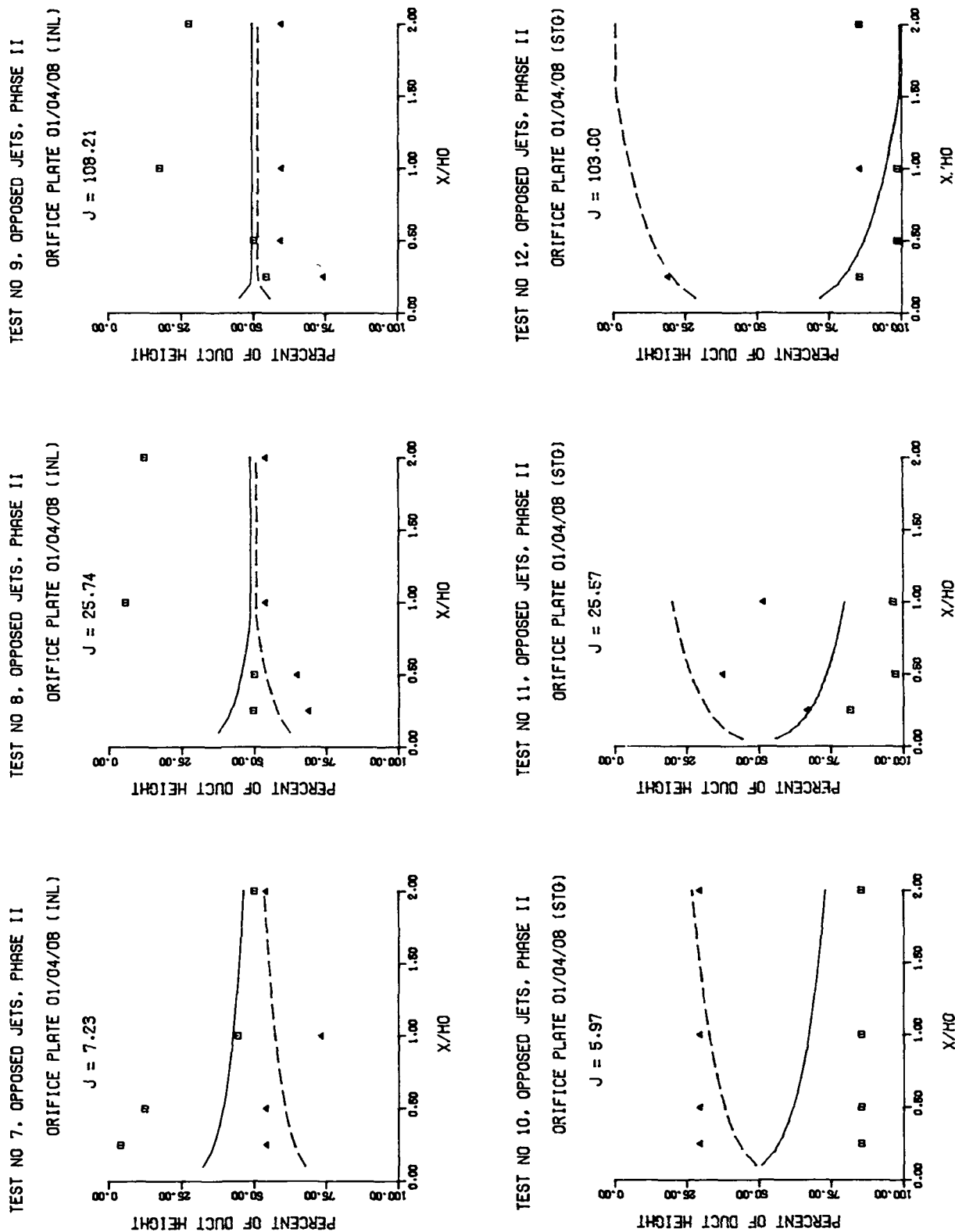
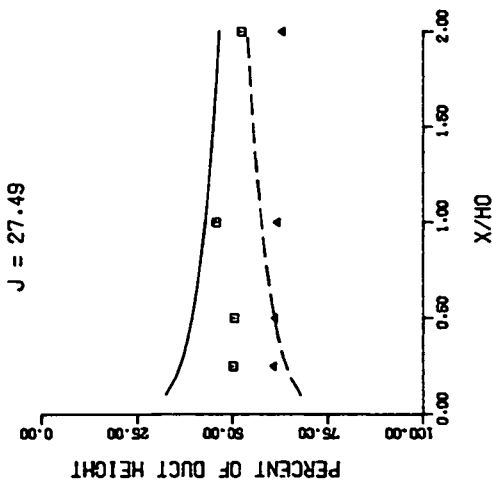
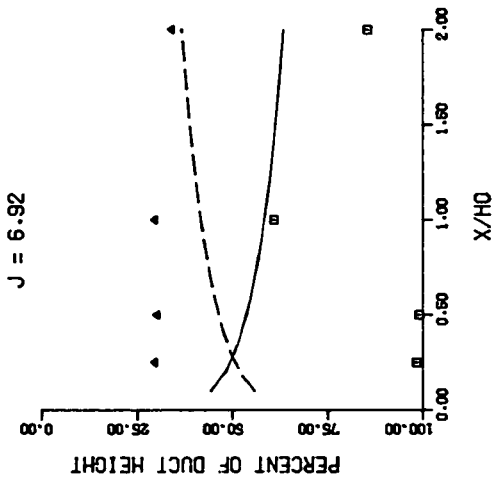


Figure 86. Predicted and Measured Velocity Trajectories for Opposed Jets, $S/D = 4$, $H_0/D = 8$.

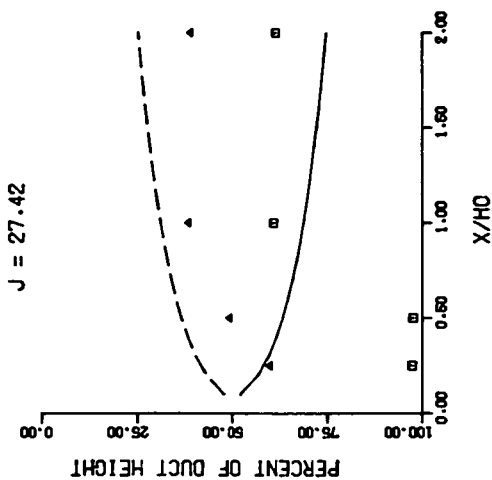
TEST NO 13, TOP COLD PROFILE, PHASE II
ORIFICE PLATE 01/02/08 (INL)



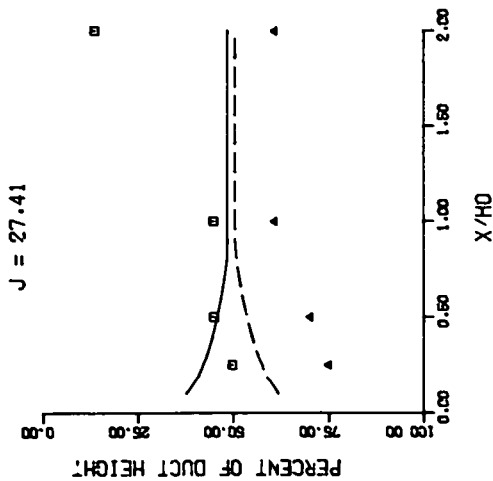
TEST NO 14, TOP COLD PROFILE, PHASE II
ORIFICE PLATE 01/02/08 (STG)



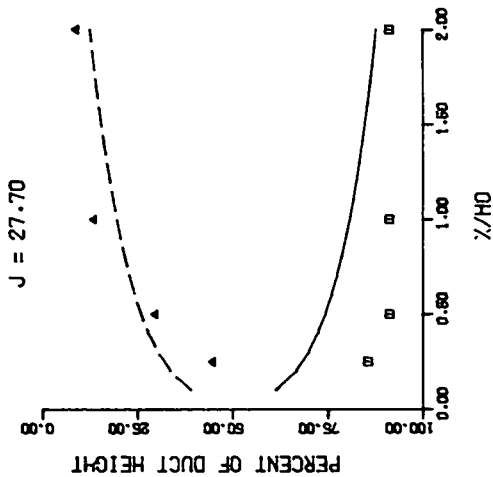
TEST NO 15, TOP COLD PROFILE, PHASE II
ORIFICE PLATE 01/02/08 (STG)



TEST NO 16, TOP COLD PROFILE, PHASE II
ORIFICE PLATE 01/04/08 (INL)



TEST NO 17, TOP COLD PROFILE, PHASE II
ORIFICE PLATE 01/04/08 (STG)



TEST NO 18, TOP COLD PROFILE, PHASE II
ORIFICE PLATE 01/04/08 (STG)

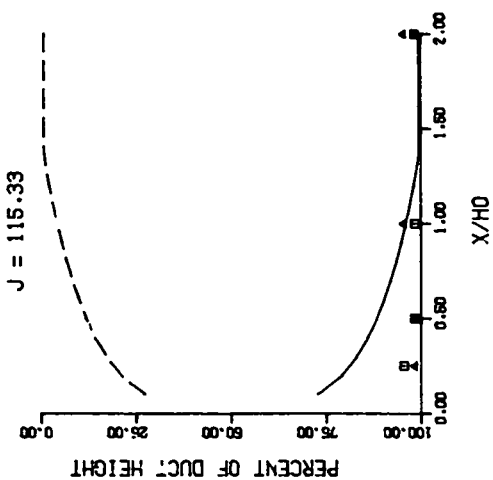
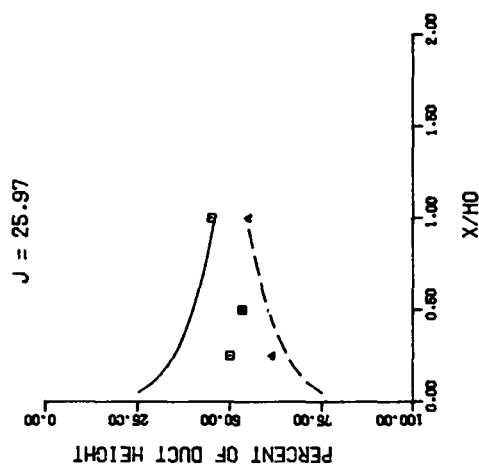
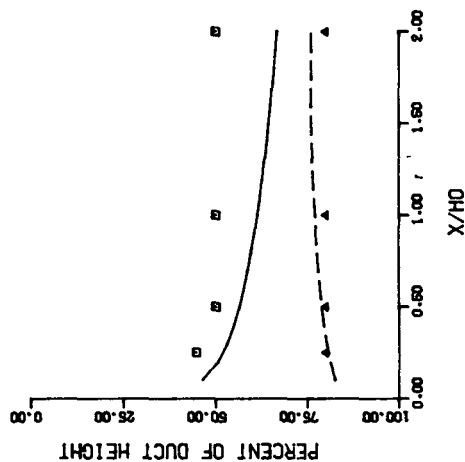


Figure 87. Predicted and Measured Velocity Trajectories for Opposed Jets
With Non-Uniform Mainstream Profile.

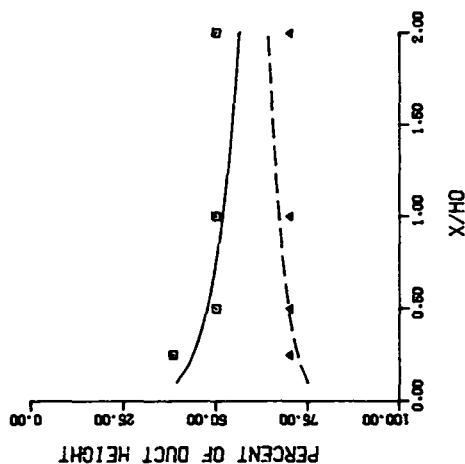
TEST NO 19. SYMMETRIC CONV DUCT-PHASE II
ORIFICE PLATE 01/02/08 (INL)



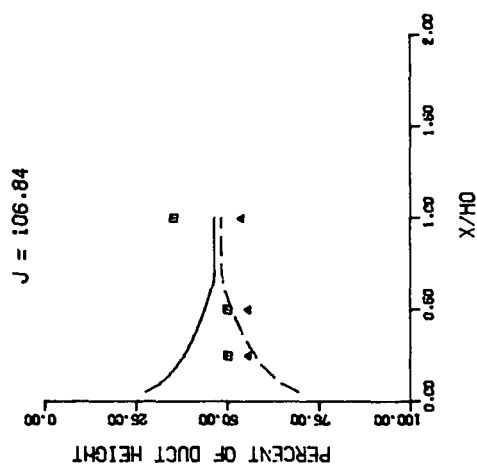
TEST NO 34. JT=58.4, JB=6.5, PHASE II
ORIFICE PLATE 01/02/08 (INL)



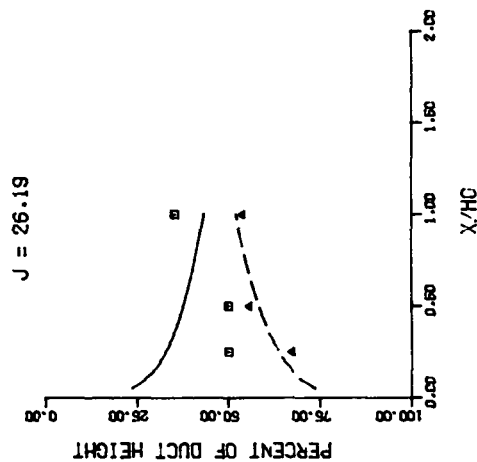
TEST NO 33. JT=40.9, JB=14.7, PHASE II
ORIFICE PLATE 01/02/08 (INL)



TEST NO 36. ASYMM CONV DUCT, PHASE II
ORIFICE PLATE 01/02/08 (INL)



TEST NO 35. ASYMM CONV DUCT, PHASE II
ORIFICE PLATE 01/02/08 (INL)



TEST NO 20. SYMMETRIC CONV DUCT-PHASE II
ORIFICE PLATE 01/02/08 (INL)

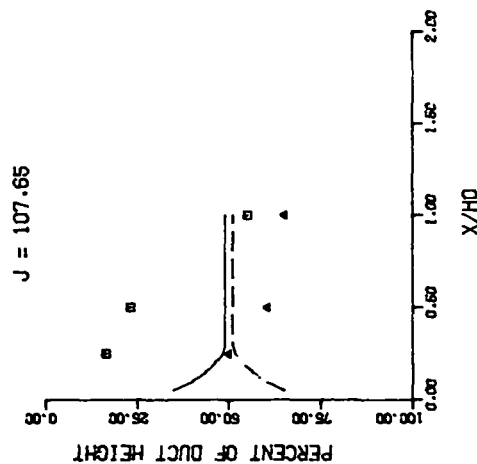
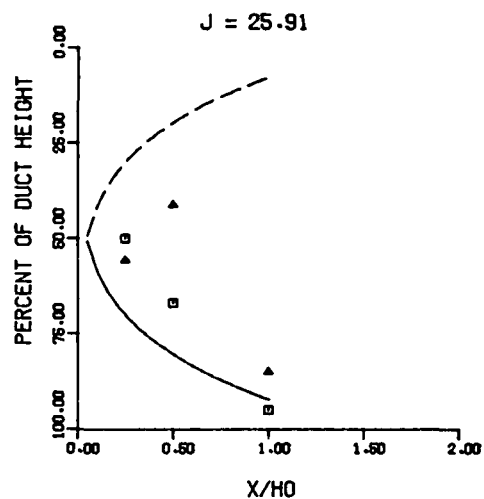


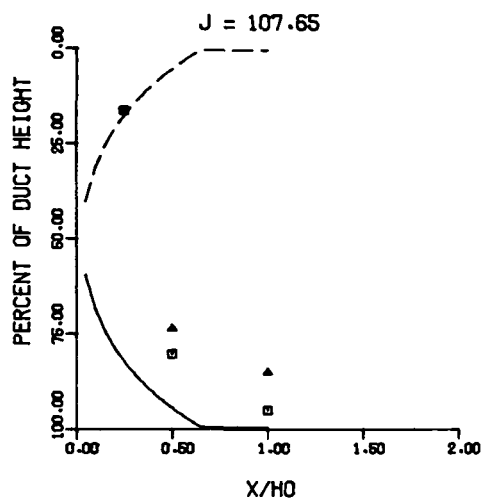
Figure 88. Predicted and Measured Velocity Trajectories with Unequal Momentum Flux Ratios, Flow Area Convergence, for Opposed Jets;
 $S/D = 2, H_0/D = 8.$

ORIGINAL PAGE IS
OF POOR QUALITY

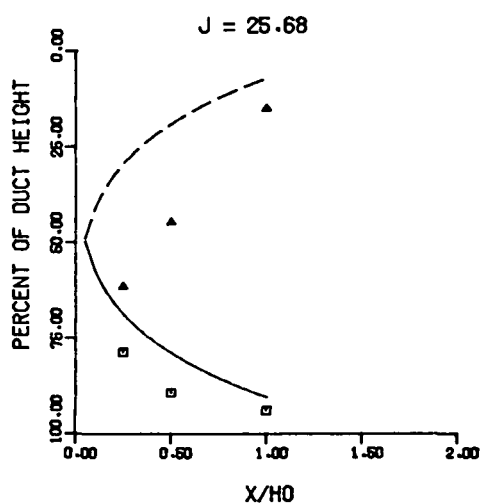
TEST NO 21, SYMM CONV DUCT, PHASE II
ORIFICE PLATE 01/04/08 (STG)



TEST NO 22, SYMM CONV DUCT, PHASE II
ORIFICE PLATE 01/04/08 (STG)



TEST NO 37, ASYMM CONV DUCT - PHASE II
ORIFICE PLATE 01/04/08 (STG)



TEST NO 38, ASYMM CONV DUCT - PHASE II
ORIFICE PLATE 01/04/08 (STG)

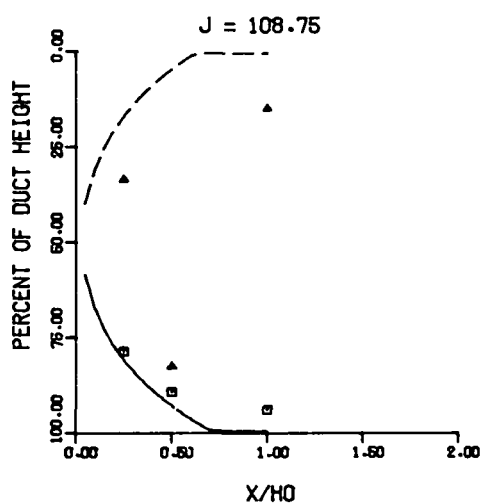


Figure 89. Predicted and Measured Velocity Trajectories for Opposed Jets in Convergent Ducts, $S/D = 4$, $H_0/D = 8$.

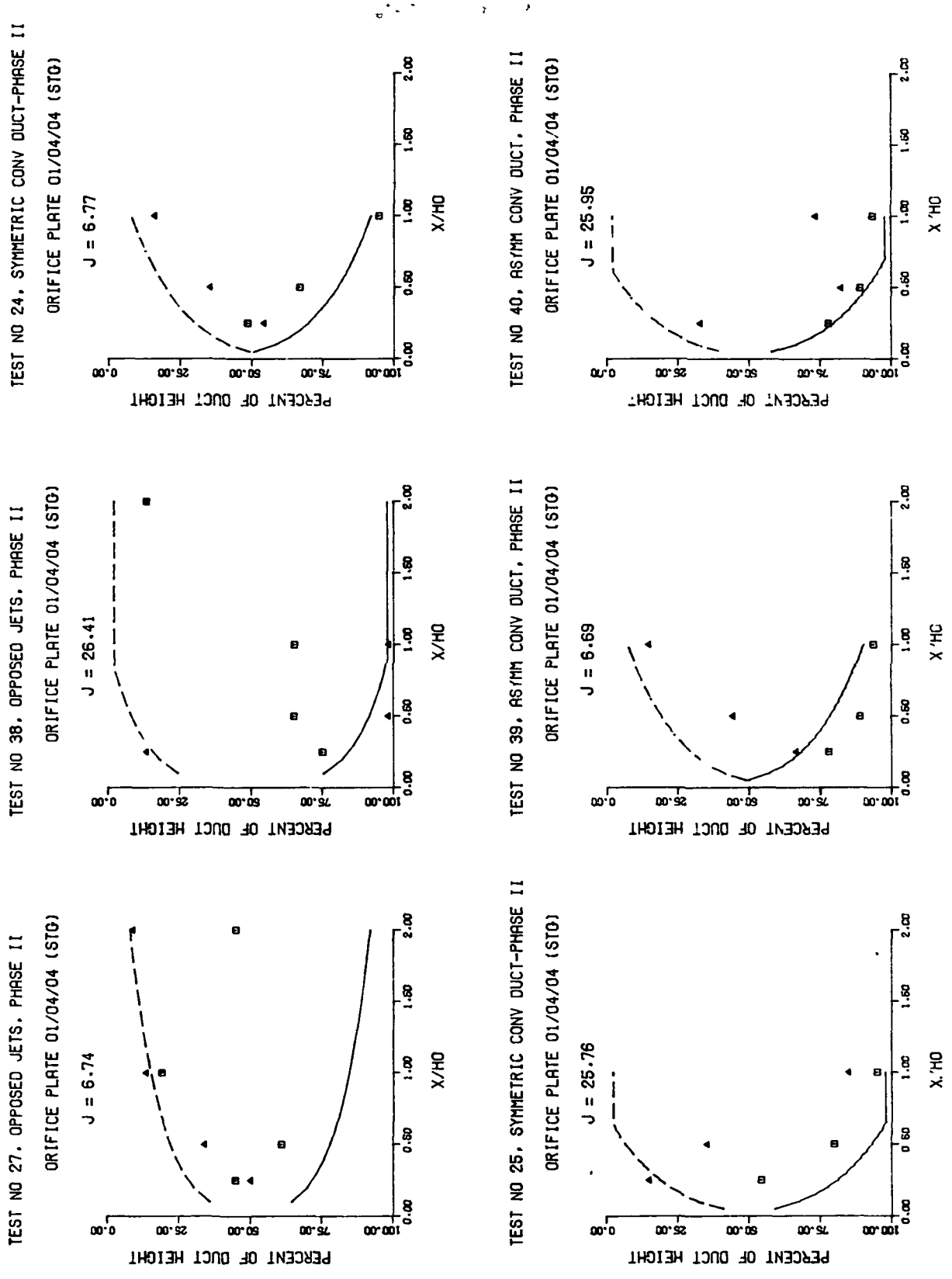
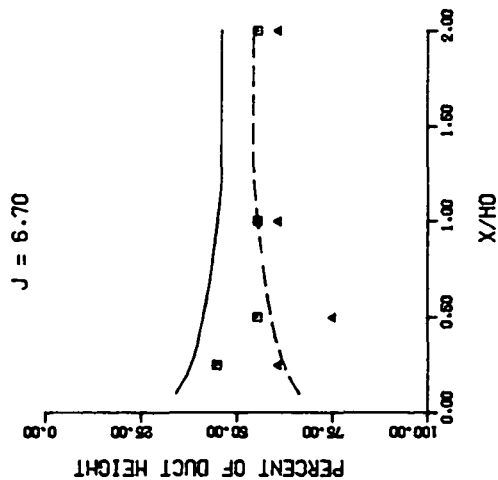
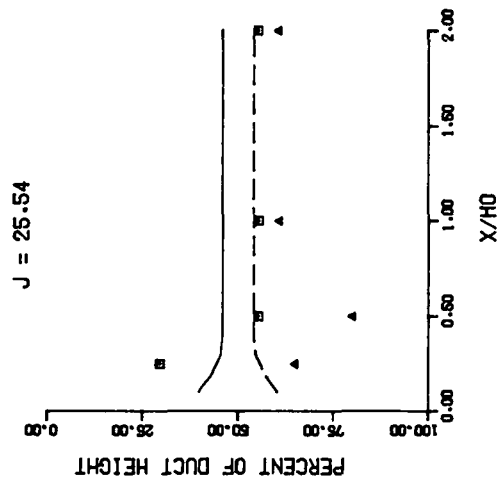


Figure 90. Predicted and Measured Velocity Trajectories for Opposed Jets with $S/D = 4$, $H_0/D = 8$.

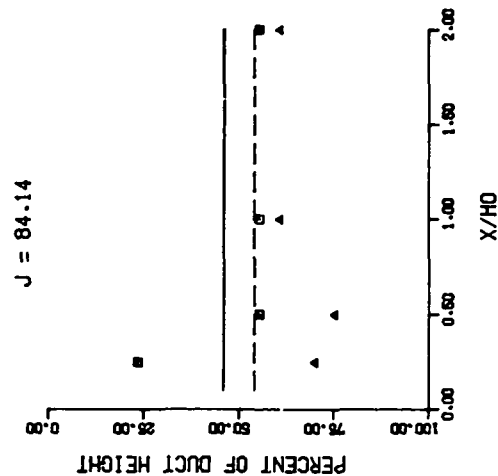
TEST NO 46, OPPOSED JETS, PHASE II
ORIFICE PLATE 01/02/04 (INL)



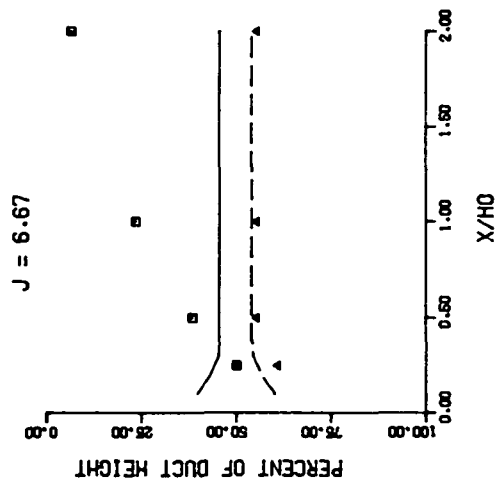
TEST NO 47, OPPOSED JETS, PHASE II
ORIFICE PLATE 01/02/04 (INL)



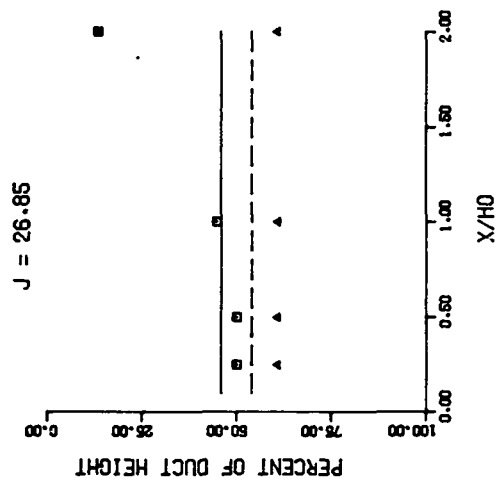
TEST NO 48, OPPOSED JETS - PHASE II
ORIFICE PLATE 01/02/04 (INL)



TEST NO 51, OPPOSED JETS - PHASE II
ORIFICE PLATE 01/04/04 (INL)



TEST NO 29, OPPOSED JETS, PHASE II
ORIFICE PLATE 01/04/04 (INL)



TEST NO 30, OPPOSED JETS, PHASE II
ORIFICE PLATE 01/04/04 (INL)

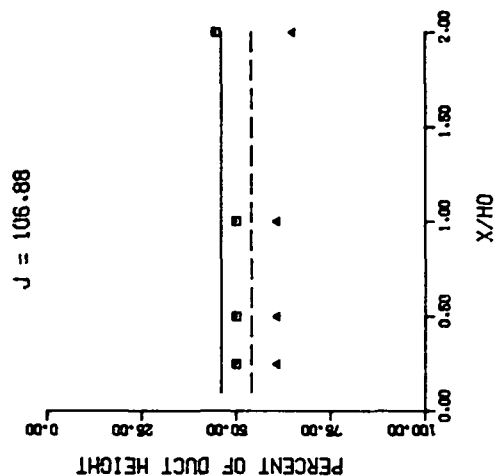
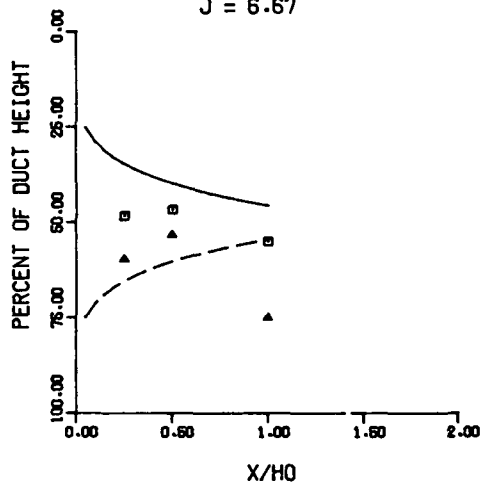


Figure 91. Comparison Between Predicted and Measured Velocity Trajectories
For Opposed In-line Jets with $H_0/D = 4$ in a Straight Duct.

TEST NO 25. SYMM CONV DUCT, PHASE II

ORIFICE PLATE 01/02/04 (INL)

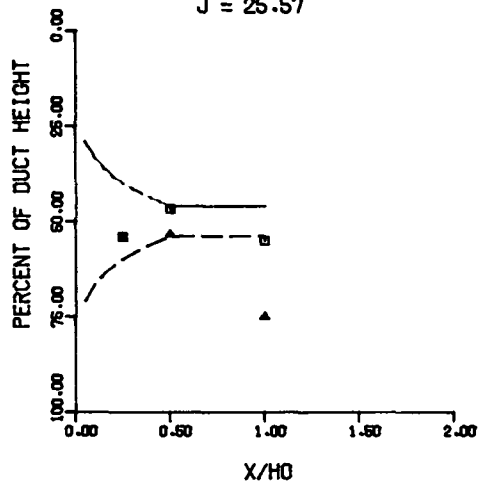
$J = 6.67$



TEST NO 26. SYMM CONV DUCT, PHASE II

ORIFICE PLATE 01/02/04 (INL)

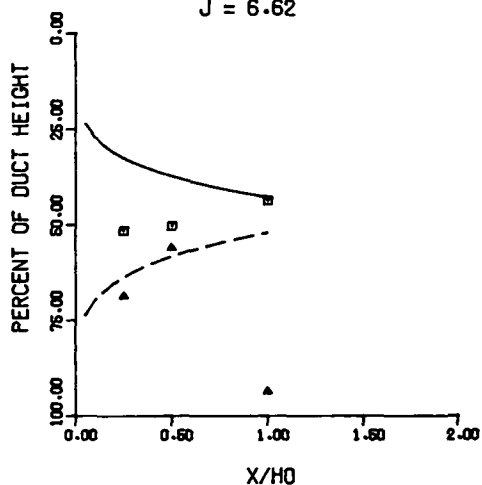
$J = 25.57$



TEST NO 41. ASYMM CONV DUCT - PHASE II

ORIFICE PLATE 01/02/04 (INL)

$J = 6.62$



TEST NO 42. ASYMM CONV DUCT - PHASE II

ORIFICE PLATE 01/02/04 (INL)

$J = 26.12$

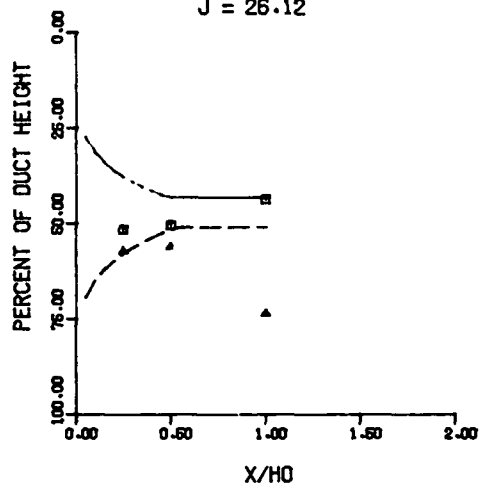
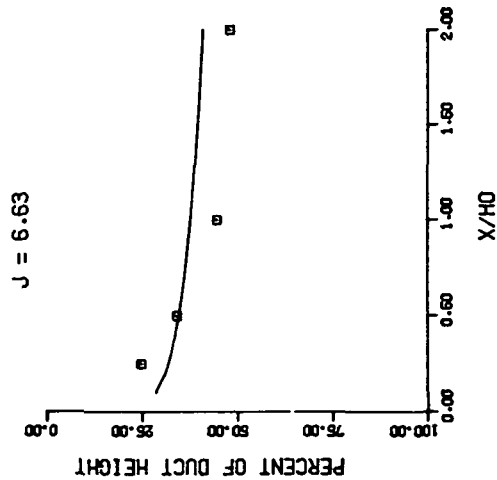
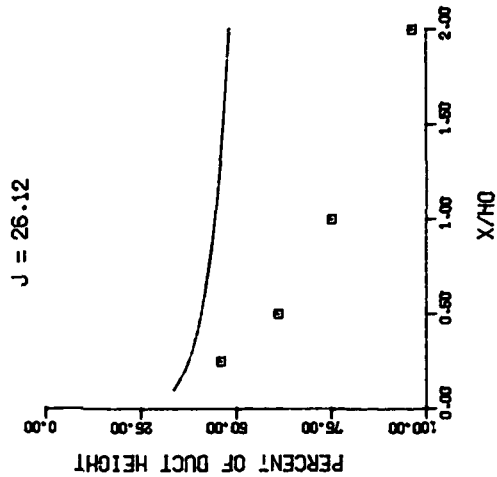


Figure 92. Predicted and Measured Velocity Trajectories with Opposed Jets in Convergent Ducts, $S/D = 2$, $H_0/D = 4$.

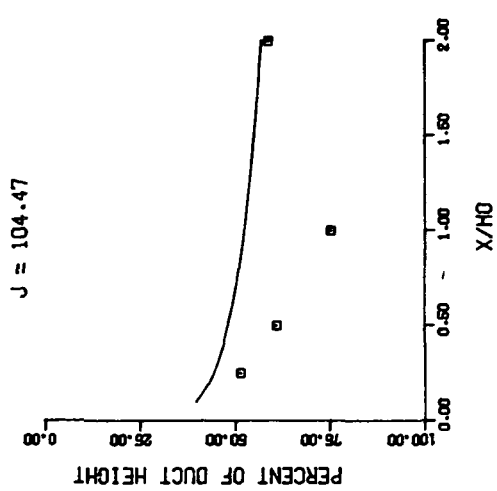
TEST NO 31A, ONE-SIDED JET, PHASE II
0.5144 CM WIDE SLOT



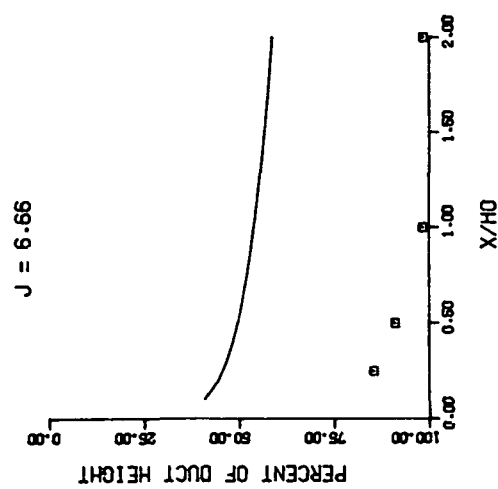
TEST NO 31B, ONE-SIDED JET, PHASE II
0.5144 CM WIDE SLOT



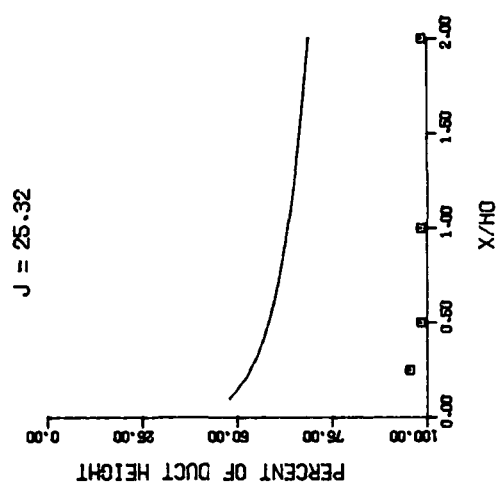
TEST NO 31C, ONE-SIDED JET - PHASE II
0.5144 CM WIDE SLOT



TEST NO 46A, ONE-SIDED JET - PHASE II
1.024 CM WIDE SLOT



TEST NO 46B, ONE-SIDED JET - PHASE II
1.024 CM WIDE SLOT



TEST NO 46C, ONE-SIDED JET - PHASE II
1.024 CM WIDE SLOT

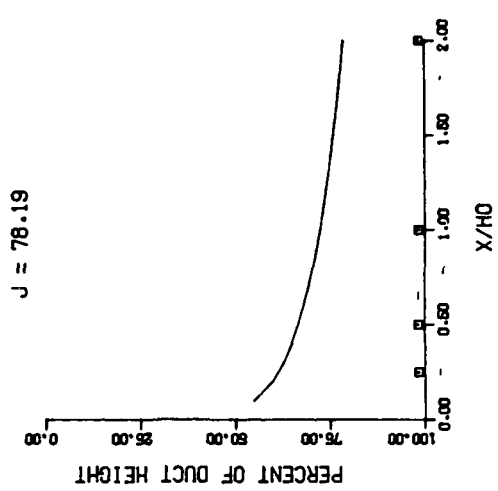
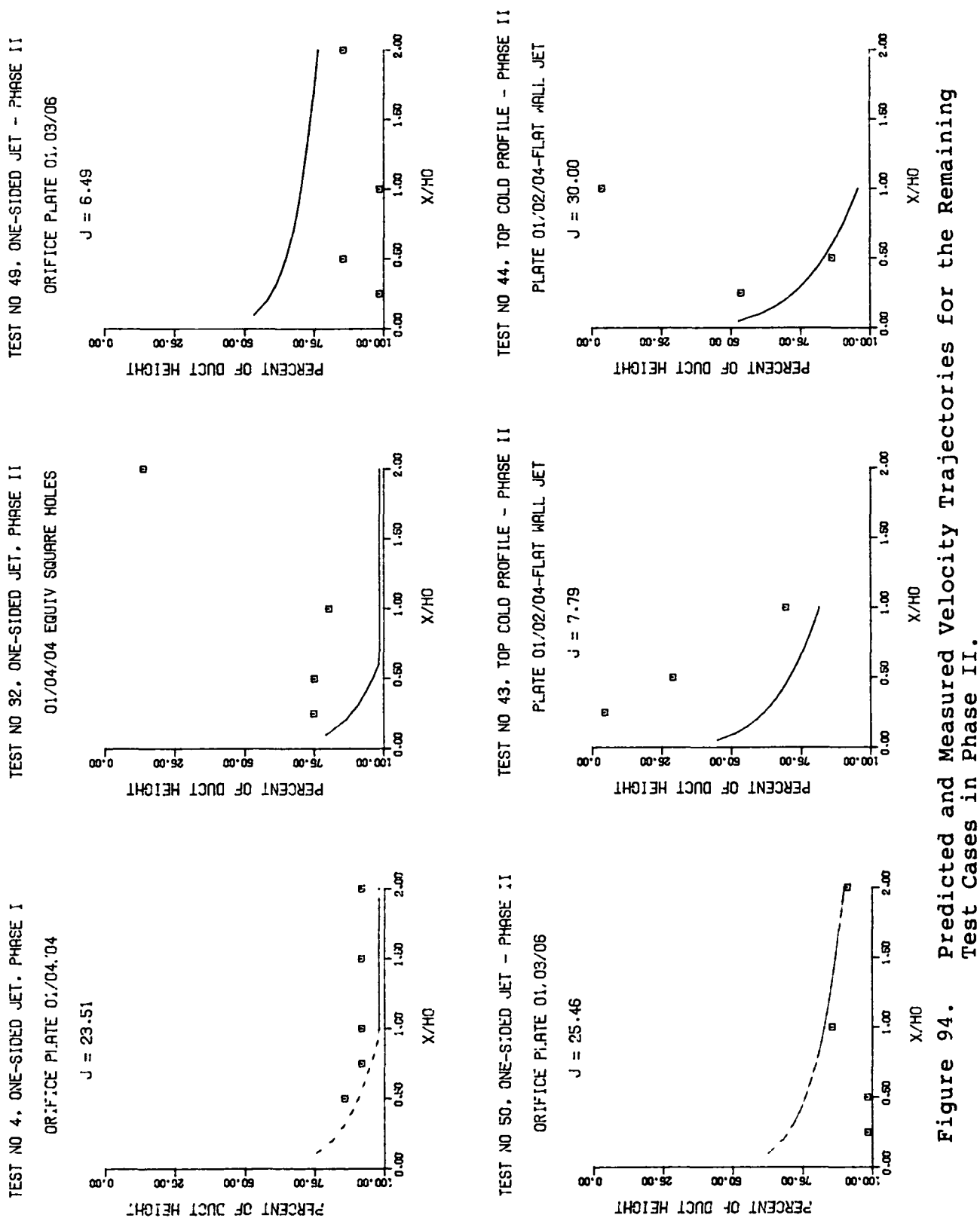


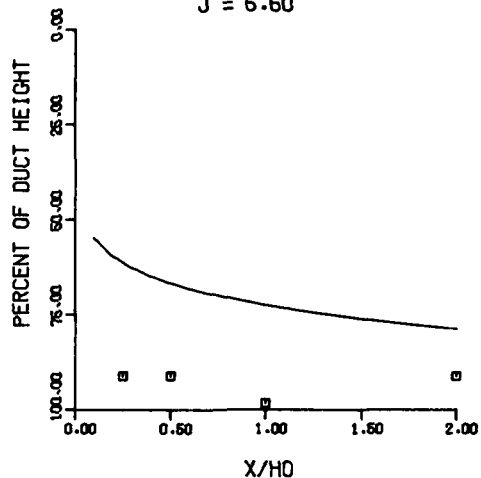
Figure 93. Predicted and Measured Velocity Trajectories for 2-D Slots.



TEST NO 1. ONE-SIDED JET, PHASE III

STREAMLINED SLOTS, $AJ/AM=0.098$

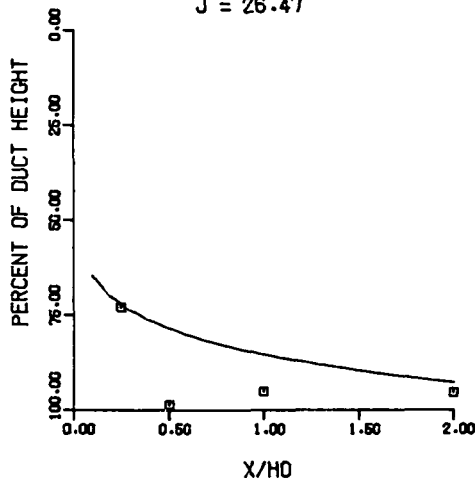
$J = 6.60$



TEST NO 2. ONE-SIDED JET, PHASE III

STREAMLINED SLOTS, $AJ/AM=0.098$

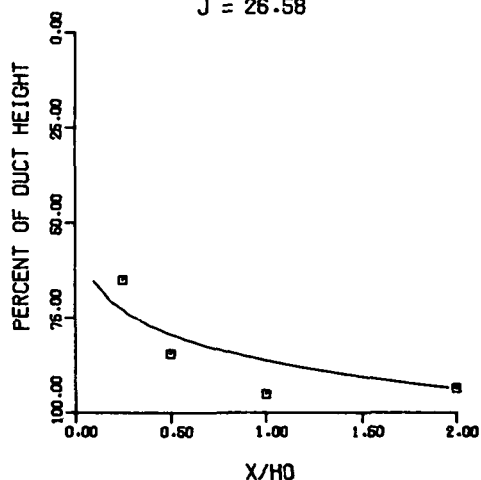
$J = 26.47$



TEST NO 3. ONE-SIDED JET - PHASE III

BLUFF SLOTS, $AJ/AM=0.098$

$J = 26.58$



TEST NO 4. ONE-SIDED JET - PHASE III

BLUFF SLOTS, $AJ/AM=0.098$

$J = 106.44$

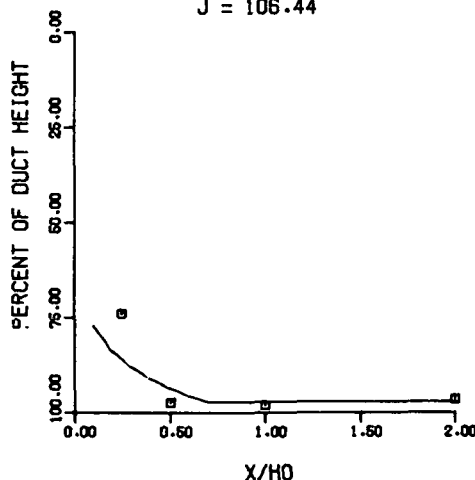
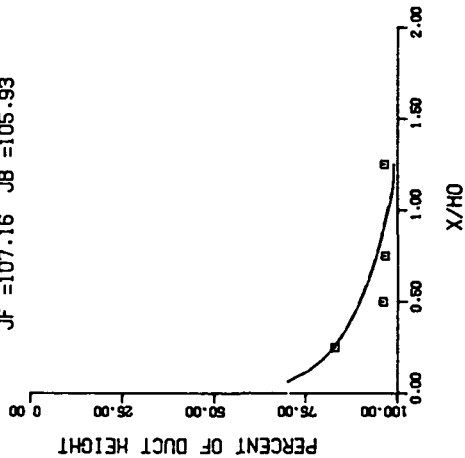


Figure 95. Predicted and Measured Velocity Trajectories for Streamlined and Bluff Slots (Equivalent Site and Spacing to Orifice Plate 01/02/04).

TEST NO 7, AXIALLY STAGED JET, PHASE III

ORIFICE PLATE M3(INL)

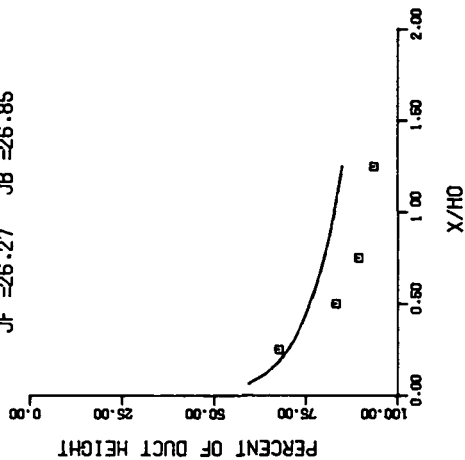
JF =107.16 JB =105.93



TEST NO 6, AXIALLY STAGED JET, PHASE III

ORIFICE PLATE M3(INL)

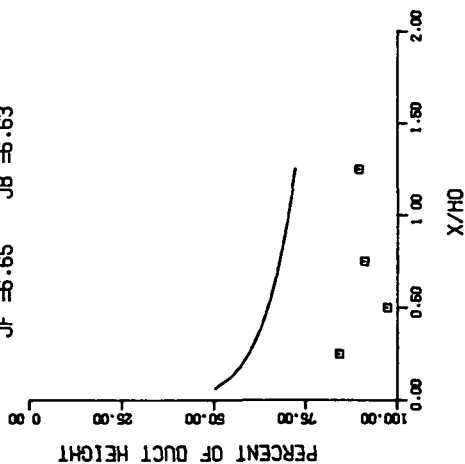
JF =26.27 JB =26.85



TEST NO 5, AXIALLY STAGED JET, PHASE III

ORIFICE PLATE - M3(INL)

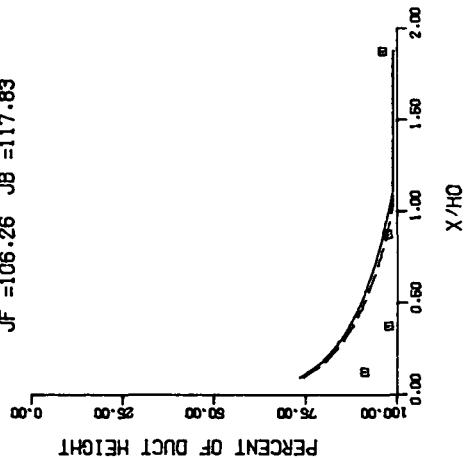
JF =6.65 JB =6.63



TEST NO 12, AXIALLY STAGED JET, PHASE III

ORIFICE PLATE - M5

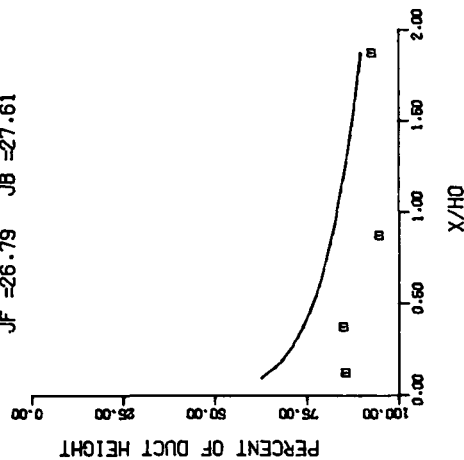
JF =106.26 JB =117.83



TEST NO 11, AXIALLY STAGED JET, PHASE III

ORIFICE PLATE - M5

JF =26.79 JB =27.61



TEST NO 10, AXIALLY STAGED JET, PHASE III

ORIFICE PLATE M5

JF =6.72 JB =6.89

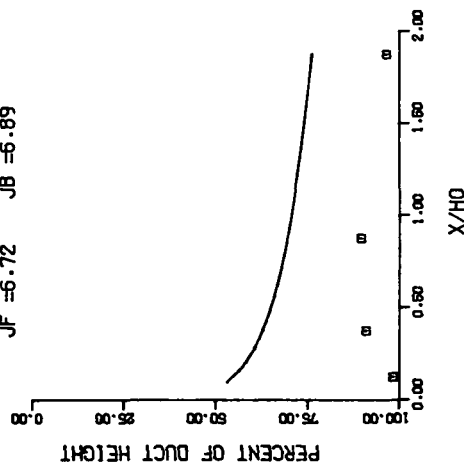
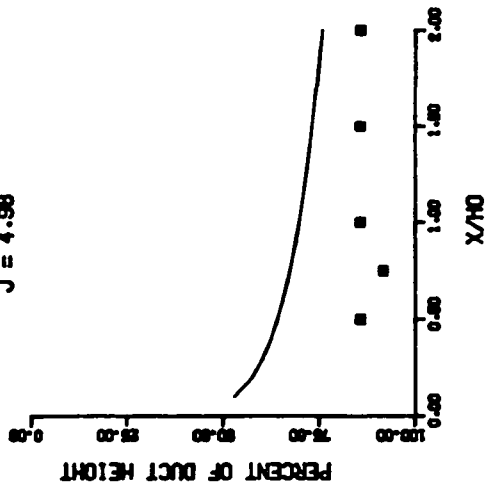


Figure 96. Predicted and Measured Velocity Trajectories for Double Row of Jets (Plate M-3 and M-5).

TEST NO 1. SINGLE SIDED ROW OF JETS

ORIFICE PLATE 01/02/04

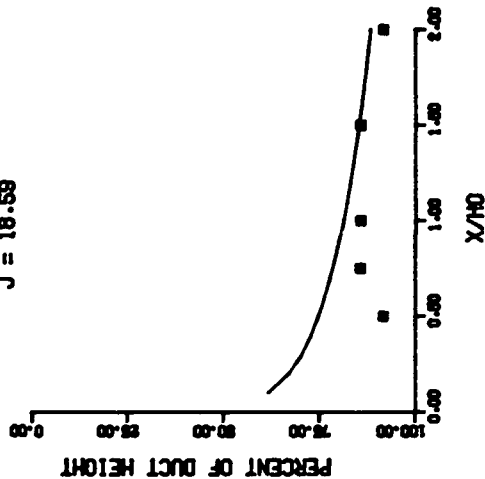
$J = 4.98$



TEST NO 2. SINGLE SIDED ROW OF JETS

ORIFICE PLATE 01/02/04

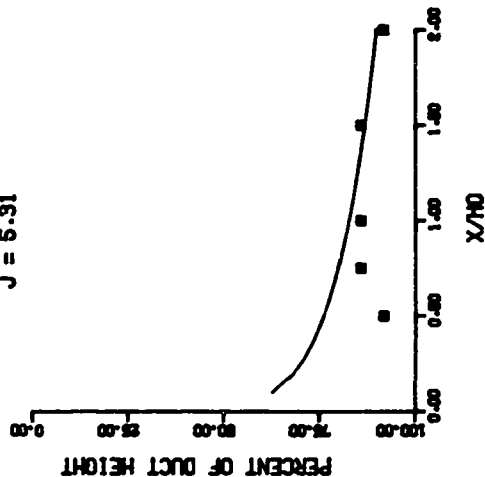
$J = 18.59$



TEST NO 3. SINGLE SIDED ROW OF JETS

ORIFICE PLATE 01/04/04

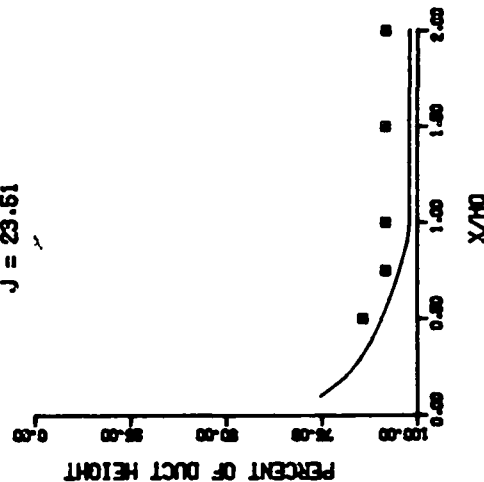
$J = 5.31$



TEST NO 4. SINGLE SIDED ROW OF JETS

ORIFICE PLATE 01/04/04

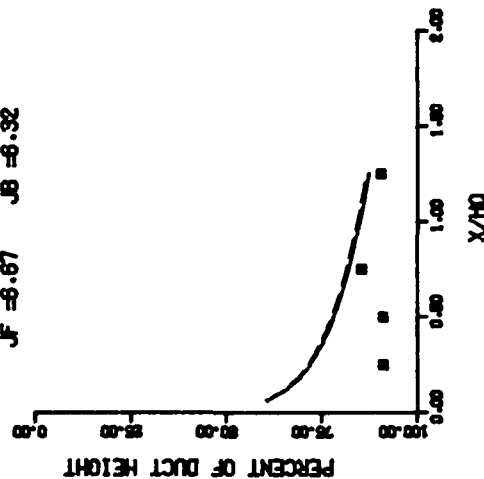
$J = 23.51$



TEST NO 8. AXIALLY STAGGED STAGGERED JETS

ORIFICE PLATE - M-4

$JF = 6.67$ $JB = 6.32$



TEST NO 9. AXIALLY STAGGED STAGGERED JETS

ORIFICE PLATE - M-4

$JF = 28.78$ $JB = 28.69$

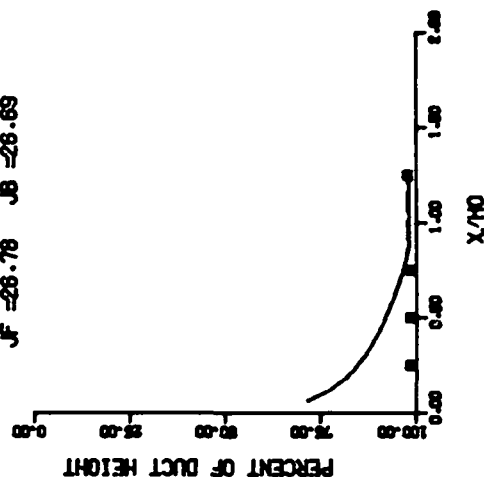


Figure 97. Comparison of Predicted and Measured Velocity Trajectories for

Plate 01/02/04, Plate M-4, and Equivalent Single Row of Jet Configurations.

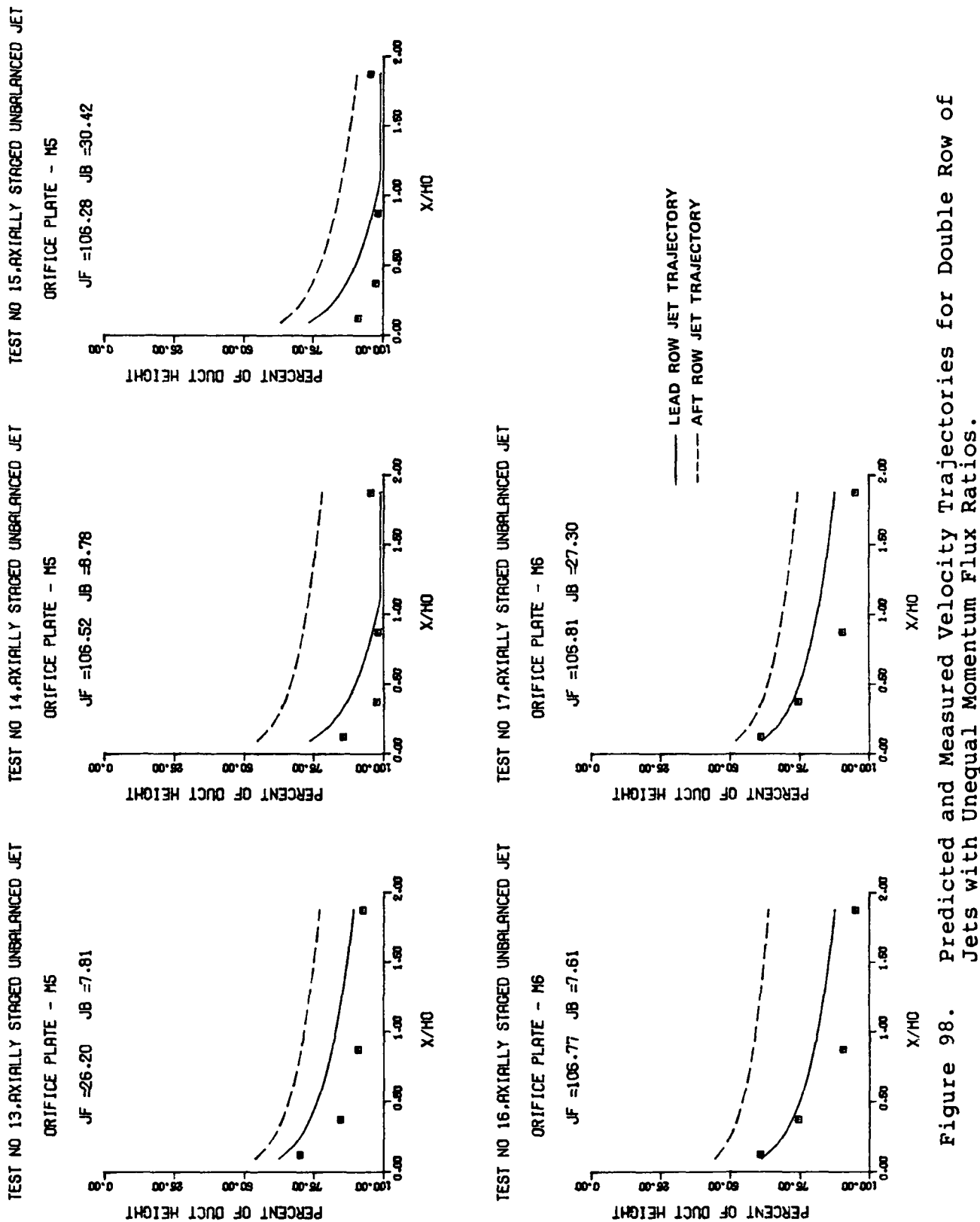
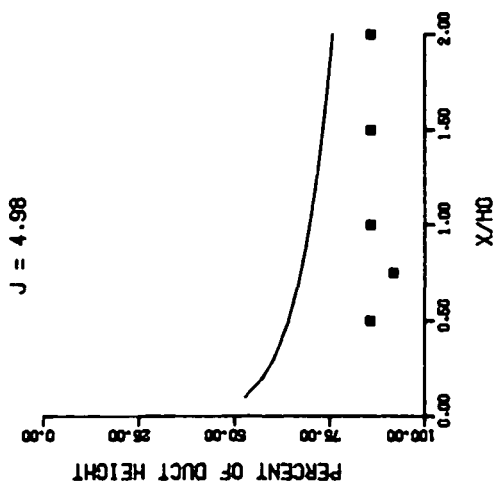
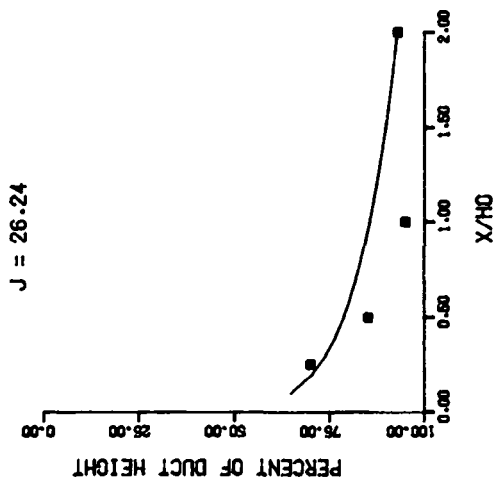


Figure 98. Predicted and Measured Velocity Trajectories for Double Row of Jets with Unequal Momentum Flux Ratios.

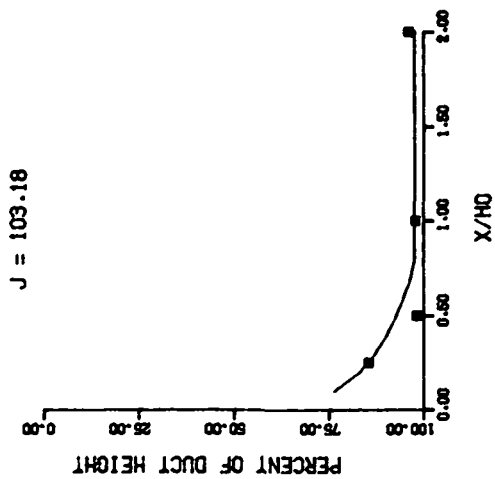
TEST NO 1. ONE-SIDED JET, PHASE I
ORIFICE PLATE 01/02/04



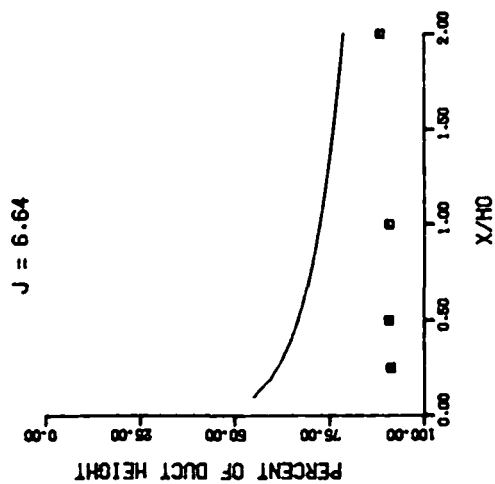
TEST NO 21. ONE-SIDED JET, PHASE III
ORIFICE PLATE 01/02/04



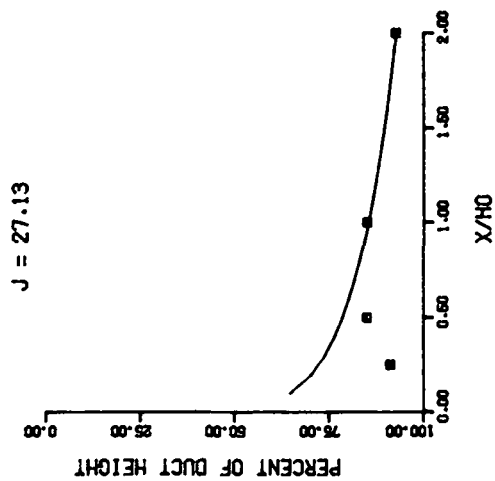
TEST NO 22. ONE-SIDED JET, PHASE III
ORIFICE PLATE 01/02/04



TEST NO 18. ONE-SIDED JET, PHASE III
45 DEG SLOTS. $RJ/RH = .098$



TEST NO 19. ONE-SIDED JET, PHASE III
45 DEG SLOTS. $RJ/RH = .098$



TEST NO 20. ONE-SIDED JET - PHASE III
45 DEG SLOTS. $RJ/RH = 0.098$

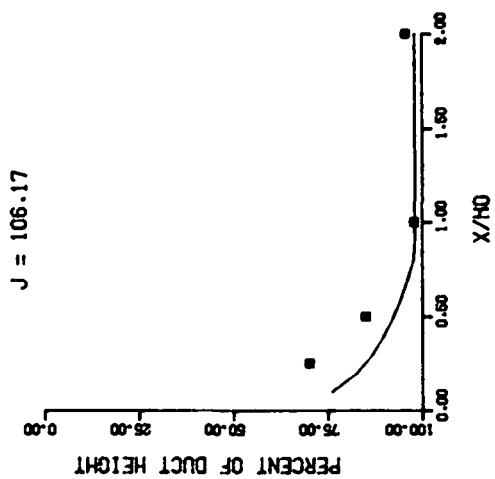
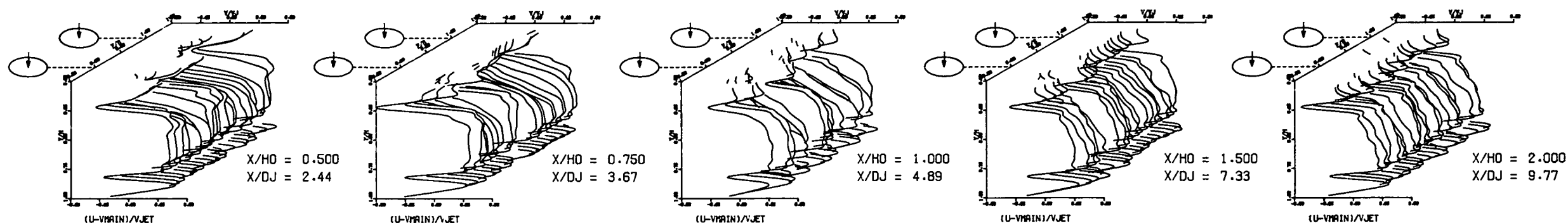


Figure 99. Comparison of Predicted and Measured Velocity Trajectories for 45-degree Slot and Equivalent Circular Holes.

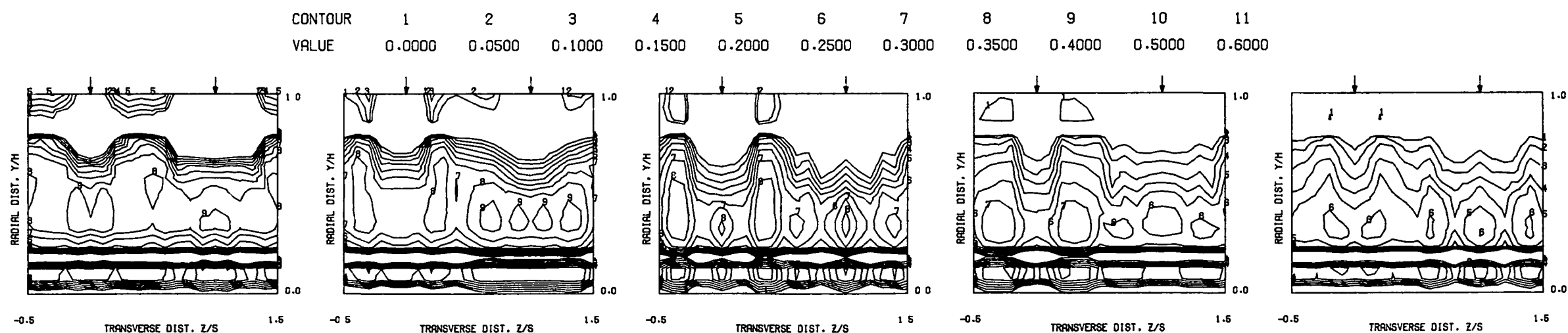
ORIGINAL PAGE IS
OF POOR QUALITY

ORIGINAL PAGE IS
OF POOR QUALITY

S = 0.0508 METERS S/DJ = 2.443 HO/DJ = 4.887 VMAIN = 4.8 M/SEC VJET = 7.9 M/SEC TMAIN = 361.0 K TJET = 171.2 K THEB = 0.1759 BLORAT = 3.243 DENRATIO = 2.113 TRATIO = 0.474



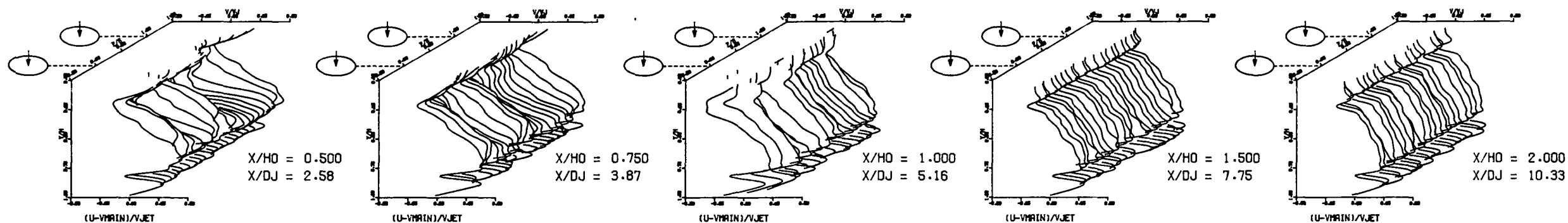
MEASURED VELOCITY PROFILES FOR TEST NO 1, TEST SECTION I, ONE-SIDED JET, $J = 4.98$, $S/D = 2.00$, $H/D = 4.00$



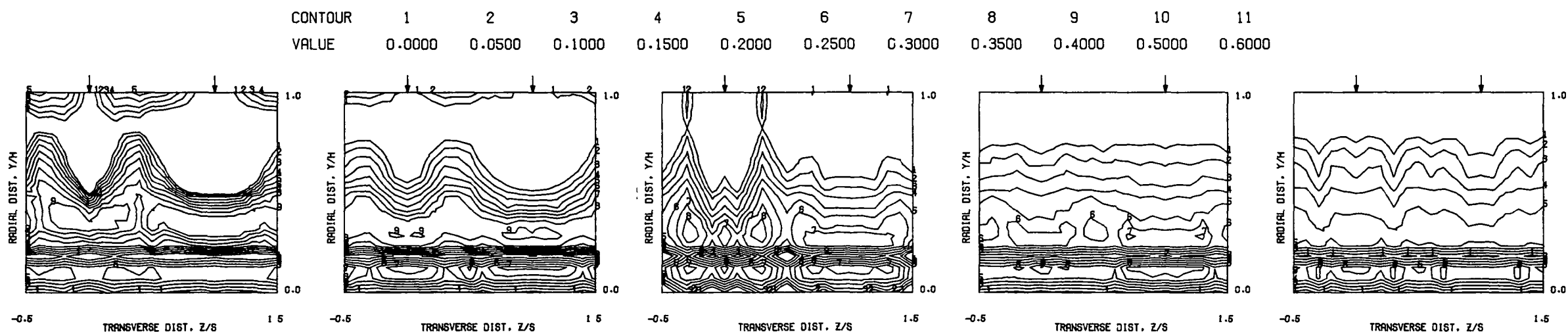
MEASURED VELOCITY PROFILES FOR TEST NO 1, TEST SECTION I, ONE-SIDED JET, $J = 4.98$, $S/D = 2.00$, $H/D = 4.00$

Figure 100. Measured Velocity
Distributions for Test No. 1 of DJM Phase I
Testing.

S = 0.0508 METERS S/DJ = 2.582 HO/DJ = 5.164 VMAIN = 5.0 M/SEC VJET = 15.9 M/SEC TMAIN = 361.8 K TJET = 171.1 K THEB = 0.2705 BLORAT = 6.281 DENRATIO = 2.132 TRATIO = 0.473



MEASURED VELOCITY PROFILES FOR TEST NO 2, TEST SECTION I, ONE-SIDED JET, $J = 18.59$, $S/D = 2.00$, $H/D = 4.00$



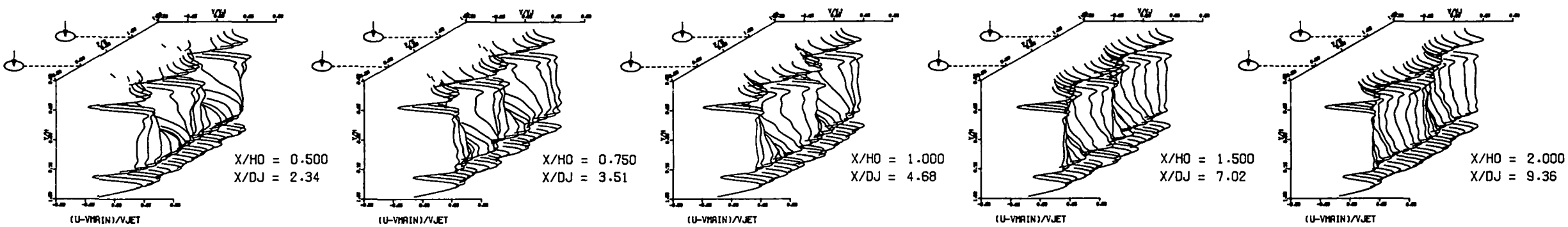
MEASURED VELOCITY PROFILES FOR TEST NO 2, TEST SECTION I, ONE-SIDED JET, $J = 18.59$, $S/D = 2.00$, $H/D = 4.00$

Figure 101. Measured Velocity Distributions for Test No. 2 of DJM Phase I Testing.

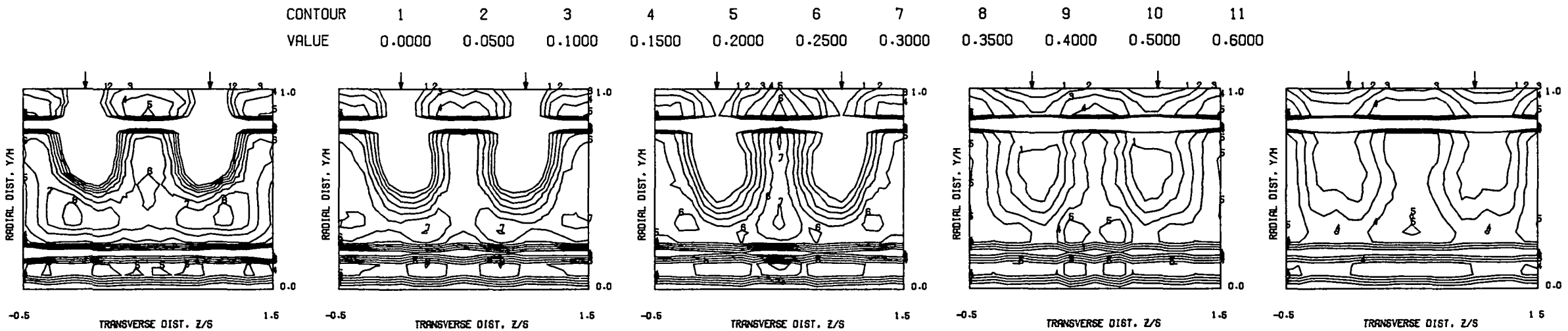
FOLDOUT FRAME

FOLDOUT FRAME

S = 0.1016 METERS S/DJ = 4.682 HO/DJ = 4.682 VMAIN = 4.6 M/SEC VJET = 7.9 M/SEC TMAIN = 360.7 K TJET = 170.5 K THEB = 0.1074 BLORAT= 3.356 DENRATIO= 2.122 TRATIO=0.473



MEASURED VELOCITY PROFILES FOR TEST NO 3,TEST SECTION I, ONE-SIDED JET , J = 5.31 , S/D = 4.00 , H/D = 4.00



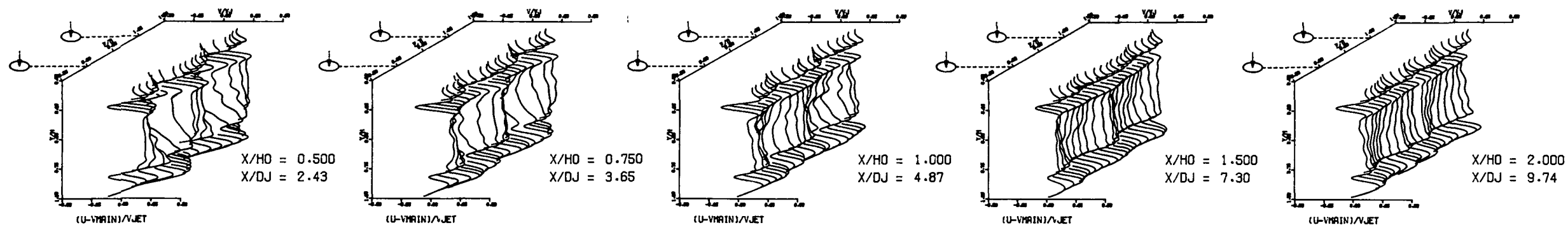
MEASURED VELOCITY PROFILES FOR TEST NO 3,TEST SECTION I, ONE-SIDED JET , J = 5.31 , S/D = 4.00 , H/D = 4.00

Figure 102. Measured Velocity Distributions for Test No. 3 of DJM Phase I Testing.

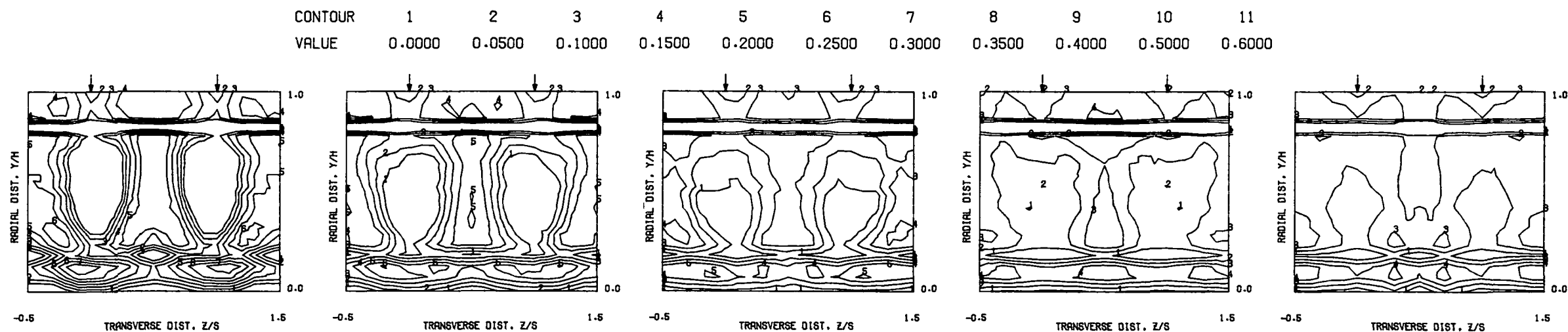
FOLDOUT FRAME

FOLDOUT FRAME

S = 0.1016 METERS S/DJ = 4.869 HO/DJ = 4.869 VMAIN = 4.5 M/SEC VJET = 15.9 M/SEC TMAIN = 361.8 K TJET = 168.9 K THEB = 0.1915 BLORAT= 7.148 DENRATIO= 2.174 TRATIO=0.467



MEASURED VELOCITY PROFILES FOR TEST NO 4, TEST SECTION I, ONE-SIDED JET, $J = 23.51$, $S/D = 4.00$, $H/D = 4.00$



MEASURED VELOCITY PROFILES FOR TEST NO 4, TEST SECTION I, ONE-SIDED JET, $J = 23.51$, $S/D = 4.00$, $H/D = 4.00$

Figure 103. Measured Velocity Distributions for Test No. 4 of DJM Phase I Testing.

FOLDOUT FRAME

FOLDOUT FRAME

S = 0.0254 METERS S/DJ = 2.582 HO/DJ = 10.328 VMAIN = 4.6 M/SEC VJET = 15.8 M/SEC TMAIN = 360.4 K TJET = 171.3 K THEB = 0.1687 BLORAT= 6.890 DENRATIO= 2.128 TRATIO=0.475

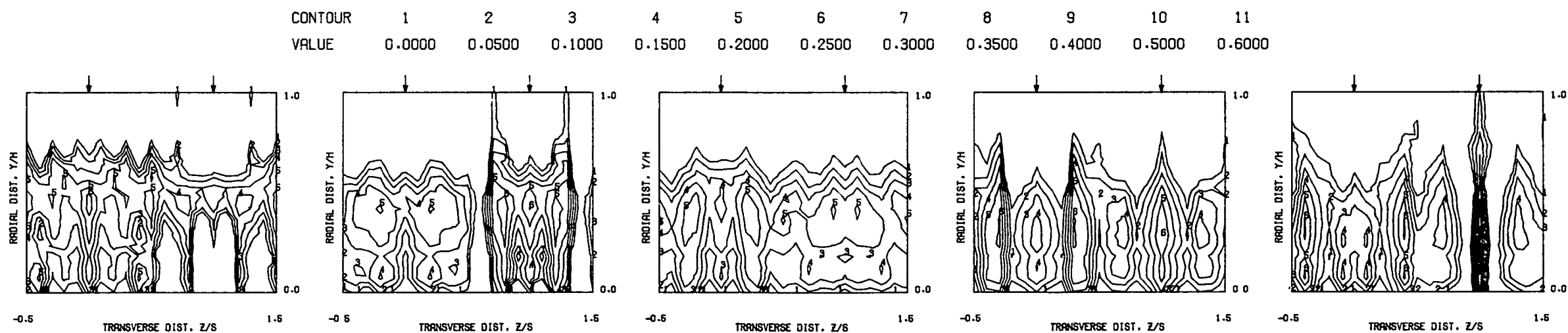
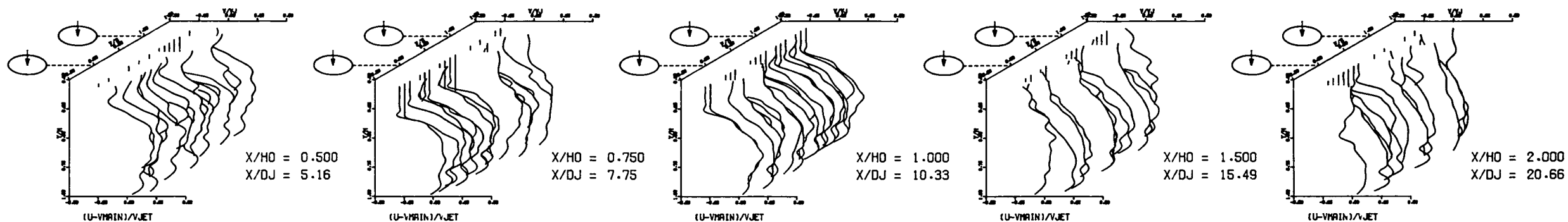


Figure 104. Measured Velocity Distributions for Test No. 5 of DJM Phase I Testing.

ORIGINAL PAGE IS
OF POOR QUALITY

ORIGINAL PAGE IS
OF POOR QUALITY

S = 0.0254 METERS S/DJ = 2.571 HO/DJ = 10.285 VMAIN = 4.6 M/SEC VJET = 31.6 M/SEC TMAIN = 360.9 K TJET = 166.2 K THEB = 0.3018 BLORAT = 14.554 DENRATIO = 2.287 TRATIO = 0.460

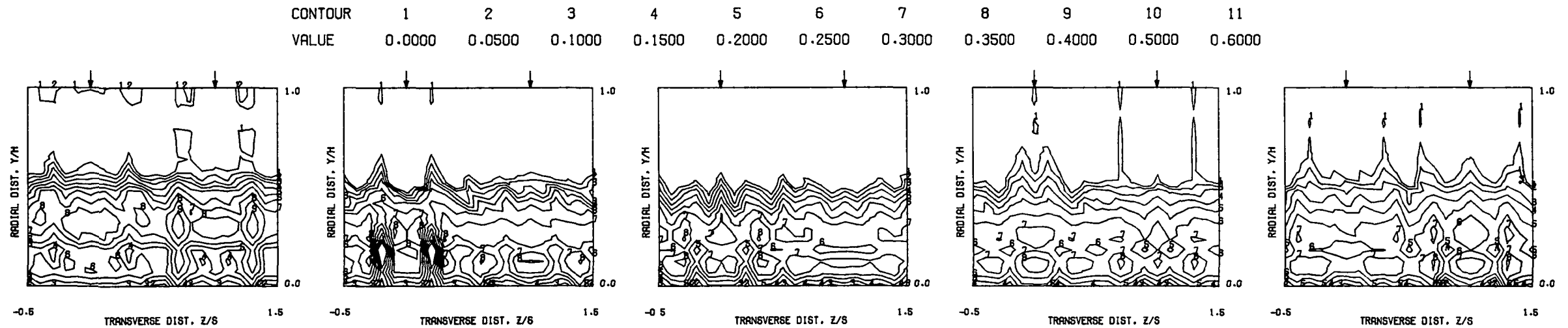
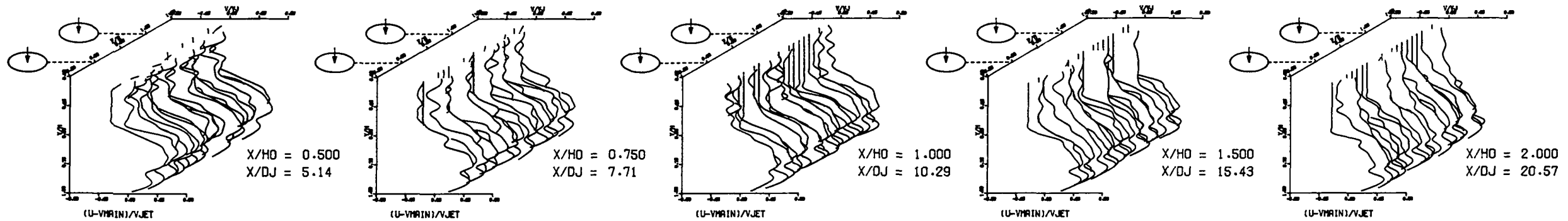


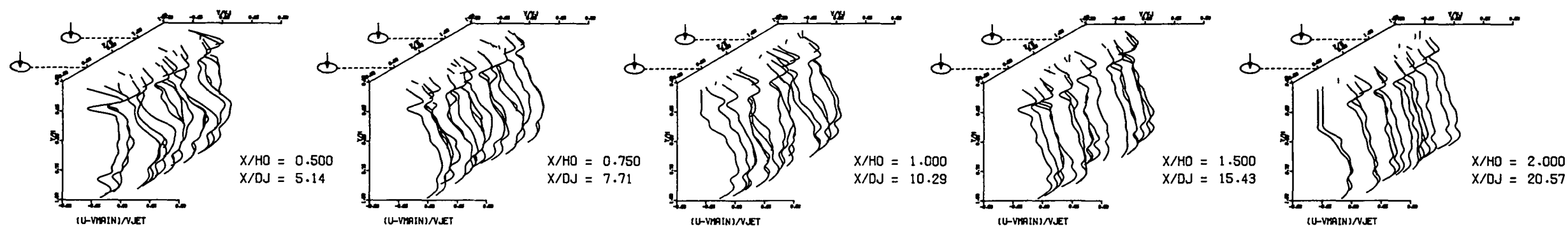
Figure 105. Measured Velocity Distributions for Test No. 6 of DJM Phase I Testing.

FOLDOUT FRAME

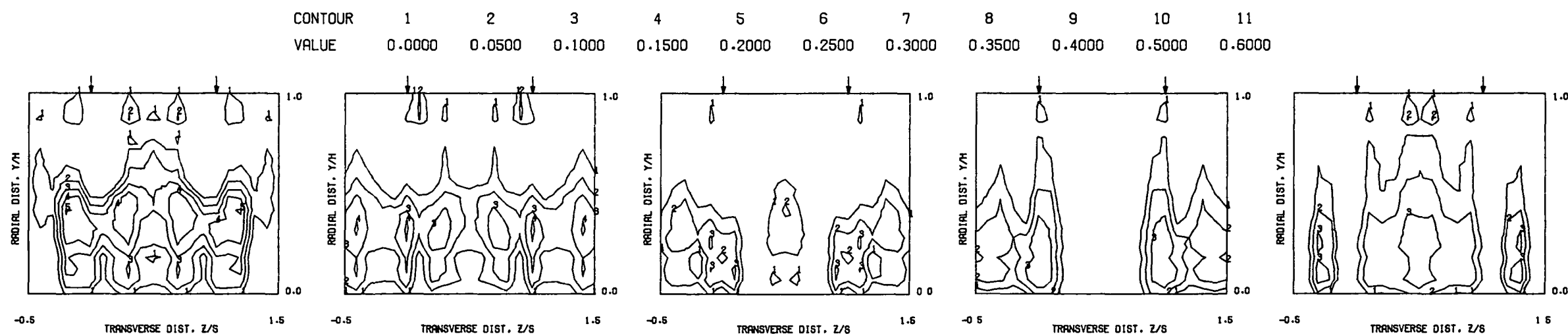
2 FOLDOUT FRAME

ORIGINAL PAGE IS
OF POOR QUALITY

S = 0.0508 METERS S/DJ = 5.143 HO/DJ = 10.285 VMAIN = 4.6 M/SEC VJET = 16.1 M/SEC TMAIN = 361.9 K TJET = 167.8 K THEB = 0.1048 BLORAT = 7.127 DENRATIO = 2.192 TRATIO = 0.464



MEASURED VELOCITY PROFILES FOR TEST NO 7, TEST SECTION I, ONE-SIDED JET, $J = 28.37$, $S/D = 4.00$, $H/D = 8.00$



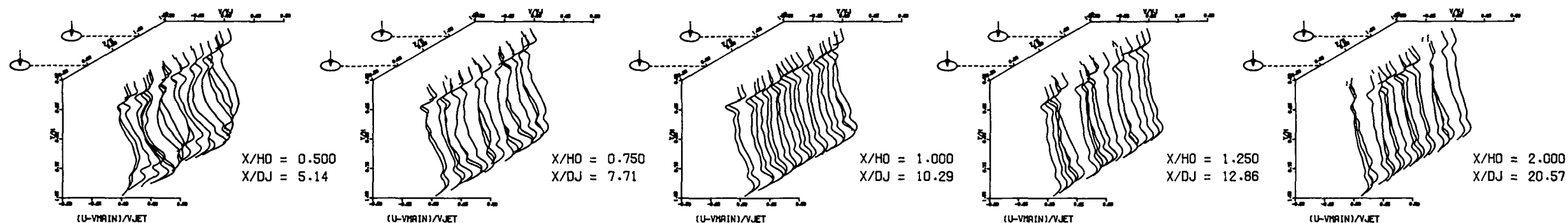
MEASURED VELOCITY PROFILES FOR TEST NO 7, TEST SECTION I, ONE-SIDED JET, $J = 28.37$, $S/D = 4.00$, $H/D = 8.00$

Figure 106. Measured Velocity
Distributions for Test No. 7 of DJM Phase I
Testing.

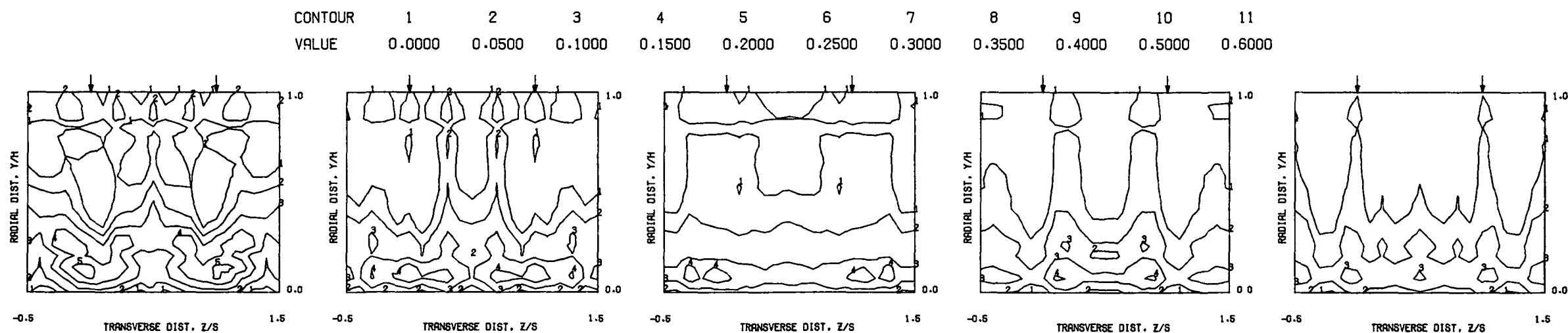
FOLDOUT FRAME

FOLDOUT FRAME

S = 0.0508 METERS S/DJ = 5.143 HO/DJ = 10.285 VMAIN = 4.6 M/SEC VJET = 31.7 M/SEC TMAIN = 360.7 K TJET = 165.9 K THEB = 0.1808 BLORAT= 14.866 DENRATIO= 2.303 TRATIO=0.460



MEASURED VELOCITY PROFILES FOR TEST NO 8, TEST SECTION I, ONE-SIDED JET, $J = 96.00$, $S/D = 4.00$, $H/D = 8.00$



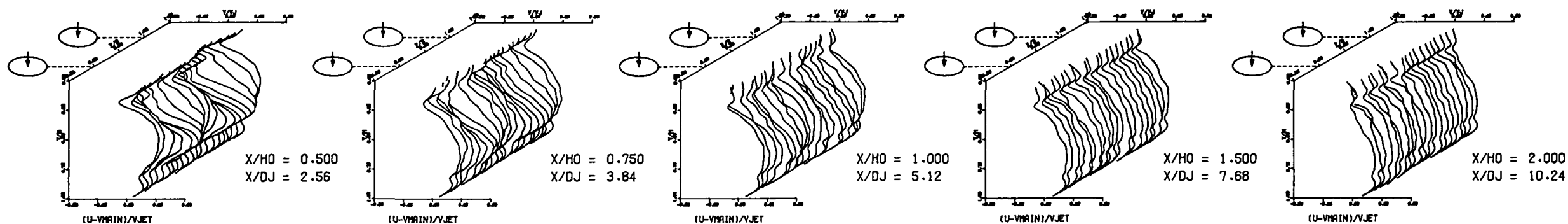
MEASURED VELOCITY PROFILES FOR TEST NO 8, TEST SECTION I, ONE-SIDED JET, $J = 96.00$, $S/D = 4.00$, $H/D = 8.00$

Figure 107. Measured Velocity Distributions for Test No. 8 of DJM Phase I Testing.

FOLDOUT FRAME

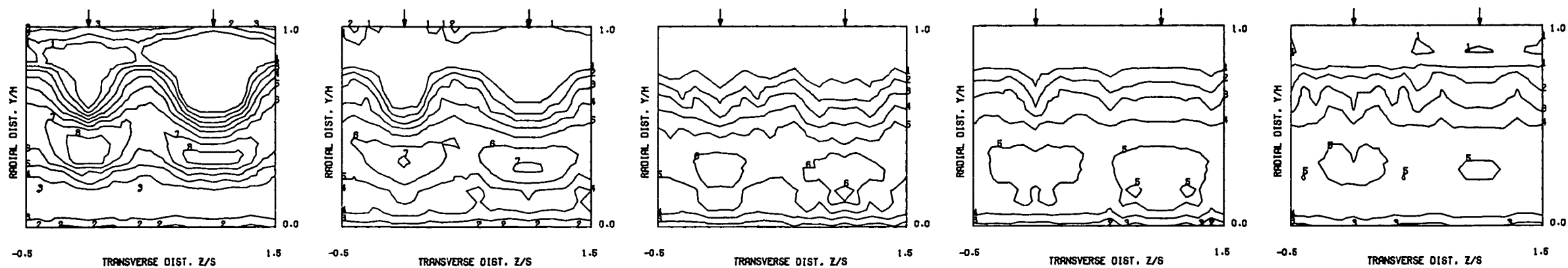
2 FOLDOUT FRAME

S = 0.0508 METERS S/DJ = 2.561 HO/DJ = 5.121 VMAIN = 4.7 M/SEC VJET = 33.3 M/SEC TMAIN = 169.9 K TJET = 284.2 K THEB = 0.1830 BLORAT= 3.765 DENRATIO= 0.617 TRATIO=1.673



MEASURED VELOCITY PROFILES FOR TEST NO 9, TEST SECTION I, HEATED JETS , J = 22.69 , S/D = 2.00 , H/D = 4.00

CONTOUR	1	2	3	4	5	6	7	8	9	10	11
VALUE	0.0000	0.0500	0.1000	0.1500	0.2000	0.2500	0.3000	0.3500	0.4000	0.5000	0.6000



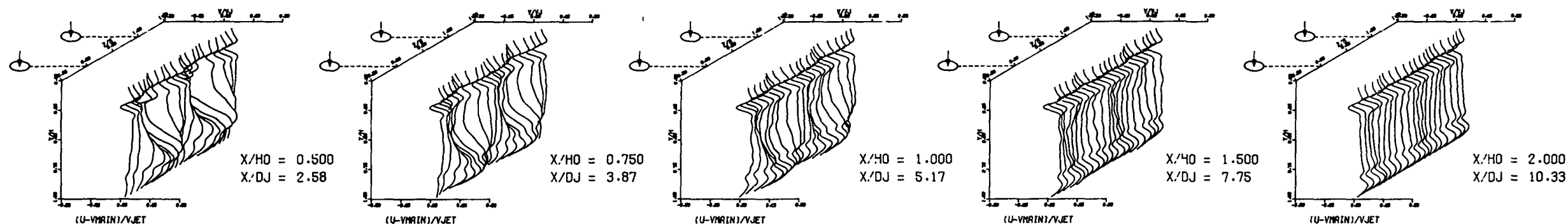
MEASURED VELOCITY PROFILES FOR TEST NO 9, TEST SECTION I, HEATED JETS , J = 22.69 , S/D = 2.00 , H/D = 4.00

Figure 108. Measured Velocity Distributions for Test No. 9 of DJM Phase I Testing.

FOLDOUT FRAME

2 FOLDOUT FRAME

S = 0.1016 METERS S/DJ = 5.165 H0/DJ = 5.165 VMAIN = 4.6 M/SEC VJET = 31.5 M/SEC TMAIN = 162.8 K TJET = 254.0 K THEB = 0.1024 BLORAT = 3.873 DENRATIO = 0.663 TRATIO = 1.560



CONTOUR VALUE 1 0.0000 2 0.0500 3 0.1000 4 0.1500 5 0.2000 6 0.2500 7 0.3000 8 0.3500 9 0.4000 10 0.5000 11 0.6000

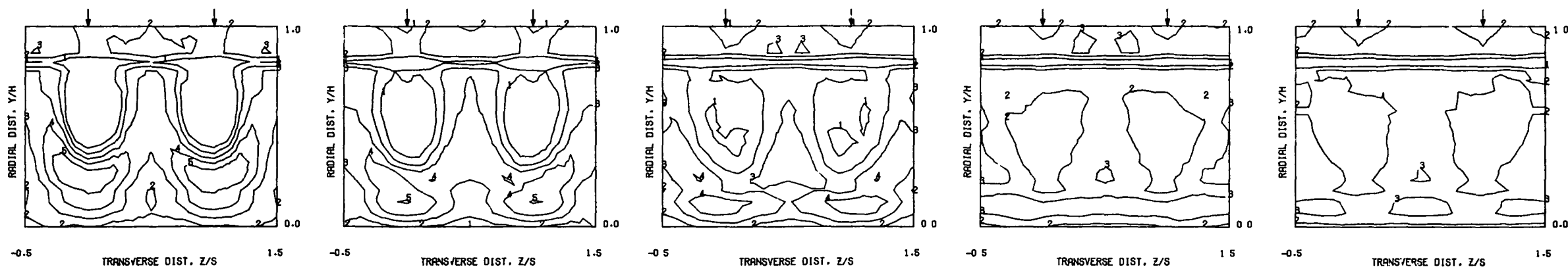


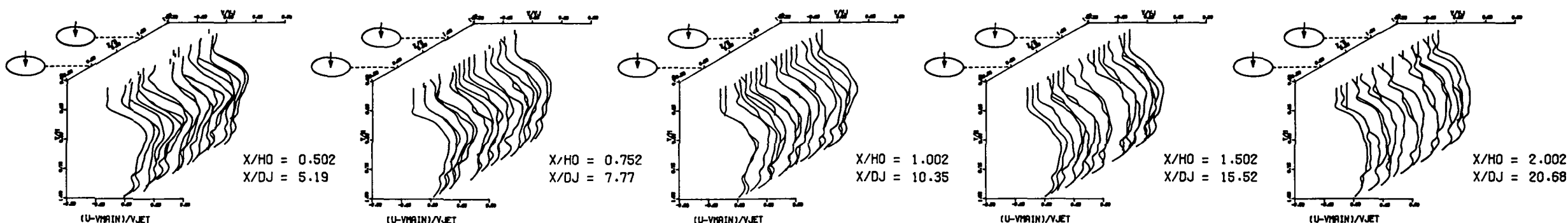
Figure 109. Measured Velocity Distributions for Test No. 10 of DJM Phase I Testing.

FOLDOUT FRAME

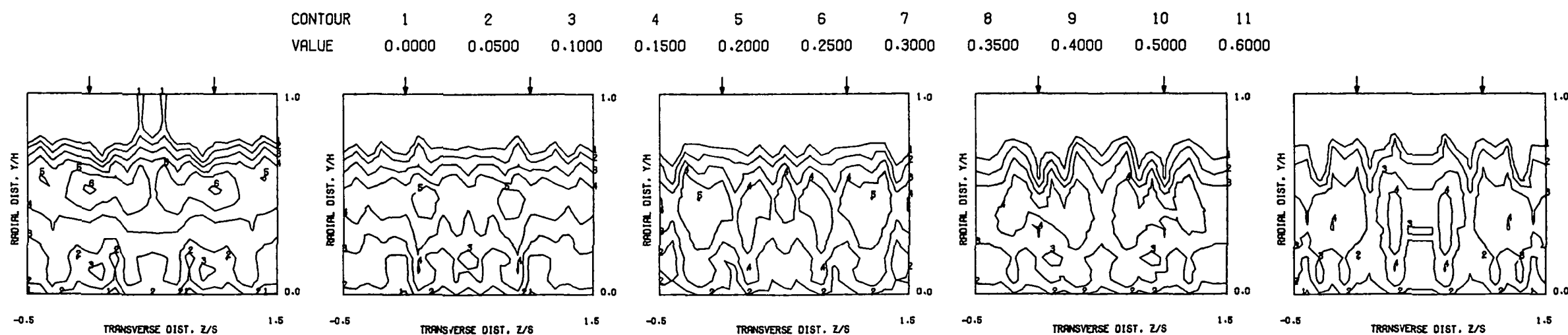
ORIGINAL PAGE IS
OF POOR QUALITY

ORIGINAL PAGE IS
OF POOR QUALITY

S = 0.0254 METERS S/DJ = 2.582 HO/DJ = 10.327 VMAIN = 4.6 M/SEC VJET = 31.1 M/SEC TMAIN = 161.3 K TJET = 247.1 K THEB = 0.1025 BLORAT= 3.875 DENRATIO= 0.672 TRATIO=1.532



MEASURED VELOCITY PROFILES FOR TEST NO 11, TEST SECTION I, HEATED JETS , J = 22.33 , S/D = 2.00 , H/D = 8.00



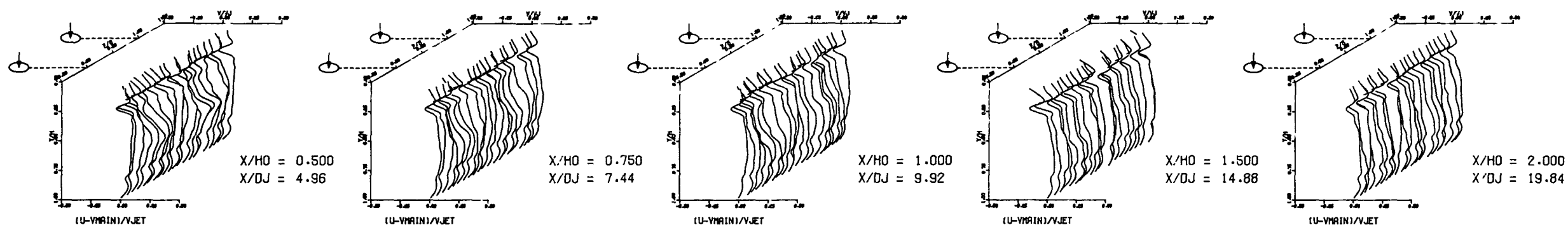
MEASURED VELOCITY PROFILES FOR TEST NO 11, TEST SECTION I, HEATED JETS , J = 22.33 , S/D = 2.00 , H/D = 8.00

Figure 110. Measured Velocity Distributions for Test No. 11 of DJM Phase I Testing.

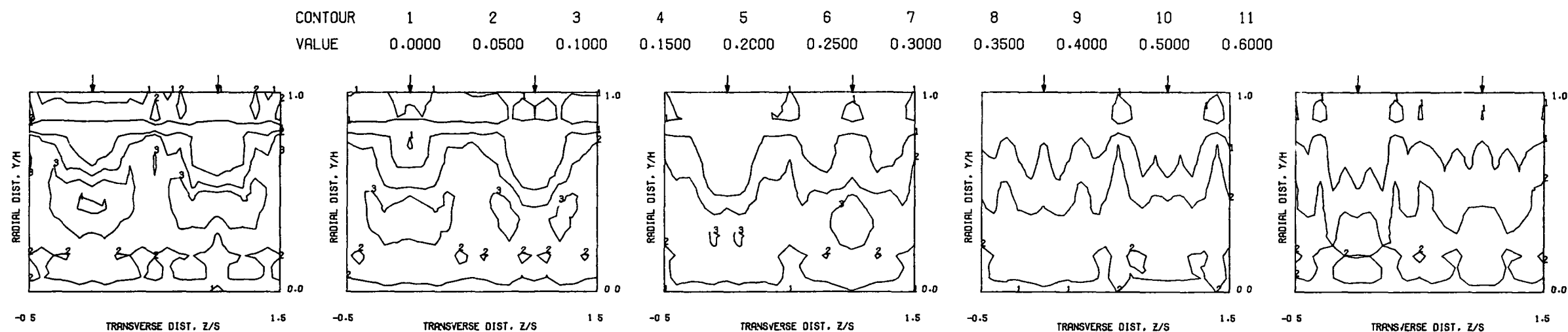
FOLDOUT FRAME

FOLDOUT FRAME

$S = 0.0508$ METERS $S/DJ = 4.961$ $HO/DJ = 9.921$ $V_{MAIN} = 4.7$ M/SEC $V_{JET} = 29.8$ M/SEC $T_{MAIN} = 163.0$ K $T_{JET} = 226.7$ K $THEB = 0.0617$ $BLOPRT = 4.117$ $DENRATIO = 0.747$ $TRATIO = 1.391$



MEASURED VELOCITY PROFILES FOR TEST NO 12, TEST SECTION I, HEATED JETS , $J = 22.68$, $S/D = 4.00$, $H/D = 8.00$



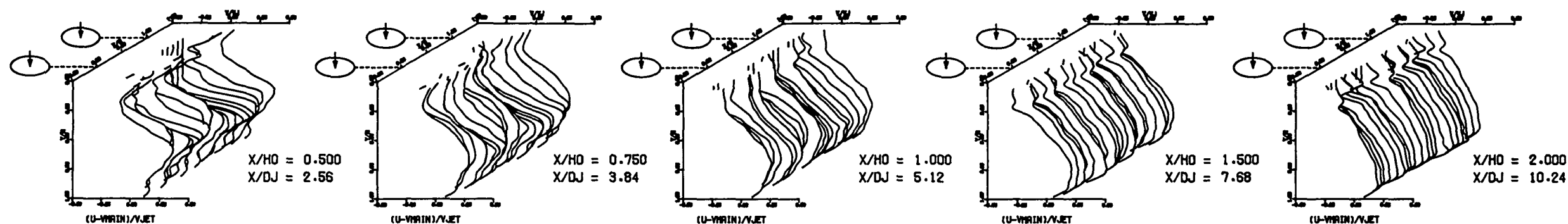
MEASURED VELOCITY PROFILES FOR TEST NO 12, TEST SECTION I, HEATED JETS , $J = 22.68$, $S/D = 4.00$, $H/D = 8.00$

Figure 111. Measured Velocity Distributions for Test No. 12 of DJM Phase I Testing.

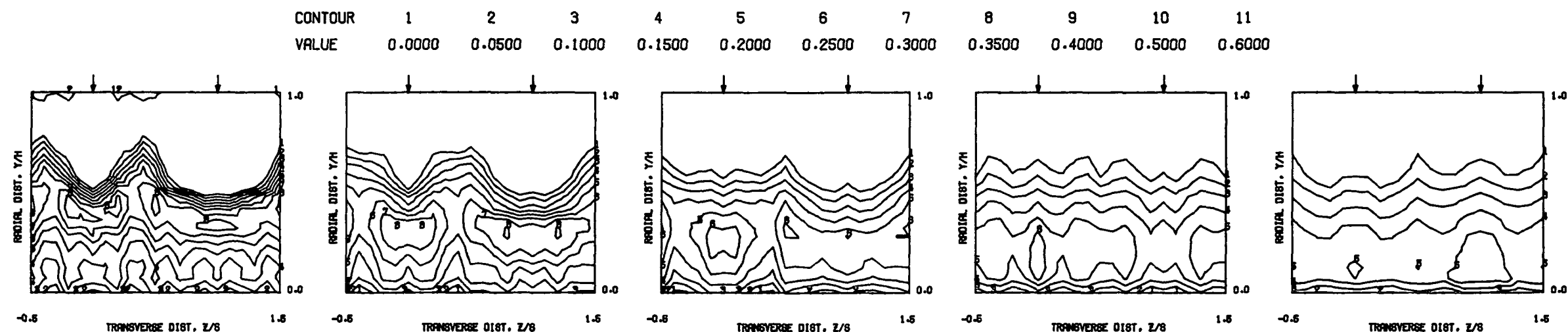
FOLDOUT FRAME

FOLDOUT FRAME

S = 0.0508 METERS S/DJ = 2.561 HO/DJ = 5.122 VMAIN = 5.1 M/SEC VJET = 18.2 M/SEC TMAIN = 290.9 K TJET = 163.1 K THEB = 0.6508 BLORAT = 7.626 DENRATIO = 1.805 TRATIO = 0.560



MEASURED VELOCITY PROFILES FOR TEST NO 13, TEST SECTION I, TOP COLD TM, J = 31.79, S/D = 2.00, H/D = 4.00



MEASURED VELOCITY PROFILES FOR TEST NO 13, TEST SECTION I, TOP COLD TM, J = 31.79, S/D = 2.00, H/D = 4.00

Figure 112. Measured Velocity Distributions for Test No. 13 of DJM Phase I Testing.

FOLDOUT FRAME

FOLDOUT FRAME

ORIGINAL PAGE 15
OF POOR QUALITY

ORIGINAL PAGE IS
OF POOR QUALITY

S = 0.1016 METERS S/DJ = 4.845 HD/DJ = 4.845 VMRAIN = 4.7 M/SEC VJET = 8.6 M/SEC THAIN = 373.5 K TJET = 169.3 K THEB = 0.3389 BLORAT = 3.847 DENRATIO = 2.210 TRATIO = 0.453

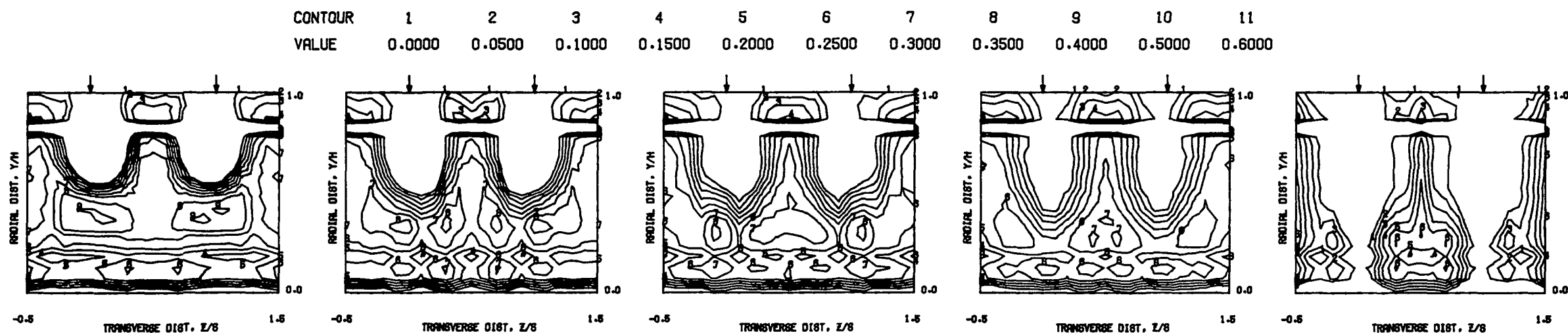
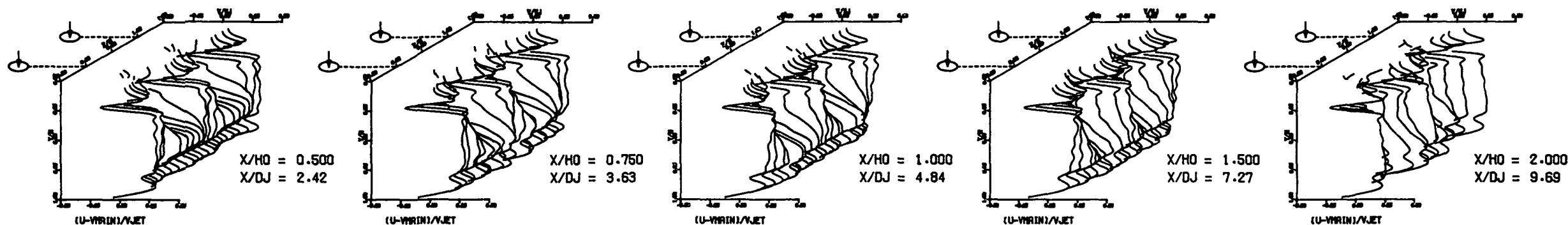
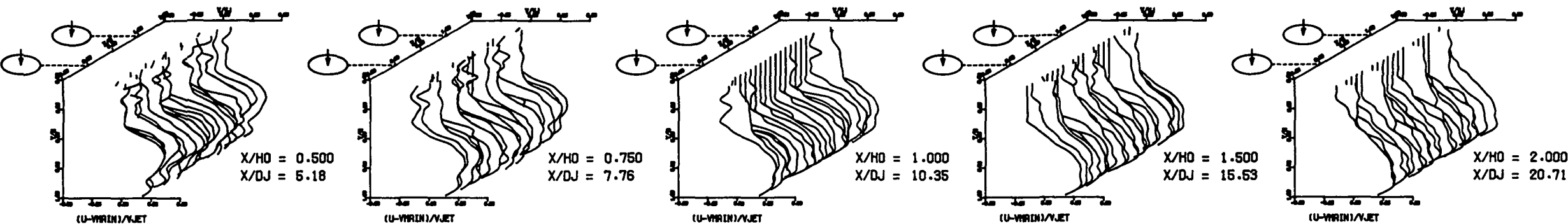


Figure 113. Measured Velocity
Distributions for Test No. 14 of DJM
Phase I Testing.

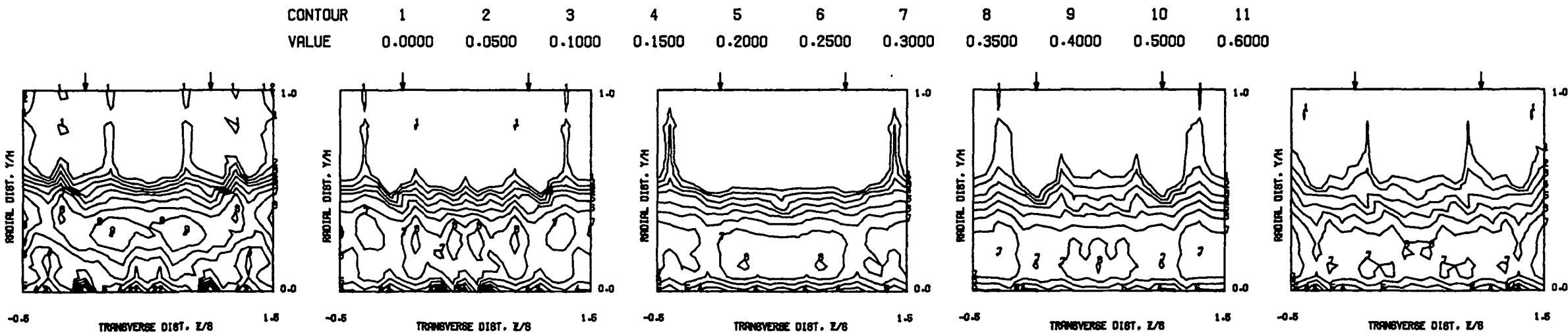
FOLDOUT FRAME

2 FOLDOUT FRAME

S = 0.0254 METERS S/DJ = 2.588 H0/DJ = 10.353 VMIN = 4.7 M/SEC VJET = 33.3 M/SEC TMAIN = 342.3 K TJET = 165.1 K THEB = 0.4692 BLORAT= 14.821 DENRATIO= 2.215 TRATIO=0.482



MEASURED VELOCITY PROFILES FOR TEST NO 15,TEST SECTION I, TOP COLD TM , J = 99.21 , S/D = 2.00 , H/D = 8.00



MEASURED VELOCITY PROFILES FOR TEST NO 15,TEST SECTION I, TOP COLD TM , J = 99.21 , S/D = 2.00 , H/D = 8.00

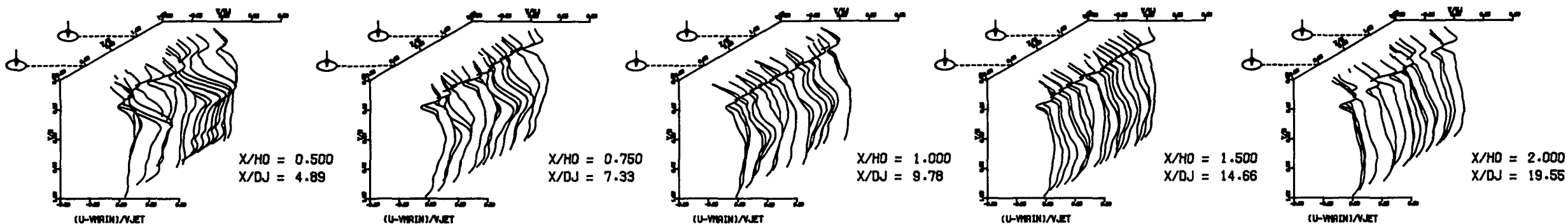
Figure 114. Measured Velocity Distributions for Test No. 15 of DJM Phase I Testing.

FOLDOUT FRAME

2 FOLDOUT FRAME

ORIGINAL PAGE IS
OF POOR QUALITY

$S = 0.0508$ METERS $S/DJ = 4.888$ $H0/DJ = 9.776$ $V_{MAIN} = 5.5$ M/SEC $V_{JET} = 19.2$ M/SEC $T_{HIN} = 315.1$ K $T_{JET} = 172.6$ K $T_{HEB} = 0.5174$ $BLORAT = 6.908$ $DENRATIO = 1.856$ $TRATIO = 0.548$



CONTOUR VALUE 1 2 3 4 5 6 7 8 9 10 11
0.0000 0.0500 0.1000 0.1500 0.2000 0.2500 0.3000 0.3500 0.4000 0.5000 0.6000

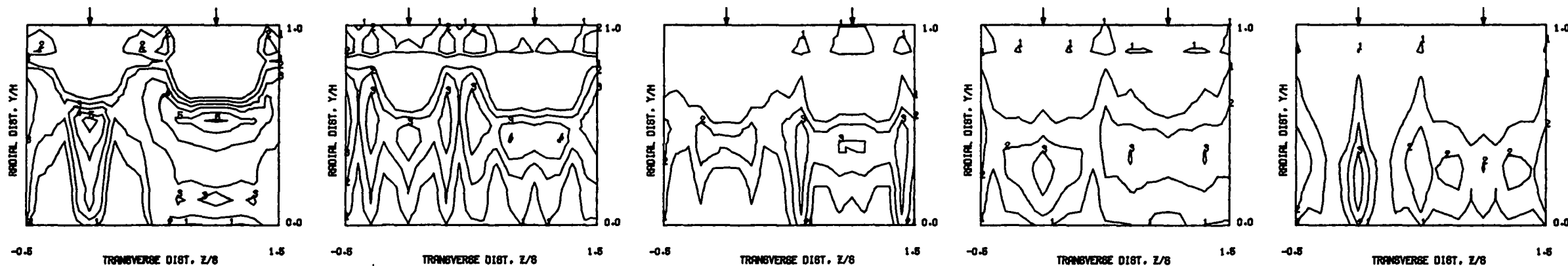
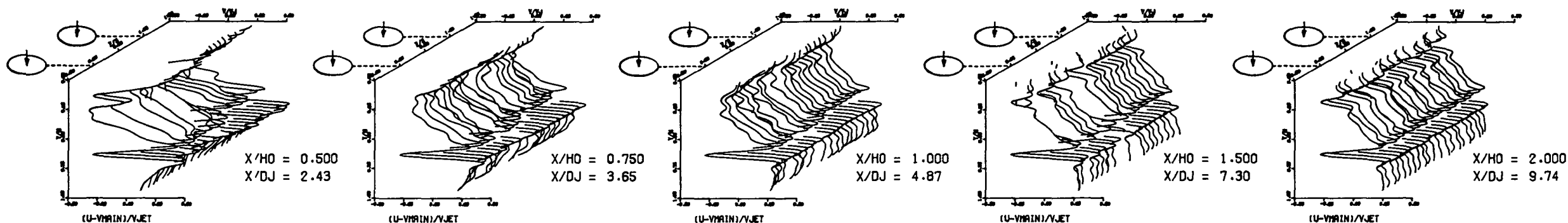


Figure 115. Measured Velocity Distributions for Test No. 16 of DJM Phase I Testing.

FOLDOUT FRAME

FOLDOUT FRAME

S = 0.0508 METERS S/DJ = 2.434 H0/DJ = 4.869 VMAIN = 5.0 M/SEC VJET = 17.7 M/SEC THAIN = 299.0 K TJET = 168.5 K THEB = 0.6001 BLORAT = 6.629 DENRATIO = 1.798 TRATIO = 0.564



CONTOUR VALUE 1 0.0000 2 0.0500 3 0.1000 4 0.1500 5 0.2000 6 0.2500 7 0.3000 8 0.3500 9 0.4000 10 0.5000 11 0.6000

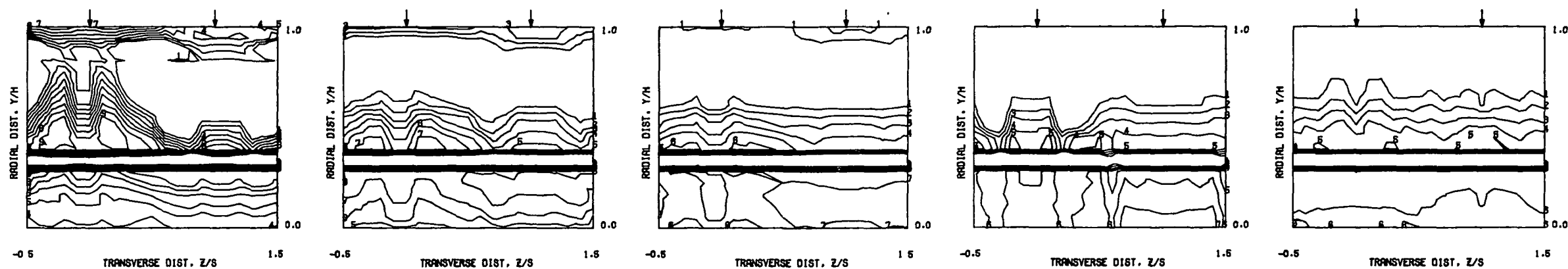


Figure 116. Measured Velocity Distributions for Test No. 17 of DJM Phase I Testing.

FOLDOUT FRAME

2 FOLDOUT FRAME

S = 0.0508 METERS S/DJ = 4.869 HO/DJ = 9.737 VMIN = 5.5 M/SEC VJET = 22.0 M/SEC TMAIN = 302.8 K TJET = 176.0 K THEB = 0.4895 BLORAT = 7.207 DENRATIO = 1.757 TRATIO = 0.581

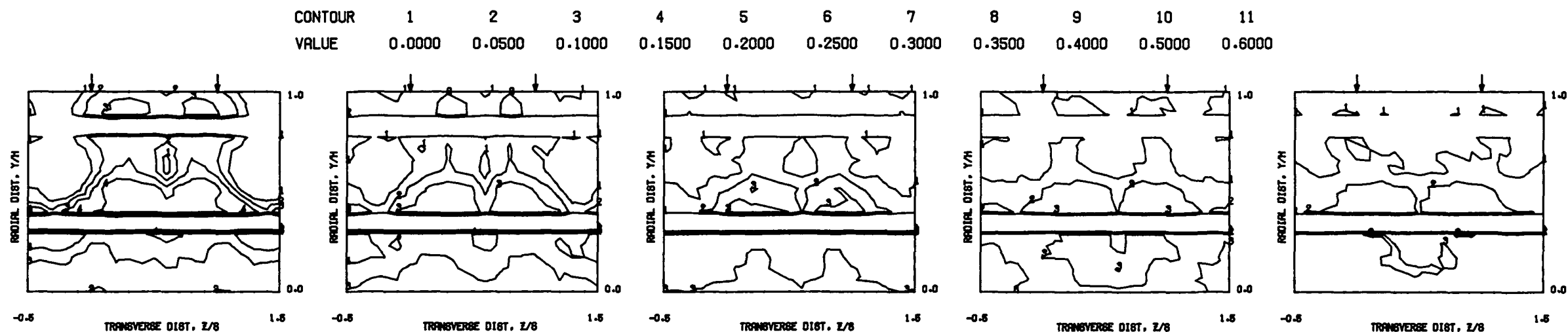
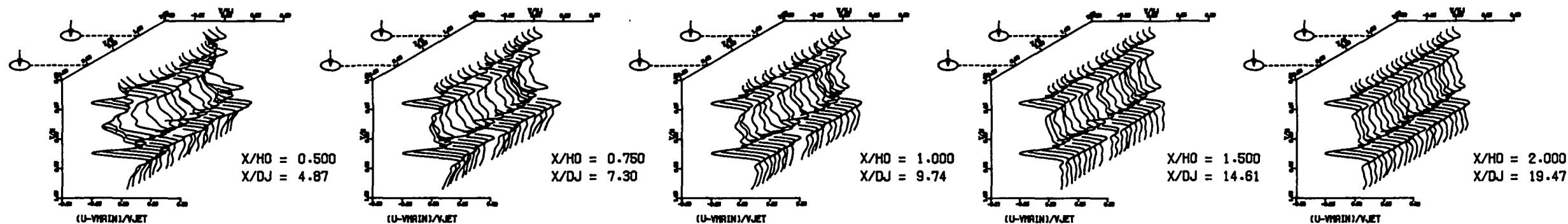
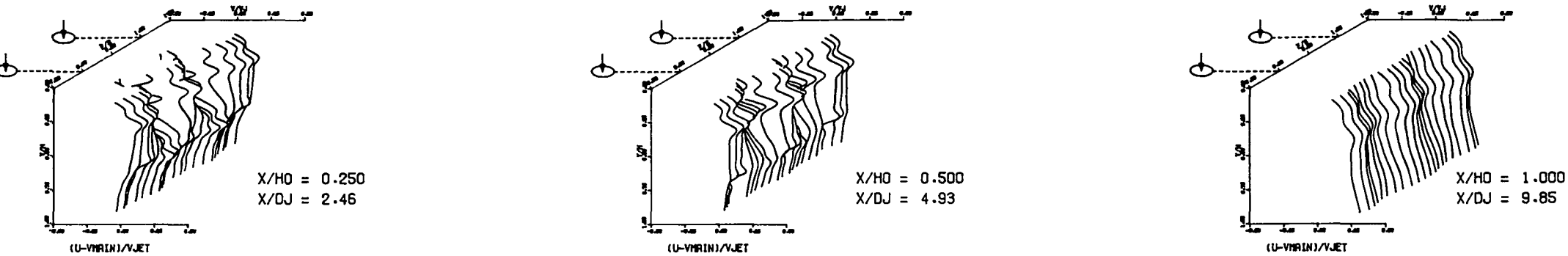


Figure 117. Measured Velocity Distributions for Test No. 18 of DJM Phase I Testing.

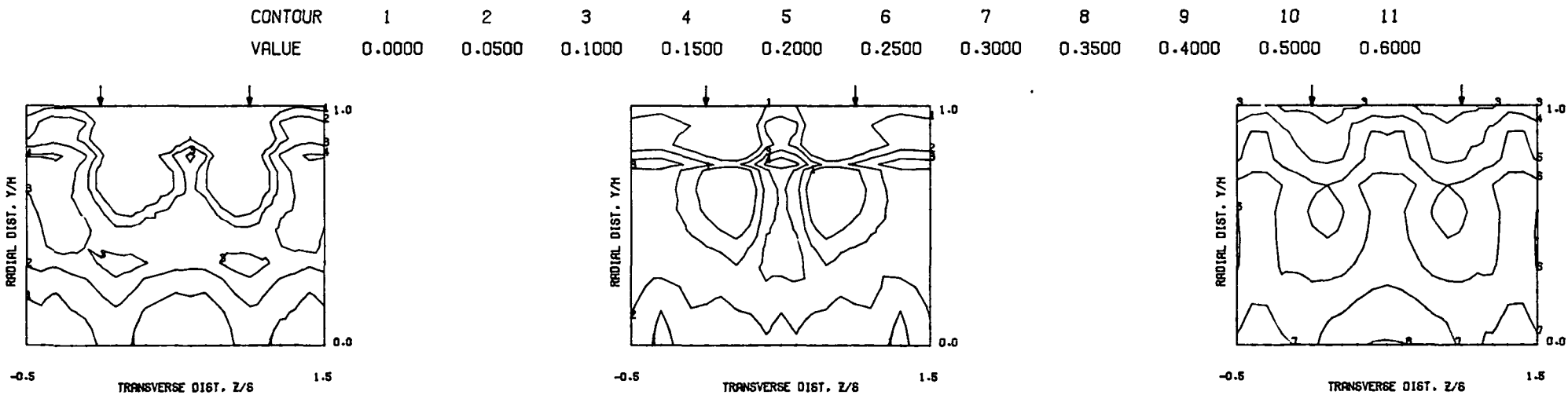
FOLDOUT FRAME

FOLDOUT FRAME

S = 0.0508 METERS S/DJ = 4.925 HO/DJ = 9.851 VMAIN = 5.2 M/SEC VJET = 16.4 M/SEC TMAIN = 358.6 K TJET = 173.5 K THEB = 0.0972 BLORAT= 6.653 DENRATIO= 2.102 TRATIO= 0.484



MEASURED VELOCITY PROFILES FOR TEST NO 23, TEST SECTION IV, TM=CONST , J = 21.05 , S/D = 4.00 , H/D = 8.00



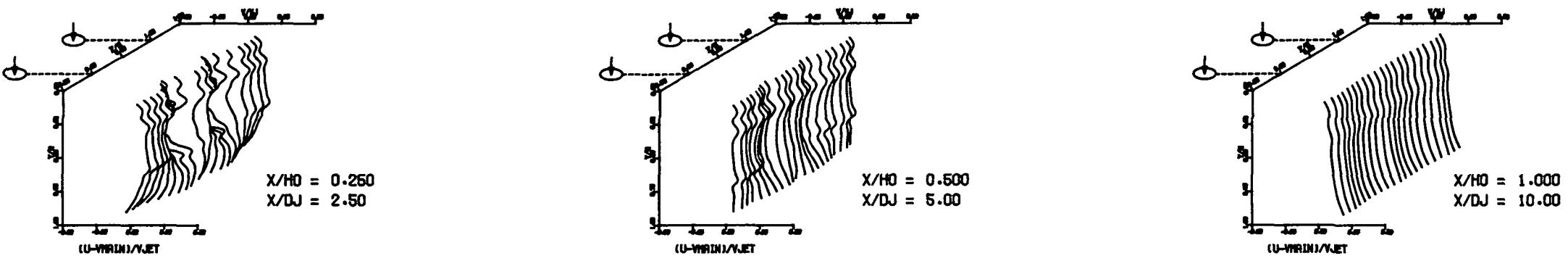
MEASURED VELOCITY PROFILES FOR TEST NO 23, TEST SECTION IV, TM=CONST , J = 21.05 , S/D = 4.00 , H/D = 8.00

Figure 118. Measured Velocity Distributions for Test No. 23 of DJM Phase I Testing.

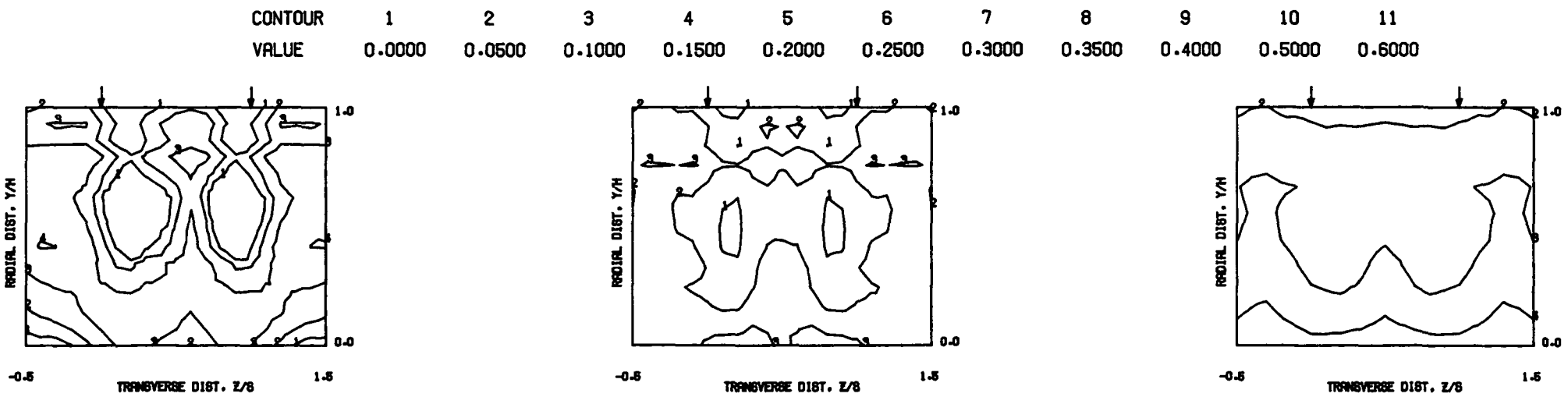
FOLDOUT FRAME

2 FOLDOUT FRAME

S = 0.0508 METERS S/DJ = 5.000 HO/DJ = 10.000 VMAIN = 5.1 M/SEC VJET = 32.0 M/SEC TMAIN = 357.1 K TJET = 172.8 K THEB = 0.1781 BLORAT= 13.792 DENRATIO= 2.217 TRATIO=0.484



MEASURED VELOCITY PROFILES FOR TEST NO 24, TEST SECTION IV, TM=CONST , J = 85.81 , S/D = 4.00 , H/D = 8.00



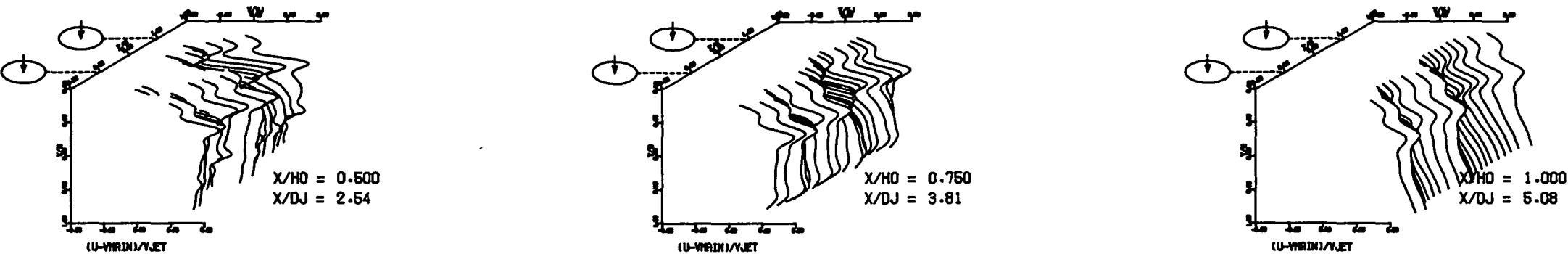
MEASURED VELOCITY PROFILES FOR TEST NO 24, TEST SECTION IV, TM=CONST , J = 85.81 , S/D = 4.00 , H/D = 8.00

Figure 119. Measured Velocity Distributions for Test No. 24 of DJM Phase I Testing.

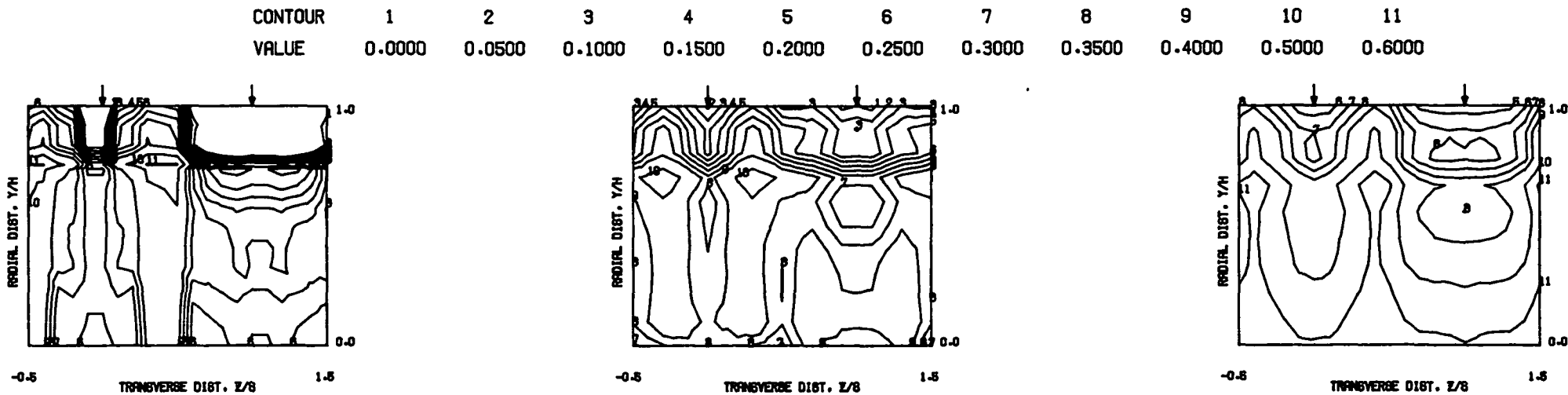
FOLDOUT FRAME

2 FOLDOUT FRAME

S = 0.0508 METERS S/DJ = 2.538 HO/DJ = 5.075 VMAIN = 4.6 M/SEC VJET = 8.4 M/SEC TMAIN = 357.4 K TJET = 178.7 K THEB = 0.1830 BLORAT= 3.672 DENRATIO= 2.003 TRATIO= 0.500



MEASURED VELOCITY PROFILES FOR TEST NO 25, TEST SECTION IV, $T_M=CONST$, $J = 6.73$, $S/D = 2.00$, $H/D = 4.00$



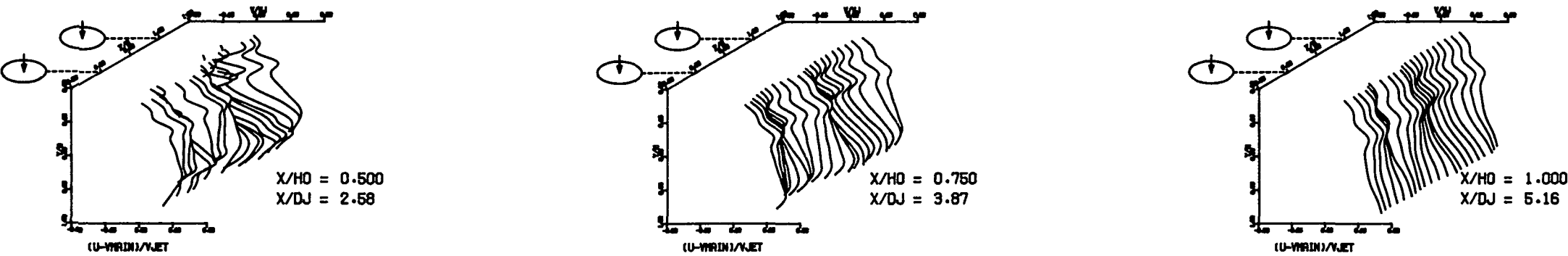
MEASURED VELOCITY PROFILES FOR TEST NO 25, TEST SECTION IV, $T_M=CONST$, $J = 6.73$, $S/D = 2.00$, $H/D = 4.00$

Figure 120. Measured Velocity Distributions for Test No. 25 of DJM Phase I Testing.

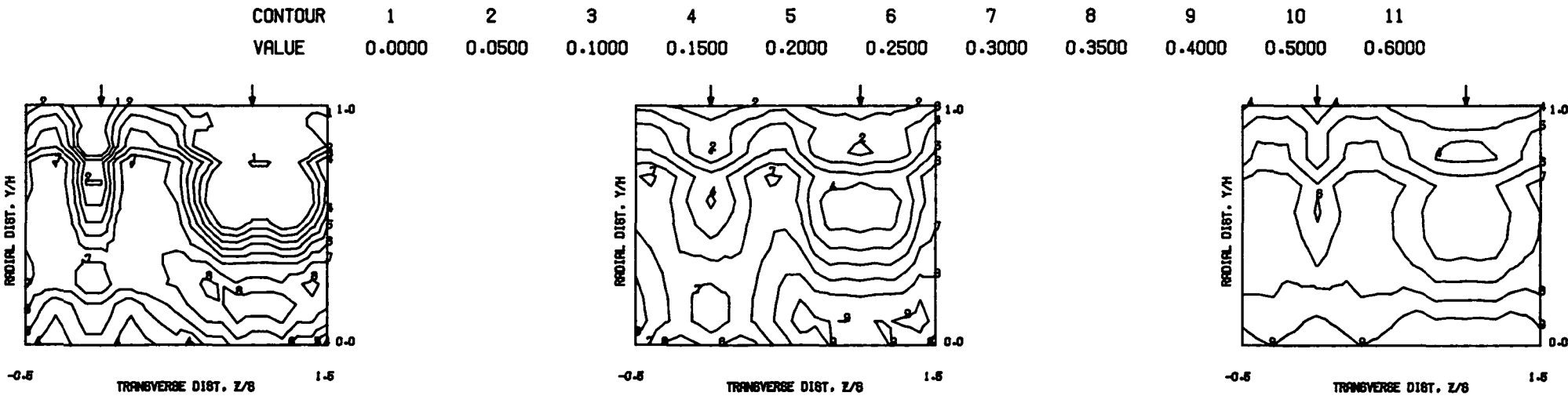
FOLDOUT FRAME

2 FOLDOUT FRAME

S = 0.0508 METERS S/DJ = 2.582 HO/DJ = 5.164 VMAIN = 4.5 M/SEC VJET = 16.8 M/SEC TMAIN = 355.9 K TJET = 183.2 K THEB = 0.2988 BLORAT= 7.233 DENRATIO= 1.958 TRATIO= 0.515



MEASURED VELOCITY PROFILES FOR TEST NO 26, TEST SECTION IV, TM=CONST , J = 26.73 , S/D = 2.00 , H/D = 4.00



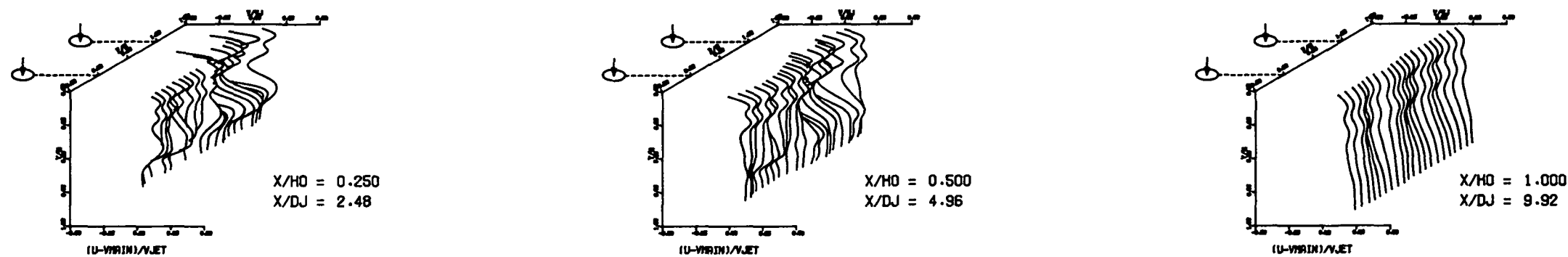
MEASURED VELOCITY PROFILES FOR TEST NO 26, TEST SECTION IV, TM=CONST , J = 26.73 , S/D = 2.00 , H/D = 4.00

Figure 121. Measured Velocity Distributions for Test No. 26 of DJM Phase I Testing.

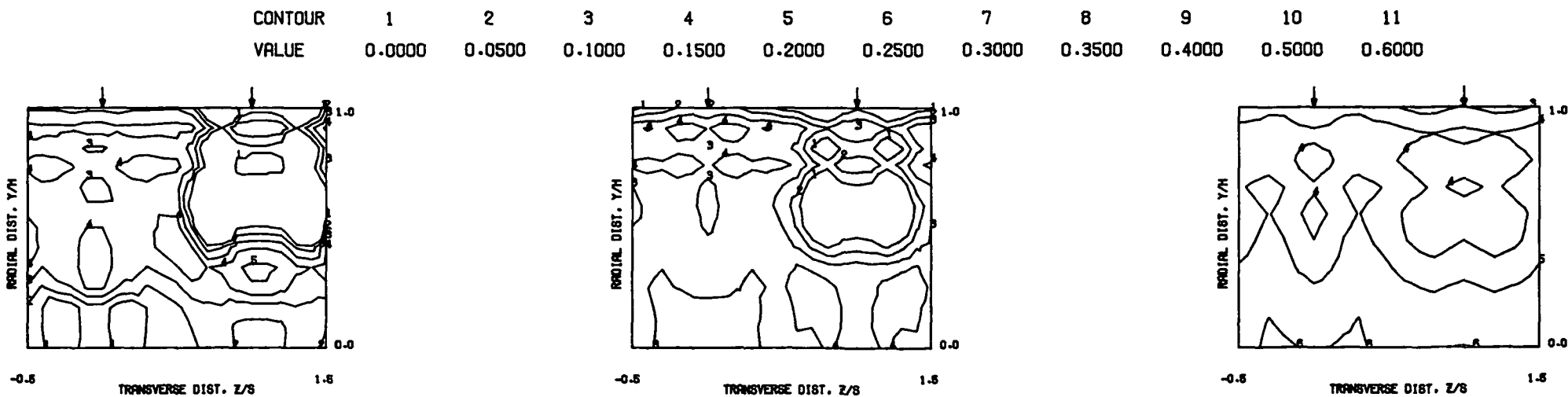
FOLDOUT FRAME

FOLDOUT FRAME

S = 0.0508 METERS S/DJ = 4.961 HO/DJ = 9.921 VMAIN = 4.9 M/SEC VJET = 17.9 M/SEC TMAIN = 359.1 K TJET = 178.0 K THEB = 0.1065 BLORAT= 7.470 DENRATIO= 2.053 TRATIO= 0.496



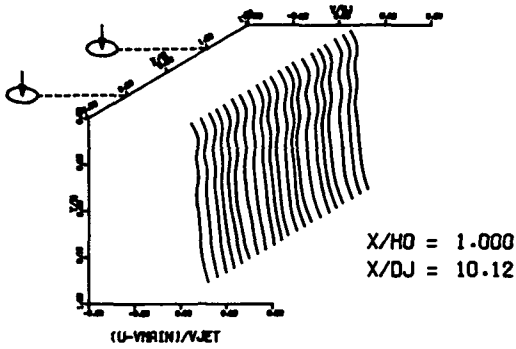
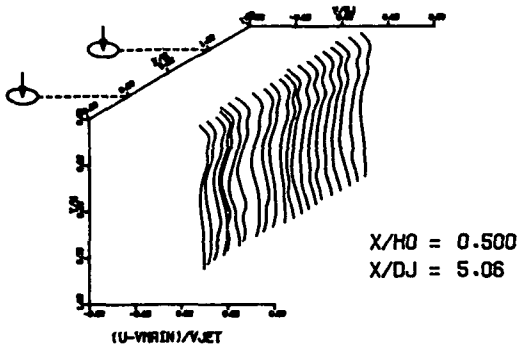
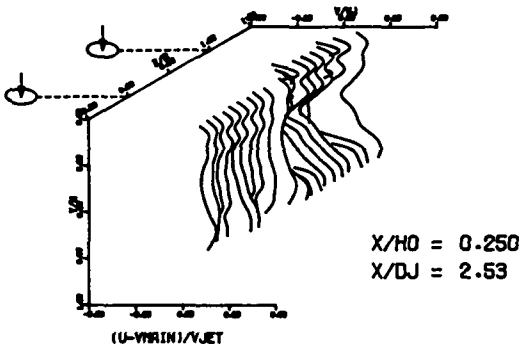
MEASURED VELOCITY PROFILES FOR TEST NO 27, TEST SECTION V, $T_M = \text{CONST}$, J = 27.18 , S/D = 4.00 , H/D = 8.00



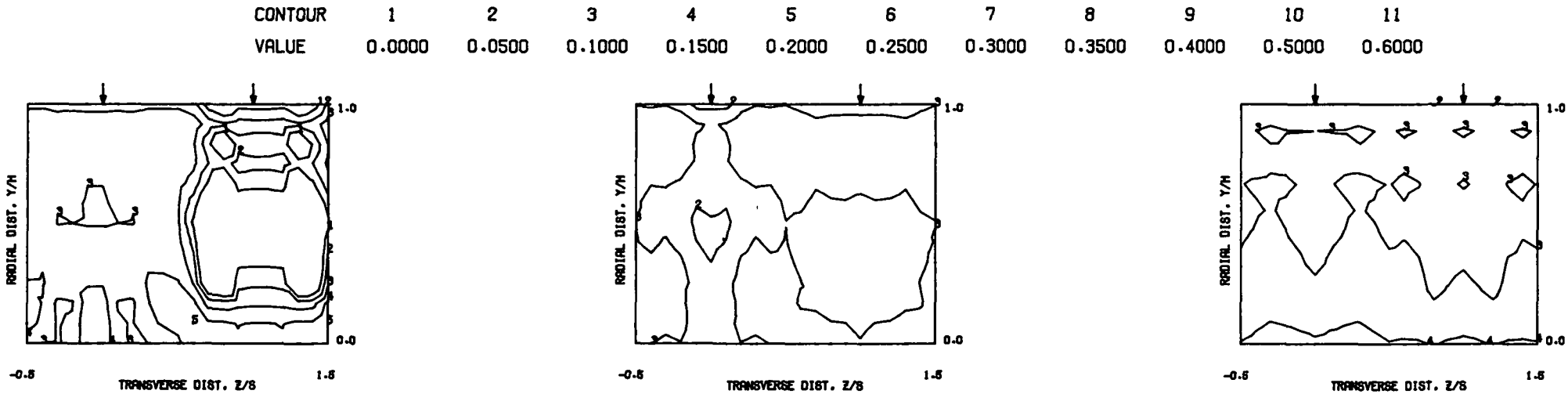
MEASURED VELOCITY PROFILES FOR TEST NO 27, TEST SECTION V, $T_M = \text{CONST}$, J = 27.18 , S/D = 4.00 , H/D = 8.00

Figure 122. Measured Velocity Distributions for Test No. 27 of DJM Phase I Testing.

S = 0.0508 METERS S/DJ = 5.061 HO/DJ = 10.121 VMAIN = 4.9 M/SEC VJET = 34.3 M/SEC TMAIN = 358.4 K TJET = 177.3 K THEB = 0.1888 BLORAT= 15.176 DENRATIO= 2.159 TRATIO=0.495



MEASURED VELOCITY PROFILES FOR TEST NO 28, TEST SECTION V, TM=CONST , J = 106.67 , S/D = 4.00 , H/D = 8.00



MEASURED VELOCITY PROFILES FOR TEST NO 28, TEST SECTION V, TM=CONST , J = 106.67 , S/D = 4.00 , H/D = 8.00

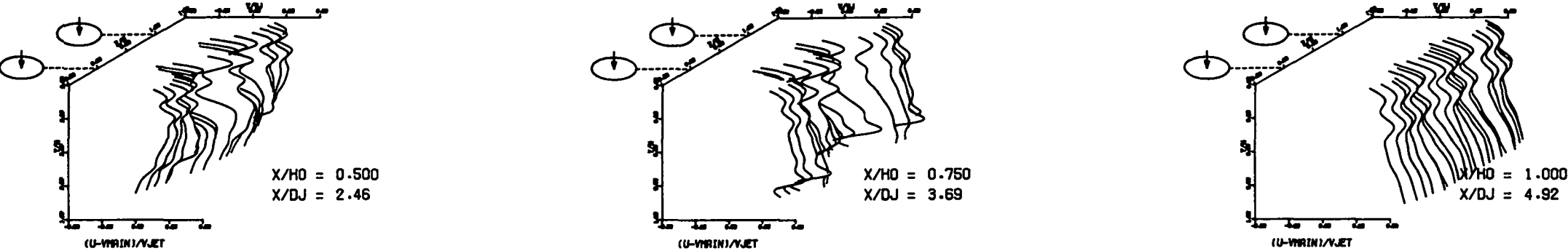
Figure 123. Measured Velocity Distributions for Test No. 28 of DJM Phase I Testing.

FOLDOUT FRAME

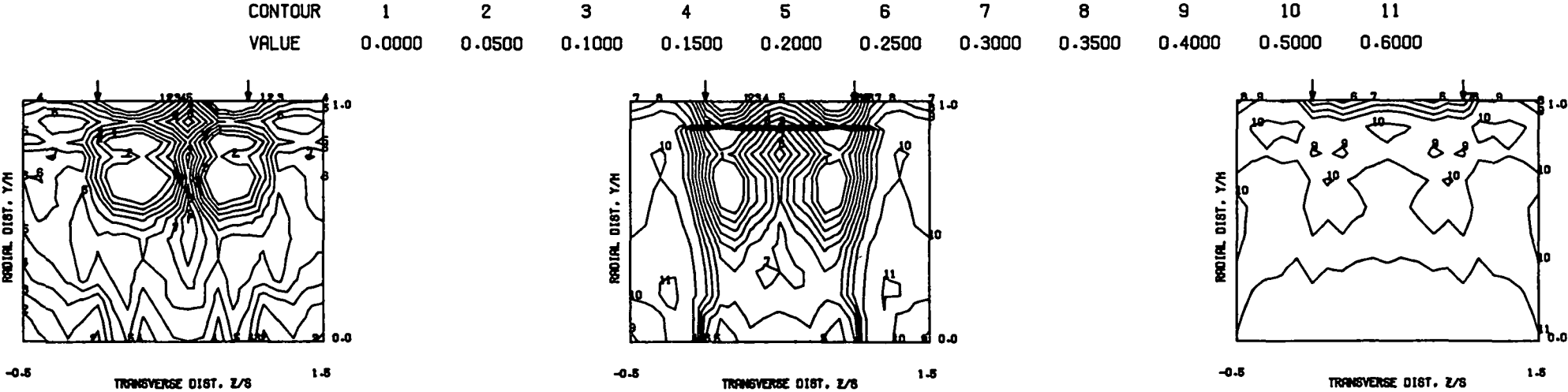
2 FOLDOUT FRAME

ORIGINAL PAGE IS
OF POOR QUALITY

S = 0.0508 METERS S/DJ = 2.462 HO/DJ = 4.924 VMAIN = 4.8 M/SEC VJET = 8.9 M/SEC TMAIN = 358.3 K TJET = 174.2 K THEB = 0.1983 BLORAT = 3.818 DENRATIO = 2.064 TRATIO = 0.486



MEASURED VELOCITY PROFILES FOR TEST NO 29, TEST SECTION V, $T_M=CONST$, $J = 7.07$, $S/D = 2.00$, $H/D = 4.00$



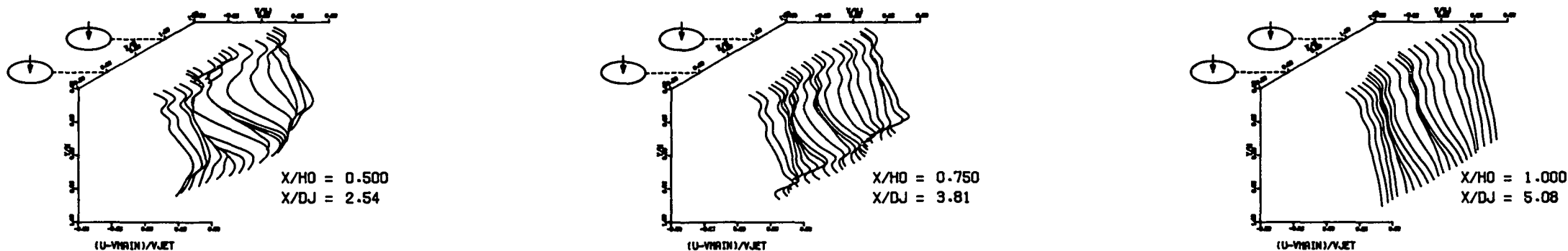
MEASURED VELOCITY PROFILES FOR TEST NO 29, TEST SECTION V, $T_M=CONST$, $J = 7.07$, $S/D = 2.00$, $H/D = 4.00$

Figure 124. Measured Velocity
Distributions for Test No. 29 of DJM
Phase I Testing.

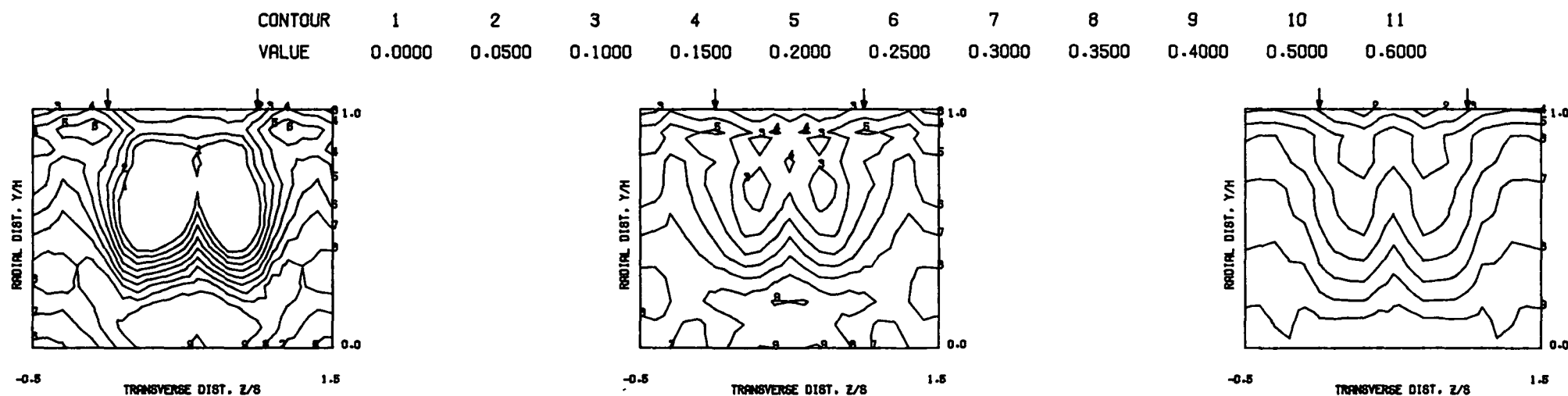
FOLDOUT FRAME

2 FOLDOUT FRAME

S = 0.0508 METERS S/DJ = 2.540 H0/DJ = 5.080 VMAIN = 4.7 M/SEC VJET = 17.2 M/SEC TMAIN = 358.7 K TJET = 174.3 K THEB = 0.3149 BLORAT= 7.549 DENRATIO= 2.087 TRATIO= 0.486



MEASURED VELOCITY PROFILES FOR TEST NO 30, TEST SECTION V, TM=CONST , J = 27.31 , S/D = 2.00 , H/D = 4.00



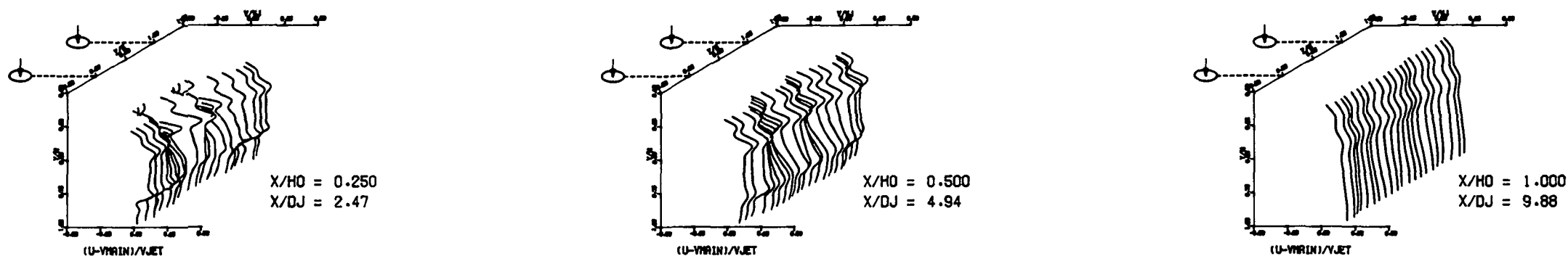
MEASURED VELOCITY PROFILES FOR TEST NO 30, TEST SECTION V, TM=CONST , J = 27.31 , S/D = 2.00 , H/D = 4.00

Figure 125. Measured Velocity Distributions for Test No. 30 of DJM Phase I Testing.

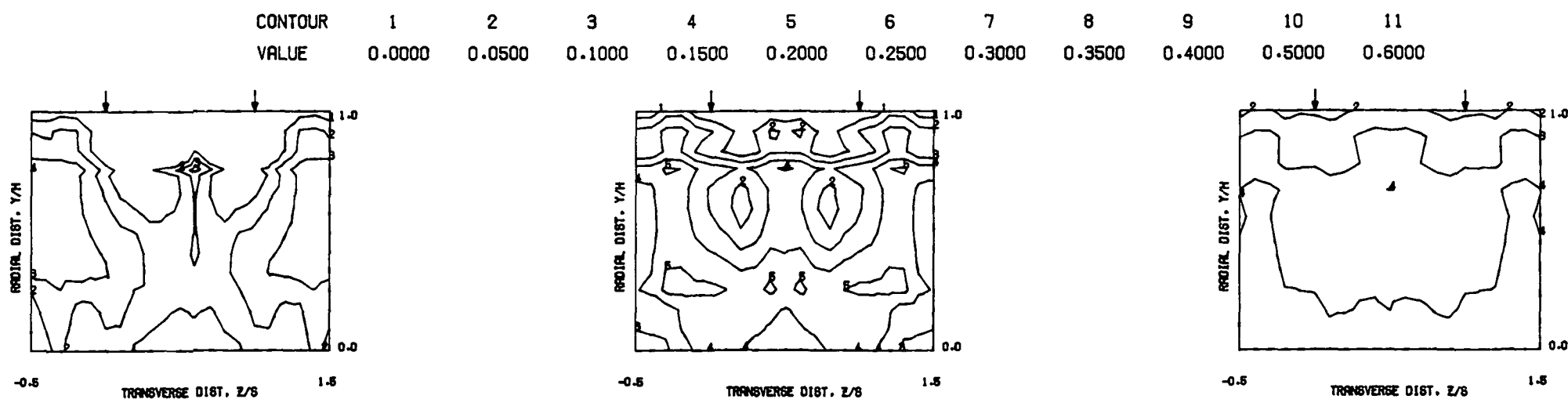
FOLDOUT FRAME

FOLDOUT FRAME

S = 0.0508 METERS S/DJ = 4.941 H0/DJ = 9.883 VMAIN = 5.0 M/SEC VJET = 17.9 M/SEC TMAIN = 360.7 K TJET = 177.5 K THEB = 0.1066 BLORAT= 7.421 DENRATIO= 2.072 TRATIO= 0.492



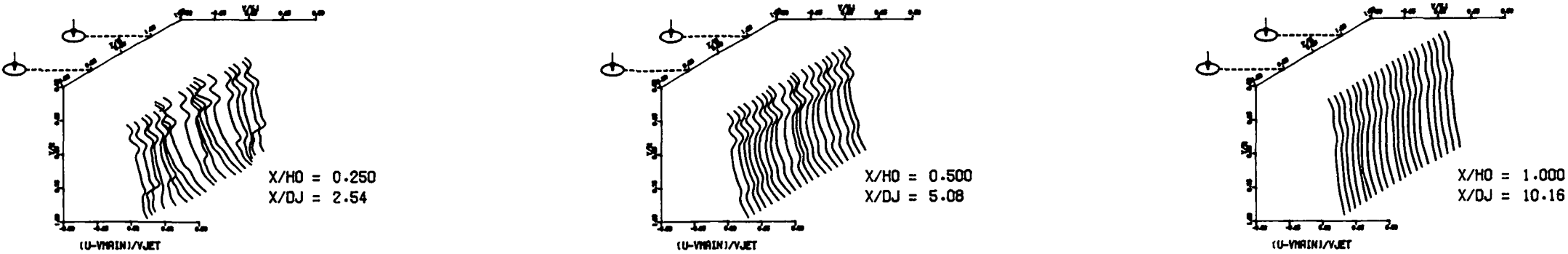
MEASURED VELOCITY PROFILES FOR TEST NO 31, TEST SECTION VI, TM=CONST , J = 26.58 , S/D = 4.00 , H/D = 8.00



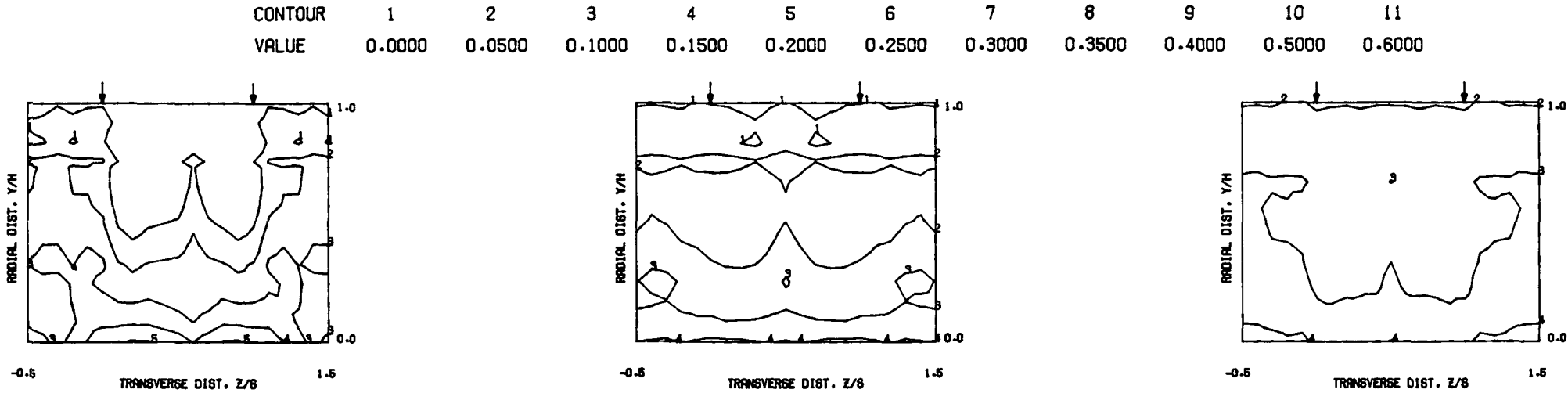
MEASURED VELOCITY PROFILES FOR TEST NO 31, TEST SECTION VI, TM=CONST , J = 26.58 , S/D = 4.00 , H/D = 8.00

Figure 126. Measured Velocity Distributions for Test No. 31 of DJM Phase I Testing.

S = 0.0508 METERS S/DJ = 5.081 HO/DJ = 10.163 VMAIN = 5.0 M/SEC VJET = 35.4 M/SEC TMAIN = 359.4 K TJET = 178.4 K THEB = 0.1887 BLORAT= 15.297 DENRATIO= 2.176 TRATIO=0.496



MEASURED VELOCITY PROFILES FOR TEST NO 32, TEST SECTION VI, TM=CONST , J = 107.57 , S/D = 4.00 , H/D = 8.00



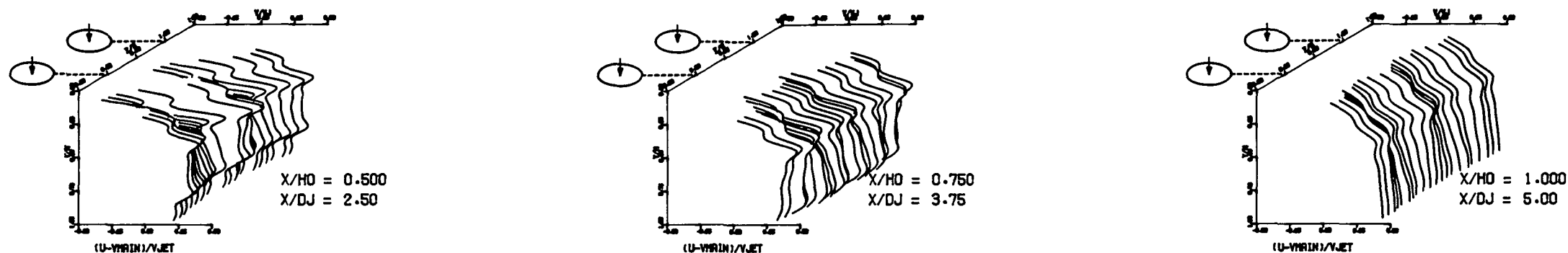
MEASURED VELOCITY PROFILES FOR TEST NO 32, TEST SECTION VI, TM=CONST , J = 107.57 , S/D = 4.00 , H/D = 8.00

Figure 127. Measured Velocity Distributions for Test No. 32 of DJM Phase I Testing.

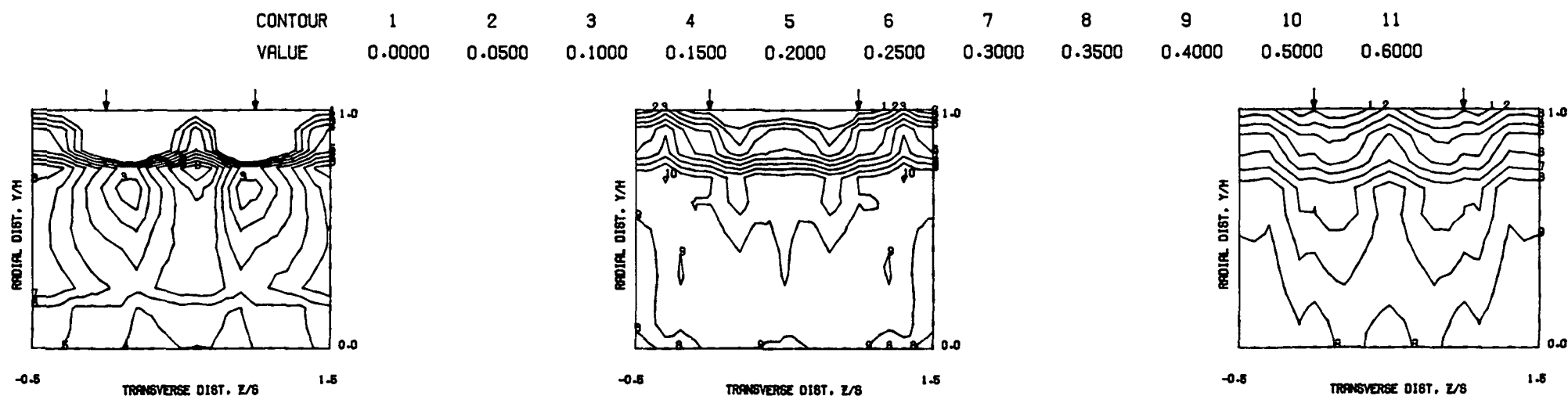
FOLDOUT FRAME

FOLDOUT FRAME

S = 0.0508 METERS S/DJ = 2.500 HO/DJ = 5.001 VMAIN = 5.0 M/SEC VJET = 9.0 M/SEC TMAIN = 361.0 K TJET = 167.4 K THEB = 0.1969 BLORAT= 3.903 DENRATIO= 2.165 TRATIO= 0.464



MEASURED VELOCITY PROFILES FOR TEST NO 33, TEST SECTION VI, TM=CONST , J = 7.04 , S/D = 2.00 , H/D = 4.00



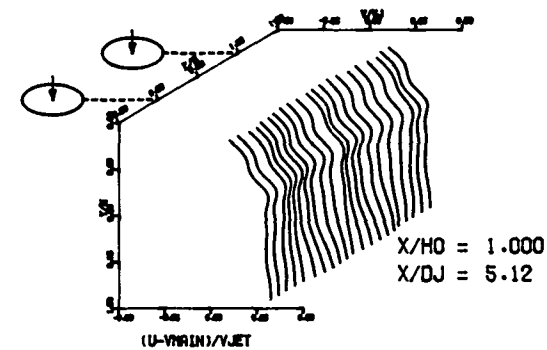
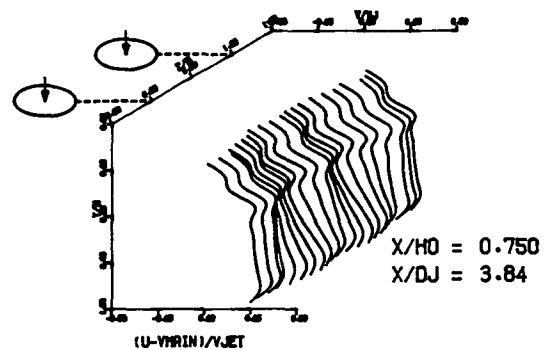
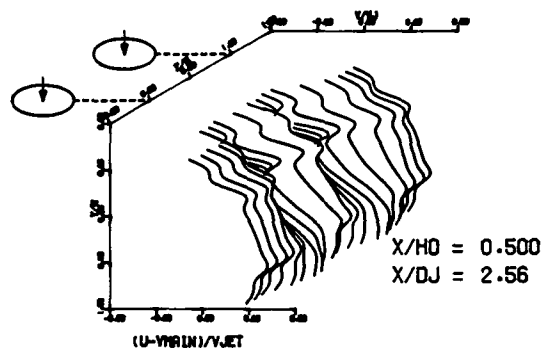
MEASURED VELOCITY PROFILES FOR TEST NO 33, TEST SECTION VI, TM=CONST , J = 7.04 , S/D = 2.00 , H/D = 4.00

Figure 128. Measured Velocity Distributions for Test No. 33 of DJM Phase I Testing.

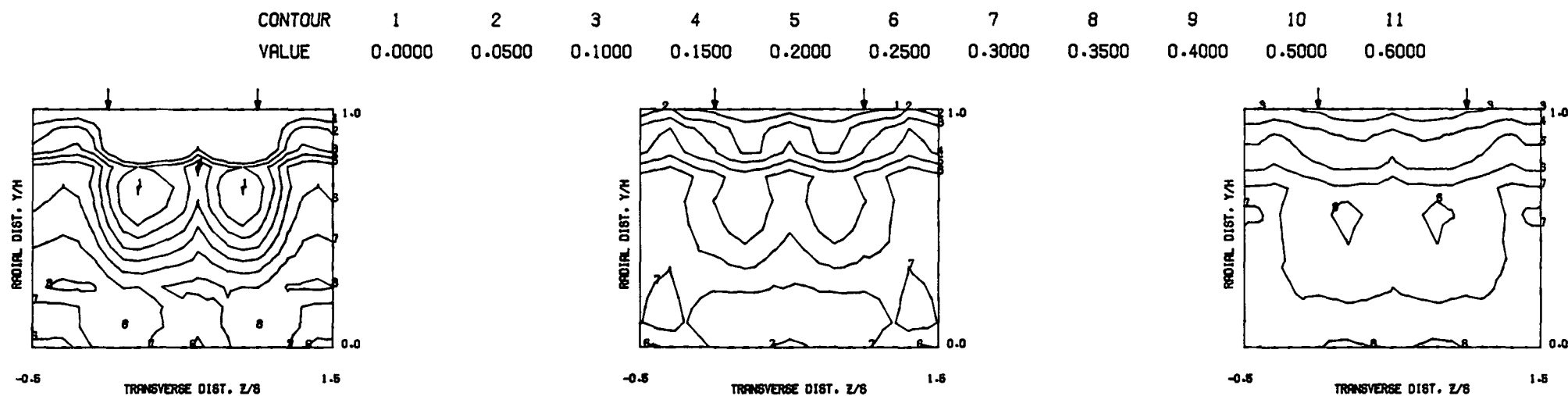
FOLDOUT FRAME

2 FOLDOUT FRAME

S = 0.0508 METERS S/DJ = 2.561 HO/DJ = 5.122 VMAIN = 5.0 M/SEC VJET = 17.0 M/SEC TMAIN = 361.6 K TJET = 164.9 K THEB = 0.3144 BLORAT= 7.657 DENRATIO= 2.225 TRATIO=0.456



MEASURED VELOCITY PROFILES FOR TEST NO 34, TEST SECTION VI, TM=CONST , J = 26.36 , S/D = 2.00 , H/D = 4.00



MEASURED VELOCITY PROFILES FOR TEST NO 34, TEST SECTION VI, TM=CONST , J = 26.36 , S/D = 2.00 , H/D = 4.00

Figure 129. Measured Velocity Distributions for Test No. 34 of DJM Phase I Testing.

FOLDOUT FRAME

2 FOLDOUT FRAME

ORIGINAL PAGE IS
OF POOR QUALITY

ORIGINAL PAGE IS
OF POOR QUALITY

$S = 0.0254$ METERS $S/DJ = 2.496$ $H/DJ = 9.983$ $V_{MAIN} = 4.7$ M/SEC $V_{JET} = 31.8$ M/SEC $T_{MAIN} = 359.0$ K $T_{JET} = 168.8$ K $THEB = 0.4879$ $BLORAT = 15.447$ $DENRATIO = 2.250$ $TRATIO = 0.470$

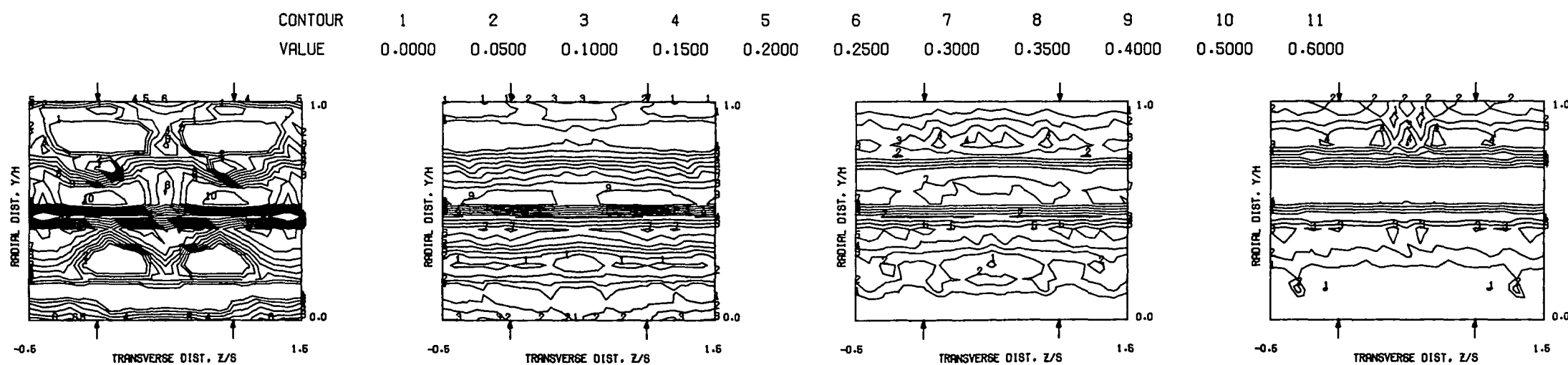
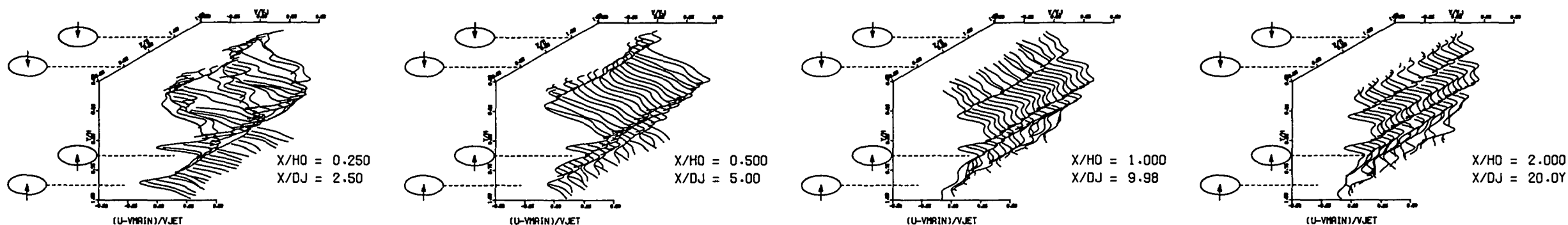
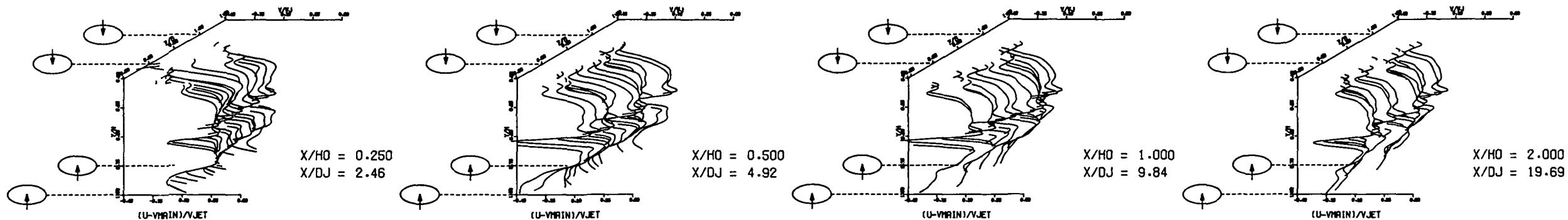
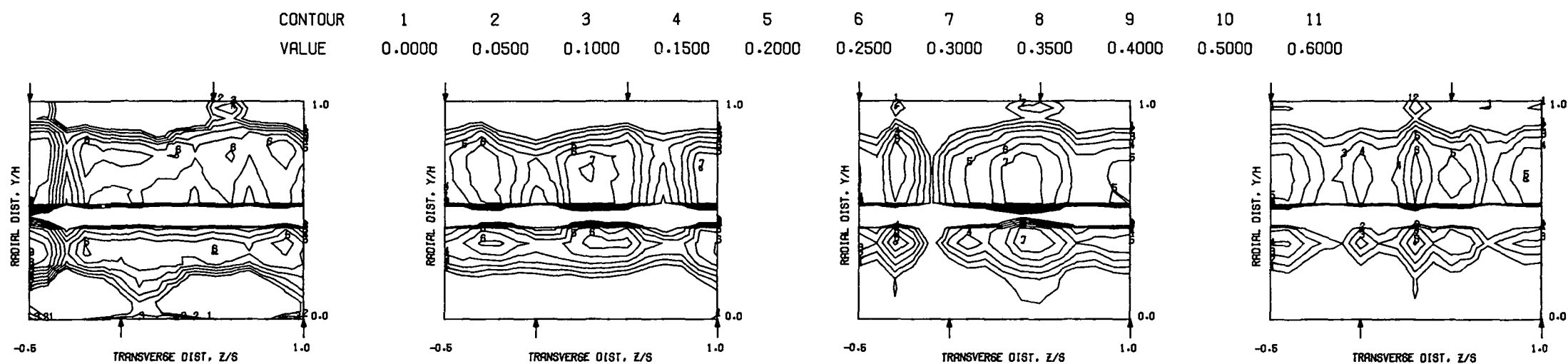


Figure 130. Measured Velocity
Distributions for Test No. 3
of DJM Phase II Testing.

S = 0.0254 METERS S/DJ = 2.461 HO/DJ = 9.844 VMAIN = 5.1 M/SEC VJET = 9.1 M/SEC TMAIN = 360.5 K TJET = 180.9 K THEB = 0.1890 BLORAT= 3.686 DENRATIO= 2.00Z TRATIO=0.502



MEASURED VELOCITY PROFILES FOR TEST NO 4,TEST SECTION I,STAGGERED JETS , J = 6.52 , S/D = 2.00 , H/D = 8.00



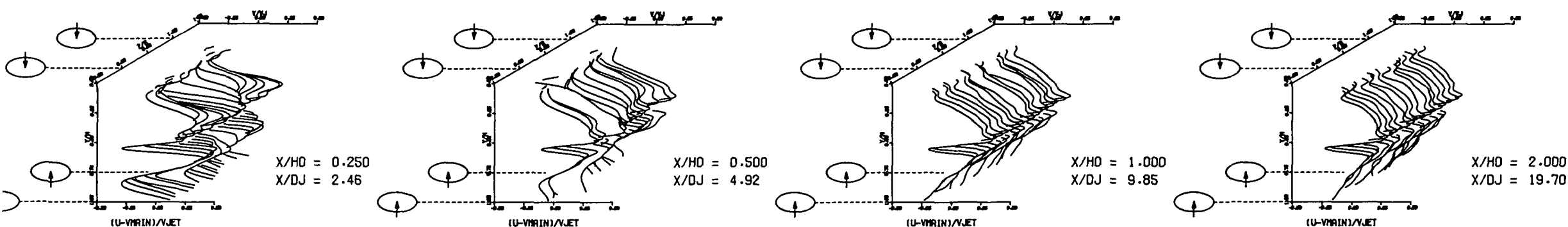
MEASURED VELOCITY PROFILES FOR TEST NO 4,TEST SECTION I,STAGGERED JETS , J = 6.52 , S/D = 2.00 , H/D = 8.00

Figure 131. Measured Velocity Distributions for Test No. 4 of DJM Phase II Testing.

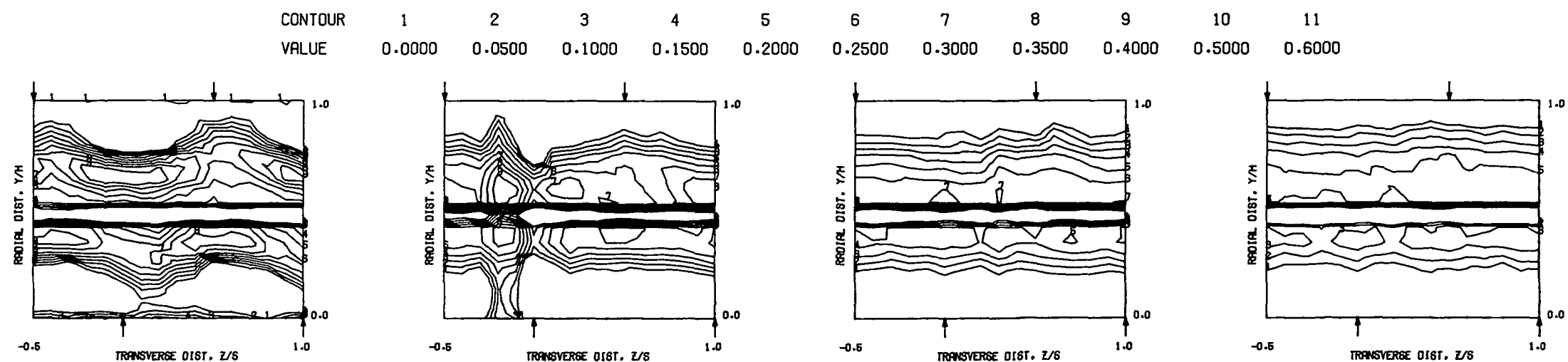
FOLDOUT FRAME

2 FOLDOUT FRAME

S = 0.0254 METERS S/DJ = 2.462 H0/DJ = 9.848 VMAIN = 5.0 M/SEC VJET = 17.3 M/SEC TMAIN = 359.0 K TJET = 174.7 K THEB = 0.3186 BLORAT = 7.393 DENRATIO = 2.086 TRATIO = 0.487



MEASURED VELOCITY PROFILES FOR TEST NO 5, TEST SECTION I, STAGGERED JETS, J = 25.15, S/D = 2.00, H/D = 8.00



MEASURED VELOCITY PROFILES FOR TEST NO 5, TEST SECTION I, STAGGERED JETS, J = 25.15, S/D = 2.00, H/D = 8.00

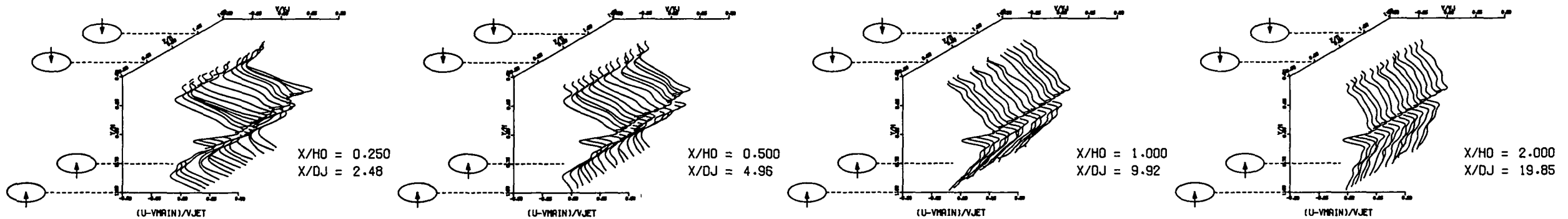
Figure 132. Measured Velocity Distributions for Test No. 5 of DJM Phase II Testing.

FOLDOUT FRAME

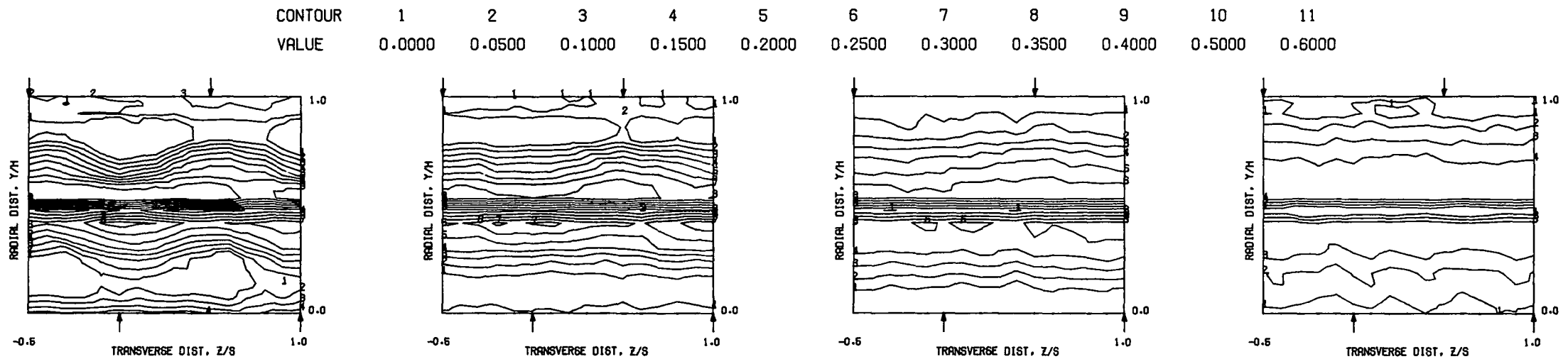
2 FOLDOUT FRAME

ORIGINAL PAGE IS
OF POOR QUALITY

S = 0.0254 METERS S/DJ = 2.481 HO/DJ = 9.924 VMAIN = 5.0 M/SEC VJET = 33.6 M/SEC TMAIN = 358.4 K TJET = 174.1 K THEB = 0.4845 BLORAT= 15.063 DENRATIO= 2.195 TRATIO= 0.486



MEASURED VELOCITY PROFILES FOR TEST NO 6, TEST SECTION I, STAGGERED JETS, J = 99.23, S/D = 2.00, H/D = 8.00



MEASURED VELOCITY PROFILES FOR TEST NO 6, TEST SECTION I, STAGGERED JETS, J = 99.23, S/D = 2.00, H/D = 8.00

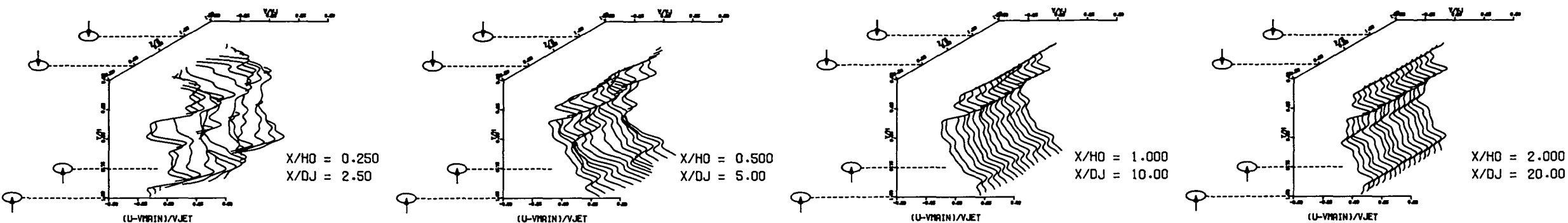
Figure 133. Measured Velocity Distributions for Test No. 6 of DJM Phase II Testing.

FOLDOUT FRAME

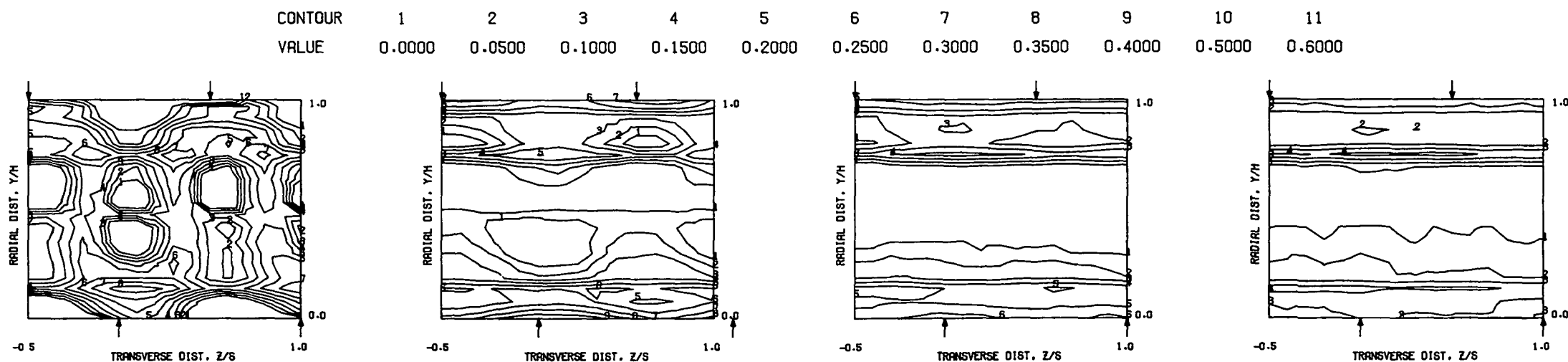
2 FOLDOUT FRAME

ORIGINAL PAGE IS
OF POOR QUALITY

S = 0.0508 METERS S/DJ = 5.000 HO/DJ = 10.000 VMAIN = 4.9 M/SEC VJET = 33.5 M/SEC TMAIN = 358.8 K TJET = 176.6 K THEB = 0.3187 BLORAT= 15.291 DENRATIO= 2.178 TRATIO=0.492



MEASURED VELOCITY PROFILES FOR TEST NO 12, TEST SECTION I, STAGGERED JET, J = 103.01, S/D = 4.00, H/D = 8.00



MEASURED VELOCITY PROFILES FOR TEST NO 12, TEST SECTION I, STAGGERED JET, J = 103.01, S/D = 4.00, H/D = 8.00

Figure 134. Measured Velocity Distributions for Test No. 12 of DJM Phase II Testing.

FOLDOUT FRAME

2 FOLDOUT FRAME

ORIGINAL PAGE IS
OF POOR QUALITY

S = 0.0254 METERS S/DJ = 2.540 H0/DJ = 10.159 VMAIN = 5.8 M/SEC VJET = 21.1 M/SEC TMAIN = 310.7 K TJET = 172.2 K THEB = 0.6402 BLORAT= 7.081 DENRATIO= 1.825 TRATIO= 0.554

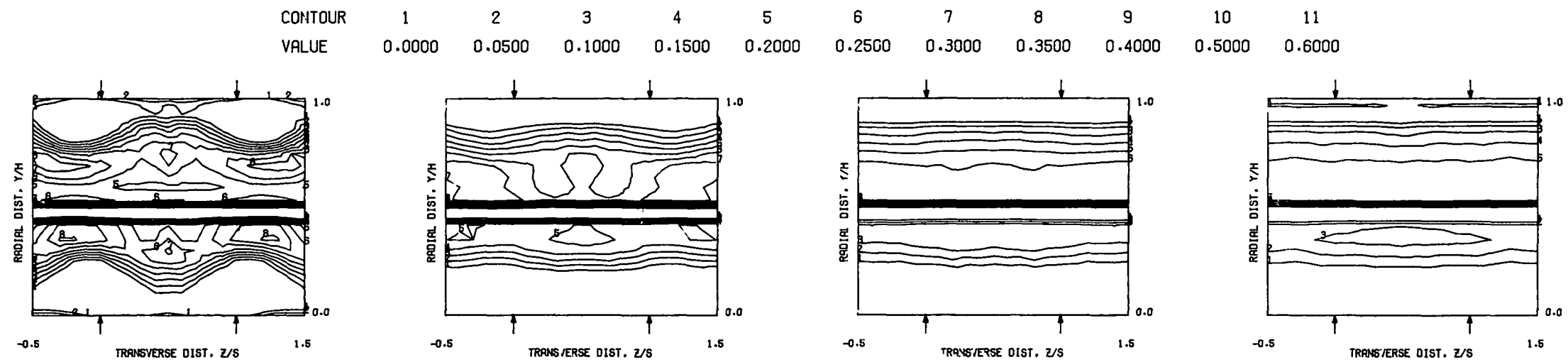
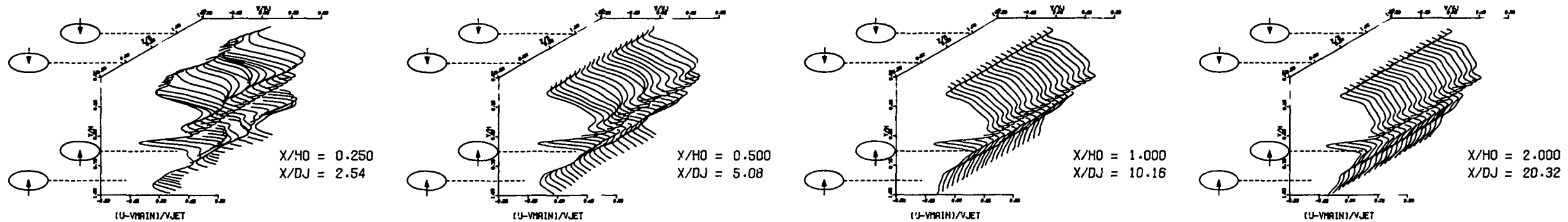
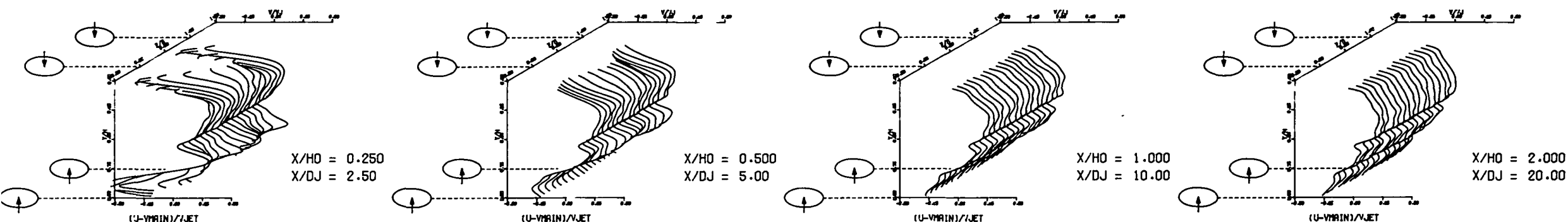


Figure 135. Measured Velocity Distributions for Test No. 13 of DJM Phase II Testing.

FOLDOUT FRAME

FOLDOUT FRAME

S = 0.0254 METERS S/DJ = 2.500 H0/DJ = 10.000 VMAIN = 5.8 M/SEC VJET = 10.8 M/SEC TMAIN = 307.7 K TJET = 178.7 K THEB = 0.5982 BLORAT= 3.457 DENRATIO= 1.725 TRATIO= 0.581



CONTOUR	1	2	3	4	5	6	7	8	9	10	11
VALUE	0.0000	0.0500	0.1000	0.1500	0.2000	0.2500	0.3000	0.3500	0.4000	0.5000	0.6000

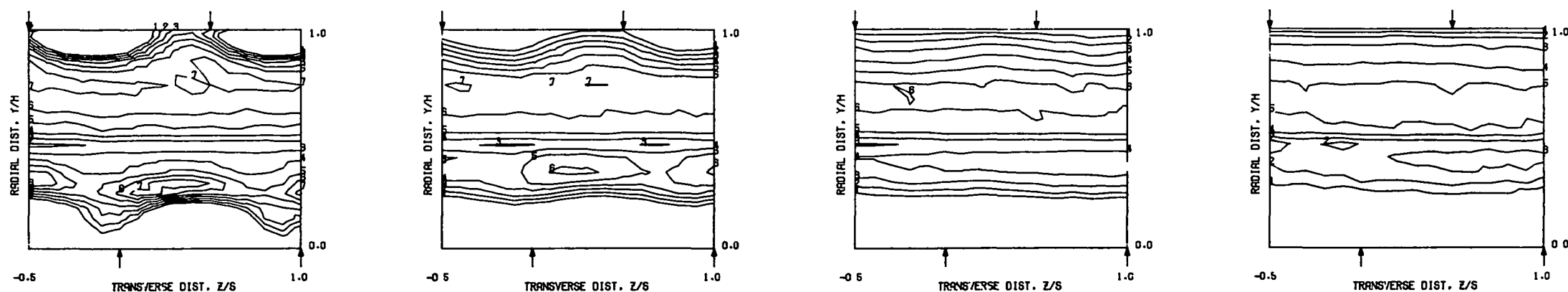


Figure 136. Measured Velocity Distributions for Test No. 14 of DJM Phase II Testing.

ORIGINAL PAGE IS
OF POOR QUALITY

S = 0.0254 METERS S/DJ = 2.520 HO/DJ = 10.080 VMAIN = 5.8 M/SEC VJET = 21.2 M/SEC TMAIN = 308.1 K TJET = 177.0 K THEB = 0.6541 BLORAT = 6.942 DENRATIO = 1.758 TRATIO = 0.574

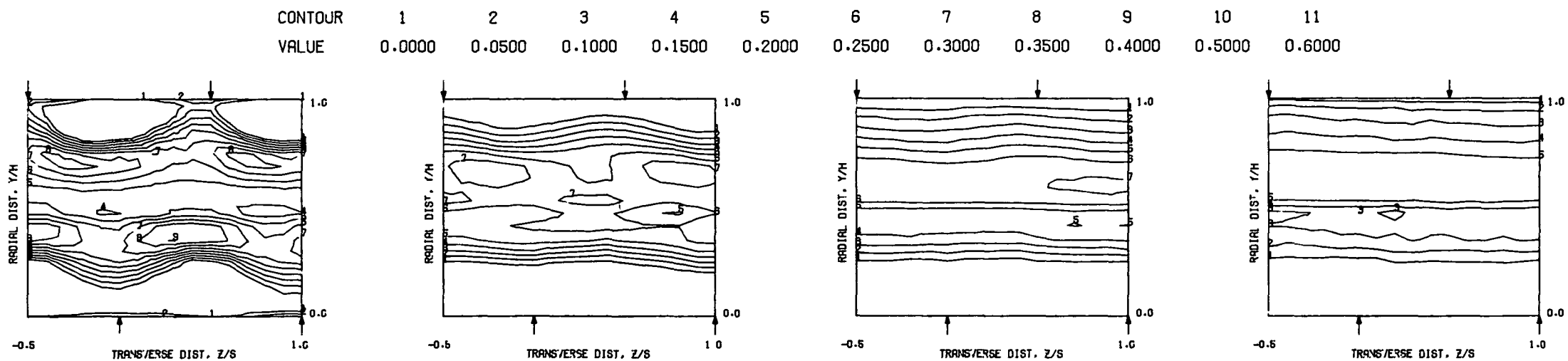
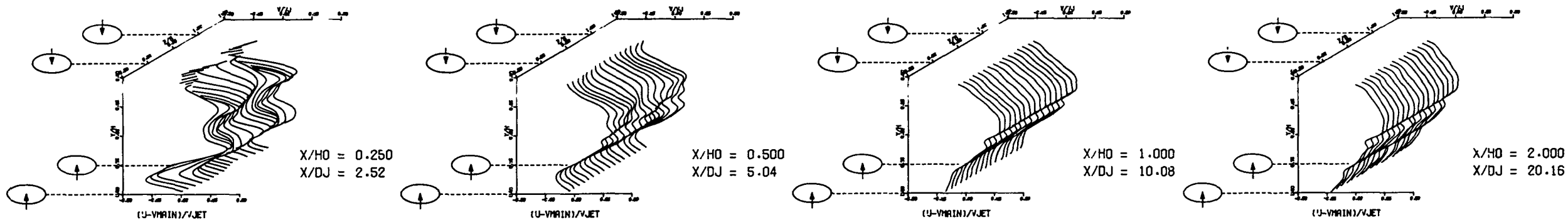
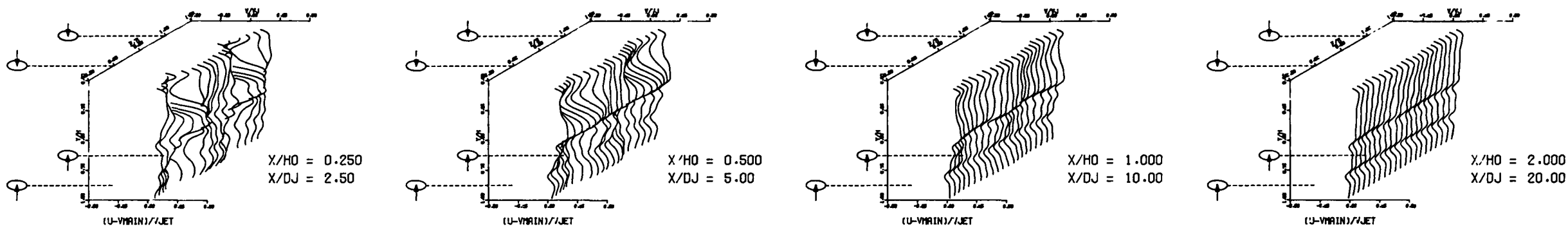


Figure 137. Measured Velocity Distributions for Test No. 15 of DJM Phase II Testing.

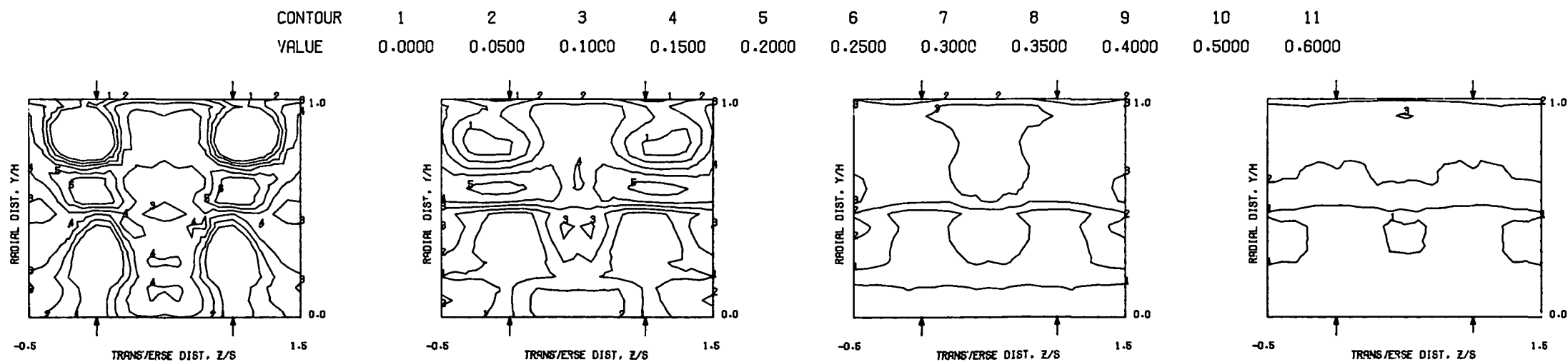
FOLDOUT FRAME

2 FOLDOUT FRAME

S = 0.0508 METERS S/DJ = 5.000 H0/DJ = 10.000 VMAIN = 5.7 M/SEC VJET = 20.9 M/SEC TMAIN = 305.5 K TJET = 178.5 K THEB = 0.6016 BLORAT= 6.892 DENRATIO= 1.733 TRATIO=0.584



MEASURED VELOCITY PROFILES FOR TEST NO 16, TOP COLD TMAIN, IN-LINE JETS , J = 27.42 , S/D = 4.00 , H/D = 8.00



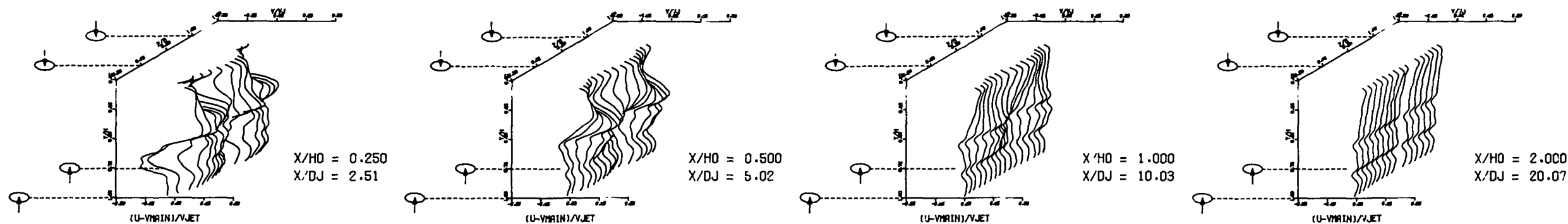
MEASURED VELOCITY PROFILES FOR TEST NO 16, TOP COLD TMAIN, IN-LINE JETS , J = 27.42 , S/D = 4.00 , H/D = 8.00

Figure 138. Measured Velocity Distributions for Test No. 16 of DJM Phase II Testing.

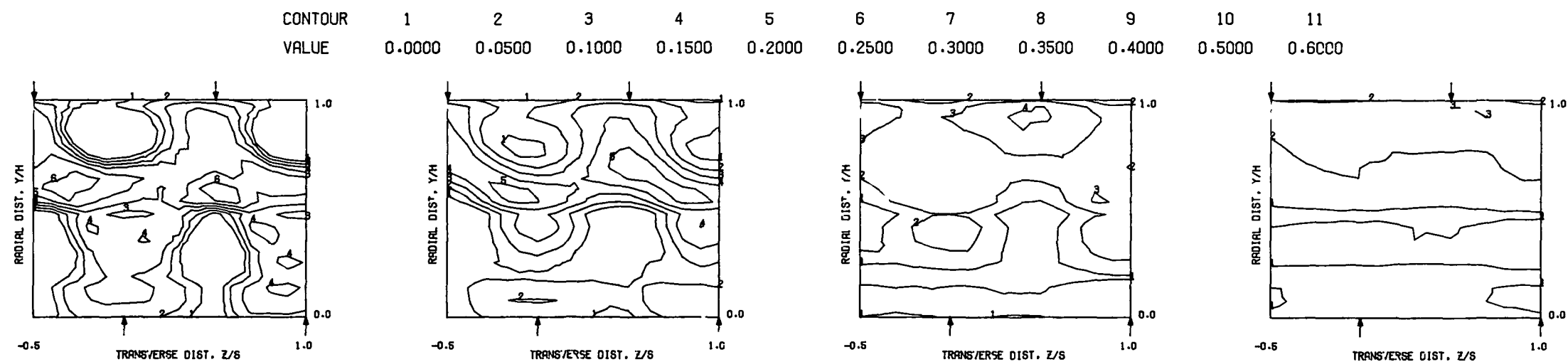
FOLDOUT FRAME

2 FOLDOUT FRAME

S = 0.0508 METERS S/DJ = 5.017 HO/DJ = 10.033 VMAIN = 5.7 M/SEC VJET = 21.0 M/SEC TMAIN = 304.5 K TJET = 175.2 K THEB = 0.6003 BLORAT= 6.980 DENRATIO= 1.759 TRATIO=0.575



MEASURED VELOCITY PROFILES FOR TEST NO 17, TOP COLD TMAIN, STAGGERED JET, J = 27.70, S/D = 4.00, H/D = 8.00



MEASURED VELOCITY PROFILES FOR TEST NO 17, TOP COLD TMAIN, STAGGERED JET, J = 27.70, S/D = 4.00, H/D = 8.00

Figure 139. Measured Velocity Distributions for Test No. 17 of DJM Phase II Testing.

1 FOLDOUT FRAME

2 FOLDOUT FRAME

FOLDOUT FRAME

FOLDOUT FRAME

S = 0.0508 METERS S/DJ = 5.040 H0/DJ = 10.080 VMAIN = 5.8 M/SEC VJET = 42.0 M/SEC TMAIN = 306.2 K TJET = 174.2 K THEB = 0.6589 BLORAT = 14.698 DENRATIO = 1.873 TRATIO = 0.569

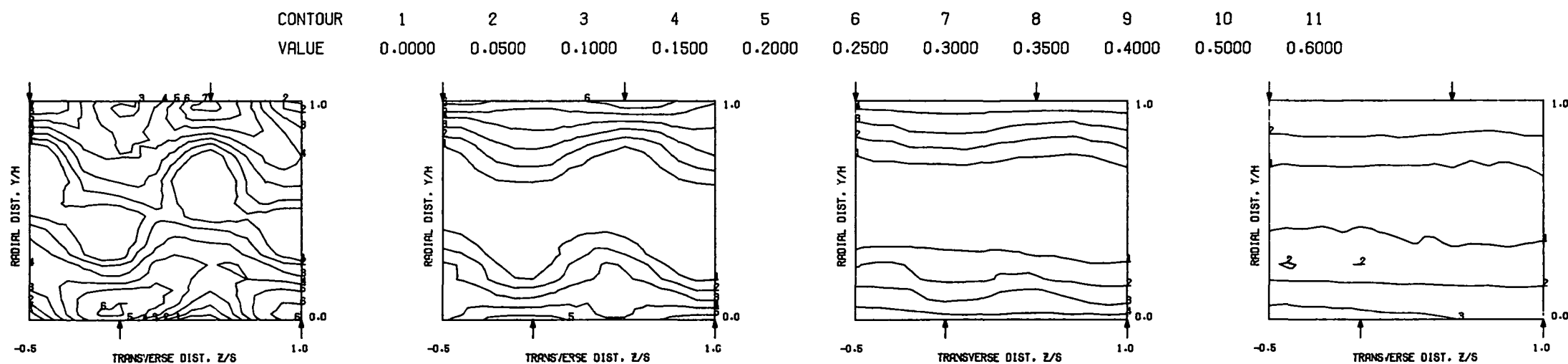
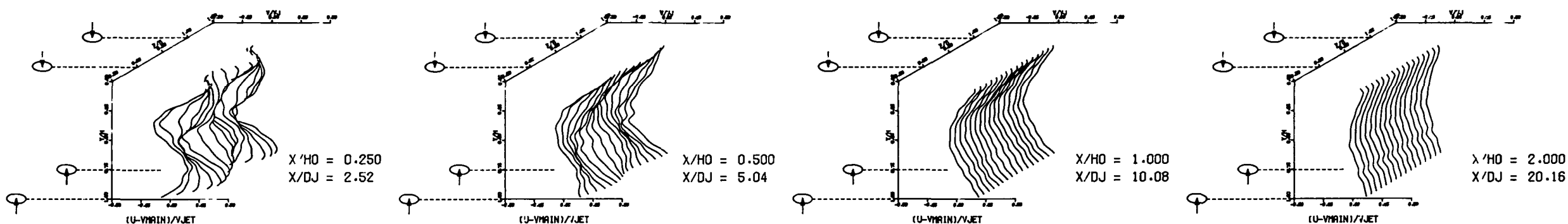


Figure 140. Measured Velocity Distributions for Test No. 18 of DJM Phase II Testing.

ORIGINAL PAGE IS
OF POOR QUALITY

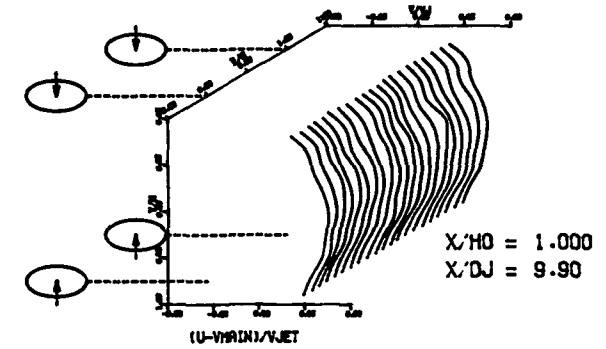
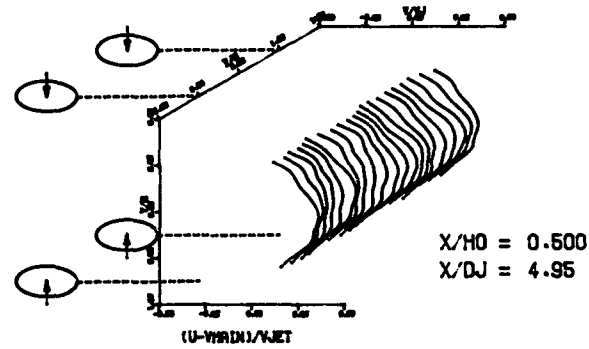
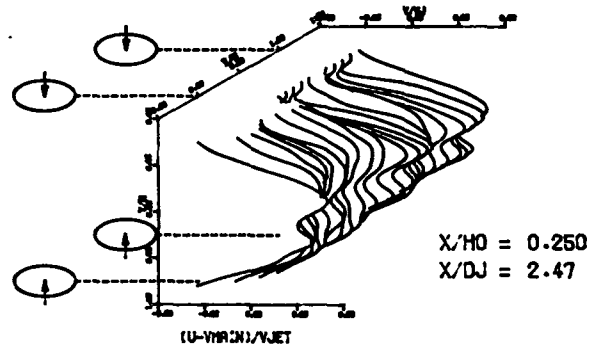
ORIGINAL PAGE IS
OF POOR QUALITY

C-4

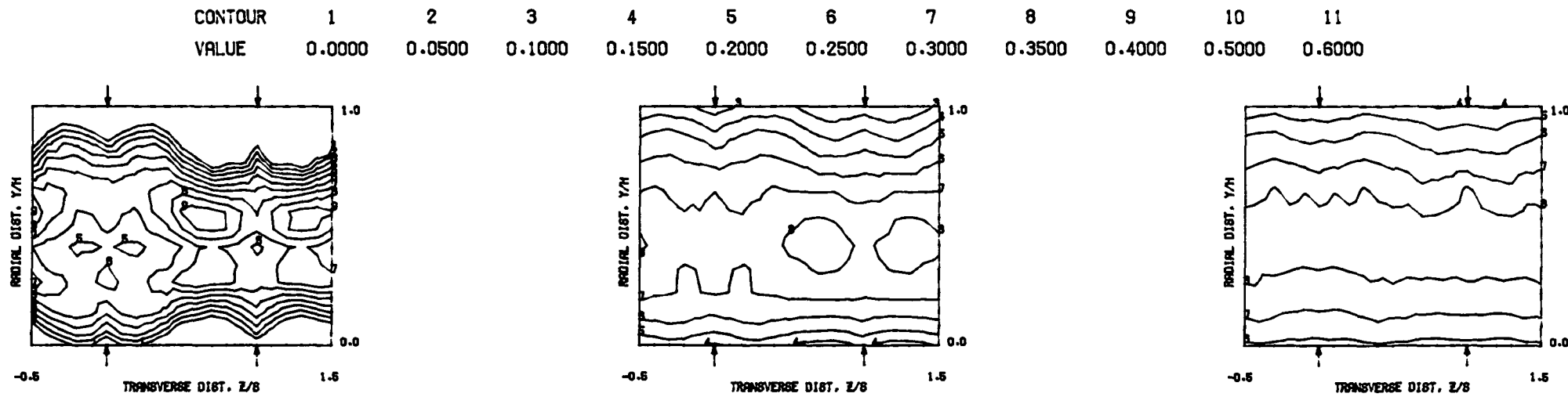
~~FOLDOUT FRAME~~

~~FOLDOUT FRAME~~

S = 0.0254 METERS S/DJ = 2.475 HQ/DJ = 9.899 VMAIN = 5.0 M/SEC VJET = 17.2 M/SEC TMAIN = 358.2 K TJET = 165.7 K THEB = 0.3253 BLORAT = 7.560 DENRATIO = 2.201 TRATIO = 0.463



MEASURED VELOCITY PROFILES FOR TEST NO 19, SYMM CONV DUCT, IN-LINE JETS , J = 25.97 , S/D = 2.00 , H/D = 8.00



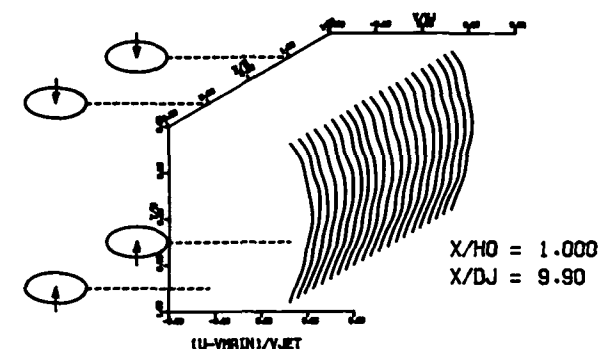
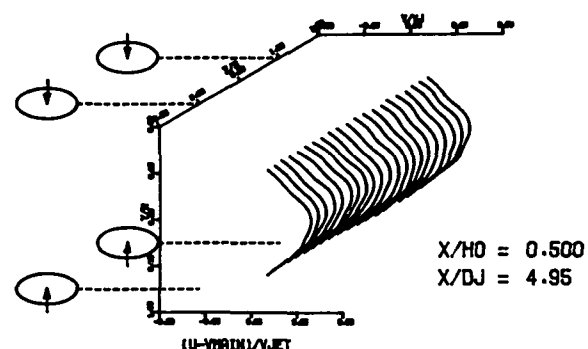
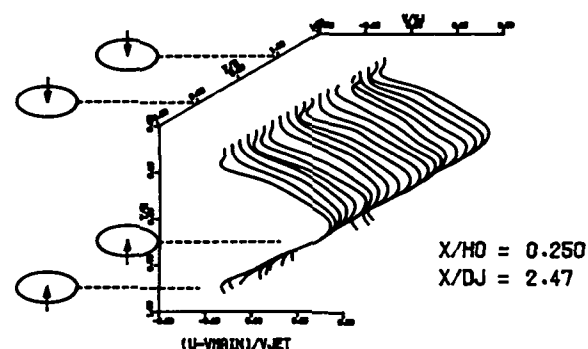
MEASURED VELOCITY PROFILES FOR TEST NO 19, SYMM CONV DUCT, IN-LINE JETS , J = 25.97 , S/D = 2.00 , H/D = 8.00

Figure 141. Measured Velocity Distributions for Test No. 19 of DJM Phase II Testing.

FOLDOUT FRAME

2 FOLDOUT FRAME

S = 0.0254 METERS S/DJ = 2.475 HO/DJ = 9.899 VMIN = 5.0 M/SEC VJET = 33.9 M/SEC TMIN = 358.1 K TJET = 165.0 K THEB = 0.5019 BLORAT= 15.664 DENRATIO= 2.305 TRATIO= 0.461



MEASURED VELOCITY PROFILES FOR TEST NO 20, SYMM CONV DUCT, IN-LINE JETS , J = 106.45 , S/D = 2.00 , H/D = 8.00

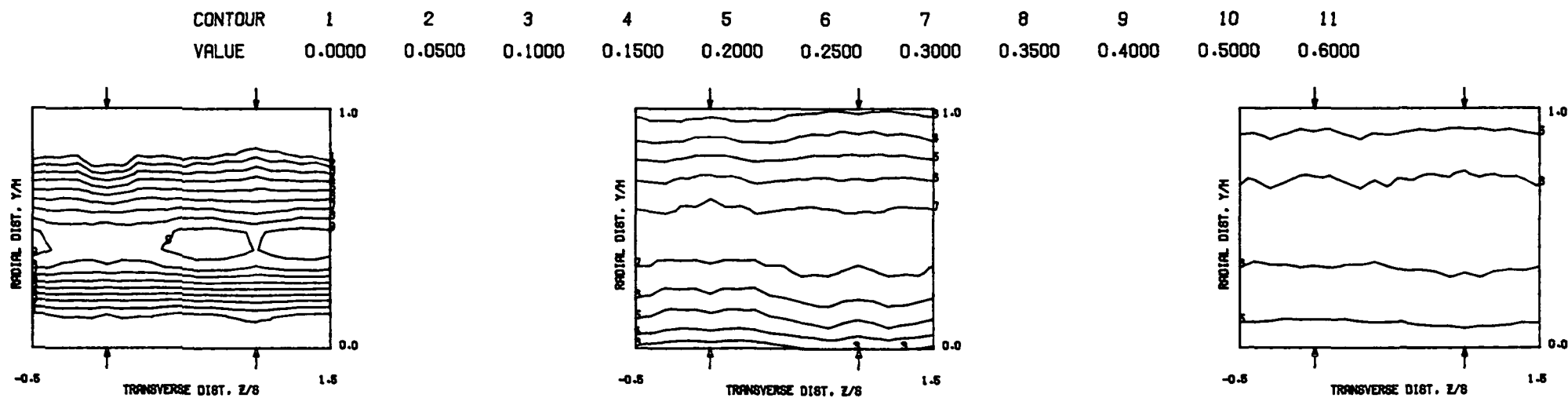
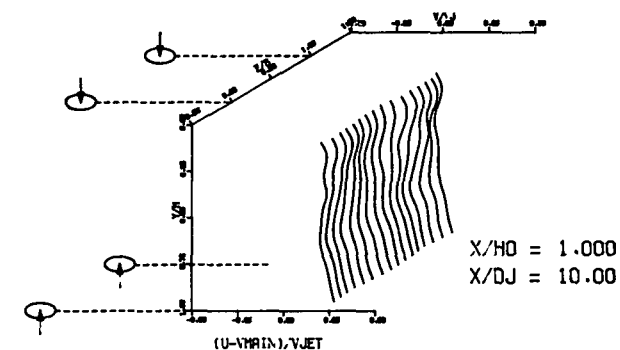
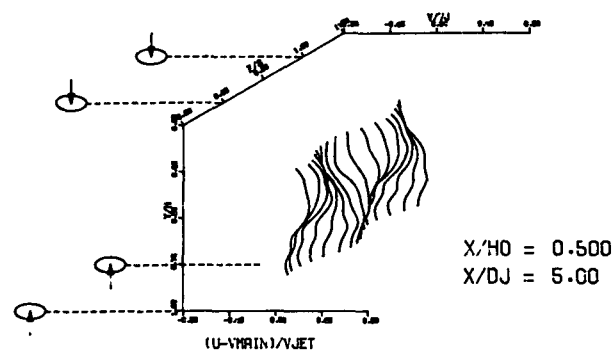
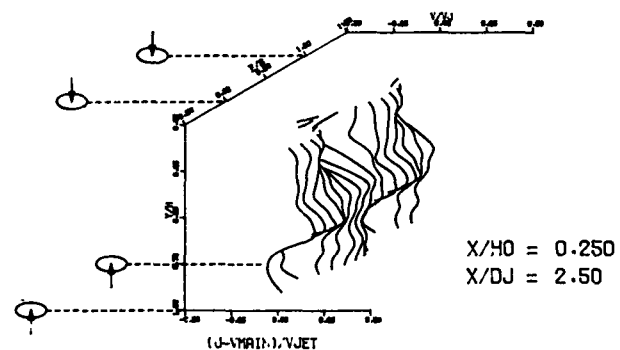


Figure 142. Measured Velocity Distributions for Test No. 20 of DJM Phase II Testing.

FOLDOUT FRAME

2 FOLDOUT FRAME

S = 0.0508 METERS S/DJ = 5.000 HO/DJ = 10.000 VMAIN = 5.0 M/SEC VJET = 17.4 M/SEC TMAIN = 358.1 K TJET = 168.3 K THEB = 0.1929 BLORAT= 7.464 DENRATIO= 2.149 TRATIO= 0.470



MEASURED VELOCITY PROFILES FOR TEST NO 21, SYMM CONV DUCT, STAGGERED JET, J = 25.92, S/D = 4.00, H/D = 8.00

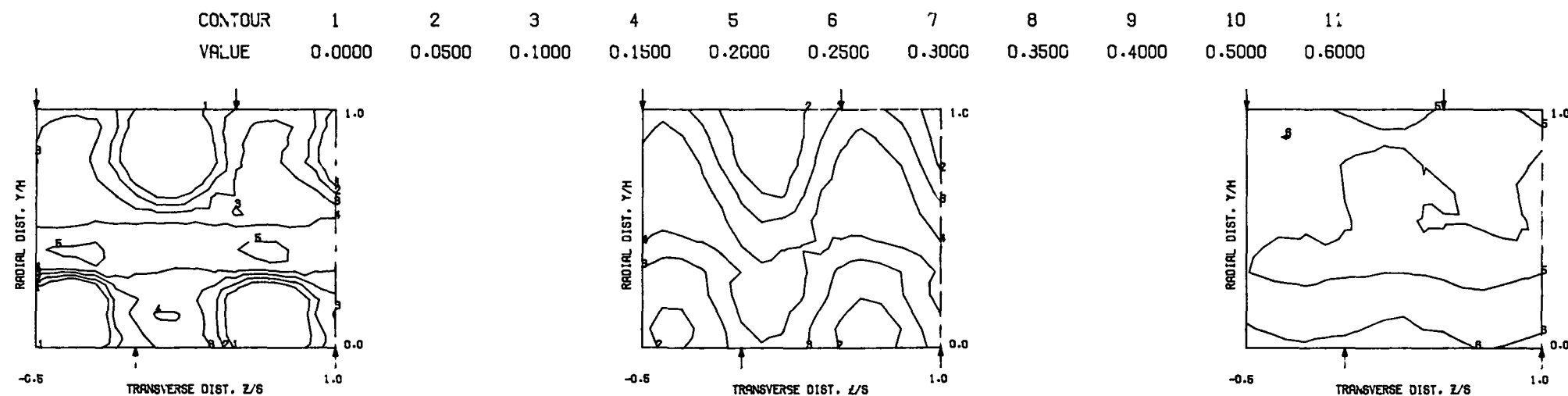
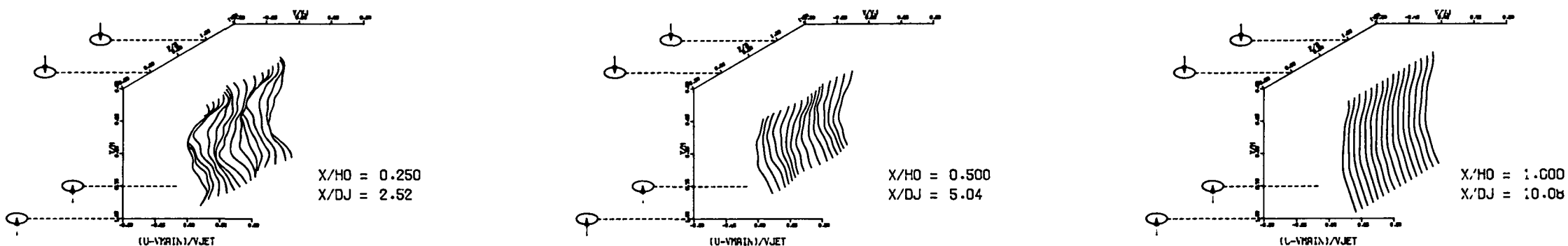


Figure 143. Measured Velocity Distributions for Test No. 21 of DJM Phase II Testing.

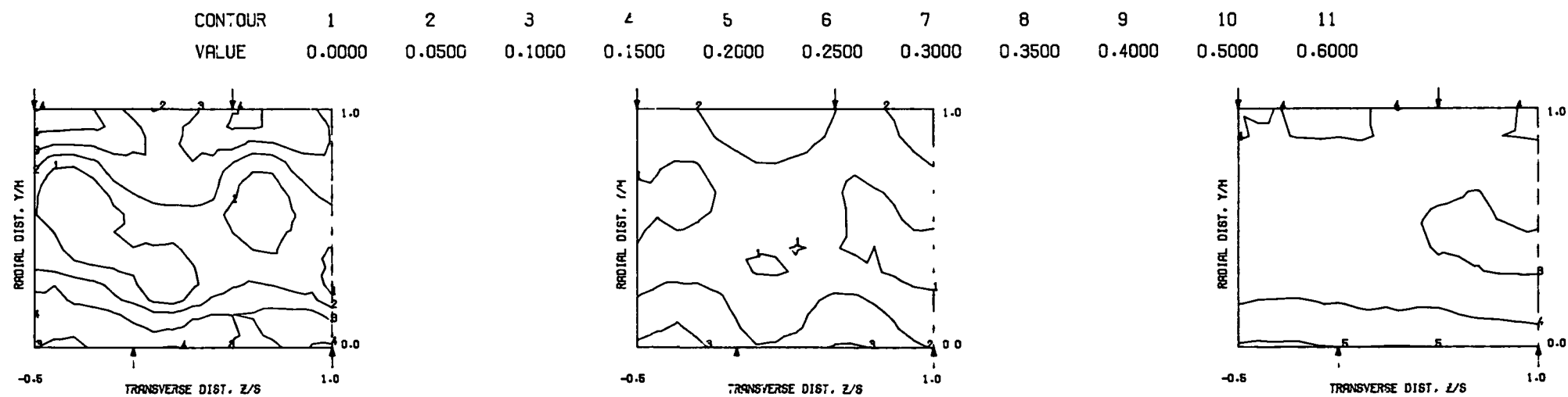
FOLDOUT FRAME

FOLDOUT FRAME

S = 0.0508 METERS S/DJ = 5.040 HO/DJ = 10.080 VMAIN = 5.0 M/SEC VJET = 34.4 M/SEC TMAIN = 357.9 K TJET = 165.8 K THEB = 0.3260 BLORAT= 15.640 DENRATIO= 2.272 TRATIO=0.463



MEASURED VELOCITY PROFILES FOR TEST NO 22, SYMM CONV DUCT, STAGGERED JET, J = 107.66, S/D = 4.00, H/D = 8.00



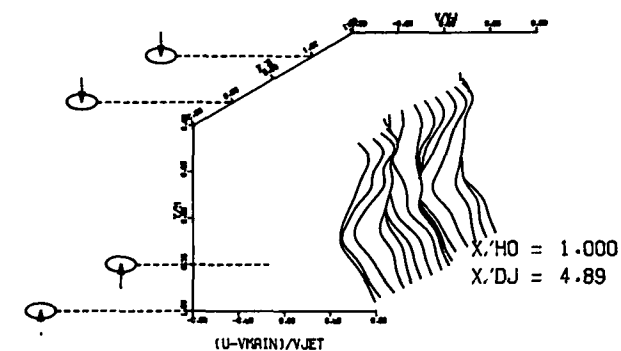
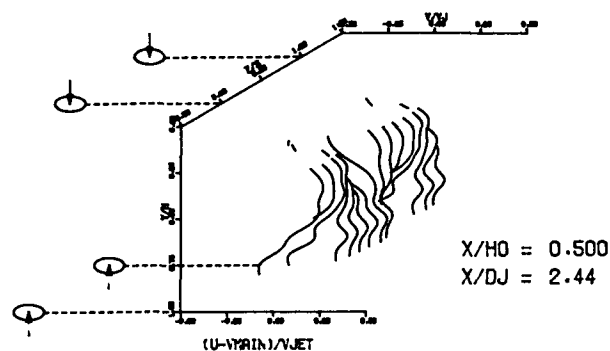
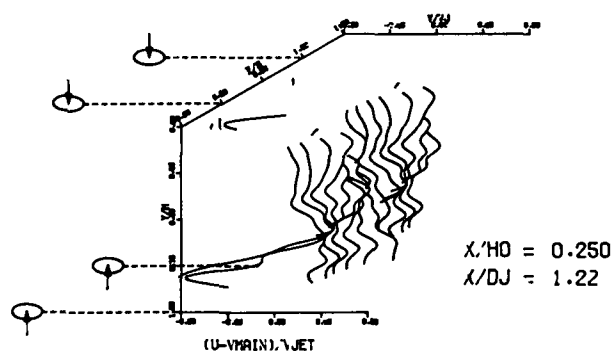
MEASURED VELOCITY PROFILES FOR TEST NO 22, SYMM CONV DUCT, STAGGERED JET, J = 107.66, S/D = 4.00, H/D = 8.00

Figure 144. Measured Velocity Distributions for Test No. 22 of DJM Phase II Testing.

ORIGINAL PAGE IS
OF POOR QUALITY

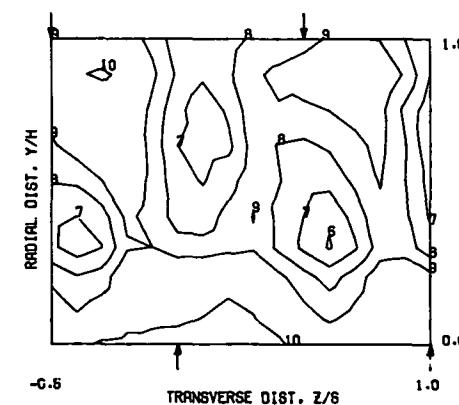
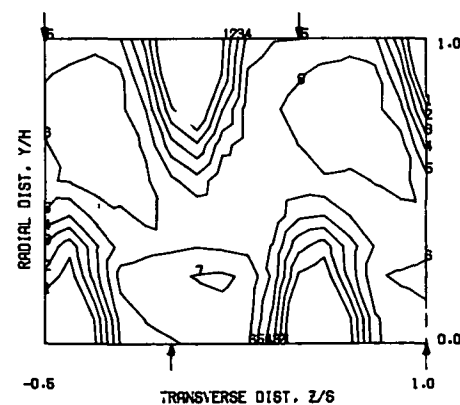
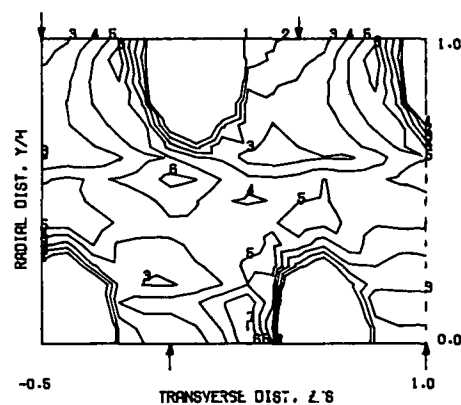
ORIGINAL PAGE IS
OF POOR QUALITY

S = 0.1016 METERS S/DJ = 4.886 HO/DJ = 4.886 VMAIN = 5.0 M/SEC VJET = 9.1 M/SEC TMAIN = 358.3 K TJET = 172.8 K THEB = 0.1994 BLORAT = 3.753 DENRATIO = 2.079 TRATIO = 0.48



MEASURED VELOCITY PROFILES FOR TEST NO 23, SYMM CONV DUCT, STAGGERED JET, $J = 6.77$, $S/D = 4.00$, $H/D = 4.00$

CONTOUR	1	2	3	4	5	6	7	8	9	10	11
VALUE	0.0000	0.0500	0.1000	0.1500	0.2000	0.2500	0.3000	0.3500	0.4000	0.5000	0.6000



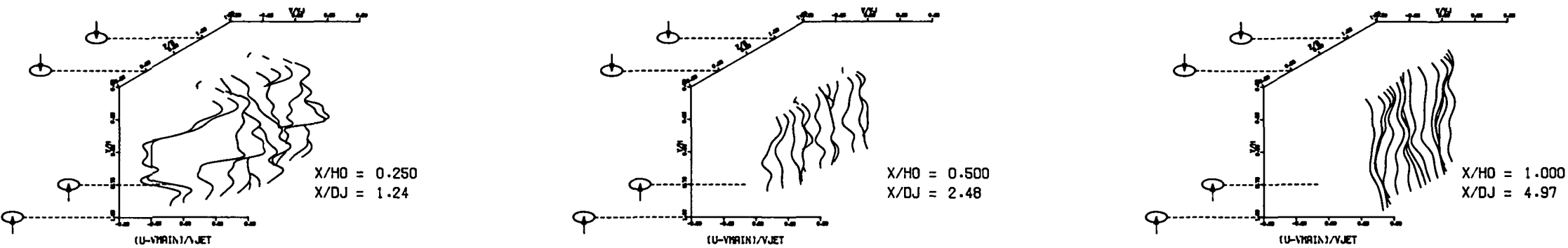
MEASURED VELOCITY PROFILES FOR TEST NO 23, SYMM CONV DUCT, STAGGERED JET, $J = 6.77$, $S/D = 4.00$, $H/D = 4.00$

Figure 145. Measured Velocity Distributions for Test No. 23 of DJM Phase II Testing.

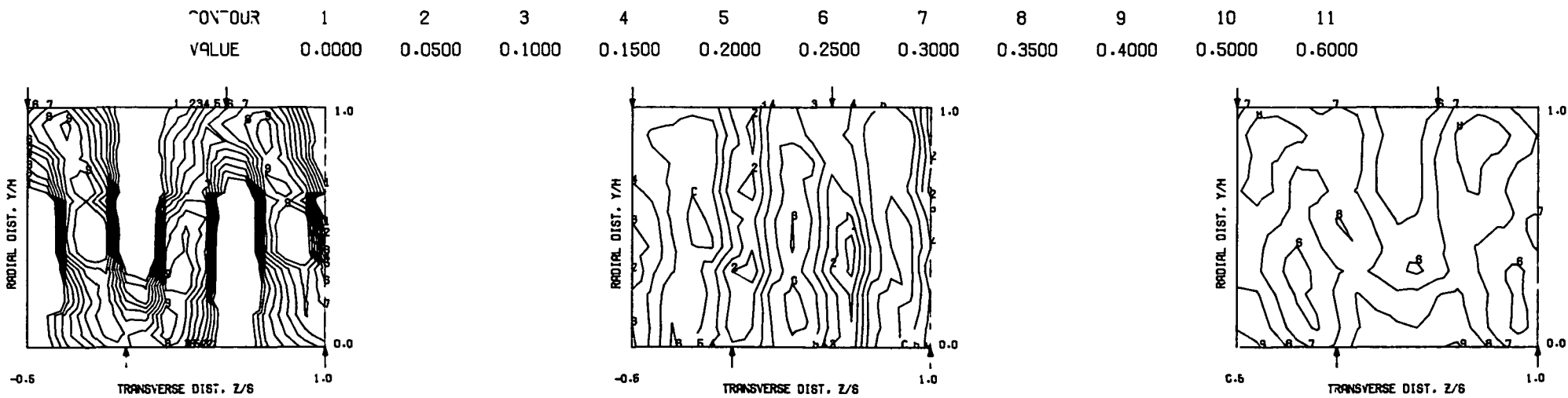
FOLDOUT FRAME

FOLDOUT FRAME

S = 0.1016 METERS S/DJ = 4.969 HO/DJ = 4.969 VMAIN = 5.0 M/SEC VJET = 17.3 M/SEC TMAIN = 358.1 K TJET = 169.0 K THEB = 0.3272 BLORAT= 7.449 DENRATIO= 2.154 TRATIO=0.472



MEASURED VELOCITY PROFILES FOR TEST NO 24, SYMM CONV DUCT, STAGGERED JET , J = 25.76 , S/D = 4.00 , H/D = 4.00



MEASURED VELOCITY PROFILES FOR TEST NO 24, SYMM CONV DUCT, STAGGERED JET , J = 25.76 , S/D = 4.00 , H/D = 4.00

Figure 146. Measured Velocity Distributions for Test No. 24 of DJM Phase II Testing.

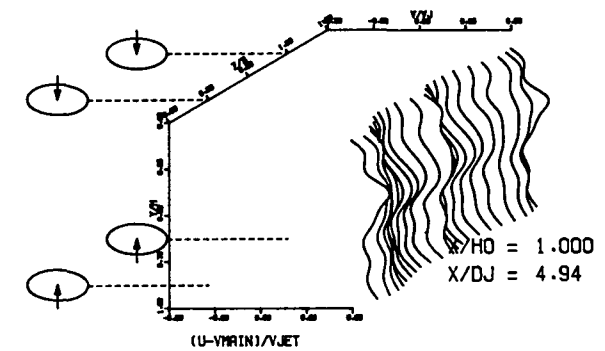
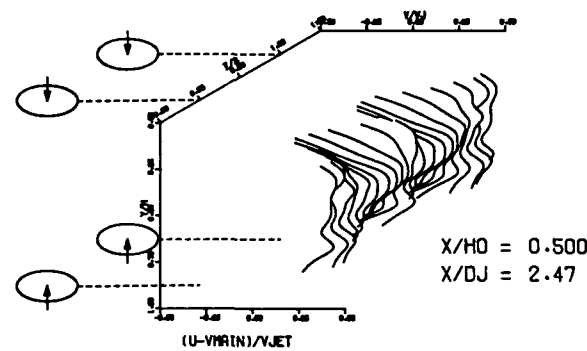
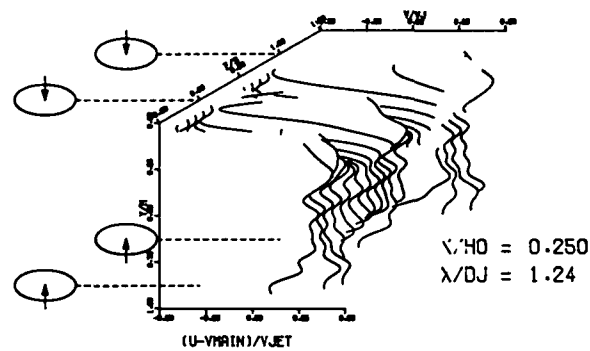
FOLDOUT FRAME

2 FOLDOUT FRAME

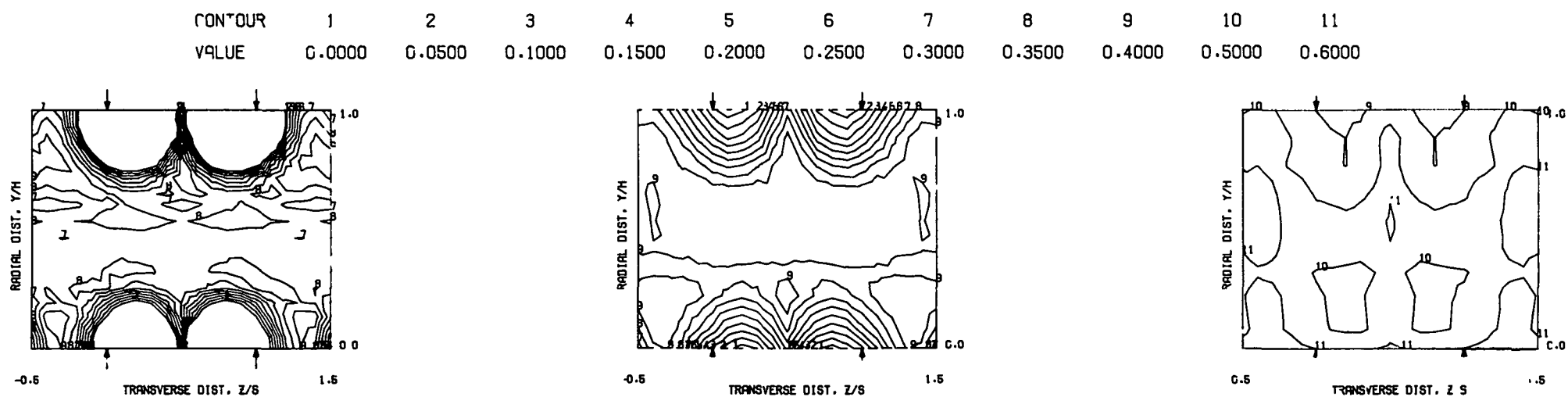
ORIGINAL PAGE IS
OF POOR QUALITY

ORIGINAL PAGE IS
OF POOR QUALITY

S = 0.0508 METERS S/DJ = 2.471 HO/DJ = 4.942 VMAIN = 5.0 M/SEC VJET = 8.8 M/SEC TMAIN = 358.4 K TJET = 166.9 K THEB = 0.3283 BLORAT = 3.791 DENRATIO = 2.156 TRATIO = 0.466



MEASURED VELOCITY PROFILES FOR TEST NO 25, SYMM CONV DUCT, IN-LINE JETS, J = 6.67, S/D = 2.00, H/D = 4.00



MEASURED VELOCITY PROFILES FOR TEST NO 25, SYMM CONV DUCT, IN-LINE JETS, J = 6.67, S/D = 2.00, H/D = 4.00

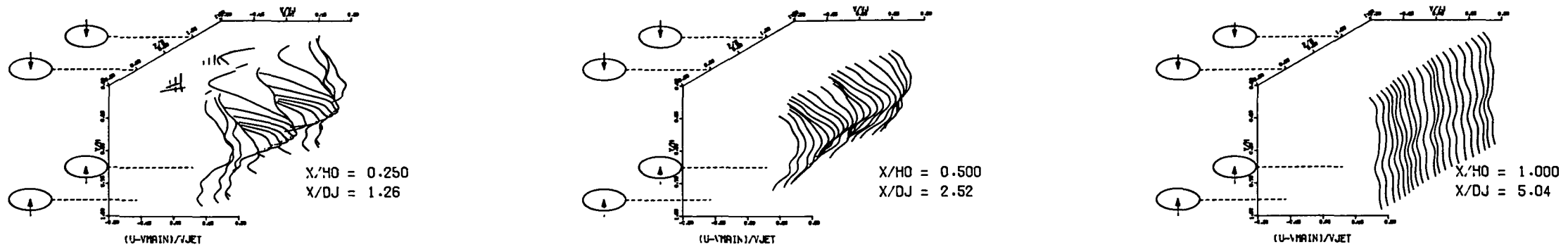
Figure 147. Measured Velocity Distributions for Test No. 25 of DJM Phase II Testing.

FOLDOUT FRAME

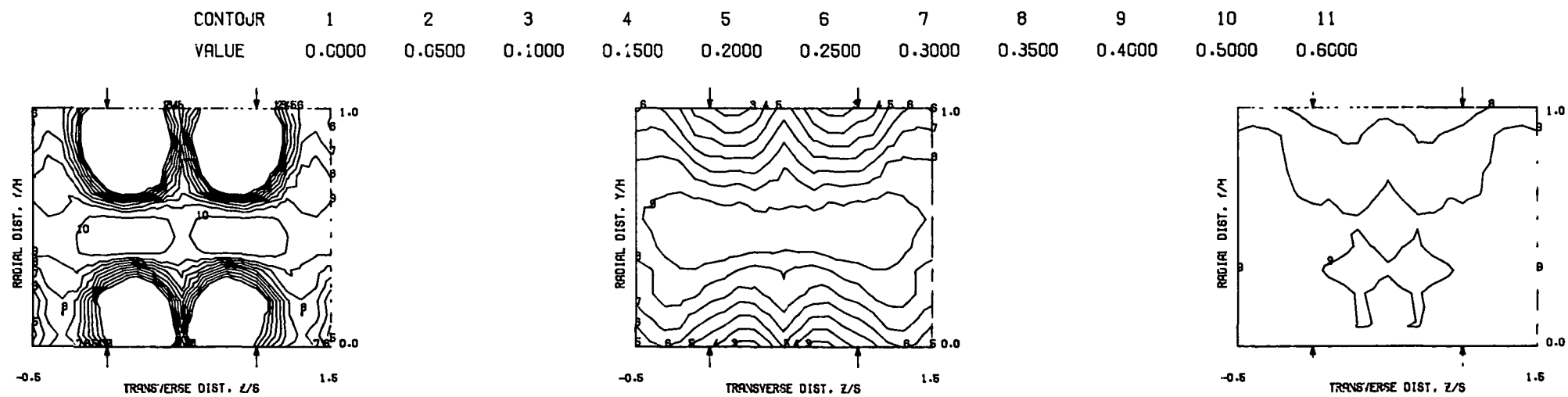
FOLDOUT FRAME

ORIGINAL PAGE IS
OF POOR QUALITY

S = 0.0508 METERS S/DJ = 2.526 HO/DJ = 5.039 VMAIN = 5.0 M/SEC VJET = 17.2 M/SEC TMAIN = 358.2 K TJET = 167.1 K THEB = 0.4810 BLORAT = 7.456 DENRATIO = 2.174 TRATIO = 0.467



MEASURED VELOCITY PROFILES FOR TEST NO 26, SYMM CONV DUCT, IN-LINE JETS , J = 25.58 , S/D = 2.00 , H/D = 4.00



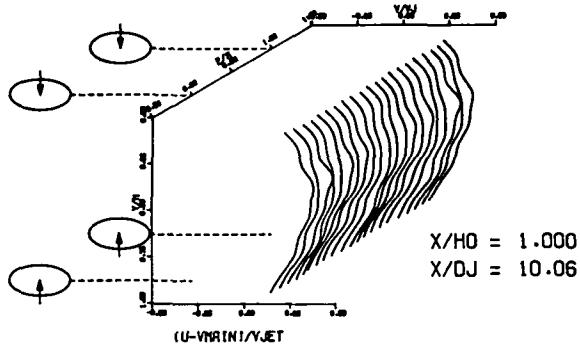
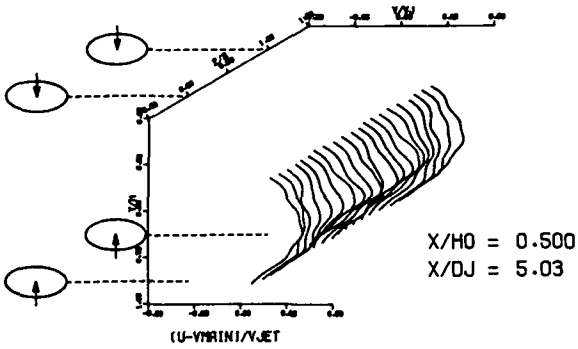
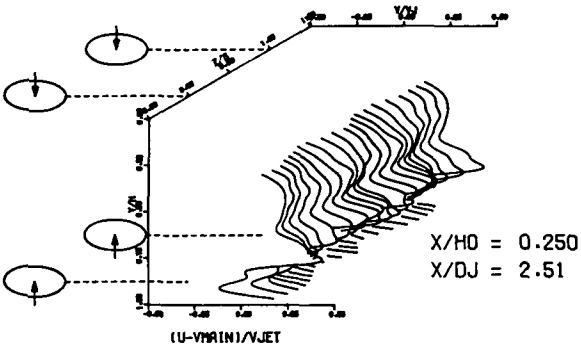
MEASURED VELOCITY PROFILES FOR TEST NO 26, SYMM CONV DUCT, IN-LINE JETS , J = 25.58 , S/D = 2.00 , H/D = 4.00

Figure 148. Measured Velocity
Distributions for Test No. 26
of DJM Phase II Testing.

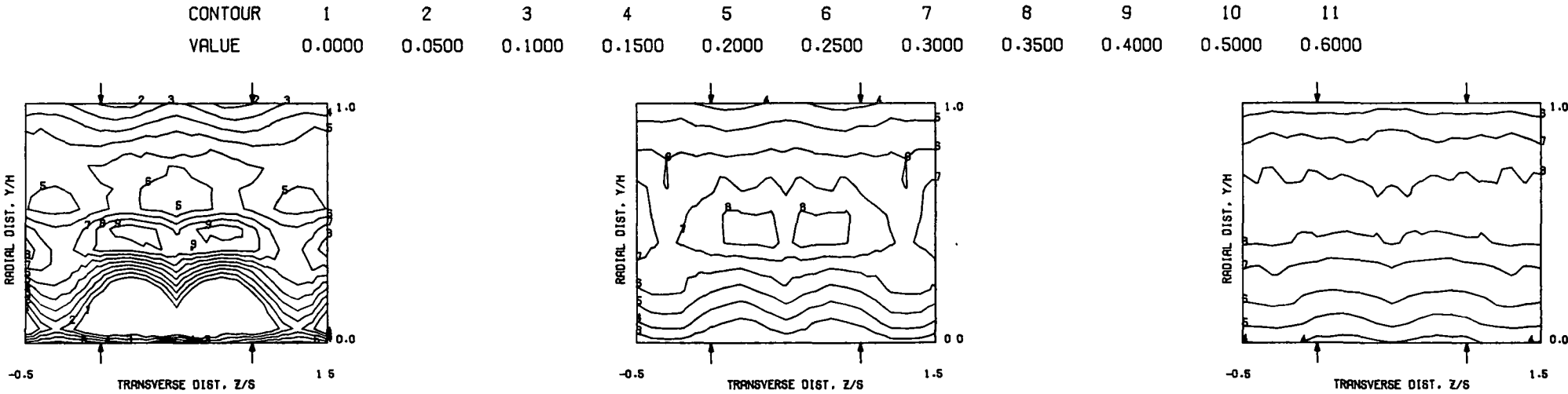
FOLDOUT FRAME

2 FOLDOUT FRAME

S = 0.0254 METERS S/DJ = 2.514 H0/DJ = 10.057 VMAIN = 5.0 M/SEC VJET = 17.4 M/SEC TMAIN = 358.3 K TJET = 168.5 K THEB = 0.3185 BLORAT= 7.512 DENRATIO= 2.155 TRATIO= 0.470



MEASURED VELOCITY PROFILES FOR TEST NO 35,ASYMM CONV DUCT,IN-LINE JETS , J = 26.20 , S/D = 2.00 , H/D = 8.00



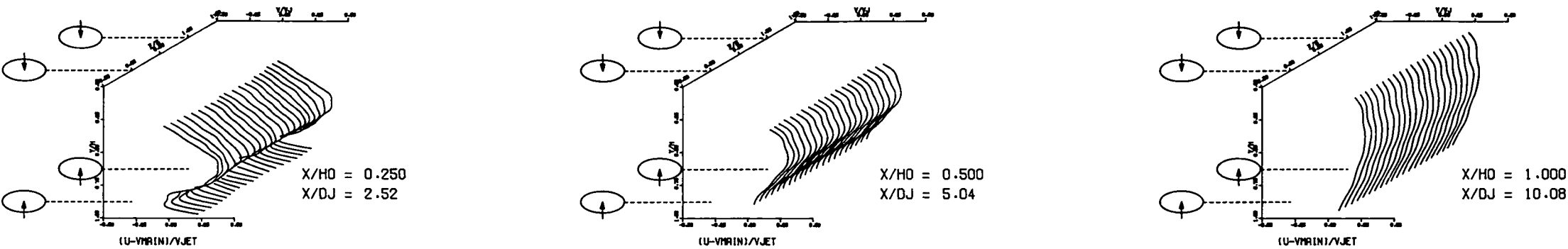
MEASURED VELOCITY PROFILES FOR TEST NO 35,ASYMM CONV DUCT,IN-LINE JETS , J = 26.20 , S/D = 2.00 , H/D = 8.00

Figure 149. Measured Velocity Distributions for Test No. 35 of DJM Phase II Testing.

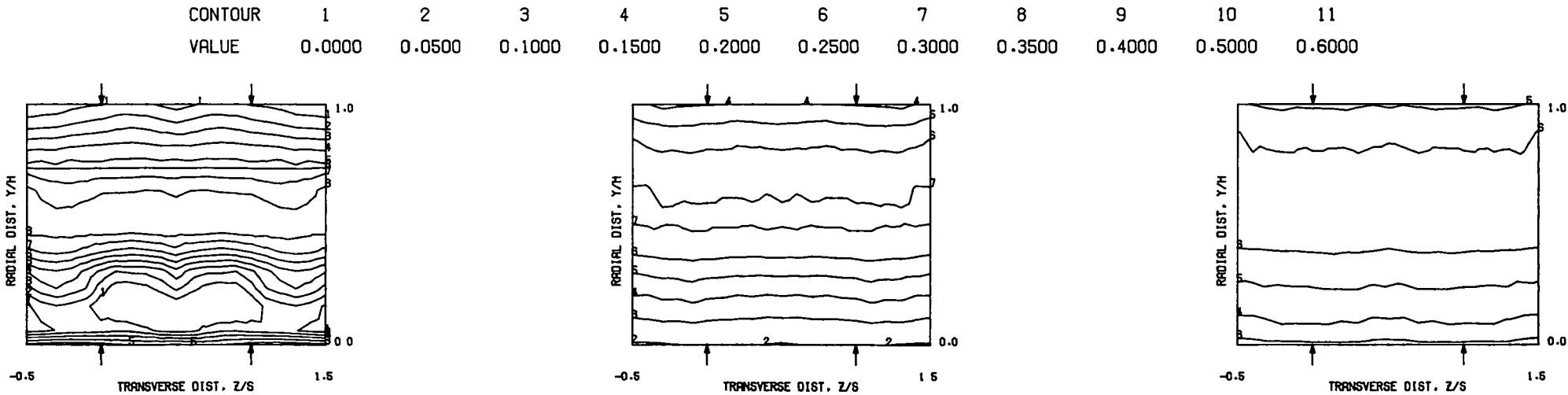
FOLDOUT FRAME

2 FOLDOUT FRAME

S = 0.0254 METERS S/DJ = 2.520 H0/DJ = 10.080 VMAIN = 5.0 M/SEC VJET = 34.4 M/SEC TMAIN = 358.0 K TJET = 167.3 K THEB = 0.4902 BLORAT= 15.590 DENRATIO= 2.275 TRATIO=0.467



MEASURED VELOCITY PROFILES FOR TEST NO 36,ASYMM CONV DUCT,IN-LINE JETS , J = 106.85 , S/D = 2.00 , H/D = 8.00



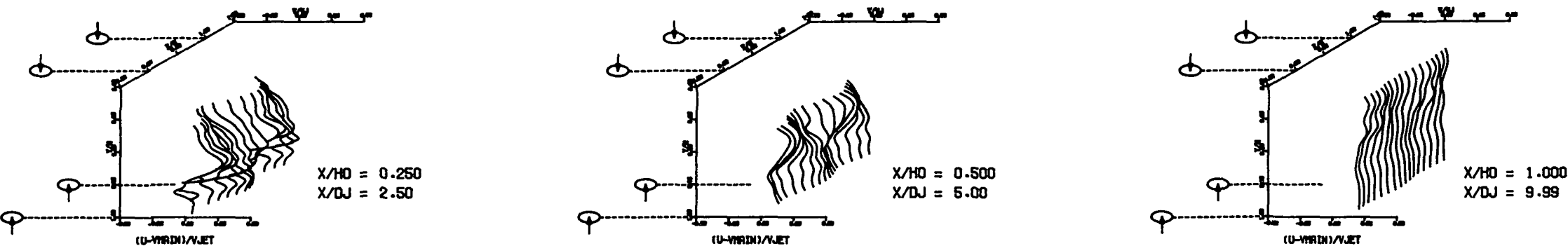
MEASURED VELOCITY PROFILES FOR TEST NO 36,ASYMM CONV DUCT,IN-LINE JETS , J = 106.85 , S/D = 2.00 , H/D = 8.00

Figure 150. Measured Velocity Distributions for Test No. 36 of DJM Phase II Testing.

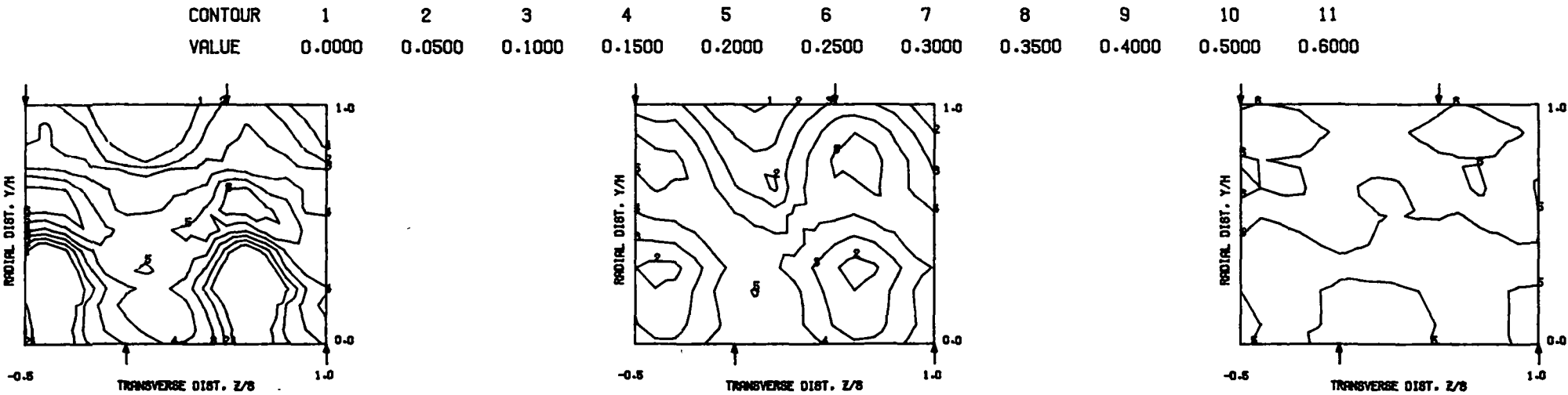
FOLDOUT FRAME

2 FOLDOUT FRAME

S = 0.0508 METERS S/DJ = 4.993 HO/DJ = 9.987 VMAIN = 5.0 M/SEC VJET = 17.5 M/SEC TMAIN = 358.7 K TJET = 172.6 K THEB = 0.1882 BLORAT = 7.343 DENRATIO = 2.100 TRATIO = 0.48



MEASURED VELOCITY PROFILES FOR TEST NO 37,ASYM CONV DUCT,STAGGERED JET , J = 25.68 , S/D = 4.00 , H/D = 8.00



MEASURED VELOCITY PROFILES FOR TEST NO 37,ASYM CONV DUCT,STAGGERED JET , J = 25.68 , S/D = 4.00 , H/D = 8.00

Figure 151. Measured Velocity Distributions for Test No. 37 of DJM Phase II Testing.

FOLDOUT FRAME

2 FOLDOUT FRAME

S = 0.0508 METERS S/DJ = 5.040 HO/DJ = 10.080 VMAIN = 5.0 M/SEC VJET = 34.7 M/SEC TMAIN = 358.7 K TJET = 168.5 K THEB = 0.3245 BLORAT= 15.678 DENRATIO= 2.260 TRATIO=0.470

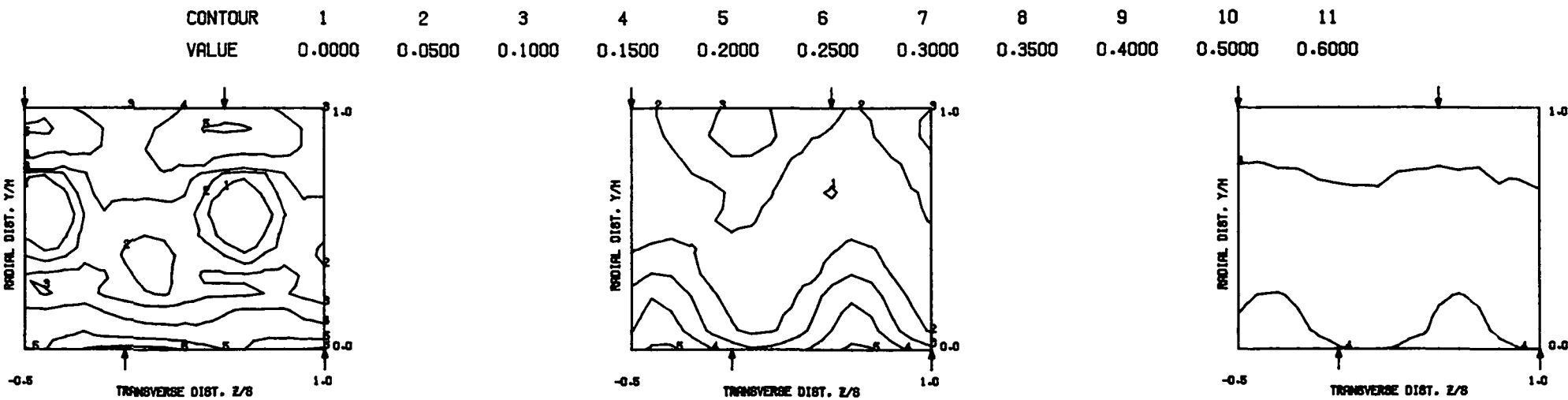
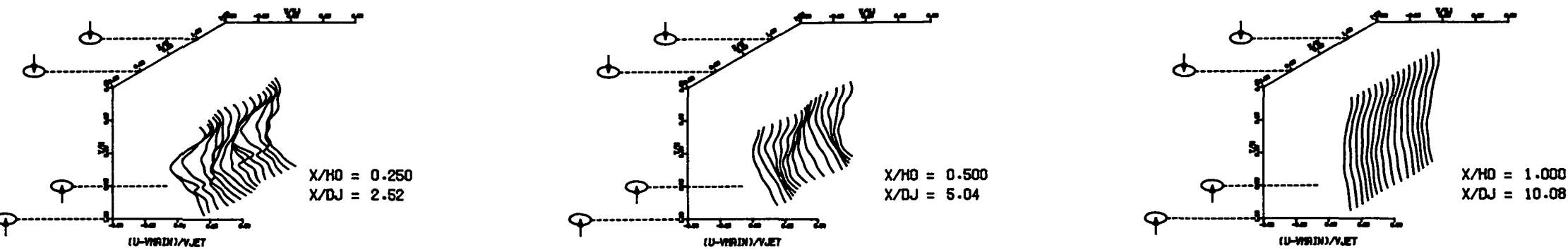
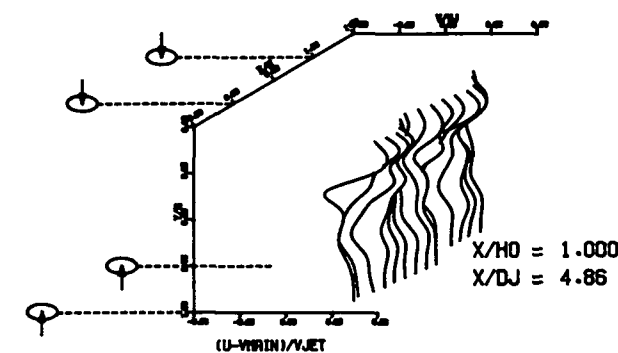
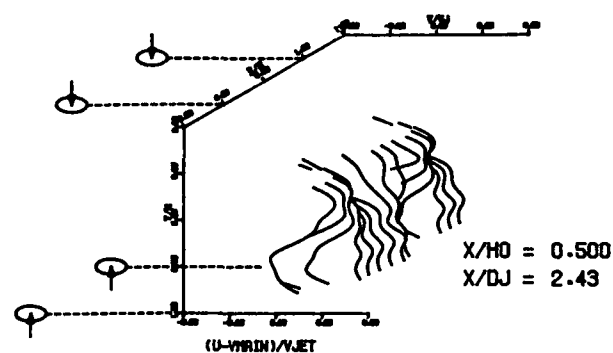
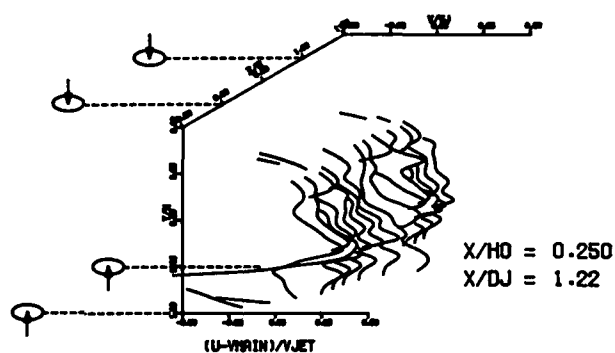


Figure 152. Measured Velocity Distributions for Test No. 38 of DJM Phase II Testing.

FOLDOUT FRAME

2 FOLDOUT FRAME

S = 0.1016 METERS S/DJ = 4.862 HO/DJ = 4.862 VMAIN = 5.0 M/SEC VJET = 9.0 M/SEC TMAIN = 358.6 K TJET = 173.3 K THEB = 0.1994 BLORAT= 3.726 DENRATIO= 2.075 TRATIO= 0.48



MEASURED VELOCITY PROFILES FOR TEST NO 39,ASYM CONV DUCT,STAGGERED JET , J = 6.69 , S/D = 4.00 , H/D = 4.00

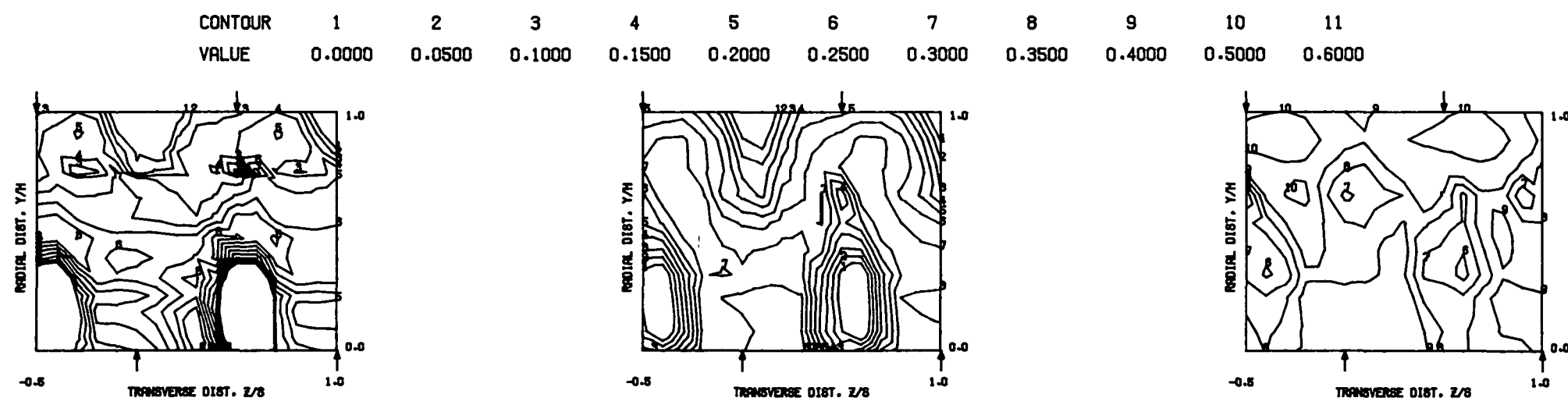
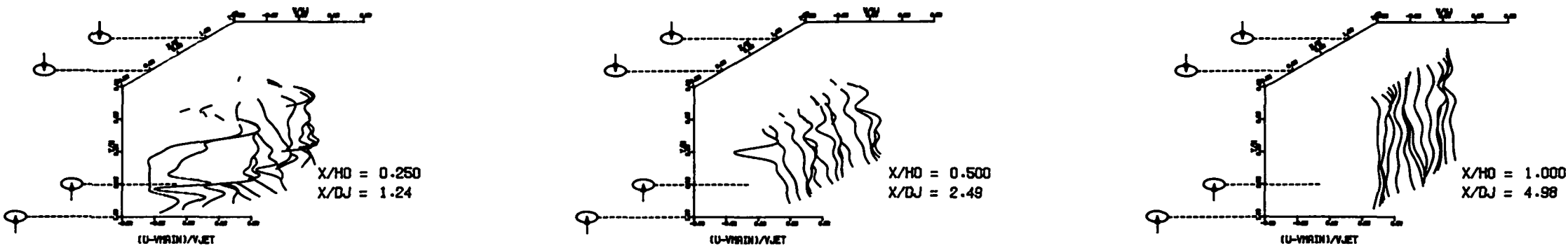


Figure 153. Measured Velocity Distributions for Test No. 39 of DJM Phase II Testing.

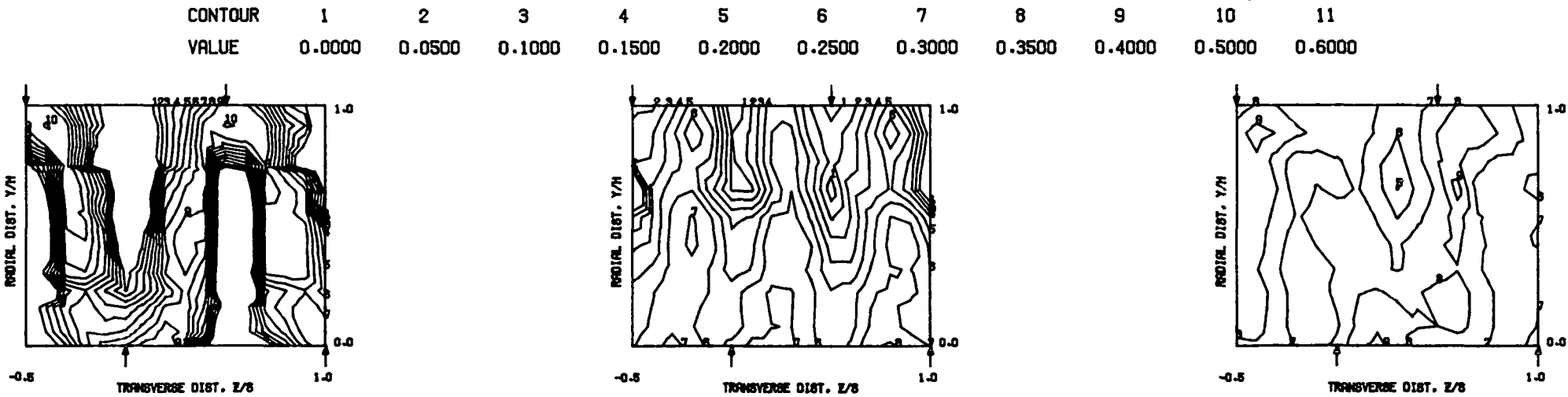
FOLDOUT FRAME

FOLDOUT FRAME

S ≈ 0.1016 METERS S/DJ = 4.977 H0/DJ = 4.977 VMAIN = 5.0 M/SEC VJET = 17.5 M/SEC TMAIN = 358.7 K TJET = 168.2 K THEB = 0.3248 BLORAT= 7.493 DENRATIO= 2.164 TRATIO=0.469



MEASURED VELOCITY PROFILES FOR TEST NO 40,ASYM CONV DUCT,STAGGERED JET , J = 25.95 , S/D = 4.00 , H/D = 4.00



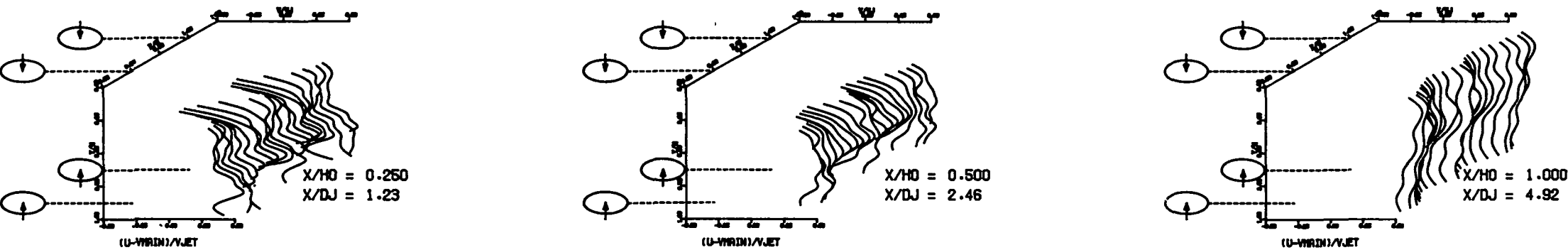
MEASURED VELOCITY PROFILES FOR TEST NO 40,ASYM CONV DUCT,STAGGERED JET , J = 25.95 , S/D = 4.00 , H/D = 4.00

Figure 154. Measured Velocity Distributions for Test No. 40 of DJM Phase II Testing.

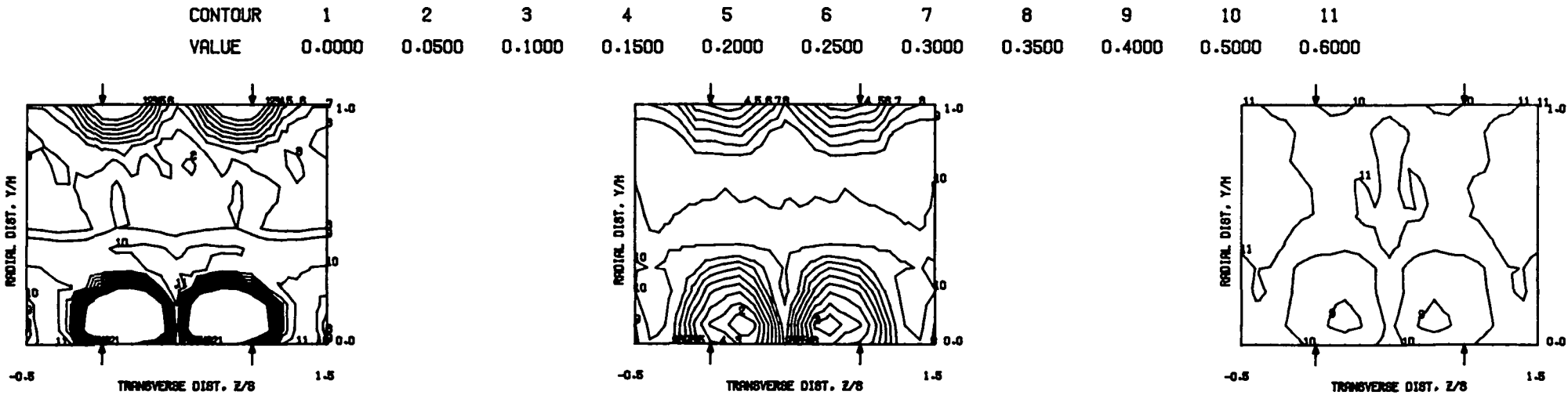
FOLDOUT FRAME

FOLDOUT FRAME

S = 0.0508 METERS S/DJ = 2.462 HO/DJ = 4.924 VMRAIN = 5.0 M/SEC VJET = 8.9 M/SEC TMAIN = 358.6 K TJET = 169.7 K THEB = 0.3272 BLORAT= 3.747 DENRATIO= 2.122 TRATIO=0.473



MEASURED VELOCITY PROFILES FOR TEST NO 41,ASYMM CONV DUCT,IN-LINE JETS , J = 6.62 , S/D = 2.00 , H/D = 4.00



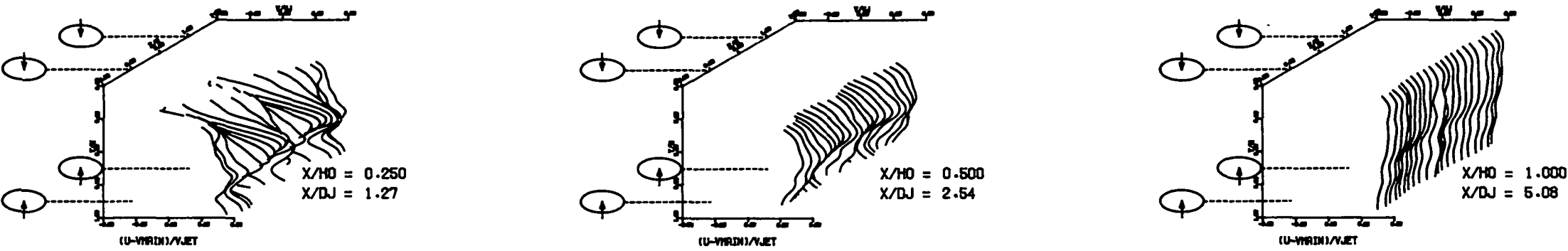
MEASURED VELOCITY PROFILES FOR TEST NO 41,ASYMM CONV DUCT,IN-LINE JETS , J = 6.62 , S/D = 2.00 , H/D = 4.00

Figure 155. Measured Velocity Distributions for Test No. 41 of DJM Phase II Testing.

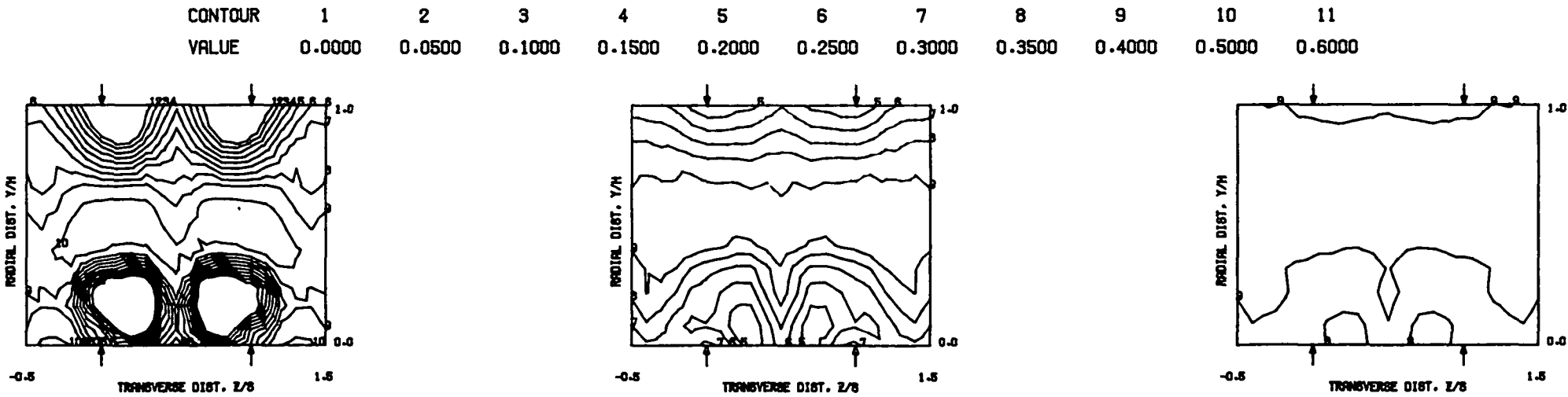
FOLDOUT FRAME

2 FOLDOUT FRAME

S = 0.0508 METERS S/DJ = 2.540 HO/DJ = 5.080 VMAIN = 5.0 M/SEC VJET = 17.4 M/SEC TMAIN = 358.2 K TJET = 168.0 K THEB = 0.4774 BLORAT= 7.518 DENRATIO= 2.164 TRATIO= 0.469



MEASURED VELOCITY PROFILES FOR TEST NO 42,ASYMM CONV DUCT,IN-LINE JETS , J = 26.12 , S/D = 2.00 , H/D = 4.00

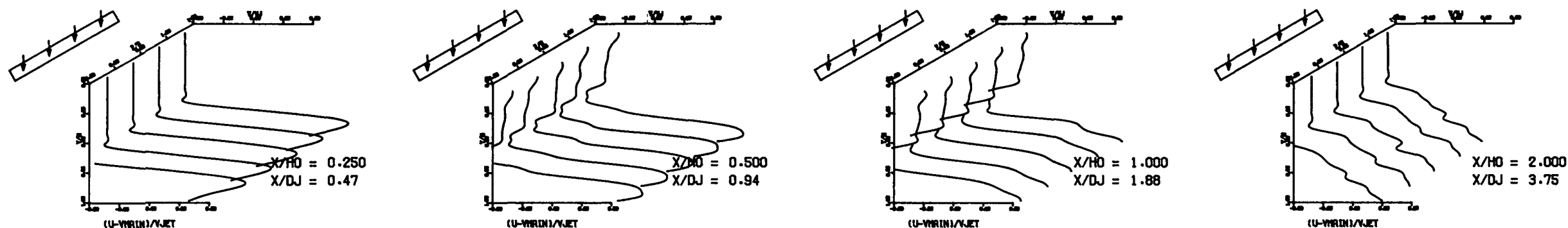


MEASURED VELOCITY PROFILES FOR TEST NO 42,ASYMM CONV DUCT,IN-LINE JETS , J = 26.12 , S/D = 2.00 , H/D = 4.00

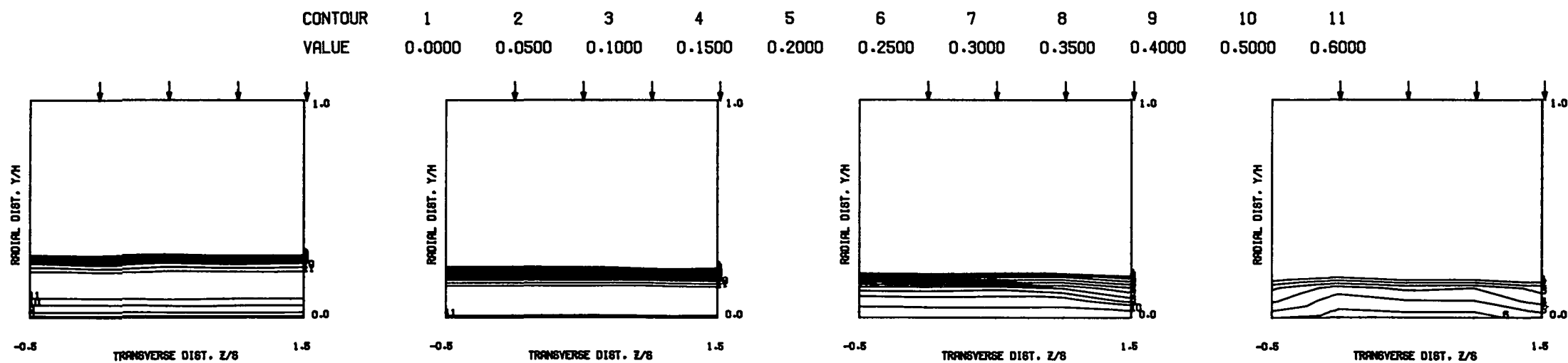
Figure 156. Measured Velocity Distributions for Test No. 42 of DJM Phase II Testing.

FOLDOUT FRAME

S = 0.0102 METERS S/DJ = 0.189 HO/DJ = 1.876 VMAIN = 5.0 M/SEC VJET = 9.0 M/SEC TMAIN = 358.1 K TJET = 171.0 K THEB = 0.2179 BLORAT= 3.744 DENRATIO= 2.104 TRATIO=0.477



MEASURED VELOCITY PROFILES FOR TEST NO 45A, 10.24 MM 2-D SLOT, TM=CONST, J = 6.66, S/D = 1.00, H/D = 9.92



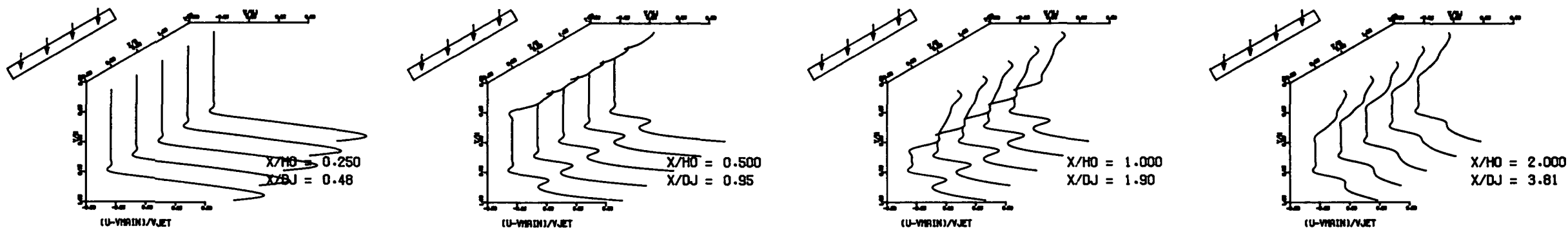
MEASURED VELOCITY PROFILES FOR TEST NO 45A, 10.24 MM 2-D SLOT, TM=CONST, J = 6.66, S/D = 1.00, H/D = 9.92

Figure 157. Measured Velocity Distributions for Test No. 45A of DJM Phase II Testing.

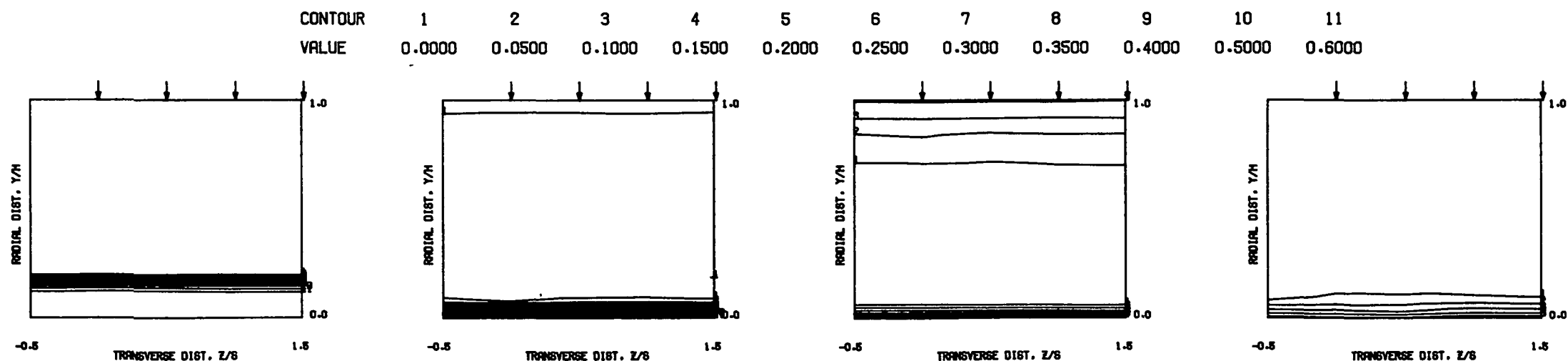
FOLDOUT FRAME

2 FOLDOUT FRAME

S = 0.0102 METERS S/DJ = 0.192 HO/DJ = 1.905 VMAIN = 5.1 M/SEC VJET = 17.5 M/SEC TMAIN = 358.0 K TJET = 171.5 K THEB = 0.3462 BLORAT= 7.335 DENRATIO= 2.125 TRATIO=0.479



MEASURED VELOCITY PROFILES FOR TEST NO 45B, 10.24 MM 2-D SLOT, TM=CONST, J = 25.33, S/D = 1.00, H/D = 9.92



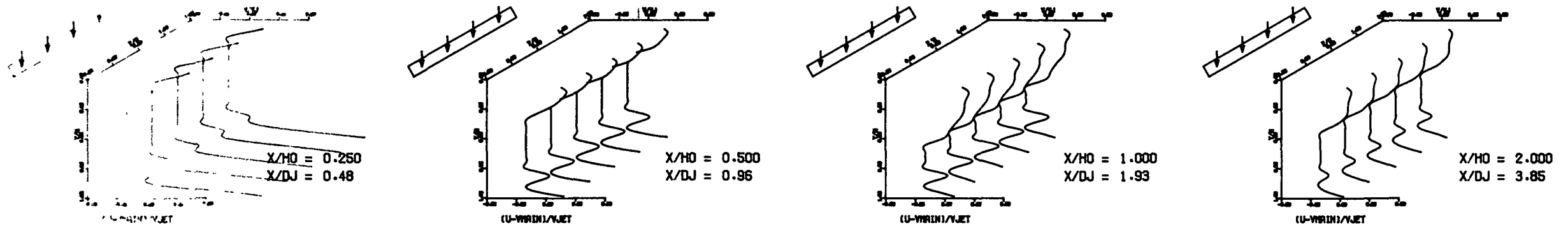
MEASURED VELOCITY PROFILES FOR TEST NO 45B, 10.24 MM 2-D SLOT, TM=CONST, J = 25.33, S/D = 1.00, H/D = 9.92

Figure 158. Measured Velocity Distributions for Test No. 45B of DJM Phase II Testing.

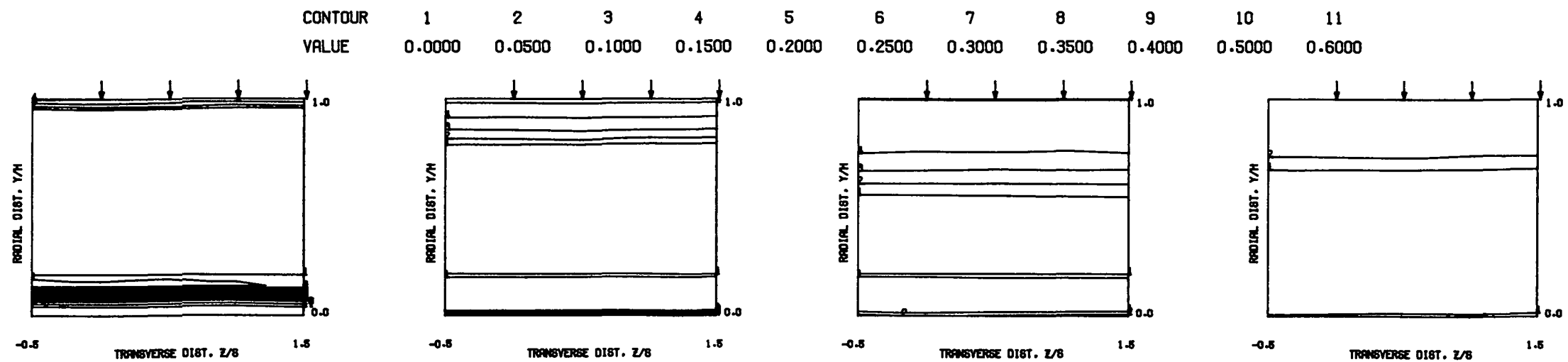
ORIGINAL PAGE IS
OF POOR QUALITY

ORIGINAL PAGE IS
OF POOR QUALITY

S = 0.0102 METERS S/DJ = 0.194 HO/DJ = 1.926 VMAIN = 5.1 M/SEC VJET = 30.2 M/SEC TMAIN = 357.7 K TJET = 170.8 K THEB = 0.4820 BLORAT= 13.185 DENRATIO= 2.223 TRATIO=0.478



MEASURED VELOCITY PROFILES FOR TEST NO 45C, 10.24 MM 2-D SLOT, TM=CONST, J = 78.20, S/D = 1.00, H/D = 9.92



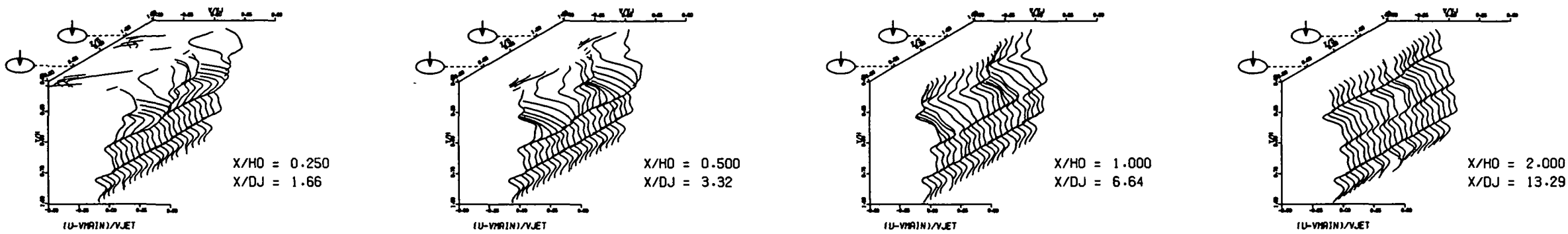
MEASURED VELOCITY PROFILES FOR TEST NO 45C, 10.24 MM 2-D SLOT, TM=CONST, J = 78.20, S/D = 1.00, H/D = 9.92

Figure 159. Measured Velocity Distributions for Test No. 45C of DJM Phase II Testing.

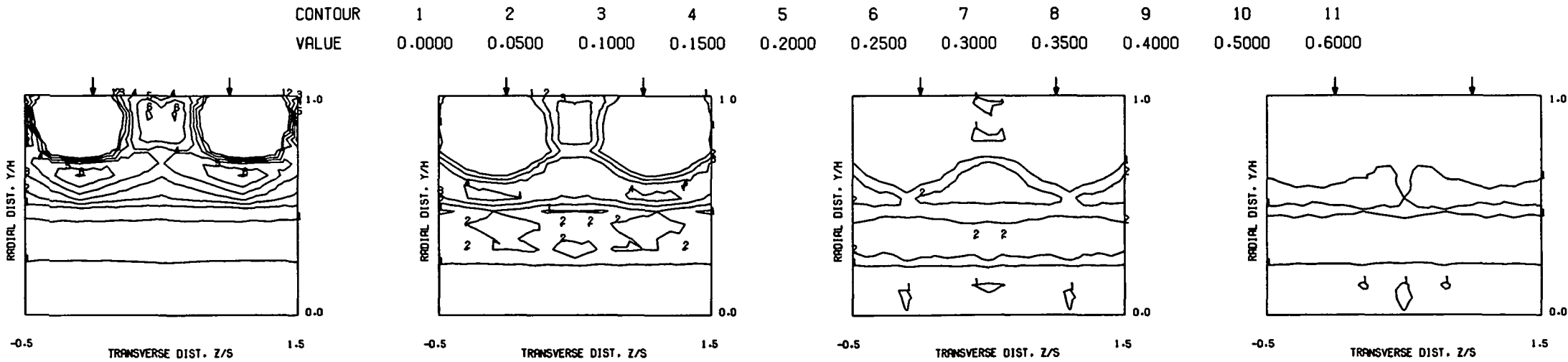
FOLDOUT FRAME

FOLDOUT FRAME

S = 0.0508 METERS S/DJ = 3.322 HO/DJ = 6.644 VMAIN = 5.1 M/SEC VJET = 9.0 M/SEC TMAIN = 358.0 K TJET = 171.9 K THEB = 0.1159 BLORAT= 3.682 DENRATIO= 2.090 TRATIO=0.480



MEASURED VELOCITY PROFILES FOR TEST NO 49, SINGLE SIDED JETS, $T_M=CONST$, $J = 6.49$, $S/D = 2.83$, $H/D = 5.66$



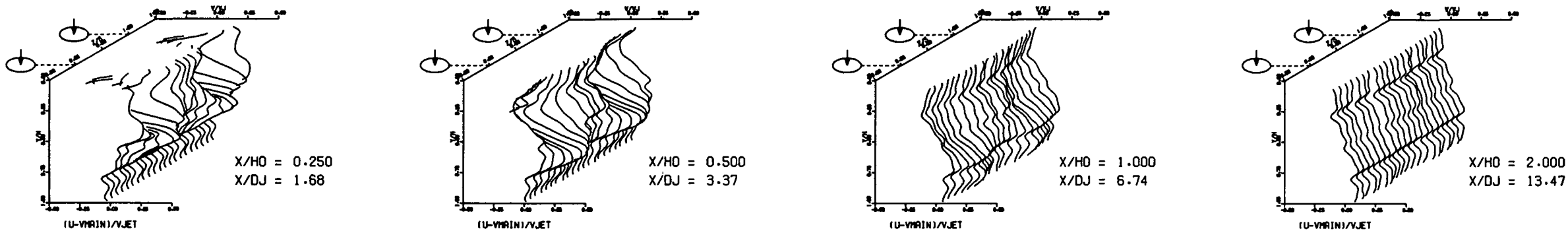
MEASURED VELOCITY PROFILES FOR TEST NO 49, SINGLE SIDED JETS, $T_M=CONST$, $J = 6.49$, $S/D = 2.83$, $H/D = 5.66$

Figure 160. Measured Velocity Distributions for Test No. 49 of DJM Phase II Testing.

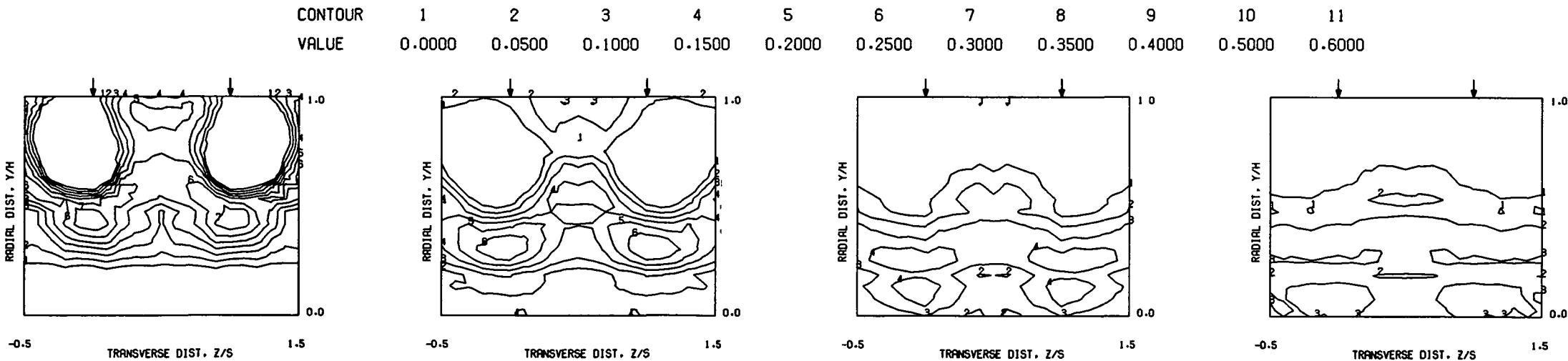
FOLDOUT FRAME

2 FOLDOUT FRAME

S = 0.0508 METERS S/DJ = 3.369 HO/DJ = 6.737 VMAIN = 5.0 M/SEC VJET = 17.2 M/SEC TMAIN = 358.3 K TJET = 166.4 K THEB = 0.2054 BLORAT= 7.468 DENRATIO= 2.191 TRATIO=0.464



MEASURED VELOCITY PROFILES FOR TEST NO 50, SINGLE SIDED JETS, $TM=CONST$, $J = 25.46$, $S/D = 2.83$, $H/D = 5.66$



MEASURED VELOCITY PROFILES FOR TEST NO 50, SINGLE SIDED JETS, $TM=CONST$, $J = 25.46$, $S/D = 2.83$, $H/D = 5.66$

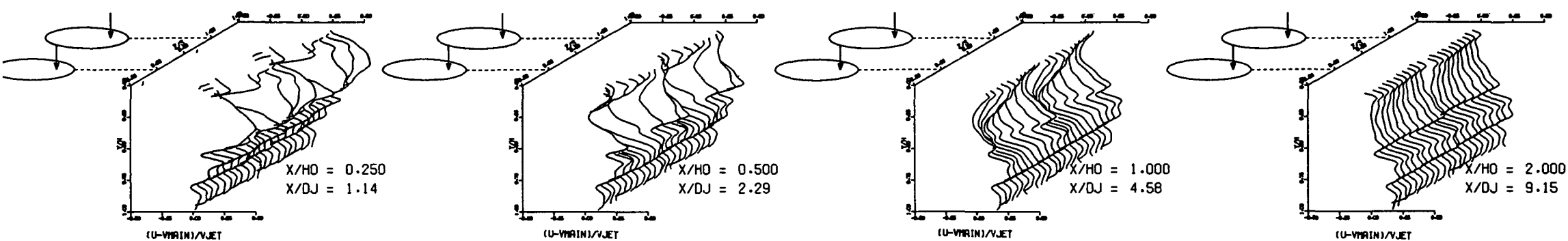
Figure 161. Measured Velocity Distributions for Test No. 50 of DJM Phase II Testing.

FOLDOUT FRAME

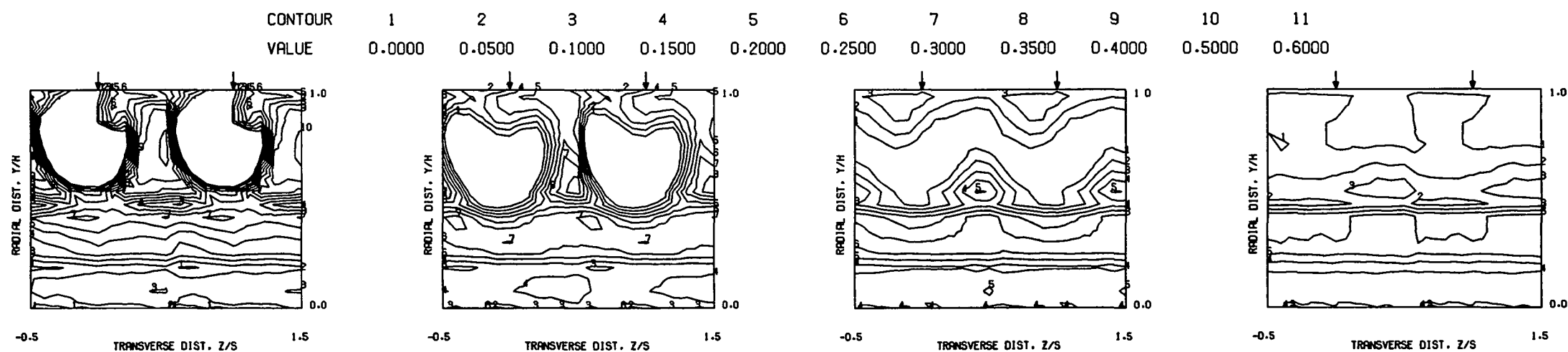
2 FOLDOUT FRAME

ORIGINAL PAGE IS
OF POOR QUALITY

S = 0.0508 METERS S/DJ = 2.288 H/DJ = 4.576 VMAIN = 17.8 M/SEC VJET = 30.9 M/SEC TMAIN = 690.1 K TJET = 317.1 K THEB = 0.2216 BLORAT = 3.795 DENRATIO = 2.181 TRATIO = 0.460



MEASURED VELOCITY PROFILES FOR TEST NO 1, TM=CONST, STREAMLINED SLOTS, $J = 6.60$, $S/D = 2.00$, $H/D = 4.00$



MEASURED VELOCITY CONTOURS FOR TEST NO 1, S.L. SLOT, $J=6.60$, $S/D=2.00$, $H/D=4.00$

Figure 162. Measured Velocity
Distributions for Test No. 1
of DJM Phase III Testing.

ORIGINAL PAGE IS
OF POOR QUALITY

S = 0.0508 METERS S/DJ = 2.379 HO/DJ = 4.758 VMAIN = 16.7 M/SEC VJET = 58.5 M/SEC TMAIN = 661.0 K TJET = 307.3 K THEB = 0.3447 BLORAT= 7.581 DENRATIO= 2.171 TRATIO= 0.465

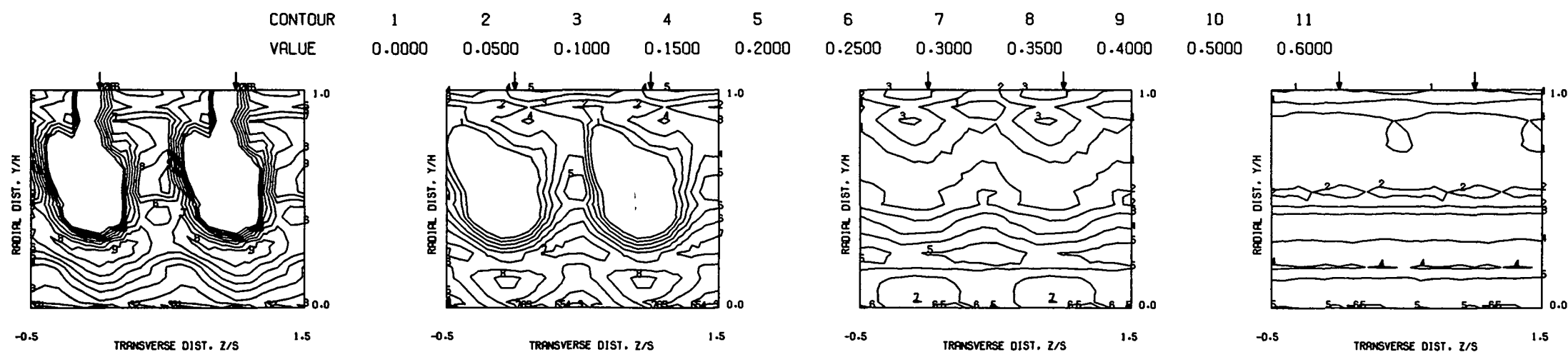
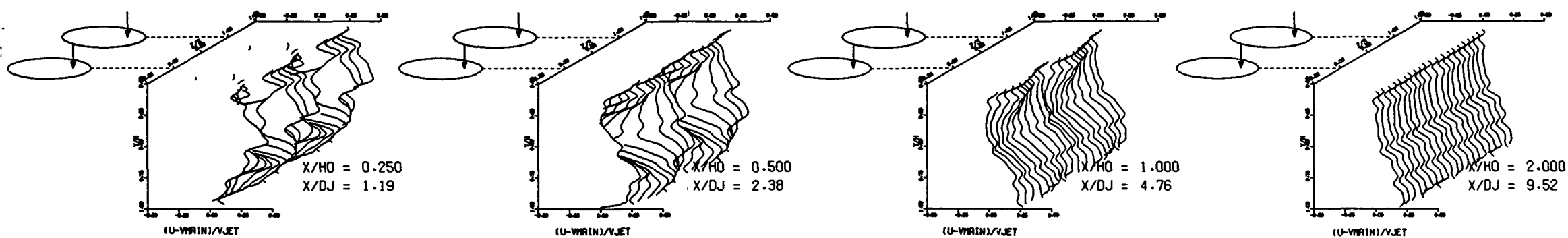


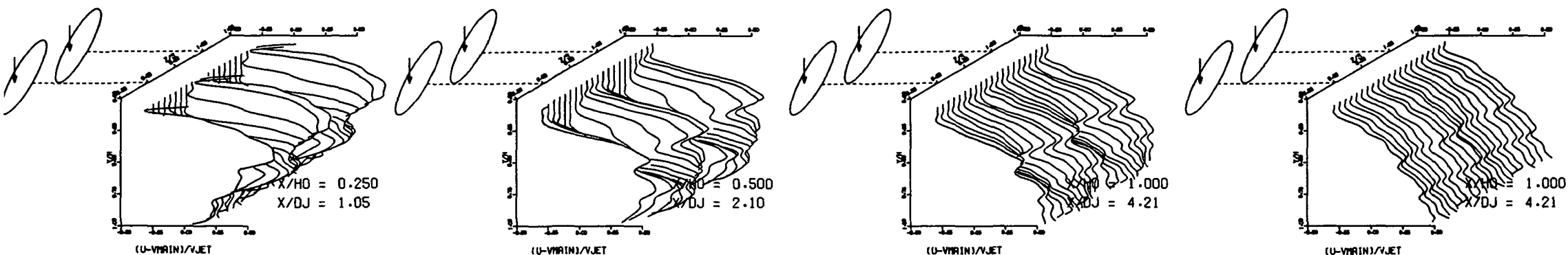
Figure 163. Measured Velocity
Distributions for Test No. 2
of DJM Phase III Testing.

ORIGINAL PAGE IS
OF POOR QUALITY

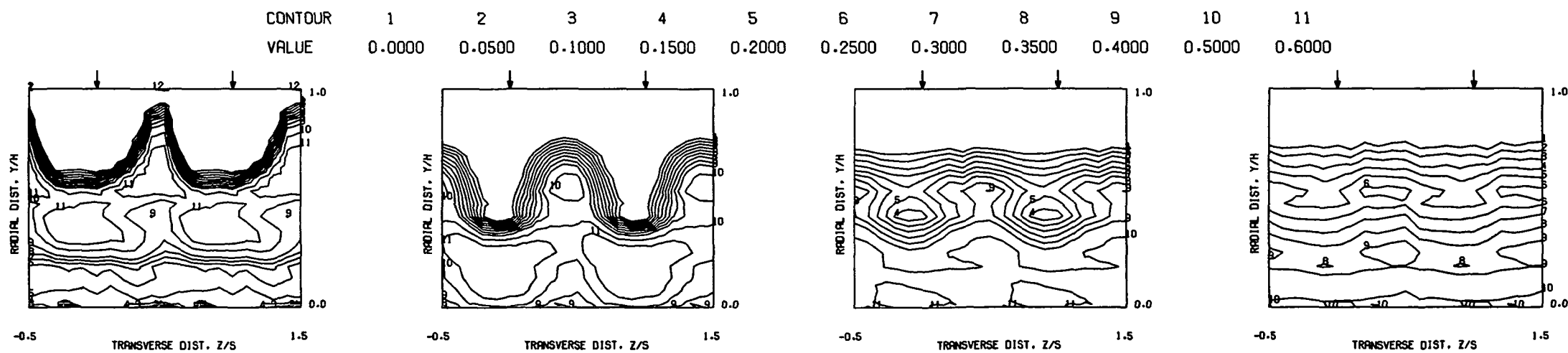
FOLDOUT FRAME

2 FOLDOUT FRAME

S = 0.0508 METERS S/DJ = 2.104 HO/DJ = 4.207 VMAIN = 17.2 M/SEC VJET = 60.3 M/SEC TMAIN = 675.0 K TJET = 316.5 K THEB = 0.4026 BLORAT= 7.592 DENRATIO= 2.168 TRATIO= 0.469



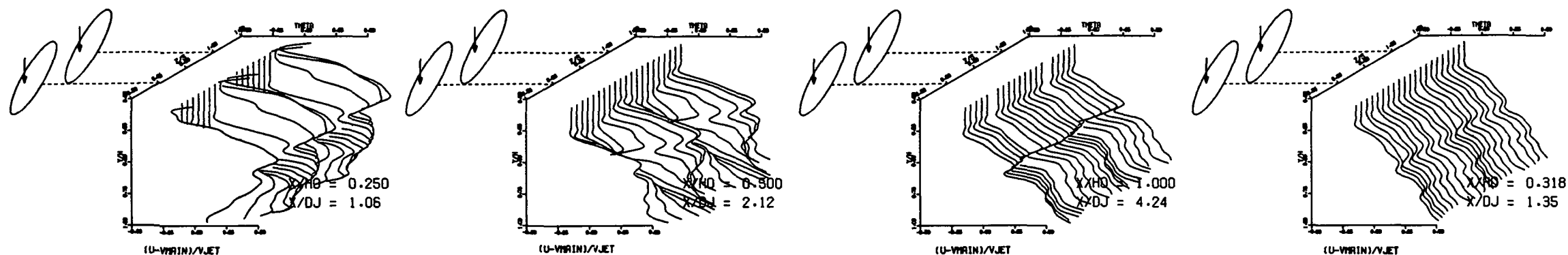
MEASURED VELOCITY PROFILES FOR TEST NO 3, TM=CONST, BLUFF SLOTS , J = 26.59 , S/D = 2.00 , H/D = 4.00



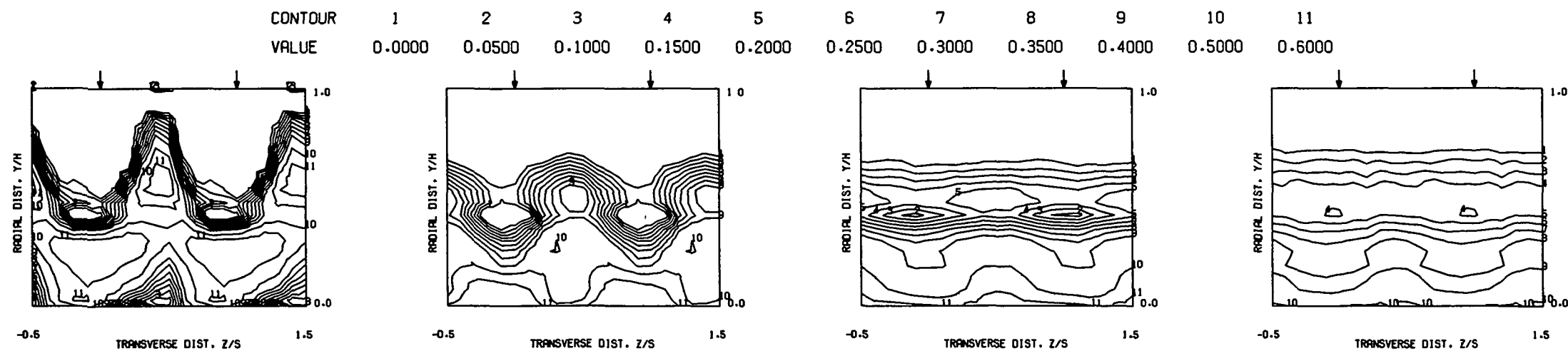
MEASURED VELOCITY CONTOURS FOR TEST NO 3, BLUFF SLOT, J=26.59, S/D=2.00, H/D=4.00

Figure 164. Measured Velocity Distributions for Test No. 3 of DJM Phase III Testing.

S = 0.0508 METERS S/DJ = 2.118 H/DJ = 4.237 VMAIN = 12.6 M/SEC VJET = 88.8 M/SEC TMAIN = 655.3 K TJET = 315.0 K THEB = 0.5705 BLORAT= 15.183 DENRATIO= 2.161 TRATIO= 0.481



MEASURED VELOCITY PROFILES FOR TEST NO 4, TM=CONST, BLUFF SLOTS , J = 106.69 , S/D = 2.00 , H/D = 4.00



MEASURED VELOCITY CONTOURS FOR TEST NO 4, BLUFF SLOT, J=106.5, S/D=2.00, H/D=4.00

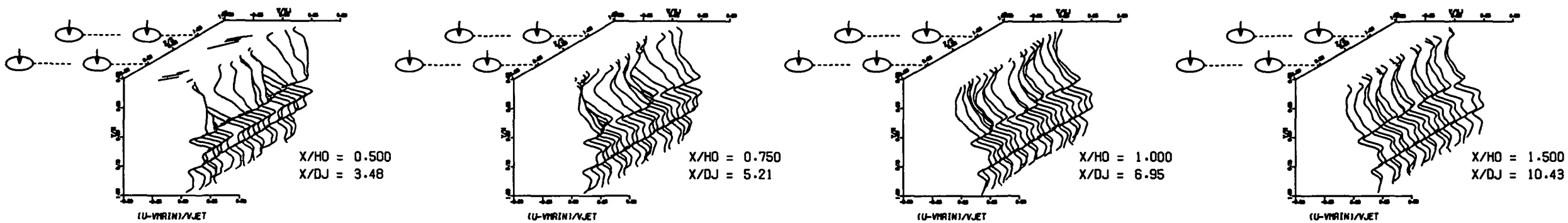
Figure 165. Measured Velocity Distributions for Test No. 4 of DJM Phase III Testing.

FOLDOUT FRAME

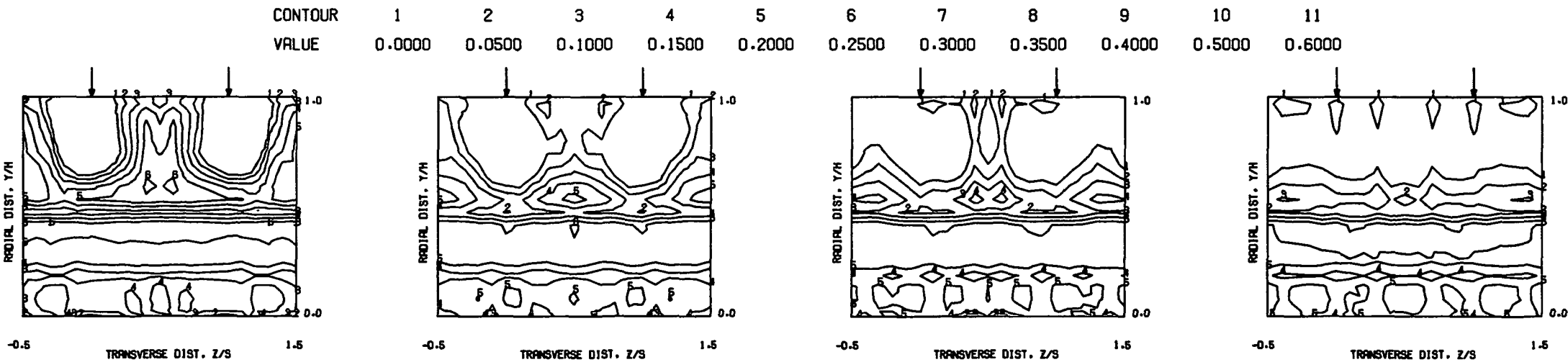
FOLDOUT FRAME

ORIGINAL PAGE IS
OF POOR QUALITY

S = 0.0508 METERS S/DJ = 3.476 HD/DJ = 6.952 VMAIN = 5.4 M/SEC VJET = 9.4 M/SEC TMAIN = 383.5 K TJET = 177.3 K THEB = 0.1978 BLORAT= 3.800 DENRATIO= 2.172 TRATIO=0.462



MEASURED VELOCITY PROFILES FOR TEST NO 5, TM=CONST, PLATE M-3 (INL) , J = 6.65 , S/D = 2.83 , H/D = 5.66



MEASURED VELOCITY PROFILES FOR TEST NO 5, TM=CONST, PLATE M-3 (INL) , J = 6.65 , S/D = 2.83 , H/D = 5.66

Figure 166. Measured Velocity
Distributions for Test No. 5
of DJM Phase III Testing.

FOLDOUT FRAME

FOLDOUT FRAME

S = 0.0508 METERS S/DJ = 3.510 H0/DJ = 7.020 VMAIN = 5.2 M/SEC VJET = 18.1 M/SEC TMAIN = 370.0 K TJET = 172.5 K THEB = 0.3268 BLORAT = 7.574 DENRATIO = 2.184 TRATIO = 0.466

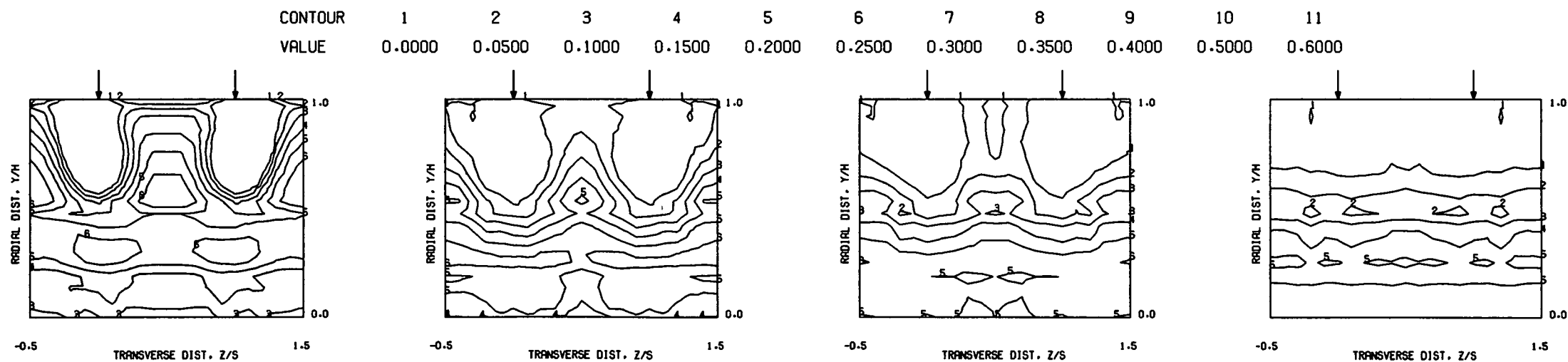
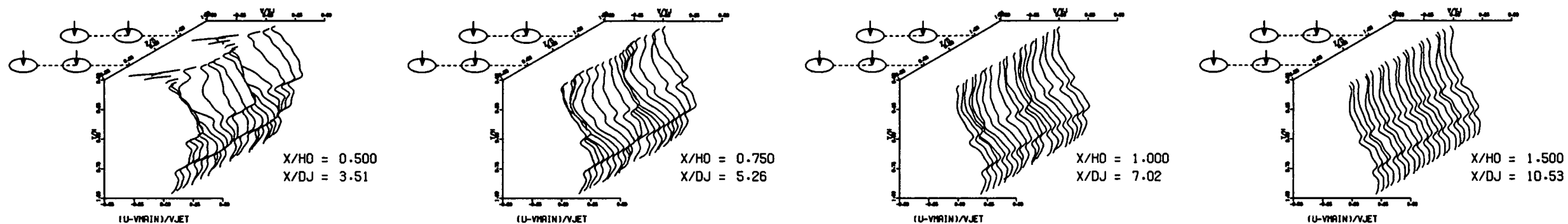


Figure 167. Measured Velocity Distributions for Test No. 6 of DJM Phase III Testing.

FOLDOUT FRAME

FOLDOUT FRAME

S = 0.0508 METERS S/DJ = 3.618 H0/DJ = 7.236 VMAIN = 5.0 M/SEC VJET = 34.7 M/SEC TMAIN = 353.7 K TJET = 172.0 K THEB = 0.4780 BLORAT= 15.307 DENRATIO= 2.186 TRATIO= 0.486

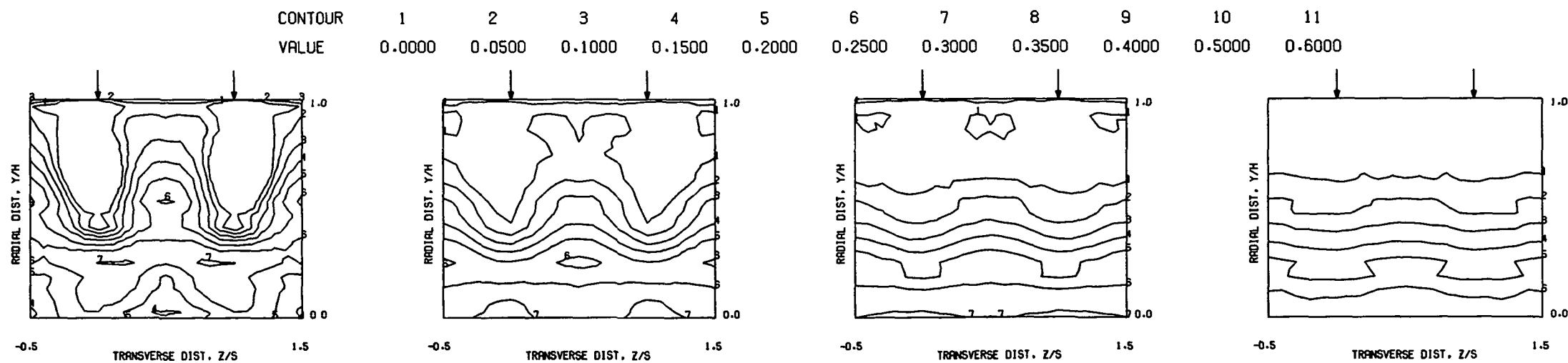
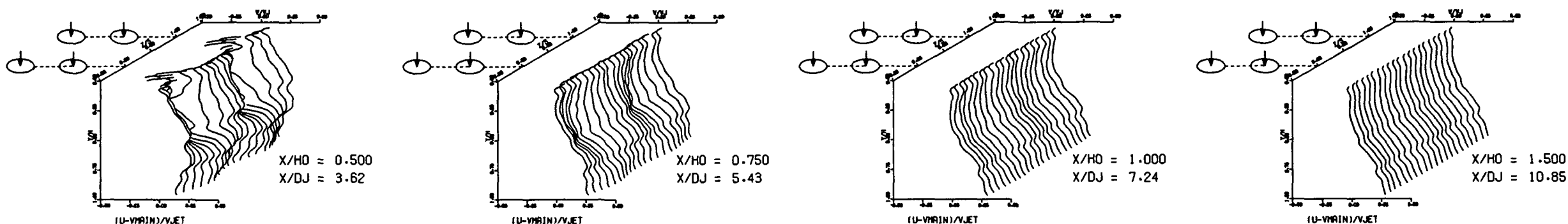


Figure 168. Measured Velocity Distributions for Test No. 7 of DJM Phase III Testing.

FOLDOUT FRAME

2 FOLDOUT FRAME

S = 0.1016 METERS S/DJ = 4.716 HO/DJ = 4.716 VMAIN = 5.3 M/SEC VJET = 9.3 M/SEC TMAIN = 378.9 K TJET = 174.5 K THEB = 0.2151 BLORAT= 3.817 DENRATIO= 2.183 TRATIO=0.460

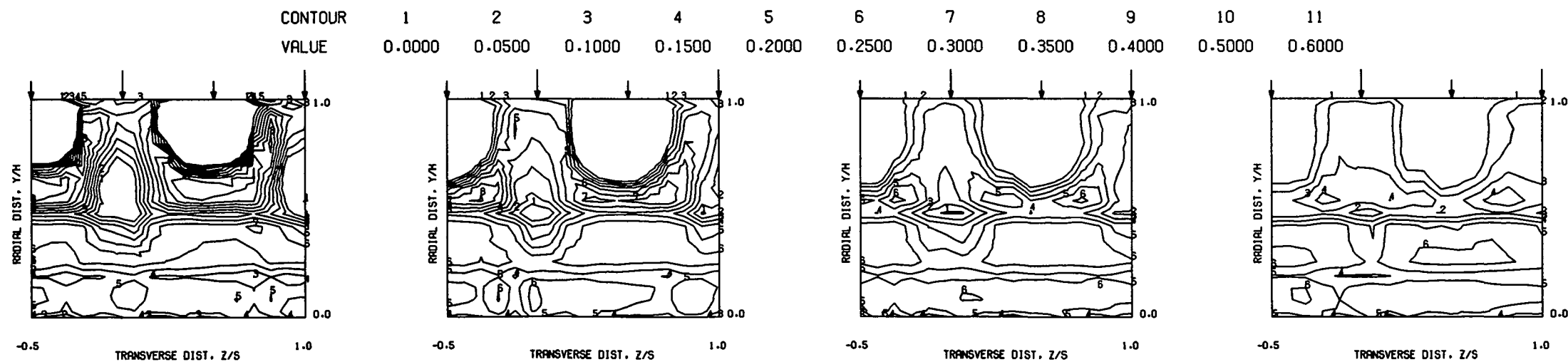
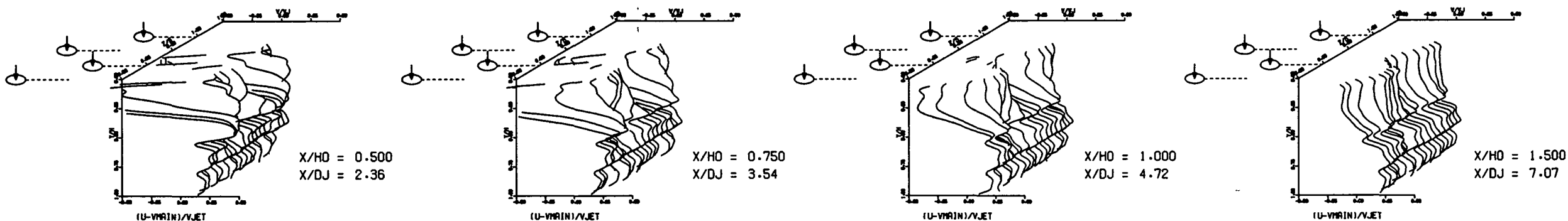


Figure 169. Measured Velocity Distributions for Test No. 8 of DJM Phase III Testing.

FOLDOUT FRAME

2 FOLDOUT FRAME

S = 0.1016 METERS S/DJ = 4.964 HO/DJ = 4.964 VMAIN = 5.3 M/SEC VJET = 18.5 M/SEC TMAIN = 373.1 K TJET = 174.2 K THEB = 0.3314 BLORAT= 7.650 DENRATIO= 2.185 TRATIO=0.467

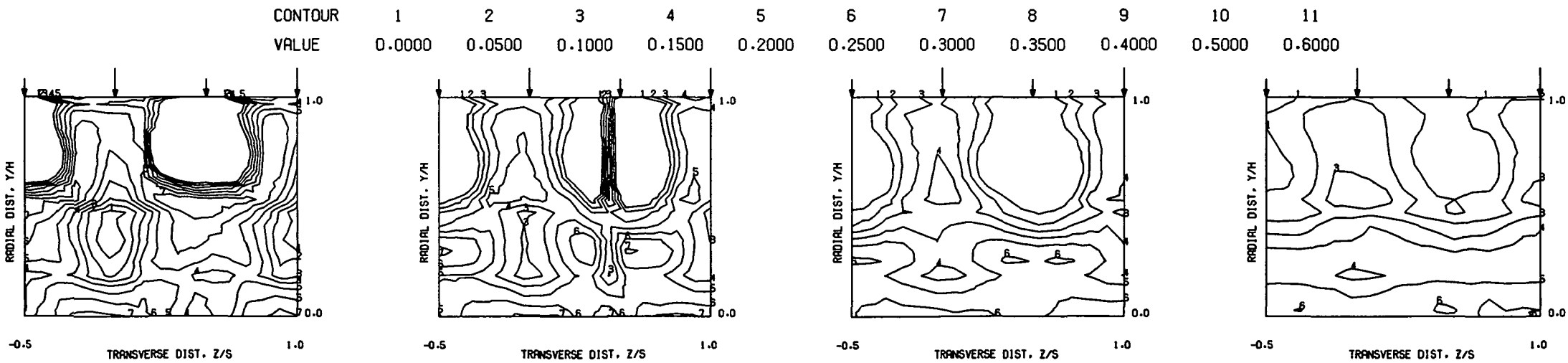
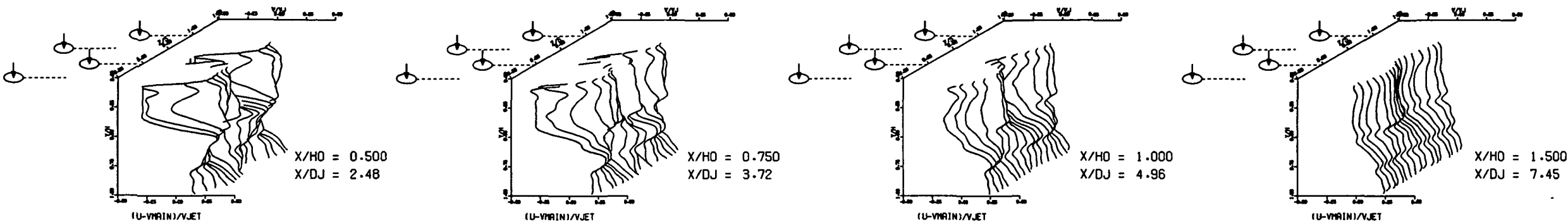


Figure 170. Measured Velocity Distributions for Test No. 9 of DJM Phase III Testing.

FOLDOUT FRAME

2 FOLDOUT FRAME

ORIGINAL PAGE IS
OF POOR QUALITY

S = 0.0508 METERS S/DJ = 3.280 H0/DJ = 6.560 VMRAIN = 5.4 M/SEC VJET = 9.5 M/SEC TMAIN = 386.4 K TJET = 178.4 K THEB = 0.2194 BLORAT = 3.825 DENRATIO = 2.178 TRATIO = 0.462

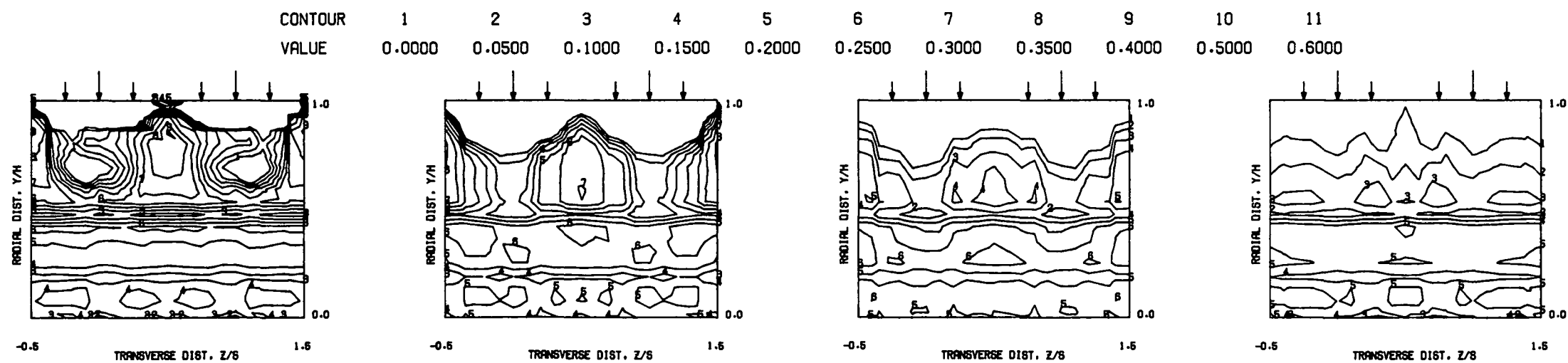
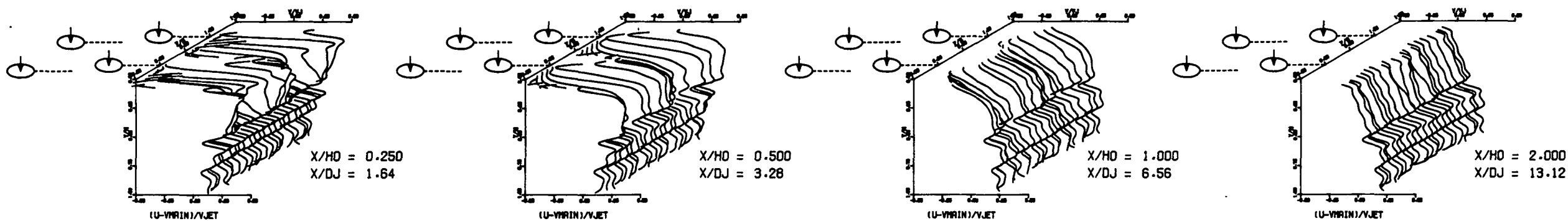


Figure 171. Measured Velocity Distributions for Test No. 10 of DJM Phase III Testing.

FOLDOUT FRAME

2 FOLDOUT FRAME

S = 0.0508 METERS S/DJ = 3.417 HO/DJ = 6.835 VMAIN = 5.3 M/SEC VJET = 18.4 M/SEC TMAIN = 376.2 K TJET = 174.2 K THEB = 0.3422 BLORAT= 7.683 DENRATIO= 2.203 TRATIO=0.463

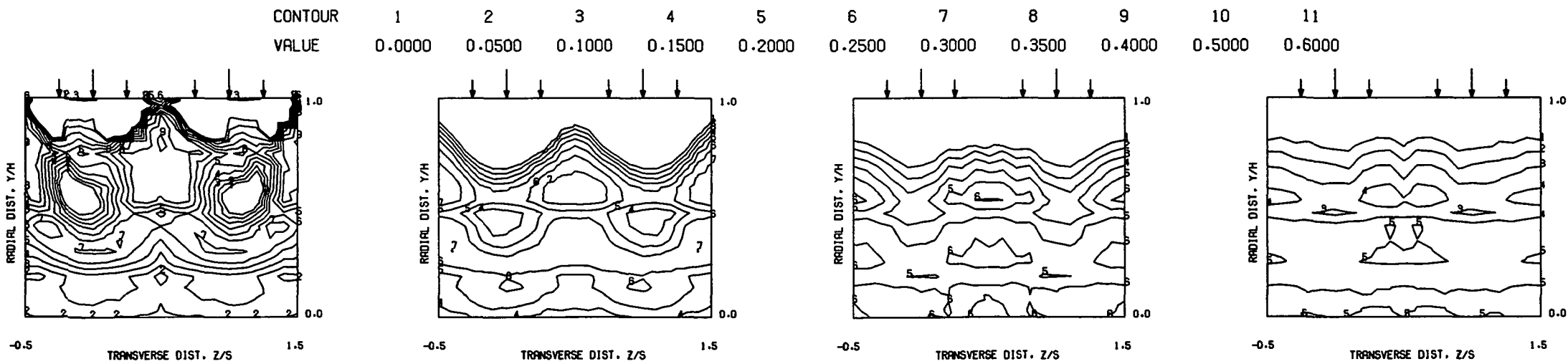
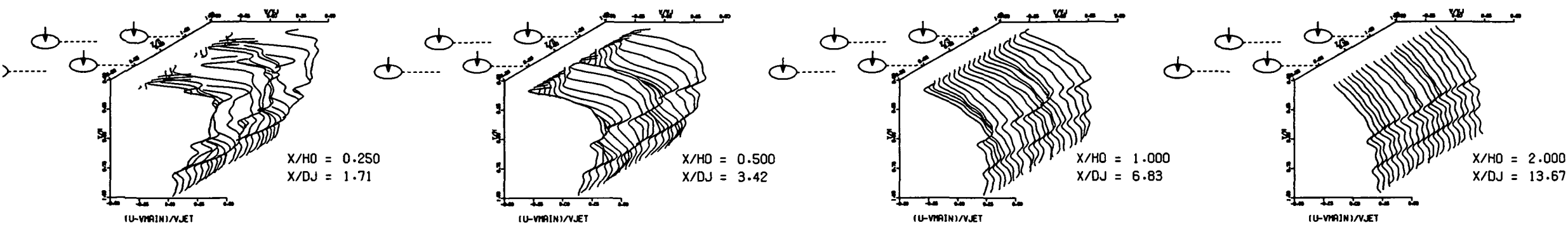


Figure 172. Measured Velocity Distributions for Test No. 11 of DJM Phase III Testing.

2 FOLDOUT FRAME

FOLDOUT FRAME

S = 0.0508 METERS S/DJ = 3.507 H0/DJ = 7.013 VMAIN = 5.0 M/SEC VJET = 34.5 M/SEC TMAIN = 358.3 K TJET = 174.3 K THEB = 0.5004 BLORAT= 15.364 DENRATIO= 2.221 TRATIO=0.481

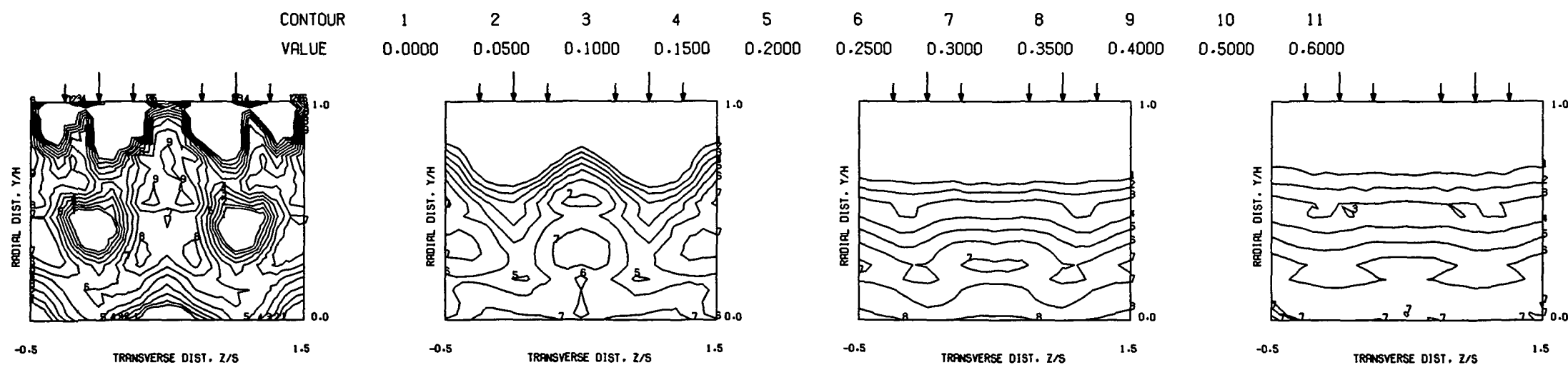
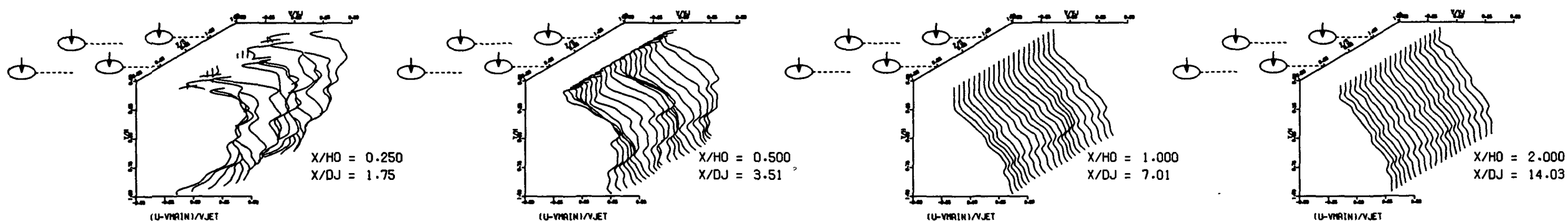


Figure 173. Measured Velocity Distributions for Test No. 12 of DJM Phase III Testing.

FOLDOUT FRAME

2 FOLDOUT FRAME

S = 0.0508 METERS S/DJ = 3.424 H0/DJ = 6.848 VMAIN = 17.0 M/SEC VJET = 58.5 M/SEC TMAIN = 672.0 K TJET = 310.1 K THEB = 0.2820 BLORAT = 7.605 DENRATIO = 2.208 TRATIO = 0.461

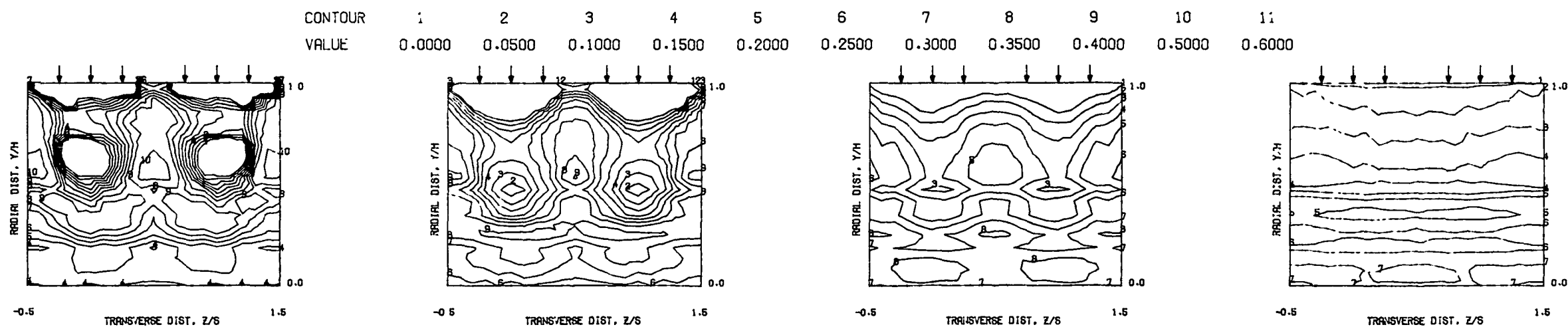
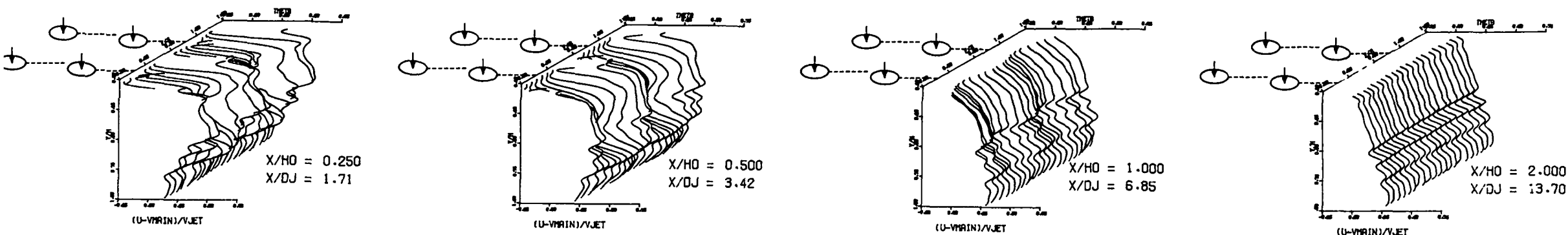
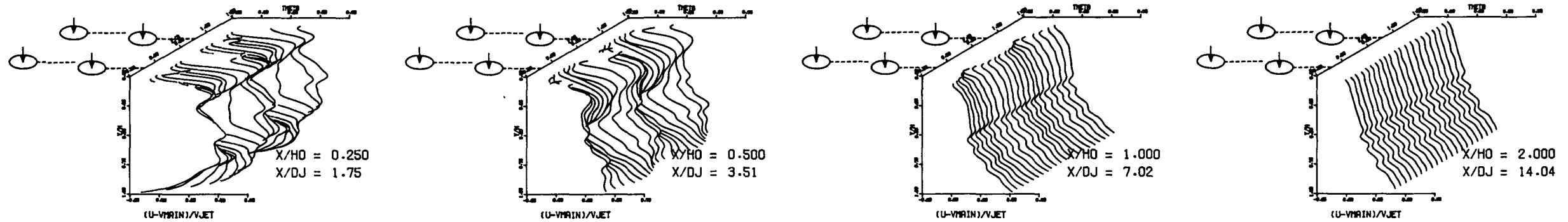


Figure 174. Measured Velocity Distributions for Test No. 13 of DJM Phase III Testing.

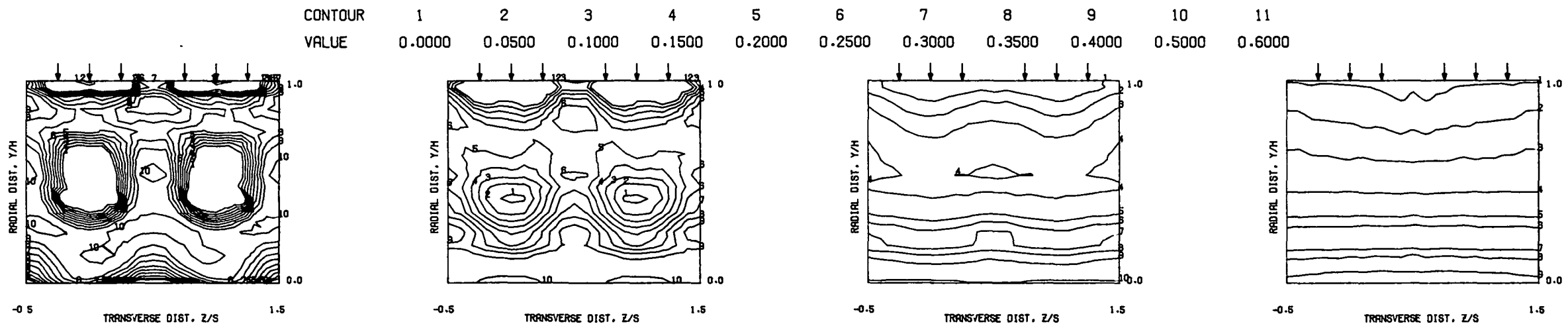
ORIGINAL PAGE IS
OF POOR QUALITY

ORIGINAL PAGE IS
OF POOR QUALITY

S = 0.0508 METERS S/DJ = 3.510 HO/DJ = 7.020 VMAIN = 16.8 M/SEC VJET = 113.0 M/SEC TMAIN = 666.3 K TJET = 304.5 K THEB = 0.3938 BLORAT = 15.834 DENRATIO = 2.353 TRATIO = 0.457



MEASURED VELOCITY PROFILES FOR TEST NO 14, TEST SECTION I, PLATE M5 , J = 106.54 , S/D = 2.83 , H/D = 5.66



MEASURED VELOCITY CONTOURS FOR TEST NO 14, PLATE M5, J1=106, J2=6, S/D=2.83, H/D=5.66

Figure 175. Measured Velocity Distributions for Test No. 14 of DJM Phase III Testing.

FOLDOUT FRAME

2 FOLDOUT FRAME

FOLDOUT FRAME

2 FOLDOUT FRAME

S = 0.0508 METERS S/DJ = 3.510 H0/DJ = 7.020 VMAIN = 16.7 M/SEC VJET = 112.9 M/SEC TMAIN = 660.0 K TJET = 305.8 K THEB = 0.4318 BLORAT= 15.708 DENRATIO= 2.321 TRATIO=0.463

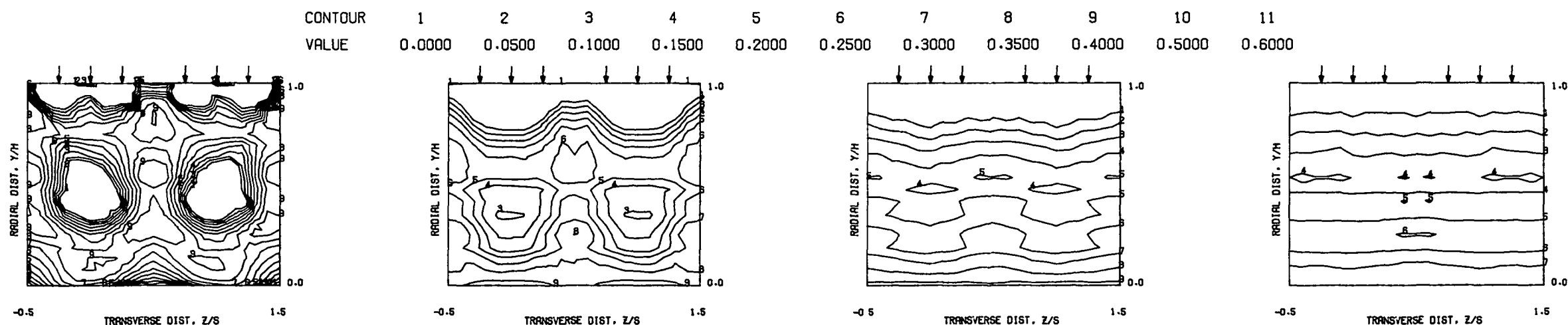
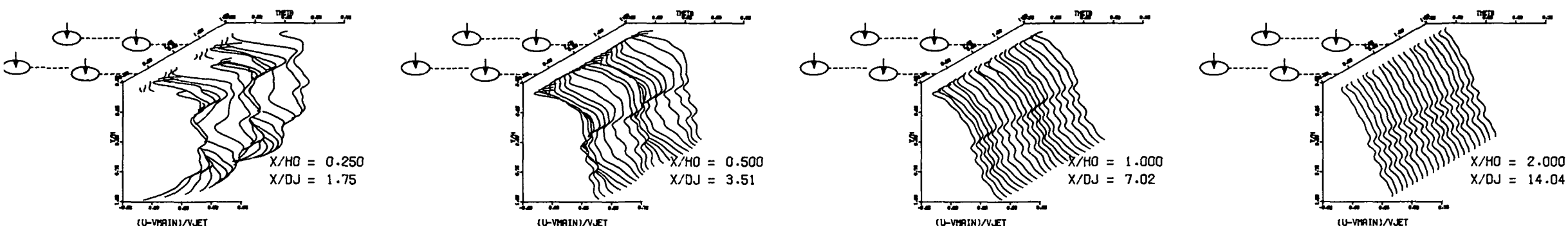


Figure 176. Measured Velocity Distributions for Test No. 15 of DJM Phase III Testing.

ORIGINAL PAGE IS
OF POOR QUALITY

ORIGINAL PAGE IS
OF POOR QUALITY

S = 0.0254 METERS S/DJ = 2.416 HO/DJ = 9.666 VMAIN = 5.1 M/SEC VJET = 34.9 M/SEC TMAIN = 364.8 K TJET = 170.4 K THEB = 0.3939 BLORAT= 15.602 DENRATIO= 2.280 TRATIO=0.467

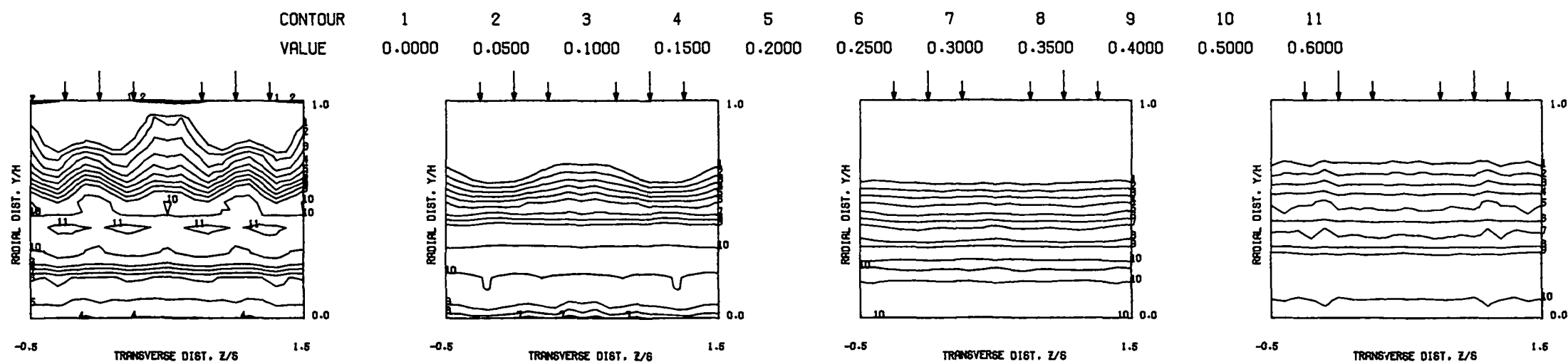
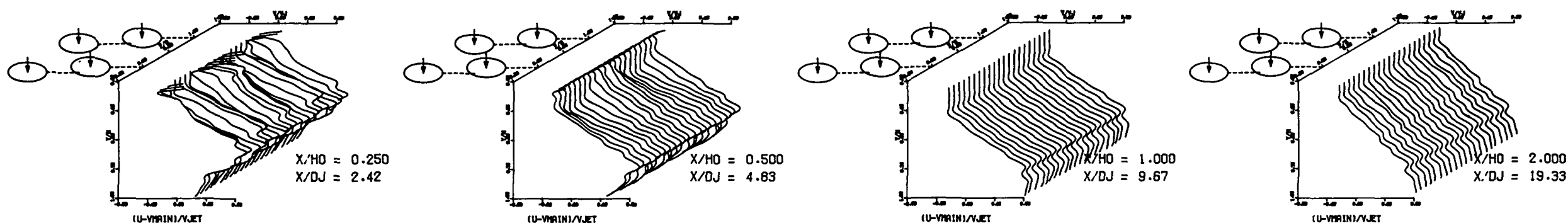


Figure 177. Measured Velocity Distributions for Test No. 16 of DJM Phase III Testing.

FOLDOUT FRAME

2 FOLDOUT FRAME

S = 0.0254 METERS S/DJ = 2.416 HO/DJ = 9.666 VMIN = 5.2 M/SEC VJET = 35.0 M/SEC TMAIN = 368.8 K TJET = 169.5 K THEB = 0.4409 BLORAT= 15.745 DENRATIO= 2.321 TRATIO=0.460

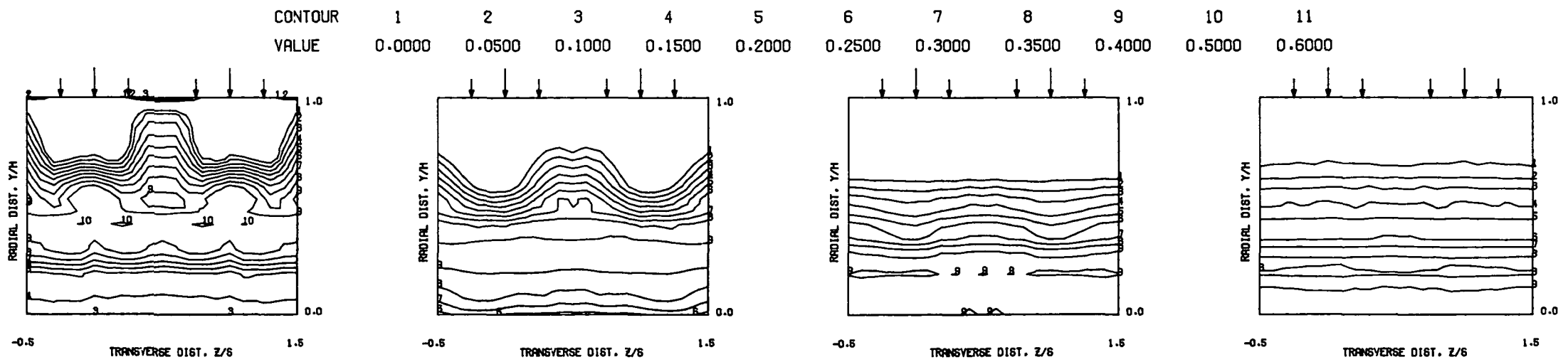
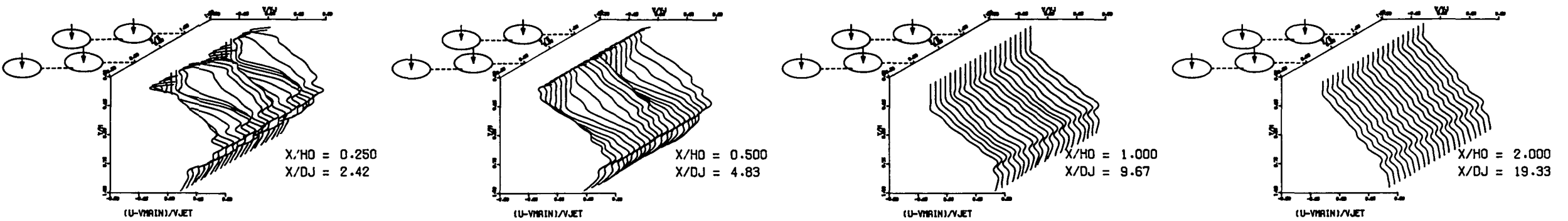
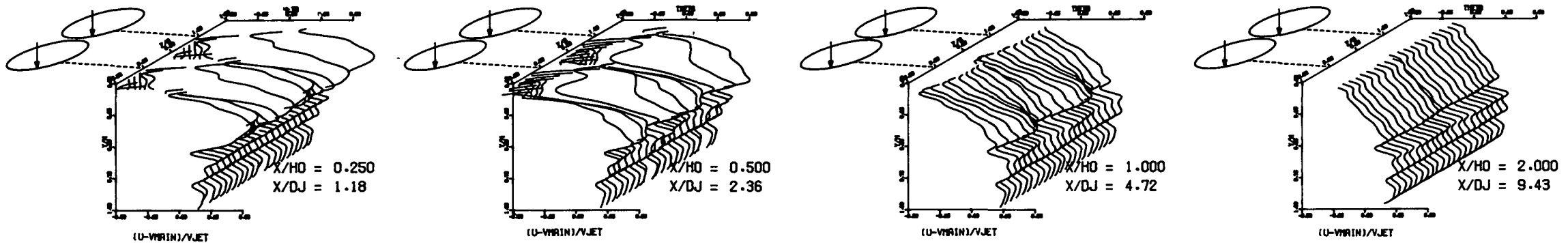


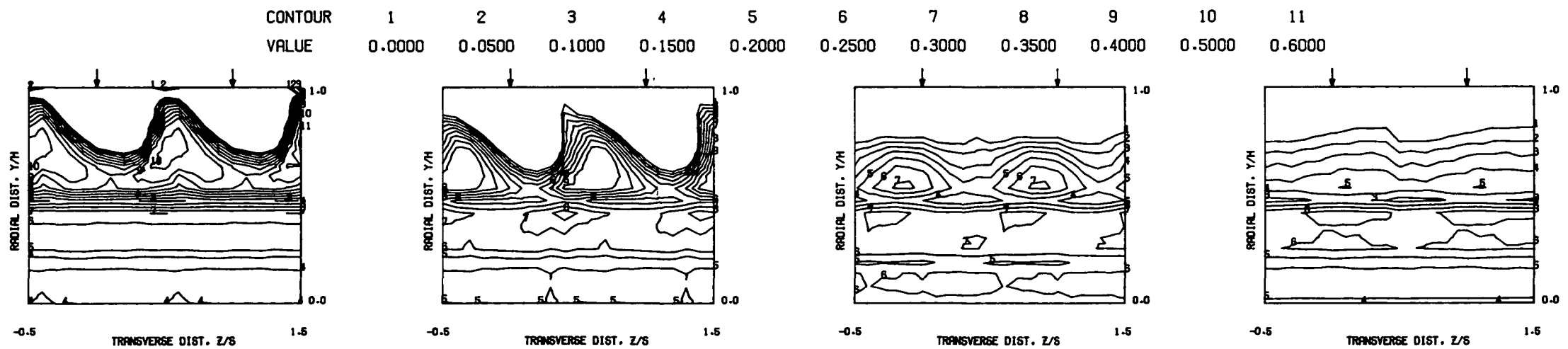
Figure 178. Measured Velocity Distributions for Test No. 17 of DJM Phase III Testing.

ORIGINAL PAGE IS
OF POOR QUALITY

S = 0.0508 METERS S/DJ = 2.358 HD/DJ = 4.716 VMAIN = 17.4 M/SEC VJET = 30.4 M/SEC TMAIN = 684.2 K TJET = 316.3 K THEB = 0.2116 BLORAT = 3.800 DENRATIO = 2.173 TRATIO = 0.462



MEASURED VELOCITY PROFILES FOR TEST NO 18. TM=CONST. 45 DEGREE SLOTS , J = 6.64 , S/D = 2.00 , H/D = 4.00



MEASURED VELOCITY CONTOURS FOR TEST NO 18, PLATE M-7. J=6.64, S/D=2.00, H/D=4.00

Figure 179. Measured Velocity
Distributions for Test No. 18
of DJM Phase III Testing.

FOLDOUT FRAME

FOLDOUT FRAME

S = 0.0508 METERS S/DJ = 2.458 H0/DJ = 4.916 VMAIN = 17.2 M SEC VJET = 60.5 M/SEC TMAIN = 675.5 K TJET = 314.5 K THEB = 0.3336 BLORAT = 7.702 DENRATIO = 2.186 TRATIO = 0.466

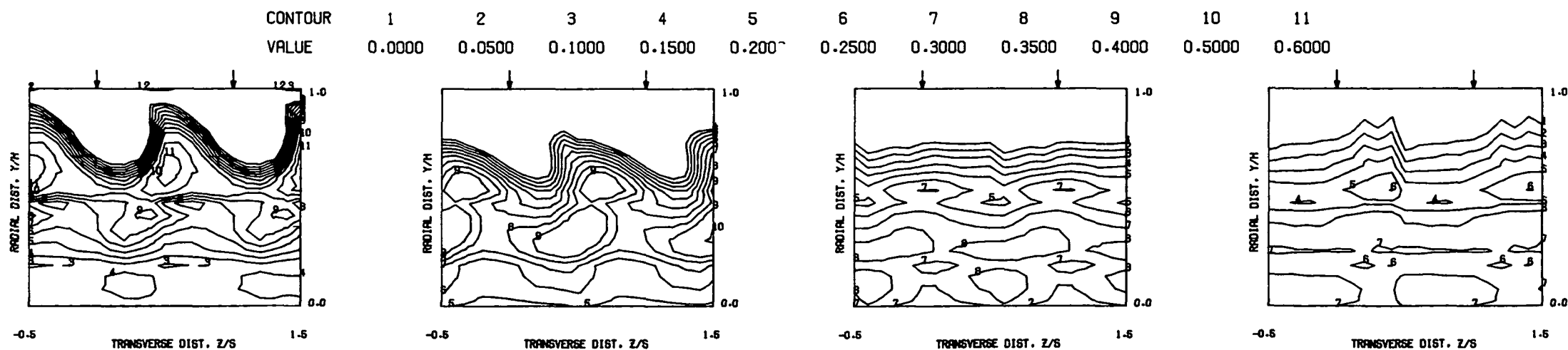
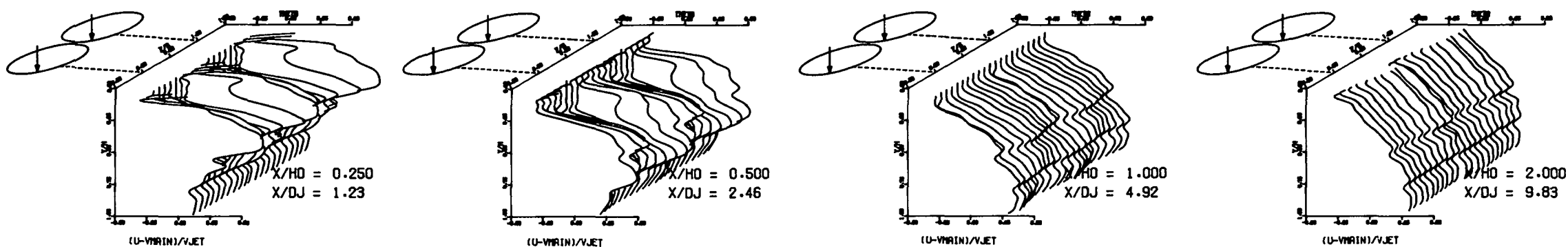
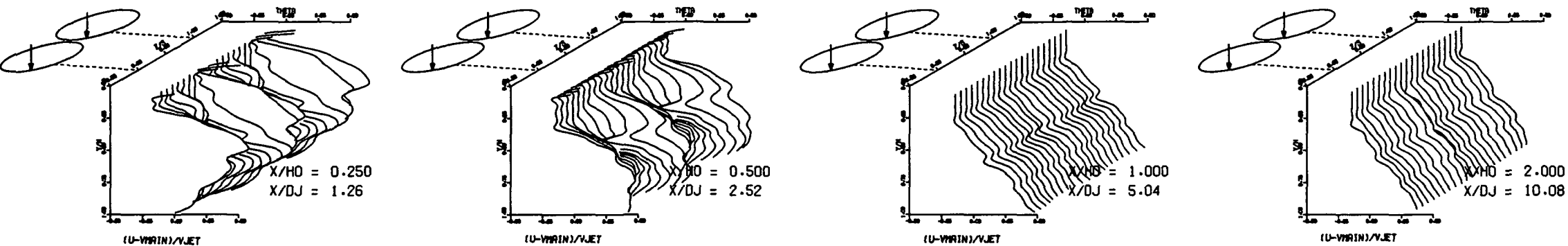


Figure 180. Measured Velocity Distributions for Test No. 19 of DJM Phase III Testing.

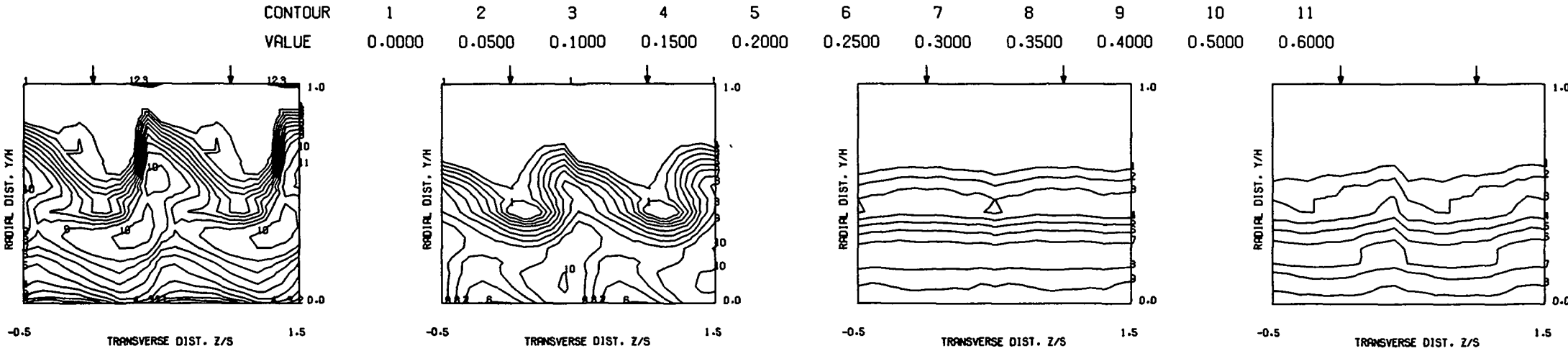
ORIGINAL PAGE IS
OF POOR QUALITY

ORIGINAL PAGE IS
OF POOR QUALITY

S = 0.0508 METERS S/DJ = 2.519 HO/DJ = 5.039 VMAIN = 16.2 M/SEC VJET = 112.0 M/SEC TMAIN = 637.4 K TJET = 307.8 K THEB = 0.4865 BLORAT= 15.314 DENRATIO= 2.209 TRATIO=0.483



MEASURED VELOCITY PROFILES FOR TEST NO 20, TM=CONST, 45 DEGREE SLOTS , J = 106.18 , S/D = 2.00 , H/D = 4.00



MEASURED VELOCITY CONTOURS FOR TEST NO 20, PLATE M-7, J=106.2, S/D=2.00, H/D=4.00

Figure 181. Measured Velocity
Distributions for Test No. 20
of DJM Phase III Testing.

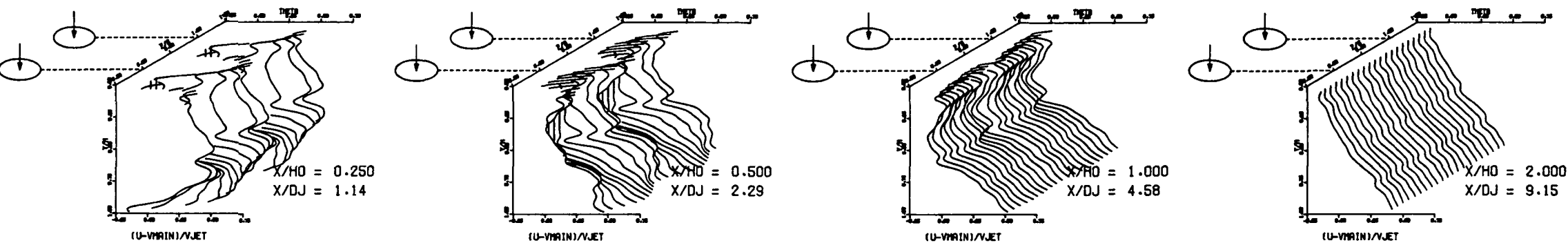
FOLDOUT FRAME

2 FOLDOUT FRAME

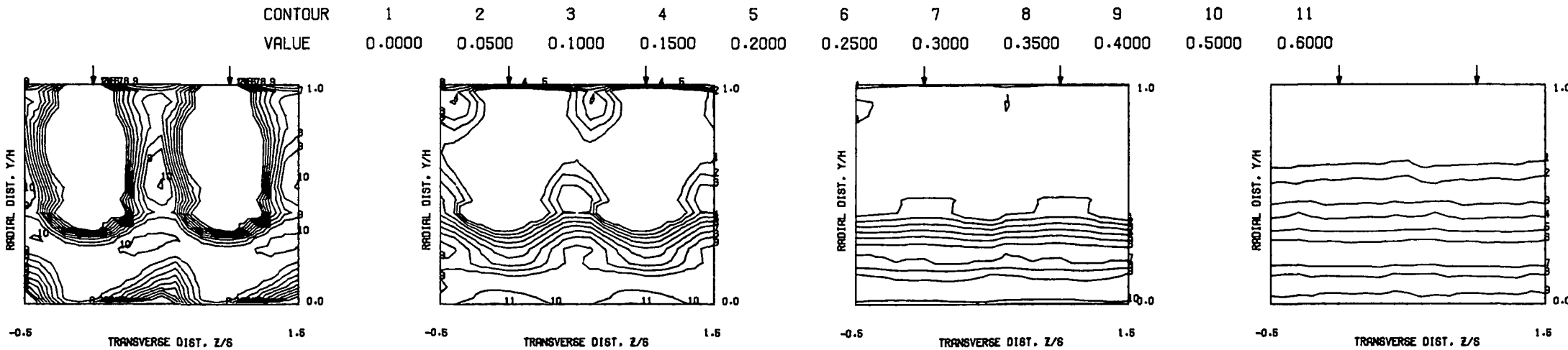
ORIGINAL PAGE IS
OF POOR QUALITY

ORIGINAL PAGE IS
OF POOR QUALITY

$S = 0.0508$ METERS $S/DJ = 2.288$ $H_0/DJ = 4.576$ $V_{MAIN} = 15.3$ M/SEC $V_{JET} = 104.3$ M/SEC $T_{MAIN} = 629.1$ K $T_{JET} = 307.0$ K $T_{HEB} = 0.5322$ $BLORAT = 15.170$ $DENRATIO = 2.230$ $TRATIO = 0.488$



MEASURED VELOCITY PROFILES FOR TEST NO 21, TEST SECTION I, $T_M = \text{CONST}$, $J = 103.19$, $S/D = 2.00$, $H/D = 4.00$



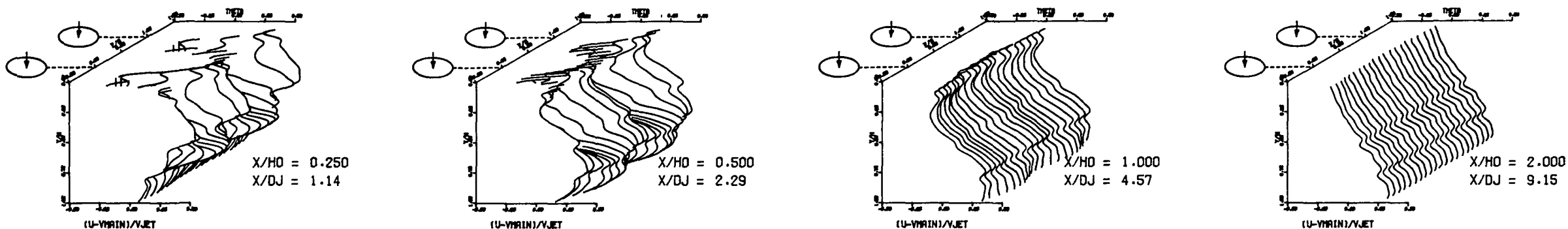
MEASURED VELOCITY CONTOURS FOR TEST NO 21, $T_M = \text{CONST}$, $J=103.2$, $S/D=2.00$, $H/D=4.00$

Figure 182. Measured Velocity
Distributions for Test No. 21
of DJM Phase III Testing.

FOLDOUT FRAME

FOLDOUT FRAME

S = 0.0508 METERS S/DJ = 2.286 H0/DJ = 4.573 VMAIN = 16.9 M/SEC VJET = 58.6 M/SEC TMAIN = 668.5 K TJET = 312.7 K THEB = 0.3626 BLORAT= 7.572 DENRATIO= 2.185 TRATIO=0.468



CONTOUR VALUE 1 0.0000 2 0.0500 3 0.1000 4 0.1500 5 0.2000 6 0.2500 7 0.3000 8 0.3500 9 0.4000 10 0.5000 11 0.6000

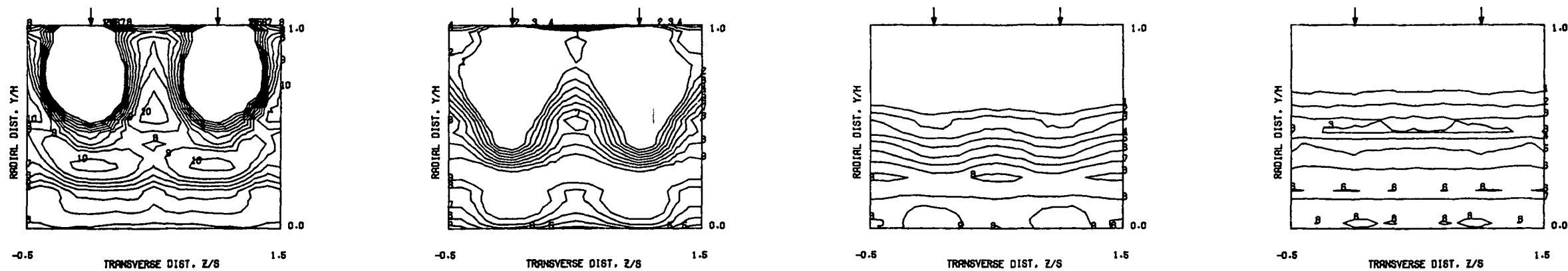


Figure 183. Measured Velocity Distributions for Test No. 22 of DJM Phase III Testing.

FOLDOUT FRAME

2 FOLDOUT FRAME

ORIGINAL PAGE IS
OF POOR QUALITY

TABLE 3 CONFIGURATIONS AND FLOW CONDITIONS FOR PHASE 1, SERIES 1 TESTS.

Test No	Test Section	Orifice Dia (CM)	S/D	H ₀ /D	Mainstream			Dilution Jet				Momentum Flux Ratio (J)	Density Ratio (Denratio)	Equilibrium Theta (Theb)	Regions of Measurement	
					Mass Flow Rate (KG/S)	Temp (Tmain) (K)	Velocity (Vmain) (M/S)	Mass Flow Rate (KG/S)	Temp (Tjet) (K)	Velocity (Vjet) (M/S)	CDJ				Axial Direction (X/H ₀)	Transverse Direction (Z/S)
1	I	2.54	2	4	0.2739	650	15.8	0.05843	308	26.0	0.670	4.98	2.11	0.176	0.5 - 2.0	0.0 to 1.0
2	I	2.54	2	4	0.2856	651	16.3	0.1059	308	52.0	0.600	18.59	2.13	0.270	0.5 - 2.0	0.0 to 1.0
3	I	2.54	4	4	0.2657	649	15.2	0.03196	307	25.9	0.730	5.31	2.12	0.107	0.5 - 2.0	-0.5 to +0.5
4	I	2.54	4	4	0.2563	651	14.9	0.06072	304	52.2	0.675	23.51	2.17	0.191	0.5 - 2.0	-0.5 to +0.5
5	I	1.27	2	8	0.2604	649	15.0	0.05285	308	51.9	0.600	22.32	2.13	0.169	0.5 - 2.0	0.0 to 1.0
6	I	1.27	2	8	0.2655	650	15.1	0.1148	299	103.6	0.605	92.63	2.29	0.302	0.5 - 2.0	0.0 to 1.0
7	I	1.27	4	8	0.2630	651	15.2	0.0308	302	52.8	0.610	28.37	2.19	0.105	0.5 - 2.0	-0.5 to +0.5
8	I	1.27	4	8	0.2623	649	15.1	0.05791	299	104.1	0.605	96.00	2.30	0.181	0.5 - 2.0	-0.5 to +0.5
9	I	2.54	2	4	0.6207	306	15.4	0.1390	511	109.4	0.610	22.69	0.62	0.183	0.5 - 2.0	0.0 to 1.0
10	I	2.54	4	4	0.6327	293	15.2	0.07215	408	103.3	0.600	22.63	0.66	0.102	0.5 - 2.0	-0.5 to +0.5
11	I	1.27	2	8	0.6393	290	15.2	0.07298	445	102.2	0.600	22.33	0.67	0.102	0.5 - 2.0	-0.5 to +0.5
12	I	1.27	4	8	0.6311	293	15.3	0.04147	457	97.6	0.650	22.68	0.65	0.062	0.5 - 2.0	0.0 to 1.0

TABLE 4 CONFIGURATIONS AND FLOW CONDITIONS FOR PHASE 1, SERIES 2 TESTS

Test No.	Test Section	Orifice Dia (CM)	S/D	H ₀ /D	Mainstream			Dilution Jet				Momentum Flux Ratio (J)	Density Ratio (Denratio)	Equilibrium Theta (Theb)	Regions of Measurement	
					Mass Flow Rate (KG/S)	Temp (Tmain) (K)	Velocity (Vmain) (M/S)	Mass Flow Rate (KG/S)	Temp (Tjet) (K)	Velocity (Vjet) (M/S)	CDJ				Axial Direction (X/H ₀)	Transverse Direction (Z/S)
13	I	2.54	2	4	0.2815	524	16.9	0.1277	294	59.7	0.610	31.79	1.81	0.312	0.5 - 2.0	0.0 to 1.0
14	I	2.54	4	4	0.2572	672	15.4	0.03311	305	28.4	0.682	6.70	2.21	0.114	0.5 - 2.0	-0.5 to +0.5
15	I	1.27	2	8	0.2777	616	15.5	0.1206	297	109.3	0.597	99.21	2.07	0.303	0.5 - 2.0	-0.5 to +0.5
16	I	1.27	4	8	0.3134	567	18.1	0.03465	311	63.0	0.670	24.38	1.86	0.100	0.5 - 2.0	0.0 to 1.0
17	I	2.54	2	4	0.3067	538	16.5	0.1347	303	57.9	0.675	24.45	1.80	0.305	0.5 - 2.0	0.0 to 1.0
18	I	1.27	4	8	0.3394	545	18.2	0.04052	317	72.2	0.675	29.55	1.76	0.107	0.5 - 2.0	-0.5 to +0.5

FOLDOUT FRAME

2 FOLDOUT FRAME

ORIGINAL PAGE IS
OF POOR QUALITY

TABLE 5 CONFIGURATIONS AND FLOW CONDITIONS FOR PHASE I, SERIES 3 TESTS.

Test No.	Test Section	Orifice Dia (CM)	S/D	H ₀ /D	Mainstream			Dilution Jet				Momentum Flux Ratio (J)	Density Ratio (Denratio)	Equilibrium Theta (Theb)	Regions of Measurement	
					Mass Flow Rate (KG/S)	Temp (Tmain) (K)	Velocity (Vmain) (M/S)	Mass Flow Rate (KG/S)	Temp (Tjet) (K)	Velocity (Vjet) (M/S)	C _{DJ}				Axial Direction (X/H ₀)	Transverse Direction (Z/S)
19	II	1.27	4	8	0.2537	656	15.9	0.02994	330	58.1	0.650	27.07	2.02	0.106	0.25 - 2.0	0.0 to 1.0
20	II	1.27	4	8	0.2543	645	15.5	0.05892	314	106.4	0.630	102.5	2.19	0.188	0.25 - 2.0	0.0 to 1.0
21	II	2.54	2	4	0.2531	654	15.8	0.06222	308	28.1	0.660	6.76	2.13	0.197	0.50 - 2.0	0.0 to 1.0
22	II	2.54	2	4	0.2534	654	15.8	0.1125	304	54.5	0.600	26.07	2.18	0.307	0.50 - 2.0	0.0 to 1.0
23	IV	1.27	4	8	0.2775	646	17.0	0.02988	312	53.8	0.660	21.05	2.10	0.097	0.25 - 1.0	-0.5 to +0.5
24	IV	1.27	4	8	0.2772	643	16.9	0.06006	311	105.1	0.640	85.81	2.07	0.178	0.25 - 1.0	-0.5 to +0.5
25	IV	2.54	2	4	0.2462	643	15.1	0.05513	322	27.7	0.620	6.73	2.00	0.183	0.50 - 1.0	0.0 to 1.0
26	IV	2.54	2	4	0.2452	641	14.9	0.1045	330	55.1	0.600	26.36	1.96	0.299	0.50 - 1.0	0.0 to 1.0
27	V	1.27	4	8	0.2619	646	16.1	0.03122	320	58.7	0.650	27.18	2.05	0.107	0.25 - 1.0	0.0 to 1.0
28	V	1.27	4	8	0.2609	645	16.0	0.06071	319	112.5	0.625	106.7	2.02	0.189	0.25 - 1.0	0.0 to 1.0
29	V	2.54	2	4	0.2560	645	15.7	0.06334	314	29.1	0.660	7.07	2.06	0.198	0.50 - 1.0	-0.5 to +0.5
30	V	2.54	2	4	0.2542	646	15.6	0.1168	314	56.4	0.620	27.31	2.09	0.315	0.50 - 1.0	-0.5 to +0.5
31	VI	1.27	4	8	0.2649	649	16.4	0.03162	320	58.6	0.655	26.58	2.07	0.107	0.25 - 1.0	-0.5 to +0.5
32	VI	1.27	4	8	0.2687	647	16.5	0.06250	321	116.0	0.620	107.6	2.18	0.189	0.25 - 1.0	-0.5 to +0.5
33	VI	2.54	2	4	0.2646	650	16.3	0.06489	301	29.5	0.640	7.04	2.17	0.197	0.50 - 1.0	-0.5 to +0.5
34	VI	2.54	2	4	0.2629	651	16.2	0.1205	297	55.9	0.610	26.36	2.23	0.314	0.50 - 1.0	-0.5 to +0.5

TABLE 6 CONFIGURATIONS AND FLOW CONDITIONS FOR PHASE I, SERIES 4 TESTS

Test No.	Test Section	Orifice Dia (CM)	S/D	H ₀ /D	Mainstream			Dilution Jet				Momentum Flux Ratio (J)	Density Ratio (Denratio)	Equilibrium Theta (Theb)	Regions of Measurement	
					Mass Flow Rate (KG/S)	Temp (Tmain) (K)	Velocity (Vmain) (M/S)	Mass Flow Rate (KG/S)	Temp (Tjet) (K)	Velocity (Vjet) (M/S)	C _{DJ}				Axial Direction (X/H ₀)	Transverse Direction (Z/S)
35	V	1.27	4	8	0.3566	561	18.7	0.03971	308	70.9	0.650	26.13	1.86	0.100	0.25 - 1.0	0.0 to 1.0
36	V	1.27	4	8	0.3579	568	18.8	0.07689	305	139.1	0.600	105.7	2.01	0.177	0.25 - 1.0	0.0 to 1.0
37	V	1.27	4	8	0.3532	417	16.0	0.02419	319	40.7	0.725	11.27	1.32	0.064	0.25 - 1.0	0.0 to 1.0
38	V	1.27	4	8	0.3645	416	16.0	0.04355	315	75.4	0.660	40.18	1.36	0.107	0.25 - 1.0	0.0 to 1.0

FOLDOUT FRAME

2 FOLDOUT FRAME

TABLE 7 CONFIGURATIONS AND FLOW CONDITIONS FOR PHASE II, SERIES 5 TESTS

Test No	Orifice Dia (CM)	S/D	H ₀ (D)	Mainstream			Top Dilution Jet					Bottom Dilution Jet					Equilibrium Theta (Thub)	Regions of Measurement	
				Mass Flow Rate (KG/S)	Temp (Tmain) (K)	Velocity (Vmain) (M/S)	Mass Flow Rate (KG/S)	Momentum Ratio J _T	Temp (T _{JT}) (K)	Velocity (V _{JT}) (M/S)	(C _D) _T	Mass Flow Rate (KG/S)	Momentum Ratio J _B	Temp (T _{JB}) (K)	Velocity (V _{JB}) (M/S)	(C _D) _B		Axial Direction X/H ₀	Transverse Direction (Z/S)
1	1 27	2 (INL)	8	0 2526	645 9	15 5	0 03109	6 81	310 4	28 1	0 665	0 03138	6 90	308 6	28 2	0 665	0 1983	0 25 - 2 0	-0 5 to +0 5
2	1 27	2 (INL)	8	0 2530	646 6	15 6	0 05893	24 94	306 8	53 3	0 650	0 0590	24 88	305 2	52 9	0 650	0 3179	0 25 - 2 0	-0 5 to +0 5
3	1 27	2 (INL)	8	0 2523	646 2	15 5	0 1204	101 8	303 9	104 3	0 640	0 1200	101 5	304 1	104 5	0 640	0 4879	0 25 - 2 0	-0 5 to +0 5
4	1 27	2 (STG)	8	0 2664	648 9	16 6	0 03118	6 52	325 7	30 0	0 660	0 03091	6 43	326 6	30 2	0 660	0 1890	0 25 - 2 0	-0 5 to 1 0
5	1 27	2 (STG)	8	0 2642	646 2	16 3	0 06199	25 15	314 5	56 7	0 660	0 06152	24 71	313 2	56 1	0 660	0 3186	0 25 - 2 0	-0 5 to 1 0
6	1 27	2 (STG)	8	0 2660	645 2	16 4	0 1252	99 23	313 5	110 2	0 650	0 1248	98 57	310 9	109 1	0 650	0 4845	0 25 - 2 0	-0 5 to 1 0
7	1 27	4 (INL)	8	0 2554	645 4	15 2	0 0159	7 23	326 3	30 2	0 670	0 01632	7 39	317 5	29 6	0 670	0 1121	0 25 - 2 0	-0 5 to +0 5
8	1 27	4 (INL)	8	0 2446	647 1	14 4	0 02952	25 74	322 2	54 5	0 650	0 02886	26 36	325 0	54 6	0 650	0 1896	0 25 - 2 0	-0 5 to +0 5
9	1 27	4 (INL)	8	0 2454	647 6	14 5	0 05932	108 2	319 8	107 7	0 650	0 05953	107 4	317 6	107 1	0 650	0 3291	0 25 - 2 0	-0 5 to +0 5
10	1 27	4 (STG)	8	0 2546	646 6	15 8	0 01435	5 97	329 1	27 6	0 670	0 01452	6 03	325 7	27 8	0 670	0 1019	0 25 - 2 0	-0 5 to 1 0
11	1 27	4 (STG)	8	0 2549	645 0	15 7	0 02974	25 57	322 2	55 8	0 660	0 02957	25 20	321 6	55 8	0 660	0 1888	0 25 - 1 0	-0 5 to 1 0
12	1 27	4 (STG)	8	0 2582	645 9	16 0	0 06076	103 0	317 9	109 9	0 640	0 0601	101 5	320 6	111 0	0 640	0 3187	0 25 - 2 0	-0 5 to 1 0

TABLE 8 CONFIGURATIONS AND FLOW CONDITIONS FOR PHASE II, SERIES 6 TESTS

Test No	Orifice Dia (CM)	S/D	H ₀ (D)	Mainstream			Top Dilution Jet					Bottom Dilution Jet					Equilibrium Theta (Thub)	Regions of Measurement	
				Mass Flow Rate (KG/S)	Temp (Tmain) (K)	Velocity (Vmain) (M/S)	Mass Flow Rate (KG/S)	Momentum Ratio J _T	Temp (T _{JT}) (K)	Velocity (V _{JT}) (M/S)	(C _D) _T	Mass Flow Rate (KG/S)	Momentum Ratio J _B	Temp (T _{JB}) (K)	Velocity (V _{JB}) (M/S)	(C _D) _B		Axial Direction X/H ₀	Transverse Direction (Z/S)
13	1 27	2 (INL)	8	0 3356	559 3	18 9	0 07235	27 49	309 9	69 3	0 620	0 07204	27 42	313 9	69 7	0 620	0 6402	0 2 - 2 0	-0 5 to +0 5
14	1 27	2 (STG)	8	0 3346	553 9	19 0	0 03633	6 92	321 7	35 5	0 640	0 03712	6 96	329 7	36 4	0 660	0 5990	0 25 - 2 0	-0 5 to 1 0
15	1 27	2 (STG)	8	0 3336	554 6	18 9	0 0716	27 42	318 5	69 6	0 630	0 07608	27 74	316 7	68 5	0 660	0 6541	0 25 - 2 0	-0 5 to 1 0
16	1 27	4 (INL)	8	0 3269	549 9	18 6	0 03539	27 42	321 3	68 5	0 640	0 0361	27 70	330 7	70 0	0 655	0 6017	0 25 - 2 0	-0 5 to +0 5
17	1 27	4 (STG)	8	0 3321	548 1	18 8	0 07975	27 71	315 4	68 7	0 636	0 08172	26 84	327 7	70 2	0 670	0 6004	0 25 - 2 0	-0 5 to 1 0
18	1 27	4 (STG)	8	0 3347	551 1	18 9	0 07606	115 3	313 5	137 7	0 630	0 08041	115 1	315 6	135 2	0 655	0 6589	0 25 - 2 0	-0 5 to 1 0

ORIGINAL PAGE IS
OF POOR QUALITY

2 FOLDOUT FRAME

1 FOLDOUT FRAME

TABLE 9. CONFIGURATIONS AND FLOW CONDITIONS FOR PHASE II, SERIES 7 TESTS WITH SYMMETRICALLY CONVERGENT TEST SECTION.

Test No	Orifice Dia (CM)	Z/D	H ₀ /D	Mainstream			Top Dilution Jet					Bottom Dilution Jet					Equilibrium Theta (Th ₀)	Regions of Measurement	
				Mass Flow Rate (KG/S)	Temp (T _{main}) (K)	Velocity (V _{main}) (M/S)	Mass Flow Rate (KG/S)	Momentum Ratio J _T	Temp (T _{J,T}) (K)	Velocity (V _{J,T}) (M/S)	(C _p) _T	Mass Flow Rate (KG/S)	Momentum Ratio J _B	Temp (T _{J,B}) (K)	Velocity (V _{J,B}) (M/S)	(C _p) _B		Axial Direction X/H ₀	Transverse Direction Z/S
19	1.27	2 (INI)	8	0.2662	644.8	16.5	0.06453	25.97	298.2	56.5	0.650	0.0638	25.57	298.2	56.3	0.650	0.3253	0.25 - 1.0	-0.5 to +0.5
20	1.27	2 (INI)	8	0.2669	644.6	16.4	0.1340	106.5	297.0	111.3	0.650	0.1348	107.7	295.0	111.3	0.650	0.5019	0.25 - 1.0	-0.5 to +0.5
21	1.27	4 (STG)	8	0.2691	644.6	16.4	0.03155	25.92	302.9	57.1	0.640	0.03275	26.69	290.2	54.7	0.640	0.1929	0.25 - 1.0	-0.5 to 1.0
22	1.27	4 (STG)	8	0.2690	644.2	16.4	0.06504	107.7	298.5	112.8	0.630	0.06506	107.7	299.9	113.7	0.630	0.3260	0.25 - 1.0	-0.5 to 1.0
23	2.54	4 (STG)	4	0.2681	644.9	16.5	0.03311	6.78	311.0	29.7	0.670	0.03367	6.75	310.4	30.0	0.680	0.1994	0.25 - 1.0	-0.5 to 1.0
24	2.54	4 (STG)	4	0.2683	644.5	16.4	0.06359	25.76	304.2	56.9	0.650	0.0669	26.0	301.1	56.7	0.675	0.3272	0.25 - 1.0	-0.5 to 1.0
25	2.54	2 (INI)	4	0.2675	645.1	16.4	0.06522	6.67	300.4	28.9	0.655	0.06554	6.70	298.9	28.9	0.655	0.3284	0.25 - 1.0	-0.5 to +0.5
26	2.54	2 (INI)	4	0.2684	644.7	16.4	0.1238	25.58	300.8	56.4	0.630	0.1250	25.90	298.9	56.6	0.630	0.4810	0.25 - 1.0	-0.5 to +0.5

ORIGINAL PAGE IS
OF POOR QUALITY

TABLE 10 CONFIGURATIONS AND FLOW CONDITIONS FOR PHASE II, SERIES 8 TESTS

Test No.	Test Section	Orifice Dia. (CM)	S D	H ₀ TF	Main Stream			Top Dilution Jet					Bottom Dilution Jet					Equilibrium Theta (Thcb)	Region of Measurement	
					Mass Flow Rate (KG/S)	Temp. (T _{main}) (K)	Velocity (V _{main}) (M/S)	Mass Flow Rate (KG/S)	Momentum Ratio J _T	Temp. (T _{JT}) (K)	Velocity (V _{JT}) (M/S)	(C _D) _T	Mass Flow Rate (KG/S)	Momentum Ratio J _B	Temp. (T _{JB}) (K)	Velocity (V _{JB}) (M/S)	(C _D) _B		Axial Direction X/H ₀	Transverse Direction Z/S
27	I	2.54	4 (STG)	4	0.2719	646.3	16.6	0.03314	6.75	313.4	30.1	0.665	0.03455	6.82	305.0	29.5	0.680	0.1993	0.25 - 2.0	-0.5 to 1.0
28	I	2.54	4 (STG)	4	0.2747	644.7	16.9	0.06534	26.41	307.4	59.4	0.650	0.06823	26.27	303.6	58.6	0.670	0.3271	0.25 - 2.0	-0.5 to 1.0
29	I	2.54	4 (INL)	4	0.2681	645.4	16.5	0.06407	26.85	307.5	58.6	0.645	0.06515	27.05	300.6	57.4	0.645	0.3253	0.25 - 2.0	-0.5 to +0.5
30	I	2.54	4 (INL)	4	0.2700	645.4	16.6	0.1306	106.9	306.9	114.9	0.640	0.1324	107.0	304.8	113.6	0.640	0.4936	0.25 - 2.0	-0.5 to +0.5
31a	I	0.5144	1	19.75	0.2739	646.0	16.8	0.03782	6.69	310.5	29.9	0.750	---	---	---	---	---	0.1213	0.25 - 2.0	0 to 40
31b	I	0.5144	1	19.75	0.2720	646.7	16.7	0.07358	26.36	308.6	21.33	0.735	---	---	---	---	---	0.2129	0.25 - 2.0	0 to 40
31c	I	0.5144	1	19.75	0.2747	646.3	16.8	0.1492	105.4	305.1	113.8	0.715	---	---	---	---	---	0.3520	0.25 - 2.0	0 to 40
32	I	2.25	2	4	0.2732	646.5	16.8	0.06414	24.23	311.0	59.1	0.670	---	---	---	---	---	0.1902	0.25 - 2.0	-0.5 to +0.5
33	I	1.27	2 (INL)	8	0.2713	645.1	16.6	0.07874	40.87	303.7	72.3	0.630	0.04895	15.20	299.1	43.2	0.640	0.3201	0.25 - 2.0	-0.5 to +0.5
34	I	1.27	2 (INL)	8	0.2703	645.3	16.6	0.09437	58.36	303.2	85.7	0.630	0.03289	6.77	300.6	28.7	0.650	0.3201	0.25 - 1.0	-0.5 to +0.5
35	III	1.27	2 (INL)	8	0.2684	645.0	16.4	0.06265	26.20	303.4	57.2	0.630	0.06279	26.12	301.0	56.7	0.630	0.3185	0.25 - 1.0	-0.5 to +0.5
36	III	1.27	2 (INL)	8	0.2698	644.5	16.4	0.1300	106.9	301.1	112.8	0.630	0.1294	106.4	301.6	113.4	0.630	0.4902	0.25 - 1.0	-0.5 to +0.5
37	III	1.27	4 (STG)	8	0.2683	645.6	16.4	0.03104	25.68	310.7	57.5	0.640	0.03115	25.67	309.0	57.7	0.640	0.1882	0.25 - 1.0	-0.5 to 1.0
38	III	1.27	4 (STG)	8	0.2680	645.6	16.4	0.06494	108.8	303.3	113.8	0.630	0.06379	105.8	303.3	113.8	0.630	0.3245	0.25 - 1.0	-0.5 to 1.0
39	III	2.54	4 (STG)	4	0.2707	645.6	16.5	0.03352	6.69	311.9	29.7	0.675	0.0339	6.75	307.5	29.5	0.675	0.1994	0.25 - 1.0	-0.5 to 1.0
40	III	2.54	4 (STG)	4	0.2727	645.7	16.6	0.06481	25.95	302.7	57.4	0.645	0.06635	26.34	293.6	55.4	0.645	0.3247	0.25 - 1.0	-0.5 to 1.0
41	III	2.54	2 (INL)	4	0.2723	645.6	16.5	0.06612	6.62	305.5	29.2	0.660	0.06633	6.65	304.9	29.3	0.660	0.3272	0.25 - 1.0	-0.5 to +0.5
42	III	2.54	2 (INL)	4	0.2726	645.8	16.4	0.1248	26.12	302.5	57.2	0.620	0.1243	26.0	303.0	57.4	0.620	0.4774	0.25 - 1.0	-0.5 to +0.5

ORIGINAL PAGE IS
OF POOR QUALITY

TABLE 10. CONFIGURATIONS AND FLOW CONDITIONS FOR PHASE II, SERIES 8 TESTS (CONTINUED)

Test No	Test Section	Orifice Dia (CM)	S/D	H ₀ /D	Mainstream			Top Dilution Jet					Bottom Dilution Jet					Equilibrium Theta (Theb)	Regions of Measurement	
					Mass Flow Rate (KG/S)	Temp (T _{main}) (K)	Velocity (V _{main}) (M/S)	Mass Flow Rate (KG/S)	Momentum Ratio J _T	Temp (T _{J_T}) (K)	Velocity (V _{J_T}) (M/S)	(C _D) _T	Mass Flow Rate (KG/S)	Momentum Ratio J _B	Temp (T _{J_B}) (K)	Velocity (V _{J_B}) (M/S)	(C _D) _B		Axial Direction X/H ₀	Transverse Direction Z/S
43	III	2.54	2	4	0.3348	506.5	17.9	0.07832	7.79	310.2	34.9	0.665	--	--	--	--	--	0.5873	0.25 - 1.0	-0.5 to +0.5
44	III	2.54	2	4	0.3350	508.4	17.9	0.1526	30.00	307.9	67.9	0.650	--	--	--	--	--	0.6460	0.25 - 1.0	-0.5 to +0.5
45a	I	1.024	1	9.92	0.2688	644.7	16.5	0.0749	6.66	307.8	29.4	0.750	--	--	--	--	--	0.2179	0.25 - 2.0	0.0 to 4.0
45b	I	1.024	1	9.92	0.2708	644.4	16.6	0.1434	25.33	308.7	57.3	0.725	--	--	--	--	--	0.3462	0.25 - 2.0	0.0 to 4.0
45c	I	1.024	1	9.92	0.2735	644.9	16.7	0.2545	78.20	307.5	98.9	0.710	---	---	---	---	---	0.4820	0.25 - 2.0	0.0 to 4.0
46	I	2.54	2 (INL)	4	0.2707	644.3	16.5	0.06667	6.70	304.8	29.4	0.665	0.06656	6.67	304.6	29.4	0.665	0.3299	0.25 - 2.0	-0.5 to +0.5
47	I	2.54	2 (INL)	4	0.2710	644.3	16.6	0.1276	25.54	302.2	57.0	0.645	0.1273	25.52	303.6	57.3	0.645	0.4846	0.25 - 2.0	-0.5 to +0.5
48	I	2.54	2 (INL)	4	0.2710	644.1	16.5	0.2334	84.14	302.5	101.4	0.640	0.2334	84.04	302.5	101.2	0.640	0.6327	0.25 - 2.0	-0.5 to +0.5
49	I	1.80	2.83	5.67	0.2701	644.4	16.7	0.03539	6.49	309.5	29.4	0.725	---	---	---	---	---	0.1159	0.25 - 2.0	-0.5 to +0.5
50	I	1.80	2.83	5.67	0.2679	644.9	16.5	0.06924	25.46	299.5	56.3	0.705	--	--	--	--	--	0.2054	0.25 - 2.0	-0.5 to +0.5
51	I	2.54	4 (INL)	4	0.2679	644.3	16.5	0.03334	6.67	305.6	29.2	0.675	0.03421	6.80	295.8	28.6	0.675	0.2014	0.25 - 1.0	-0.5 to +0.5

ORIGINAL PAGE IS
OF POOR QUALITY

TABLE 11 CONFIGURATIONS AND FLOW CONDITIONS FOR PHASE III, SERIES 9 TESTS

Test No	Orifice Plate	Orifice Dia (LM)	$\frac{S}{H_0}$	Mainstream			Fore Dilution Jet					Aft Dilution Jet					Equilibrium Theta (Theb)	Regions of Measurement	
				Mass Flow Rate (KG/S)	Temp (Tmain) (K)	Velocity (Vmain) (M/S)	Mass Flow Rate (KG/S)	Momentum Ratio J_p	Temp (T _{Jp}) (K)	Velocity (V _{Jp}) (M/S)	(C _D) _P	Mass Flow Rate (KG/S)	Momentum Ratio J_A	Temp (T _{JA}) (K)	Velocity (V _{JA}) (M/S)	(C _D) _A		Axial Direction X/H ₀	Transverse Direction (Z/S)
1	M-1	2.54	0.5	0.2683	690.1	17.8	0.07636	6.60	317.1	30.9	0.764	--	--	--	--	--	0.2216	0.25-2.0	-0.5 to +0.5
2	M-1	2.54	0.5	0.2661	661.0	16.7	0.1339	26.47	307.3	58.5	0.707	--	--	--	--	--	0.3447	0.25-2.0	-0.5 to +0.5
3	M-2	2.54	0.5	0.2676	675.0	17.2	0.1803	26.59	316.5	60.3	0.904	--	--	--	--	--	0.4026	0.25-2.0	-0.5 to +0.5
4	M-2	2.54	0.5	0.2025	655.3	12.6	0.2690	106.5	315.0	88.6	0.891	--	--	--	--	--	0.5705	0.25-2.0	-0.5 to +0.5
5	M-3	1.80 1.80	0.5 0.5	0.2674	690.3	17.7	0.03302	6.65	319.2	30.9	0.662	0.03291	6.63	320.5	30.95	0.662	0.1978	0.5-1.5	-0.5 to +0.5
6	M-3	1.80 1.80	0.5 0.5	0.2687	665.9	17.1	0.06488	26.27	310.4	59.2	0.650	0.06555	26.85	310.9	59.9	0.650	0.3268	0.5-1.5	-0.5 to +0.5
7	M-3	1.80 1.80	0.5 0.5	0.2681	636.7	16.3	0.1231	107.2	309.6	113.9	0.611	0.1224	106.0	310.2	113.2	0.611	0.4780	0.5-1.5	-0.5 to +0.5
8	M-4	2.54 2.54	1.0 1.0	0.2668	682.0	17.4	0.03596	6.67	314.0	30.4	0.719	0.03715	6.32	314.1	29.6	0.764	0.2151	0.5-1.5	-0.5 to +0.5
9	M-4	2.54 2.54	1.0 1.0	0.2694	671.6	17.3	0.06567	26.77	313.5	60.7	0.649	0.06786	26.68	314.8	60.8	0.675	0.3314	0.5-1.5	-0.5 to +0.5
10	M-5	1.80 1.27	0.5 0.25	0.2672	695.5	17.8	0.03730	6.72	321.1	31.2	0.744	0.03781	6.67	320.4	31.1	0.756	0.2194	0.25-2.0	-0.5 to +0.5
11	M-5	1.80 1.27	0.5 0.25	0.2675	677.2	17.3	0.06911	26.79	313.5	60.2	0.685	0.07006	26.63	312.9	60.1	0.700	0.3422	0.25-2.0	-0.5 to +0.5
12	M-5	1.80 1.27	0.5 0.25	0.2670	645.0	16.4	0.1310	106.3	313.7	113.3	0.651	0.1365	106.4	313.2	114.7	0.685	0.5004	0.25-2.0	-0.5 to +0.5

TABLE 12 CONFIGURATIONS AND FLOW CONDITIONS FOR PHASE III, SERIES 10 TESTS

Test No	Orifice Plate	Orifice Dia (LM)	$\frac{S}{H_0}$	Mainstream			Fore Dilution Jet					Aft Dilution Jet					Equilibrium Theta (Theb)	Regions of Measurement	
				Mass Flow Rate (KG/S)	Temp (Tmain) (K)	Velocity (Vmain) (M/S)	Mass Flow Rate (KG/S)	Momentum Ratio J_p	Temp (T _{Jp}) (K)	Velocity (V _{Jp}) (M/S)	(C _D) _P	Mass Flow Rate (KG/S)	Momentum Ratio J_A	Temp (T _{JA}) (K)	Velocity (V _{JA}) (M/S)	(C _D) _A		Axial Direction X/H ₀	Transverse Direction (Z/S)
13	M-5	1.80 1.27	0.5 0.25	0.2657	672.0	17.0	0.06769	26.20	310.1	58.5	0.683	0.03663	6.36	310.9	29.1	0.756	0.2821	0.25-2.0	-0.5 to +0.5
14	M-5	1.80 1.27	0.5 0.25	0.2650	666.3	16.8	0.1338	106.5	304.5	113.0	0.650	0.03662	6.48	312.5	29.2	0.756	0.3938	0.25-2.0	-0.5 to +0.5
15	M-5	1.80 1.27	0.5 0.25	0.2655	660.0	16.7	0.1329	106.3	305.8	112.9	0.650	0.06941	26.37	302.3	57.6	0.700	0.4318	0.25-2.0	-0.5 to +0.5
16	M-6	1.27 1.80	0.25 0.5	0.2670	656.6	16.7	0.1401	106.8	306.7	114.4	0.685	0.03726	6.46	290.6	28.2	0.744	0.3939	0.25-2.0	-0.5 to +0.5
17	M-6	1.27 1.80	0.25 0.5	0.2671	663.8	16.9	0.1414	106.8	305.1	114.8	0.685	0.07057	26.49	297.3	57.9	0.695	0.4409	0.25-2.0	-0.5 to +0.5
18	M-7	2.54	0.5	0.2666	684.2	17.4	0.07156	6.64	316.3	30.4	0.719	--	--	--	--	--	0.2116	0.25-2.0	-0.5 to +0.5
19	M-7	2.54	0.5	0.2672	675.5	17.2	0.1338	27.13	314.5	60.5	0.662	--	--	--	--	--	0.3336	0.25-2.0	-0.5 to +0.5
20	M-7	2.54	0.5	0.2672	637.4	16.2	0.2532	106.2	307.8	112.0	0.630	--	--	--	--	--	0.4862	0.25-2.0	-0.5 to +0.5
21	A	2.54	0.5	0.2574	629.1	15.3	0.2929	103.2	307.0	104.3	0.764	--	--	--	--	--	0.5322	0.25-2.0	-0.5 to +0.5
22	A	2.54	0.5	0.2663	668.5	16.9	0.1515	26.24	312.5	58.6	0.765	--	--	--	--	--	0.3626	0.25-2.0	-0.5 to +0.5

ORIGINAL PAGE IS
OF POOR QUALITY

REFERENCES

1. Srinivasan, R., Berenfeld, A., and Mongia H.C., "Dilution Jet Mixing Program - Phase I Report," NASA CR-168031, 1982.
2. Srinivasan, R., Coleman, E., and Johnson, K., "Dilution Jet Mixing Program - Phase II Report," NASA CR-174624, 1984.
3. Srinivasan, R., Meyers, G., Coleman, E., and White, C., "Dilution Jet Mixing Program - Phase III Report," NASA CR-174884, 1985.
4. Srinivasan, R., et al., "Aerothermal Modeling Program: Phase I Final Report" Garrett Turbine Engine Company, Phoenix, Arizona, Garrett 21-4742, August 1983 (NASA CR-168243).
5. Holdeman, J.D., and Walker, R.E., "Mixing of a Row of Jets with a Confined Crossflow," AIAA Journal, Vol. 15, No. 2, Feb. 1977, pp. 243-249 (also AIAA-76-48 and NASA TM X-71787).
6. Walker, R.E. and Eberhardt, R.G., "Multiple Jet Study Data Correlations," NASA CR-134795, 1975.

C - 5